Applications of Quartz Crystal Microbalance Technology in Petroleum Engineering, Demonstrated by Studies of Wax, Asphaltenes, Hydrates, Ice, Diesel Additives and Anti-deposition Coatings

Rhoderick William BURGASS

Thesis submitted for the degree of Doctor of Philosophy

Heriot-Watt University

Institute of Petroleum Engineering

May 2015

ABSTRACT

This thesis describes the development and uses of equipment and methods based upon the use of quartz crystal microbalance (QCM) technology for measurements involving major Flow Assurance issues, namely wax, asphaltene and hydrate in addition to ice formation in processing facilities, deposition of diesel performance additives in injectors and evaluation of anti-depositional paint coatings.

For wax, the use of QCM for accurate measurements of the solubility of wax in synthetic binary and quaternary mixtures of n-alkanes is demonstrated and validated against literature data and model predictions. The use of the QCM for measurements of wax appearance temperature (WAT) and wax disappearance temperature (WDT) for stabilised and live reservoir fluids is presented. The development of QCM based equipment for investigating the effect of temperature gradient on wax deposition tendency at ambient and high pressure is described. The development and validation of the application of QCM technology for comparing and optimising dose rates for wax inhibitors at atmospheric and high pressure is presented. Wax case studies employing the developed equipment and methods are included.

In the case of asphaltenes the potential use of QCM based equipment for measuring asphaltene onset in standard solvent titration measurements is shown. In addition by comparing step-wise and continuous injection results, potential errors in asphaltene stability measurements are highlighted. QCM tests with live fluids show that asphaltene onset can be readily detected in reservoir fluids at high pressure/high temperature conditions. In addition reversibility of asphaltene deposition can be demonstrated. Measurement of the effectiveness of asphaltene inhibitor treatments in terms of reducing solids deposition is demonstrated at operating conditions. Asphaltene case studies using the developed equipment and methods are presented.

With hydrates, the development of QCM based equipment for measurement of hydrate dissociation points is presented. The use of QCM to identify solids forming in a dew pointing and mercaptan removal unit is described. The development of high pressure/high temperature equipment to detect deposition of diesel performance additives in injectors is presented. Finally the evaluation of anti-deposition coatings for scale and wax is described.

DEDICATION

This thesis is dedicated to Josie, Jayne, Inga and Geoff.

ACKNOWLEDGEMENTS

I would especially like to thank Bahman Tohidi for his guidance and encouragement and for being a good friend and colleague for over 20 years.

I would like to thank Adrian Todd and Ali Danesh who gave me the opportunity to work in Petroleum Engineering Research.

I would like to thank the Industry and Government sponsors whose support enabled the studies presented in this thesis to be conducted.

TABLE OF CONTENTS

LIST OF PUBLICATIONS BY THE CANDIDATE

Publications as first author.

Burgass, R., Tohidi, B., Danesh, A. and Todd, A.C., *Application of Quartz Crystal Microbalance to Gas Hydrate Stability Zone Measurements,* 4th International Conference on Gas Hydrates, Yokohama, Japan, 19-23 May (2002).

Burgass, R.W., and Tohidi, B., Robinson, I., *Reducing the Risks of Solid Deposition by using Internal Pipeline Coating,* 15th International Conference on Pipeline Protection, Aachen, Germany, 29-31 October (2003).

Burgass, R.W., and Tohidi, B., *Development and Validation of Small Volume Multi-Tasking Flow Assurance Tool,* SPE Asia Pacific Oil and Gas Conference and Exhibition, Jakarta, Indonesia 20-22 September (2011).

Burgass, R., Chapoy, A., Duchet-Suchaux, P., and Tohidi, B., *Experimental Water Content Measurements of Carbon Dioxide in Equilibrium with Hydrates at 223.15 to 263.15 K and 1.0 to 10.0 MPa,* Journal of Chemical Thermodynamics, volume 69, Pages 1-5, February (2014).

Burgass, R., Chapoy, A., and Tohidi, B., *Low Temperature Water Content in Natural Gas Systems: New Measurements and Modelling,* Proceedings of the 8th International Conference on Gas Hydrates (ICGH8-2014), Beijing, China, 28 July - 1 August (2014).

Co-author in 132 papers as detailed at link given below references. Selected papers listed below.

Chapoy, A., Burgass, R. W., Tohidi Kalorazi, B. & Alsiyabi, I. *Hydrate and phase behavior modeling in CO_2-rich pipelines*, 12 Feb 2015 In : Journal of Chemical and Engineering Data. 60, 2, p. 447-453 7 p.

Chapoy, A., Mazloum Vajari, S., Burgass, R. W., Haghighi, H. & Tohidi Kalorazi, B. *Clathrate hydrate equilibria in mixed monoethylene glycol and electrolyte aqueous solutions*, May 2012 In : Journal of Chemical Thermodynamics. 48, p. 7-12 6 p.

Chapoy, A., Burgass, R. W., Tohidi Kalorazi, B., Austell, J. M. & Eickhoff, C. *Effect of common impurities on the phase behavior of carbon-dioxide-rich systems: minimizing the risk of hydrate formation and two-phase flow*, Dec 2011 In : SPE Journal. 16, 4, p. 921-930 10 p.

Hemmingsen, P. V., Burgass, R. W., Pedersen, K. S., Kinnari, K. & Sorensen, H. *Hydrate temperature depression of MEG solutions at concentrations up to 60 wt%: Experimental data and simulation results*, Aug 2011 In : Fluid Phase Equilibria. 307, 2, p. 175-179 5 p.

Zhang, L., Burgass, R. W., Chapoy, A., Tohidi Kalorazi, B. & Solbraa, E. *Measurement and modeling of CO2 frost points in the CO2-methane systems*, Jun 2011 In : Journal of Chemical and Engineering Data. 56, 6, p. 2971-2975 5 p.

Zhang, L., Burgass, R. W., Chapoy, A. & Tohidi Kalorazi, B. *Measurement and modeling of water content in low temperature hydrate-methane and hydrate-natural gas systems*, Jun 2011 In : Journal of Chemical and Engineering Data. 56, 6, p. 2932-2935 4 p.

Haghighi, H., Chapoy, A., Burgass, R. W., Mazloum Vajari, S. & Tohidi Kalorazi, B. *Phase equilibria for petroleum reservoir fluids containing water and aqueous methanol solutions: experimental measurements and modelling using the CPA equation of state*, Apr 2009 In : Fluid Phase Equilibria. 278, 1-2, p. 109-116 8 p.

Haghighi, H., Burgass, R., Chapoy, A., Tohidi, B.Najibi, H., Chapoy, A., *Experimental Determination and Thermodynamic Prediction of Methane Hydrate Stability in Alcohols and Electrolyte Solutions,* Fluid Phase Equilibria, 275, 127-131 (2009).

Anderson, R., Burgass, R.W., Tohidi, B., and Østergaard, K. K. *Experimental Measurement of Gas Hydrate Stability Zones in Porous Media*, Presented at the 63rd EAGE Conference and Exhibition, Amsterdam, The Netherlands, 11-15 June (2001).

Østergaard, K.K., Tohidi, B., Burgass, R.W., Danesh, A., and Todd, A.C. *Hydrate Equilibrium Data of Multi-Component Systems in the Presence of Structure-II and Structure-H HeavyHydrate Formers*, Journal of Chemical and Engineering Data 46 (2001).

Tohidi, B., Burgass, R.W., Danesh, A., Todd, A.C., and Østergaard, K.K. *Improving the Accuracy of Gas Hydrate Dissociation Point Measurements*, Annals of the New York Academy of Sciences 912 (2000).

Østergaard, K.K., Burgass, R.W., Tohidi, B., Danesh, A., and Todd, A.C. **Advances in** *Experiments and Computer Modelling Software to Simulate Hydrate Formation with Respect to Salts and Inhibitors*, Presented at Practicalities of Predicting, Preventing and Controlling Waxes, Hydrates and Asphaltenes, 17-18 June, Aberdeen, UK, Conference Proceedings (1998).

Tohidi, B., Burgass, R. W., Danesh, A. and Todd, A. C. *Experimental Study on the Causes of Disagreements in Methane Hydrate Dissociation Data*, Annals of the New York Academy of Sciences 715 (1994).

Tohidi, B., Burgass, R. W., Danesh, A. and Todd, A. C. *Benzene Can Form Gas Hydrates*, Trans IChemE **71** A (1993).

Tohidi, B., Burgass, R. W., Danesh, A. and Todd, A. C. *Measurement and Prediction of Amount and Composition of Equilibrium Phases in Heterogeneous Systems Containing Gas Hydrates*, Presented at the SPE Student Paper Contest, September 6, Aberdeen, Scotland (1993).

Burgass, R. W., and Powell, A. A., *Evidence for Repair Processes in the Invigoration of Seeds by Hydration*, Ann Bot (1984) 53 (5): 753-757.

https://pureapps2.hw.ac.uk/portal/en/publications/search.html?search=burgass&uri=&journalName=&type=&organisationName=&organisations=&language=&publicationYearsFrom=&publicationYearsTo=&publicationcategory=&peerreview

CHAPTER 1 - INTRODUCTION

In 1995 I started work on a project aimed at investigating the use of a quartz piezoelectric torsional viscometer for measuring fluid properties downhole and in the laboratory. The viscometer had been initially developed by BP America Incorporated, however it was not fully functional and there were some issues that required to be resolved. At this time I searched for other potential options based upon using piezoelectric devices and came across the quartz crystal microbalance (QCM). The use of QCM for different applications such as thin film deposition control, surface science, assisted etching, analytical chemistry, space system contamination, and aerosol mass measurement had already been demonstrated by other workers [1, 2]. The wide range of potential uses of QCM technology in petroleum engineering immediately became apparent. This thesis gives a valuable account of the development and validation of novel uses of QCM technology in petroleum engineering in particular some of the major Flow Assurance challenges. The advances and achievements are documented and backed up by publications and projects carried out for real cases. Overall this work is an important starting point that can be used to take the technology further through development of novel methods and equipment. Since starting this work in 1995 the uses of QCM have multiplied rapidly as described in a number of publications [3-10]. In addition 500 references on QCM applications can be found at http://www.science.gov/topicpages/q/quartz+crystal+microbalance.html#.

Flow Assurance is a term widely used in the oil and gas industry, it is considered to be a translation from a Portuguese term used by Petrobras in the 1990s whose literal translation is "Guarantee of Flow". It can be considered as multiphase transport, covering the transmission of oil, gas and water in the same pipeline from the reservoir to the processing plant. Flow Assurance involves overcoming problems associated with solids that may form such as wax, asphaltene, hydrate, scale and napthenates. This thesis covers investigations into the potential uses of QCM based equipment for studying three of the major Flow Assurance issues, namely wax, asphaltene and hydrate.

Wax crystallization and deposition during production and transportation is well known to be a very costly problem [11]. Wax is the term generally given to n-alkanes higher than C_{15} that can precipitate from oil as it cools along with smaller amounts of branch-chain and cyclic

paraffins and aromatics [12]. Wax can cause problems such as depositing on pipeline walls and restricting flow, increasing oil viscosity and in the case of shut-ins joining together to form a gel. There are different strategies that have been developed for dealing with wax problems such as heating and insulation, pigging, solvent injection and inhibitors. Clearly whichever strategy is chosen depends upon a variety of factors primarily driven by economic considerations.

In order to design production and transportation facilities with respect to potential wax problems it is necessary to be able to predict, with knowledge of the reservoir fluid composition and the P/T conditions, the likelihood of wax forming and causing the problems described above. It is also desirable to be able to back up predictions with experimental measurements on fluids that are available from initial exploration. In terms of predicting wax phase equilibria there are a number of different approaches such as UNIQUAC solid solution, ideal solid solution and multi-pure solid model. At Heriot-Watt University a new approach for describing wax solids has been developed, based on the UNIQUAC equation [13]. A good model requires to accurately predict the wax phase boundary of the reservoir fluid and how much wax will form at different temperatures. A wide variety of factors will then need to be considered such as the effect of temperature gradients between fluids and pipeline walls coupled with shear rates and viscosities to build a picture of likely problems.

Development and validation of any thermodynamic model requires accurate experimental data. For wax models, a systematic approach might be considered to first ensure that the model can accurately predict the solubility of n-alkanes higher than C_{15} in lighter hydrocarbons and solvents. There is a significant amount of literature data available for binary mixtures of n-alkanes and n-alkanes with different solvents [14-19]. Much of the solubility data has been measured using a thorough systematic approach based upon visual observation of the appearance and disappearance of the solid phase avoiding the common pitfall of disregarding the requirement for sub-cooling to initiate solid formation.

For stabilised transparent or semi-transparent fluids the ASTM D 2500 – 86 cloud point or wax appearance temperature (WAT) is commonly measured. As this method cannot be used for darker coloured fluids a variety of other methods have been developed such as cross polar microscopy (CPM), dynamic filtration, viscosity, near-infra-red light attenuation, photoelectric, rheometry and differential scanning calorimetry (DSC). As many studies have

shown, due to the requirement for some degree of sub-cooling to initiate wax formation, this cannot be considered as a point of thermodynamic equilibrium and therefore cannot be used to validate any thermodynamic model. As discussed in Chapter 2 the difference between WAT and WDT is because a nucleation process with a certain activation energy will be involved in the crystallisation process and the physical expression of this is a requirement for a certain degree of supersaturation or sub-cooling. In addition due to the variety of cooling rates and the sensitivity of the method the data have been found to be inconsistent [20-22]. The true point of thermodynamic equilibrium requires to be measured by finding the temperature at which all the wax dissolves known as the wax disappearance temperature (WDT). As with the WAT, the accuracy of different methods depends upon their sensitivity.

Wax inhibitors are commonly used as a Flow Assurance tool. They are considered to act by co-crystallising with the wax making it less likely to adhere to or build up on surfaces and to form networks leading to gel formation [23]. There are a number of means available for screening wax inhibitors such as pour point and cold finger tests. In the case of cold finger tests quite large quantities of oil are required and in addition it is not possible to conduct testing at pipeline P/T conditions.

The QCM is an ultrasensitive device that can be used at a wide variety of P/T conditions. For this reason it is ideally suited to the study of solid appearance and disappearance measurements as required in the study of wax in synthetic and reservoir fluids. In addition, as it depends upon solids adhering to or building up on its surface, it is ideally suited to studying the effect of wax inhibitors. In **Chapter 2**, the development and validation of QCM based equipment and methods for measuring the WAT and WDT of stabilised and live reservoir fluids, wax adhesion tendency with different temperature gradients and the use of the equipment to screen wax inhibitors, is presented. In **Chapter 3** case studies, using the developed equipment and methods are presented.

As with wax, asphaltene is another solid that can come out of solution during production and transportation. Problems are caused by solids building up on surfaces restricting flow. Asphaltenes are high molecular components present in reservoir fluids, commonly identified by the fact that they are insoluble in n-alkanes such as pentane and heptane but soluble in aromatic solvents such as toluene. Asphaltenes precipitate from reservoir fluids as a result of reducing pressures and temperatures. Reducing reservoir pressure can cause asphaltene to

deposit on surfaces within the formation leading to reduced permeability. Both reducing pressure and temperature in pipelines can lead to asphaltene precipitation and deposition on pipeline walls. CO_2 injection and solvent treatments can also lead to asphaltene precipitation. Asphaltene problems are known to be widespread throughout the world [24-27]. Problems are usually associated with lighter fluids with relatively small amounts of asphaltene present where the asphaltenes more readily come out of solution and adhere to surfaces.

There are a number of different thermodynamic models for predicting asphaltene stability in reservoir fluids such as solubility, solid, colloidal and association EOS models. As with wax it is essential to have reliable experimental data to validate any thermodynamic model. Asphaltene stability is commonly measured on stabilised crude oils using titration with solvents such as n-pentane and n-heptane. There are a variety of methods for detecting the onset point such as NIR spectroscopy, laser light scattering, microscopy, filtration, capillary flow and vapour pressure osmometry [27-32]. There is a scarcity of information available relating to comparisons between these methods. Usually the titration is conducted using a continuous injection rate of the solvent at a variety of rates. This may not allow the fluids to reach equilibrium, hence overshooting the point of precipitation. This coupled with different detection sensitivities could lead to scattered data. As stabilised samples may lose asphaltenes through precipitation as P/T conditions change it would be better to conduct studies on live, relatively uncontaminated downhole samples.

Knowledge of the asphaltene deposition envelope allows for taking into account problems associated with asphaltene precipitation and deposition when designing production and transport facilities. Strategies for dealing with asphaltene include changing P/T conditions to avoid asphaltene deposition by heating or maintaining pressure, periodical removal by mechanical means or solvent injection and injection of inhibitors aimed at preventing asphaltenes from precipitating.

As with waxes the QCM is an ideal device for measuring asphaltene solids deposition at a wide variety of P/T conditions. **Chapter 4** describes the development of equipment and methods for measuring asphaltene onset in heptane titration tests with stabilised oil, measuring asphaltene onset in live reservoir fluids and measuring the effect of inhibitor on asphaltene deposition tendency. Case studies where the developed equipment and methods have been used are presented in **Chapter5**.

Hydrate formation is a major Flow Assurance problem, particularly for subsea pipelines where unprocessed reservoir fluids are being transported at high pressures and low temperatures. Apart from a Flow Assurance issue, hydrates are receiving considerable interest for other reasons. There are substantial amounts of gas trapped in naturally occurring hydrates throughout the world [33, 34] and thus a potentially important resource for the future. In addition there is potential to use hydrates as a means of CO_2 capture and storage of methane or hydrogen as clean energy sources [35].

As in the case of both wax and asphaltene there are different approaches for predicting hydrate formation conditions ranging from simple correlations to thermodynamic models with different equations of state options. In order to validate predictions accurate experimental hydrate dissociation points are required. There are a number of options available such as isochoric step-heating, isothermal step depressurization, visual, Cailletet, Raman Spectroscopy and high pressure DSC. As described in **Chapter 6** the use of QCM to make accurate hydrate dissociation point measurements was developed between 1995 and 1997 [36]. Due to the small amount of sample required equilibrium times are low allowing for faster measurements. The method has been adopted by other researchers [37, 38] as it allows for faster testing. The potential use of QCM based equipment to make hydrate dissociation point measurements in order to indirectly validate predictions of inhibitor distribution is presented in **Chapter 6**.

QCM based equipment has successfully been used for other studies. **Chapter 6** details its use combined with other analytical equipment to identify solids forming in a processing plant and in addition evaluate different avoidance and remediation strategies. The capability of a QCM to be used at pressures up to 40,000 psia and its potential for use in studying deposition of performance additives in diesel injectors is described in **Chapter 6**. Finally in **Chapter 6** the application of QCM based equipment for studying the performance of anti-deposition coatings applied to internal pipeline surfaces with the aim of reducing deposition of solids such as scale and wax, is presented.

1.1. References

[1] Lu, C., and Czanderna, A.W., *Applications of Piezoelectric Quartz Crystal Microbalances*, Czanderna and Lu (Eds.) Elsevier, New York, (1984).

[2] Buttry, D.A., and Ward, M., *Measurement of Interfacial Processes at Electrode Surfaces with the electrochemical Quartz Crystal Microbalance,* Chem. Reviews 92(6) (1992) 1355-1379.

[3] Ballantine, D.S.,et. al., *Acoustic Wave Sensors-Theory, Design, and Physico-Chemical Applications,* Academic Press, (1996).

[4] O'Sullivan, C.K., and Guilbault, G.G., *Commercial Quartz Crystal Microbalances-Theory and Applications,* Biosensors and Bioelectronics 14(1999) 663.

[5] Henry, C., *Measuring the Masses: Quartz Crystal Microbalances,* Anal Chem., News and Features, Oct (1996), p. 625A.

[6] Handley, J., *Quartz Crystal Microbalances Some New Innovations Stand Alongside the Standard, reliable workhorse,* Anal Chem., April (2001), 225A.

[7] Martin, S., *Closing Remarks,* Faraday Discuss 107 (1997) 463.

[8] Hillman, A.R., *The QCM in Electrochemistry,* Electrochimica Acta (Special Issue) 45(22 & 23), 304 pages, (2000).

[9] Faraday Discussions, volume 107, (1997).

[10] Cass, T. & Ligles, F.S., *Immobilized Biomolecules in Analysis - A Practical Approach,* Oxford University Press (1998); ISBN 0 19 963636 2.

[11] Sanjay, M., Baruah, S., and Singh, K., *Paraffin Problems in Crude Oil Production and Transportation: A Review,* SPE Production and Facilities, Volume 10, Number 1, pages 50-54, (1995).

[12] Jorda, R.M., *Paraffin Deposition and Prevention in Oil Wells*, JPT 1605; Trans., AIME, 237, (1966).

[13] Ji, H., Tohidi, B., Danesh, A., and Todd, A.C., *Wax Phase Equilibria: Developing a Thermodynamic Model Using a Systematic Approach*, Fluid Phase Equilibria, 216, 201-217 (2004).

[14] Seyer, W.F., and Fordyce, R., *The mutual solubilities of hydrocarbons: I the freezing point curves of dotriacontane (dicetyl) in propane and butane,* J. Am. Chem. Soc.**,** 58, 2029-31, (1936).

[15] Seyer, W.F., *Mutual Solubilities of Hydrocarbons II. The Freezing Point Curves of Dotricontane (Dicetyl) in Dodecane, Decane, Octane, Hexane, Cyclohexane and Benzene,* J. Am. Chem. Soc.**,** 60, 827-30, (1938).

[16] Holder G.A., and Winkler J., *Wax Crystallization form Distillate Fuels*, Journal of the Institute of Petroleum, Volume 51, Number 499, July (1965).

[17] Lundager Madsen, H.E., and Boistelle, R., *Solubility of Long-Chain n-Paraffins in Pentane and Heptane*, J. Chem. Soc., Faraday Trans. 1, **72**, 1078-1081, (1976).

[18] Roberts, K.I., Rousseau, R.W., and Teja, A.S., *Solubility of Long-Chain n-Alkanes in Heptane between 280 and 350 K*, J. Chem. Eng. Data, 39, 793-795, (1994).

[19] Jennings, D.W., and Weispfennig, K., *Experimental solubility data of various n-alkane waxes: effects of alkane chain length, alkane odd versus even carbon number structures, and solvent chemistry on solubility*, Fluid Phase Equilibria 227, 27-35, (2005).

[20] Rønningsen, H. P., Bjørndal, B., Hansen, A. B., and Pedersen, W. B, *Wax Precipitation from North Sea Crude Oils. 1. Crystallization and Dissolution Temperatures, and Newtonian and Non-Newtonian Flow Properties*, Energy Fuels 5, 895-907 (1991).

[21] Mongure-McClure, T.G., Tackett, J.E., and Merrill, L.S., *Comparisons of Cloud Point Measurement and Paraffin Prediction Methods*, SPE Prod. & Facilities 14 (1), February (1999).

[22] Coutinho, A.P., and Daridon, J.L., *The Limitations of the Cloud Point Measurement Techniques and the Influence of the Oil Composition on Its Detection*, Petroleum Science and Technology, 23:1113-1128, (2005).

[23] Manka, J.S., and Ziegler, K.L., *Factors Affecting the Performance of Crude Oil Wax-Control Additives*, SPE 67326, Presented at SPE Production and Operations Symposium, Oklahoma City, Oklahoma, 24-27 March (2001).

[24] Haskett, C.E, Polumbus, E.A, and Tartera, M., *A Practical Solution to the Problem of Asphaltene Deposits-Hassi Messaoud Field, Algeria*, Journal of Petroleum Technology, Volume 17, Number 4, 387-391, April (1965).

[25] Lichaa, P.M., *Asphaltene Deposition Problem in Venezuela Crude*, Can. PTJ. Oil Sands, 609-624, (1997).

[26] Kokal, S.L., and Sayegh, S.G., *Asphaltenes: the Cholesterol of Petroleum*, SPE paper 29787, presented at the SPE Middle East Oil Show in Bahrain, March 11-14, (1995).

[27] Escobedo, J., and Mansoori, G.A., *Heavy-organic particle deposition from petroleum fluid flow in oil wells and pipeline*, Pet.Sci. 7:502-508 (2010).

[28] Oliensis, G.L.. In: ASTM, Proceedings. of the 36th Annual Meeting, Chicago 33, Part II, p. 715 (1933).

[29] Hotier, G. and M. Robin, *Effects of different diluents on heavy oil products: measurement, interpretation, and a forecast of asphaltene flocculation*, Revue de l'IFP 38, 101 (1983).

[30] Fotland, P., H. Anfindsen, and F.H. Fadnes. *Detection of asphaltene precipitation and amounts precipitated by measurement of electrical conductivity,* Fluid Phase Equilibria 82, 157 (1993).

[31] Jamaluddin, A.K.M., N. Joshi, M.T. Joseph, D. D'Cruz, B. Ross, and J. Creek et al. *Laboratory Techniques to Measure Thermodynamic Asphaltene Instability* Paper # 2000–68. In: Canadian International Petroleum Conferences (2000).

[32] Yarranton, H.W., Alboudwarej, H., and Jakher, R., *Investigation of Asphaltene Association with Vapor Pressure Osmometry and Interfacial Tension Measurements*, Ind. Eng. Chem. Res., *39*, 2916-2924 (2000).

[33] Tohidi, B., and Anderson, R., *Gas Hydrates: Frozen Methane – Friend or Foe,* Teaching Earth Sciences, 29, 18-21, (2004).

[34] Giavarini, C., and Hester, K., *Gas Hydrates Immense Energy Potential and Environmental Challenges,* Springer ISBN 978-0-85729-955-0 (2011).

[35] Yang, M., Song, Y., Jiang, L., Zhu, N., Liu, Y., Zhao, Y., Dou, B., and Li, Q., *CO_2 Hydrate Formation and Diasociation in Cooled Porous Media: A Potential Technology for CO_2 Capture and Storage*, Environ. Sci. Technolog., 47 (17) pp 9739-9746, (2013).

[36] Danesh, A., Todd, A.C., Tohidi, B., and Burgass, R., *Applicability of Oscillating Quartz Crystal in Measuring Fluid Properties in Laboratory or Downhole*, EPSRC research grant final report, ref No: GR/K63641, (1997).

[37] Lee, B.R., Sa, J.H., Park, D.H., Cho, S., Lee, J., Kim, H.J., Oh, E., Jeon, S., Lee, J.D., and Lee, K.H., *"Continuous" Method for the Fast Screening of Thermodynamic Promoters of Gas Hydrates Using a Quartz Crystal Microbalance,* Energy Fuels, 26, 767-772, (2012).

[38] Park, D.H., Lee, B.R., Sa, J.H., and Lee, K.H., *Gas-Hydrate Phase Equilibrium for Mixtures of Sulfur Hexafluoride and Hydrogen,* J. Chem. Eng. Data, 57, 1433-1436, (2012).

CHAPTER 2 - DEVELOPMENT OF QCM BASED EQUIPMENT AND METHODS FOR WAX MEASUREMENTS

2.1. Introduction

Pure alkanes such as decane are liquid at 20 °C and atmospheric pressure. If the temperature of decane is reduced below its melting point, -30 °C, then it will become solid. The transition between liquid and solid may require some degree of sub-cooling, depending upon factors such as the time given and the degree of agitation. Measurement of the exact temperature can be achieved by a variety of means, possibly the simplest being to heat the solid decane in small steps allowing thermal equilibrium to be achieved at each step and visually observe whether it is solid or liquid. A small amount of a heavier component, such as icosane, can be dissolved in decane so that there is no solids present at 20 °C. If the resultant binary mixture is cooled solids will appear at some temperature. As with the liquid solid transition in a pure component some degree of sub-cooling will be required, in most cases, before the solid appears. This is because a nucleation process with a certain activation energy will be involved in the crystallisation process and the physical expression of this is a requirement for a certain degree of supersaturation or sub-cooling. This means that the point at which solids appear cannot be taken as an accurate measure of the solubility of icosane in decane, unless the cooling rate is sufficiently slow to avoid any sub-cooling.

Numerous accurate measurements of solubility for binary alkane mixtures have been made using visual means and various approaches. Holder and Winkler (1965) [1] used visual observation of continuously mixed test solutions cooled at a slow rate of 2 °F per hour. Madsen and Boistelle (1975) [2] alternatively raised and lowered the temperature of a continuously mixed sample, with steadily decreasing amplitude, whilst observing the appearance and disappearance of solids. Roberts et al. (1994) [3] used visual observation combined with heating at a rate of 2 Kelvin per hour of a continuously mixed sample. The data for the solubility of hexatriacontane in heptane measured by Roberts et al. (1994) [3] are in good agreement with those measured by Madsen and Boistelle (1975) [2]. Whichever approach is used the most important point is to obtain a reliable measurement of the solubility that can then be used to develop and tune thermodynamic models. Clearly if measurements are made with high or uneven rates of cooling and poor mixing then the results will be

unreliable due to the sub-cooling required to form the solid phase. Holder and Winkler (1965) [1] concluded that the standard test method for cloud point of petroleum oils, ASTM D 2500 – 86, could not be used to make reliable measurements because the cooling is non-uniform and irregular.

Oil and its distilled products are made up of mixtures of large numbers of components and in many cases solids will appear when the temperature is reduced from a condition where no solids are present. The solids composed of n-alkanes higher than C_{18} are normally referred to as wax. Wax can cause significant problems such as adhering to pipeline walls and restricting flow. In addition it can lead to increased viscosity reducing flow, and increasing pumping costs. In cases where flow is stopped and wax forms the fluids can gel, leading to potential restart problems. Wax formation in fuels at low temperatures can lead to engine failure. As the major concern is with the formation/appearance of wax as the fluid cools, the temperature at which this will occur is the main focus of attention. This point is commonly named the Wax Appearance Temperature (WAT).

There are a variety of experimental methods aimed at measuring the WAT such as visual i.e. ASTM D 2500 – 86, cross polar microscopy (CPM), dynamic filtration, viscosity, near-infra-red light attenuation, photoelectric, rheometry and differential scanning calorimetry (DSC) [1, 4-20]. In most cases the method requires that the test fluid is cooled from a temperature at which no wax is present at a constant rate and detecting when wax is formed. As with the binary alkane mixtures some degree of sub-cooling is, in most cases, required for the formation of a solid phase. Essentially this means that the WAT is not the correct point of thermodynamic equilibrium where a solid phase is formed and therefore it cannot be used for either tuning or validating a thermodynamic model. If a thermodynamic model is a true representation of the physical phenomena it must be able to predict the condition of thermodynamic equilibrium. As discussed below, depending upon the methodology used, the difference can be up to 20 °C.

The measured WAT has been shown to vary between different techniques [6, 8, 21] for a number of reasons. One reason is that the amount of wax that can be detected is variable depending upon the method of detection. For example DSC has been shown to be less sensitive with samples with lower wax content [13] giving lower WAT values. Methods

relying upon changes in viscosity or changes from Newtonian to non-Newtonian behaviour require some amount of wax to be present before changes can be clearly seen. Visual methods such as ASTM D 2500 – 86 can only be used on transparent or translucent fluids and the measured WAT may vary from operator to operator. A second reason for differences is the cooling rate, as shown by Paso et al. [22] using the CPM method with different cooling rates the WAT will vary, as expected the higher the cooling rate the lower the WAT will be. It is clear that methods with varying sensitivities and cooling rates will yield different WAT values. Ronningsen et al. [6] compared measurements of WAT or wax precipitation temperature, as they termed it, for 17 crude oil samples measured by microscopy, DSC and viscosity. In general the microscopy method with the lowest cooling rate of 0.5 °C per minute gave the highest WAT. The DSC cooling rate, at 10 °C per minute, was slower than the 12.5 °C per minute used in the viscosity measurements. The DSC WAT was found to be lower in many cases than the viscosity method, suggesting that it was the least sensitive. For many of the oils there was poor agreement between the measured WAT values, in some cases the difference was over 20 °C. Due to the differences between the experimental approaches to measuring WAT Coutinho and Daridon [21] suggested that other information should be used to complement or replace this measurement.

In summary WAT is not a point of thermodynamic equilibrium thus it cannot be used for modelling purposes. It can be measured by a variety of methods, however unless the cooling rate and sensitivity, regarding detecting the first solids, are the same then the results are likely to be different. Measurement of WAT is possibly of most use if the cooling rate used in the test is similar to that encountered in the field.

Accurate and reliable measurement of the temperature at which all of the wax is dissolved, commonly termed wax disappearance or dissolution temperature (WDT), will give a point of thermodynamic equilibrium that can be used to compare with predictions from thermodynamic models. The WDT of live oil will change with pressure due to the amount of light components dissolved in the liquid phase. Measurements of the WDT at different pressures will give a wax phase boundary that can be used to compare with model predictions and give useful information as a starting point for design of facilities with respect to potential problems caused by wax formation. Clearly the amount of wax that will form, the amount that will adhere to pipeline walls and the changes in viscosity are critical parameters.

Without being able to predict the wax phase envelope it is unlikely that these parameters can be predicted correctly.

As with WAT, measurement of WDT can be carried out using the same variety of procedures. In addition, similar to WAT measurement the results are likely to be different, dependent in the main part upon the sensitivity of the method. Ronningsen et al. [6] compared WDT measurements on 17 crude oil samples measured using microscopy and DSC. The same heating rate of 10 °C per minute was used. In general the measurements made using microscopy were higher indicating that the microscopy method is more sensitive when compared to DSC. Precise identification of the WDT in a real fluid is challenging as it is necessary to detect small amounts of the heaviest components that have formed wax as they are re-dissolved.

When wax formation is likely to be a flow assurance problem then there are a variety of options available. The temperature can be controlled by insulation or heating such that it does not become low enough for the wax to become problematic. In pipelines wax deposits can be removed periodically by cutting, pigging or treatment with hot oil. Another commonly used option is to add chemicals that can reduce the tendency of wax crystals to adhere to surfaces and to form matrices leading to potential gelling of the oil [23]. There are a number of chemistries that can be used such as ethylene vinyl acetate copolymers, vinyl acetate olefin copolymers, alkyl esters of styrene maleic anhydride colpolymers, alkylesters of unsaturated carboxylic acids, polyalkylacrylates, alkyl phenols and alpha olefin copolymers. Factors that can influence the performance of the additive include the polymer backbone, the length of the pendant chains, the polymer molecular weight and the dose rate. Optimising the performance of the additive is clearly important. Experimental measurements such as the ASTM D97-96A standard pour point test, cold finger, viscosity and flow-loop tests are used to compare inhibitor performance. ASTM D97-96A is a well-established and simple test, however the results can be quite scattered and as there is no indication of the wax adhesion tendency it may not be able to distinguish the best inhibitor or dose rate. Cold finger and flow-loop tests can require significant volumes of oil for extended testing. Ultimately it is better to have the capability of testing live oil samples as this can help in optimising the dose rate to be applied in the field.

Since Sauerbrey (1959) [24] proposed the use of quartz oscillators as microbalances a multitude of applications have evolved. The capability to measure very small amounts, nanogram range, of solids adhering to the surface of a piezoelectric quartz crystal through monitoring changes in resonant frequency (RF) makes the quartz crystal microbalance (QCM) a very useful analytical tool. Initial uses mainly focused on applications such as thin film deposition monitoring (Stockbridge 1966) [26]. The use of QCM's immersed in fluids was described by Nomura et al (1980) [27]. Kanazawa and Gordon (1985) [28] linked changes in QCM RF to the density and viscosity of the contacting liquid. Research at Heriot-Watt University (HWU) into uses of QCM in the oil industry started in 1995. The initial work was supported by EPSRC [28] and was aimed at evaluating the applicability of oscillating quartz crystal in measuring fluid properties in laboratory or downhole. In this work the use of QCM was demonstrated for saturation pressure, hydrate dissociation point, scale and wax measurements. The work resulted in patents for saturation point Burgass et al. [30] and hydrate dissociation point Burgass et al. [31] measurements. Spates et al. (1995) [32] patented the use of QCM technology for measurement of cloud point. This work clearly showed that for a transparent fluid the cloud point, as measured by a marked reduction in RF as a result of wax solids adhering to the QCM surface on cooling, closely matched that observed by visual means. The QCM was shown to be more sensitive than visual observation as it responded to very small amounts of solids not visible without a microscope.

This chapter describes the development of equipment and methods aimed at making accurate measurements of WAT and WDT at both ambient and high pressure, assessing wax adhesion tendency at pressure with variable temperature gradients and evaluating inhibitors at both ambient and high pressure conditions. In **Chapter 3** case studies are presented using the developed equipment and methods.

2.2. QCM background

The QCM is comprised of an AT cut disc of quartz with gold electrodes bonded to its surface, a schematic is shown in Figure 2.1 below. AT cut is the name given to a specific cut developed in 1934. Due to a number of attributes such as low sensitivity to temperature changes it is the most commonly used cut for QCM [33]. The QCM being made of a piezoelectric material will deform when a voltage is applied across it. Using an alternating electric field the QCM can be made to oscillate. At the resonant frequency (RF) of the QCM the electrical properties will change. The RF can thus be detected by measuring the

conductance over a range of RF values and finding the peak conductance. An example plot is shown in Figure 2.2. If the mass of the QCM changes due to solids adhering to its surface then the RF will reduce. The change in RF can be related to the change in mass using the Sauerbrey equation [24] as shown below (Equation 2.1). This equation can only be used in air when the following conditions are met: the deposited mass must be rigid, the deposited mass must be distributed evenly and the frequency change $\Delta f / f <$ 0.05. In the work presented in this thesis on wax and asphaltenes the QCM is being used, submersed in non-conductive liquid. In liquids the resonant frequency will be reduced as a result of changes in viscosity and density of the surrounding medium, according to Equation 2.2. In both the cases of wax and asphaltene deposition, due to the nature of the solids deposits i.e. varying degrees of viscoelasticity, uncertainties regarding parameters such as density and evenness of deposits, it is difficult to be exact regarding the amount of solids adhering. The main point is that by measuring small changes in RF, very small amounts in the nanogram range, can be detected.

$$\Delta f = -\frac{2f_0^2}{A\sqrt{\rho_q \mu_q}}\Delta m \qquad \text{Equation 2.1.}$$

f_0 – RF (Hz)

Δf – Frequency change (Hz)

Δm – Mass change (g)

A – Piezoelectrically active crystal area (Area between electrodes, cm^2)

ρ_q – Density of quartz (ρ_q = 2.648 g/cm^3)

μ_q – Shear modulus of quartz for AT-cut crystal (μ_q = 2.947 x 10^{11} $g/cm.s^2$)

$$\Delta f = -\, f_0^{3/2}(\eta_l \rho_l / \pi \rho_q \mu_q)^{1/2} \qquad \text{Equation 2.2.}$$

where ρ_l is the density of the liquid and η_l is the viscosity of the liquid [27].

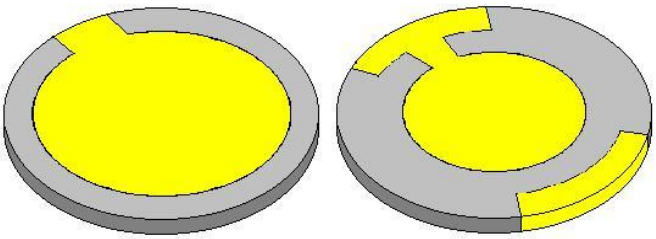

Figure 2.1. Schematic of QCM surfaces with gold plates.

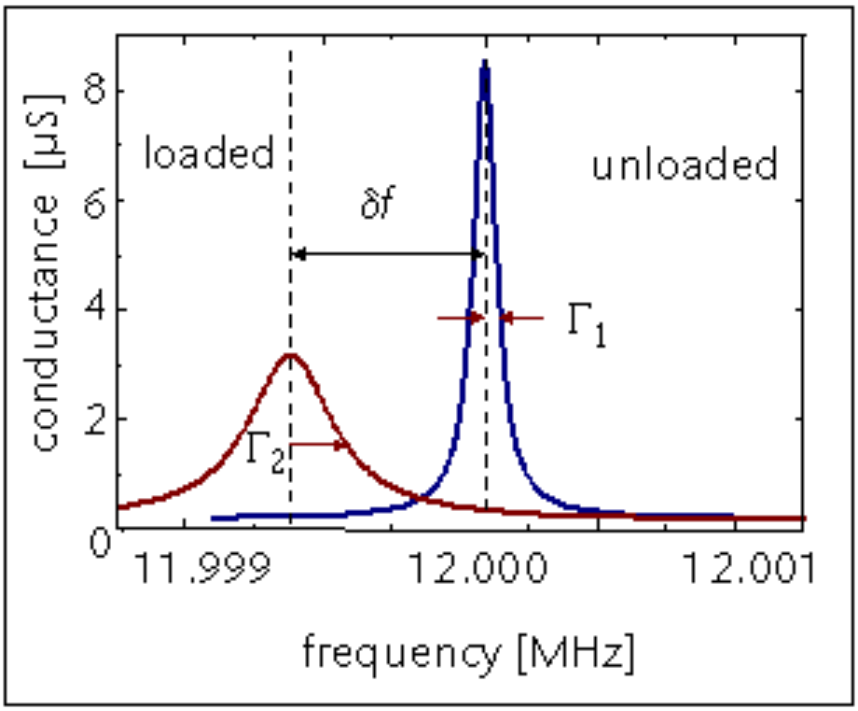

Figure 2.2. Plot showing determination of RF from measurements of conductance at a range of frequencies.

2.3. Measurement of QCM electrical properties

The QCM mechanical model can be represented by different equivalent electrical models. A simple way is an RLC circuit as shown in Figure 2.3 below. R1 represents the energy dissipated during oscillation, C1 represents the energy stored during oscillation, and L1 represents the inertial component related to the displaced mass. At the RF the impedance of the circuit is at a minimum and is equal in magnitude to R1. The electrodes bonded to the QCM surface introduce an additional capacitance (C0) in parallel with the series RLC as shown in Figure 2.4. This circuit is called the Butterworth – van Dyke (BvD) model. The

BvD model has two resonant frequencies, the series resonant frequency, f_s (as in the original RLC circuit) and the parallel RF, f_p. The impedance spectrum for the BvD model shows a minimum at f_s and a maximum at f_p. In this work a Hewlett Packard 4194A Impedance/Gain-Phase Analyzer was used to measure the QCM electrical properties. The analyzer cancels out C0 and only measures the fs. Most equipment used to measure QCM RF manually cancels out C_0, and only reports the series resonant frequency, f_s since f_s ~= f_0 and f_s is obviously dependent upon L1.

Both the RF and the conductance at RF, equal to the inverse of resistance, were recorded in the test reported in this thesis. Viscous coupling of the liquid surrounding the QCM results both in a decrease in the series RF but also in damping of the resonant oscillation. The viscous loss is manifested as an increase in series resonance resistance, hence reduction in conductance, of the QCM. Thus conductance serves as an independent measure of viscous loading by the medium at the crystal's surface. This is particularly useful when making measurements in cases where the solids formed do not adhere strongly to the QCM surface, such as in the case of macro crystalline wax or gas hydrates. In these cases there may not be a very significant change in RF but due to changes in the fluid viscosity there will be significant changes in the conductance.

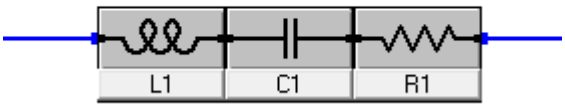

Figure 2.3. RLC circuit.

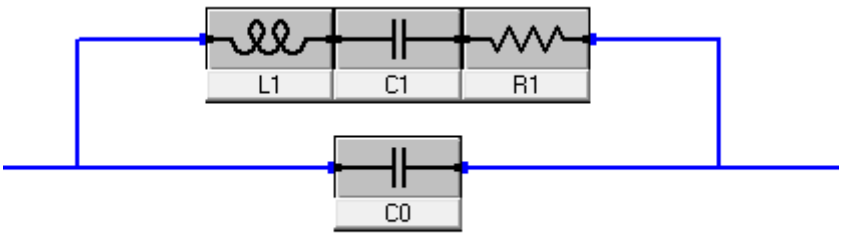

Figure 2.4. Butterworth-van Dyke equivalent circuit model.

2.4. Tests with synthetic fluids

In order to show that the QCM could be used to make accurate wax measurements it was decided to repeat some solubility measurements for hexatriacontane in heptane that have been

reported in literature by three different authors [2, 3, 32]. The agreement between the measurements is good and they were all carried out using visual means, either using slow constant rate heating or temperature cycling. Following this, measurements were made with further binary mixtures and a quaternary mixture of alkanes.

2.4.1. Experimental equipment and methods

For tests at ambient conditions the experimental set up is comprised of a 15 ml glass tube with a QCM suspended inside as shown in Figure 2.5. The tube is held in a temperature controlled bath. The temperature of the bath is measured using a platinum resistance thermocouple PRT, with an accuracy of ±0.1 °C. The electrical properties of the QCM are measured using a Hewlett Packard 4194A Impedance/Gain-Phase Analyzer as described above. The QCM used had resonant frequencies in air of close to either 5 or 6 MHz. It was found that light abrasion of the surface prior to use helped to give clearer indication of the presence of solids. In a typical test, 5 ml of test fluid was placed in the glass tube and the bath temperature was reduced at a constant rate from a starting temperature where no solids were present. The RF and conductance at RF were continuously measured and recorded using a PC running LabView software. Once wax had formed, as seen by changes in RF and conductance at RF, the sample temperature was increased at a constant rate. In order to increase the efficiency of the set up eight tubes were placed in the same bath allowing for multiple samples to be tested simultaneously. All of the alkanes and the toluene were 99+% pure supplied by Sigma Aldrich Ltd.

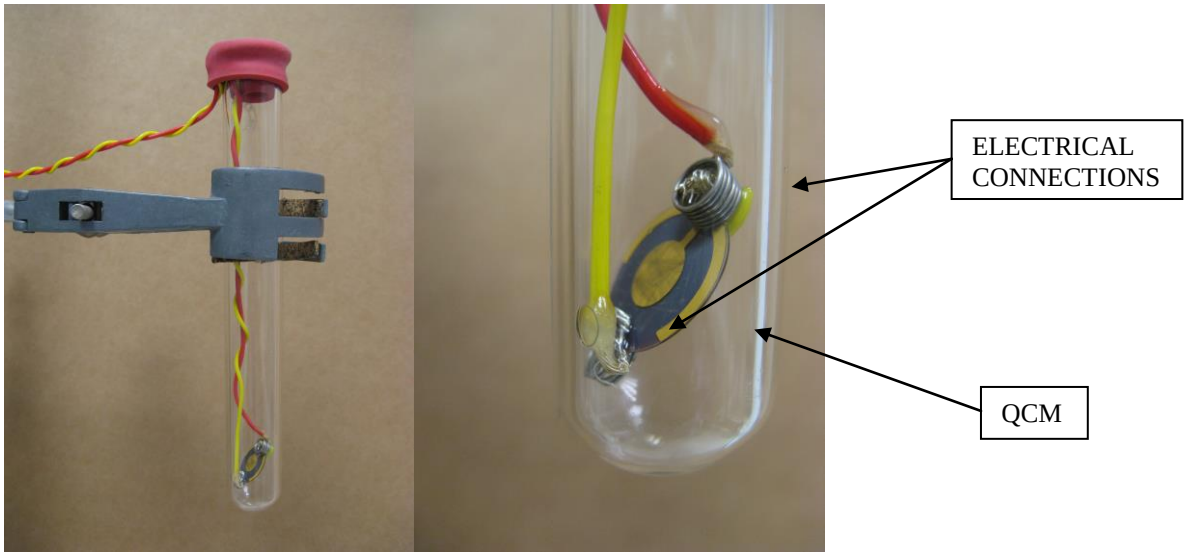

Figure 2.5. Picture of QCM glass tube assembly.

2.4.2. Binary heptane / n-hexatriacontane

Measurements were made using continuous cooling and heating at a rate of 0.3 °C per minute. It was found that there was little significant difference between the temperature at which solids formed on cooling and the temperature at which solids dissolved on heating. The dissolution temperature could be easily identified from sharp changes in plots of both RF and conductance at RF as shown in Figure 2.6. As can be seen from Figure 2.6 the conductance was reduced when solids were present, whereas the RF increased. RF normally reduces when solids adhere to the QCM surface, however in the case of waxes formed from pure alkanes, that tend to form well crystalized or macro crystalline wax the RF was found to increase. The reason for this was most probably due to uneven loading of the QCM. This was tested by depositing small amounts of solids at different points on a QCM surface, the outcome being an increase in RF. In the case of real fluids such as stabilised oil and condensate samples the wax formed tends to be microcrystalline and the loading even, resulting in reductions in both RF and conductance. In high viscosity oils measuring WAT/WDT can be difficult due to the fact that solids cannot easily move to, and adhere to the QCM surface. In these cases the best approach is to measure WAT and WDT for samples of oil diluted with n-heptane. The WAT/WDT for the oil can be determined by extrapolation from the values for the diluted samples to the value obtained with no added n-heptane.

The experimental solubility measurements for n-hexatriacontane in heptane from this work are presented in Table 2.1 and compared with literature data in Figure 2.7 below. Also included in Figure 2.7 is the predicted wax phase boundary for the binary mixture made using the Heriot-Watt Wax model, HWWAX, details of which are published by Ji et al. [33]. As can be seen from Figure 2.7 the agreement between the measured solubility data in this work using QCM, and the HWWAX predictions is good, thus validating the measurement technique. As eight or more samples can be run simultaneously with relatively small amounts of sample and no requirement for visual observation this is a good option for generating experimental data.

Table 2.1. Experimental measurements of the solubility of n-hexatriacontane in heptane.

Temperature °C ±0.3	Weight% $C_{36}H_{74}$
33.5	2.00
35.4	2.98
37.4	4.02
41.8	7.71
43.8	10.07
46.3	11.95
47.0	15.00
52.0	25.00
52.5	28.91
54.3	35.00
57.6	45.00
60.5	53.90

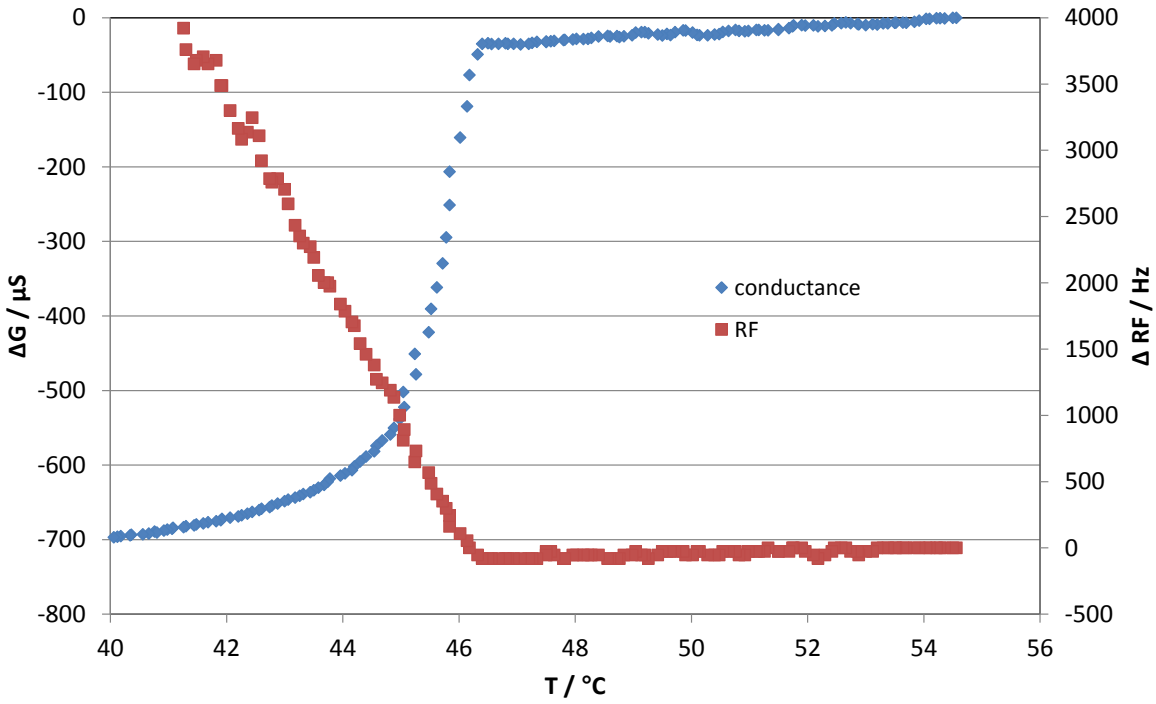

Figure 2.6. Example of changes in RF and conductance (G) at RF measured during test with binary heptane / n-hexatriacontane. Temperature increased at a rate of 0.3 °C per minute.

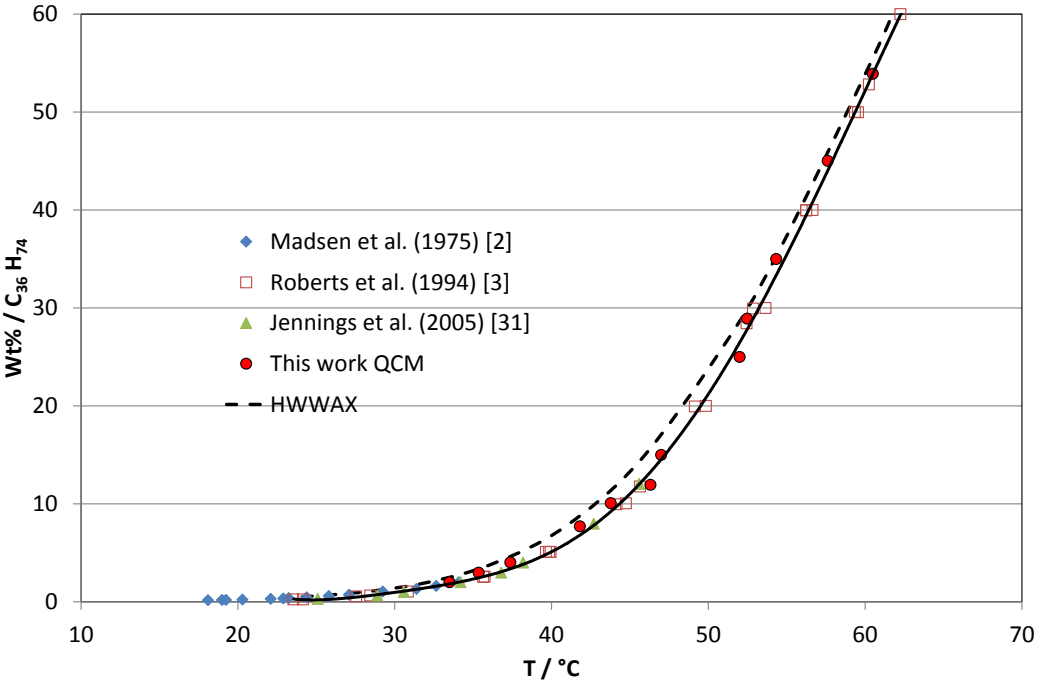

Figure 2.7. Experimental measurements for the solubility of n-hexatriacontane in heptane from this work and literature. Solid line fitted through data of Roberts et al. (1994) [3].

2.4.3. *Binary toluene / n-hexatriacontane*

Measurements were made for the solubility of n-hexatriacontane in toluene. As with the measurements with n-hexatriacontane / heptane, there was little difference found between the temperature at which solids formed on cooling and dissolved on heating. An example of the changes of conductance with cooling and heating are shown in Figure 2.8. As can be seen the temperature at which solids form and dissolve can be easily identified by a sharp change in the slope of the plot of conductance versus temperature. The solubility measurements are presented in Table 2.2 and plotted in Figure 2.9.

Table 2.2. Experimental measurements of the solubility of n-hexatriacontane in toluene.

Temperature °C ±0.3	Weight% $C_{36}H_{74}$
28.5	2.00
34.0	3.90
35.8	4.85
41.3	10.00
44.4	15.13
46.4	20.16
50.2	29.51
53.3	40.28
55.2	45.68
59.3	59.13

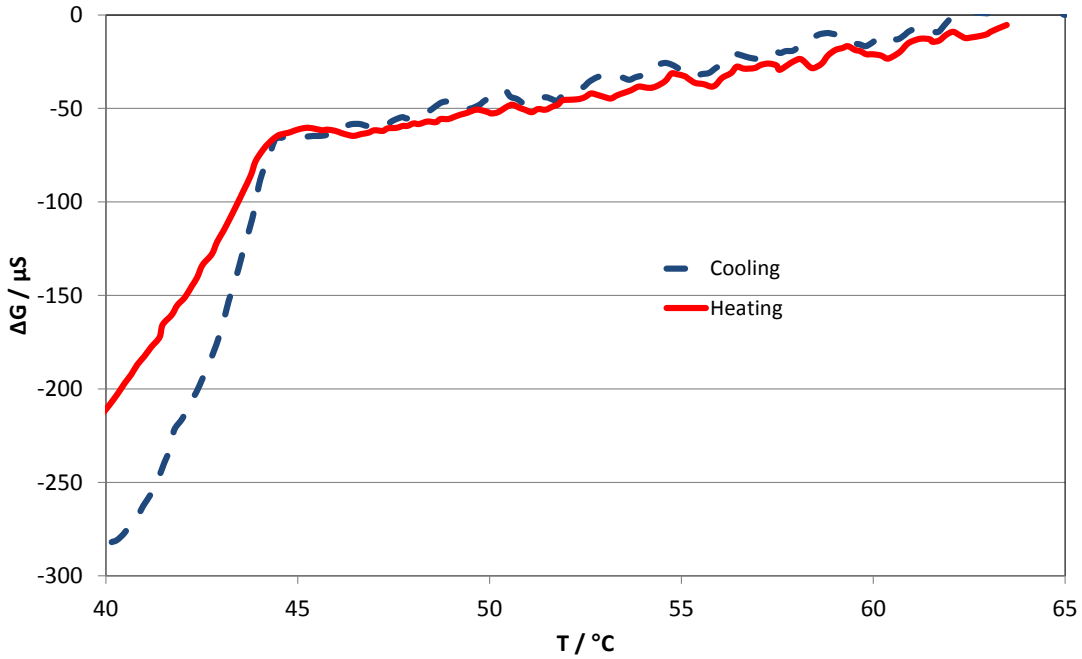

Figure 2.8. Changes in conductance (G) recorded on cooling and heating at a constant rate of 0.3 °C per minute in test with hexatriacontane and toluene.

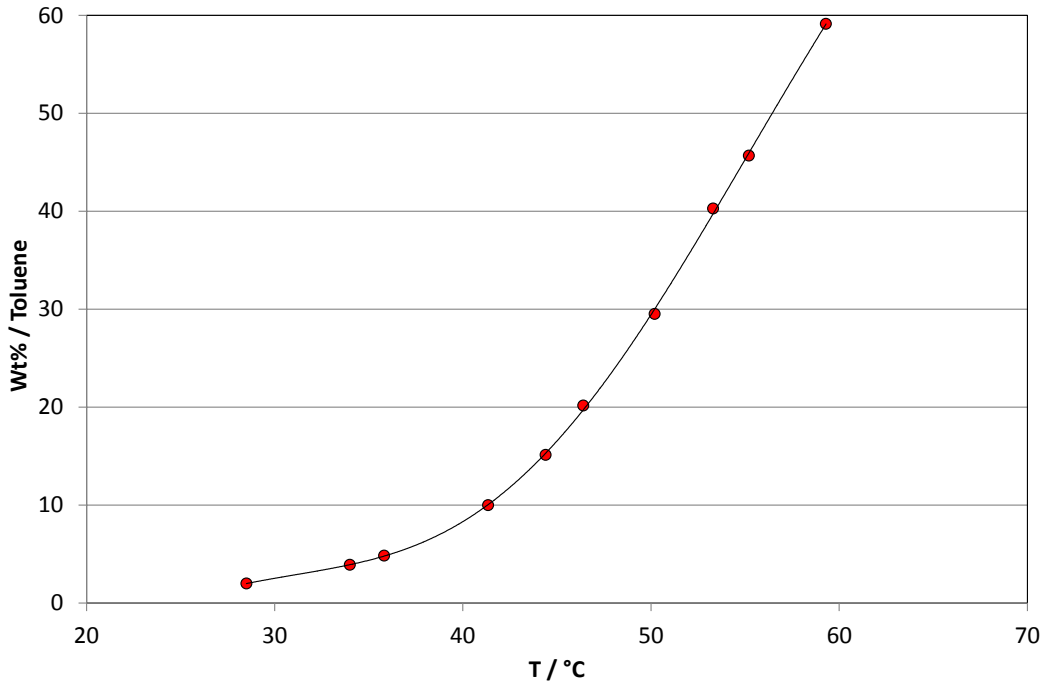

Figure 2.9. Experimental measurements for the solubility of n-hexatriacontane in toluene.

2.4.4. Binary and quaternary mixtures of alkanes

One series of tests was conducted with the quaternary mixture of normal alkanes as presented in Table 2.3 and with binary mixtures of C_{50}/C_{12}, C_{40}/C_{12}, and C_{28}/C_{12} using the same mass ratio between the C_{12} and the heavier component as that present in the quaternary mixture. In each test the sample temperature was cooled from 50 ºC to –3 ºC at a rate of

0.15 ºC per minute and then heated back to 50 ºC at the same rate. WAT and WDT were also measured visually. The conductance, measured at resonant frequency, was used to indicate the WAT and WDT. This parameter was chosen because it is easier to see WAT and WDT when plotted against temperature in cases where only small amounts of wax are formed. The data for the test with the quaternary mixture is presented in Figure 2.10 and the data for the three binary mixtures is shown in Figures 2.11 (C_{50}/C_{12}), 2.12 (C_{40}/C_{12}) and 2.13 (C_{28}/C_{12}). The WAT and WDT for each test is shown on the relevant plot, in all cases the visual measurement was in agreement with the QCM result.

There are some differences that can be noted between the binary mixtures. In the case of Figure 2.11 (C_{50}/C_{12}) the change in conductance on wax formation is not very marked, possibly due to the relatively small amount of the heavy component present. The test with C_{40}/C_{12} (Figure 2.12) shows the largest difference between the WAT and the WDT. In the tests with C_{50}/C_{12} and C_{40}/C_{12} the wax crystals were quite small whereas in the test with C_{28}/C_{12} the crystals were large and flaky. The conductance plot for the test with C_{28}/C_{12} (Figure 2.13) showed an increase in conductance after the initial formation. This may be related to the type of crystals formed. Initially on rapid crystal formation, microcrystalline wax forms and after some time the form of the crystals changes to macrocrystalline. Previous work indicated that the type of crystal formed is related to the amount of response, in terms of reduction in RF, measured by the QCM which is related to how strong the bond is between the solids and the QCM and how evenly distributed are the solids. If needle type crystals are formed there is often an increase in RF seen from the QCM, as discussed previously possibly associated with uneven distribution of solids. The greatest reduction in RF is seen with microcrystalline wax as mainly seen in stabilised crude and condensate samples. Microcrystalline wax has long been known to have excellent adhesive qualities and has previously been given the accolade of glue of the month *www.thistothat.com/gom/2000.08.shtml.*

The cooling data for the three binary mixtures and the quaternary mixture is plotted together in Figure 2.14 and that for the heating is plotted in Figure 2.15. As can be seen from Figure 2.14 the WAT of the mixture is at a temperature close to the WAT of the C_{50}/C_{12} mixture. The reduction of conductance is more marked for the mixture. It was noted that the size of the wax crystals formed in the mixture at this temperature were smaller, hence more microcrystalline than those formed in the C_{50}/C_{12}. This observation may explain the

difference between the two responses. The cooling data for the mixture shows a second change in slope at around the same temperature as the WAT for the binary C_{40}/C_{12} and C_{28}/C_{12} mixtures.

As can be seen from the heating data shown in Figure 2.15 there was not such marked changes in slope of the conductance versus temperature plot as was seen for the cooling data shown in Figure 2.14.

The main point of this work was to demonstrate that the WAT and WDT measured using a QCM corresponded to that measured visually. Other methods such as DSC, CPM, FP and FTIR do not show such a match as shown in literature (Monger-McClure et al. (1999) [8]. In addition in work with DSC conducted in this laboratory the visual and DSC data did not match for WAT and WDT. It is reasonable to assume that the QCM method, having been proven to be reliable in the case of clear mixtures of alkanes, will also be reliable for opaque fluids where no visual observations are possible. A second point from this work is that the QCM shows the WAT and WDT for the different n-alkanes in the studied mixture. This may be useful in the development and validation of mathematical wax models such as HWWAX.

Table 2.3. Composition of synthetic fluid used in WAT/WDT QCM tests.

Component	Mass%
C_{50}	0.020
C_{40}	0.038
C_{28}	2.001
C_{12}	97.941

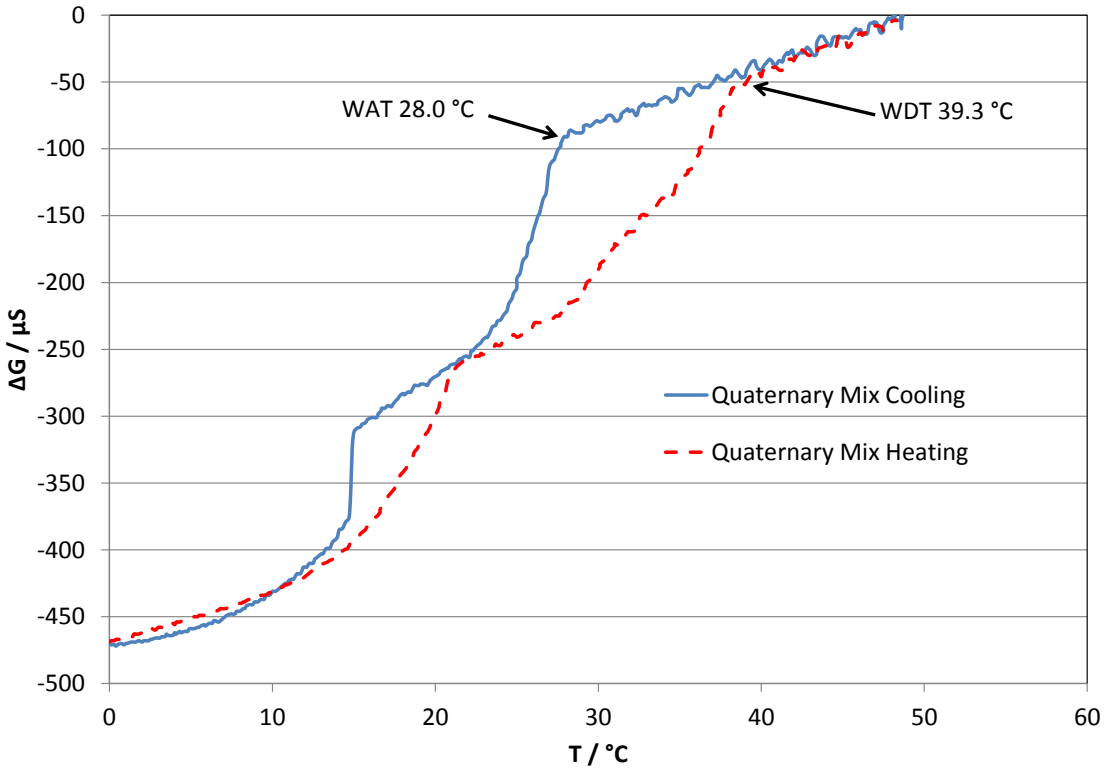

Figure 2.10. Plot of change in conductance (G) with temperature measured on cooling and heating quaternary mixture of n-alkanes (Table 2.3). Rate of temperature change 0.15 ºC per minute.

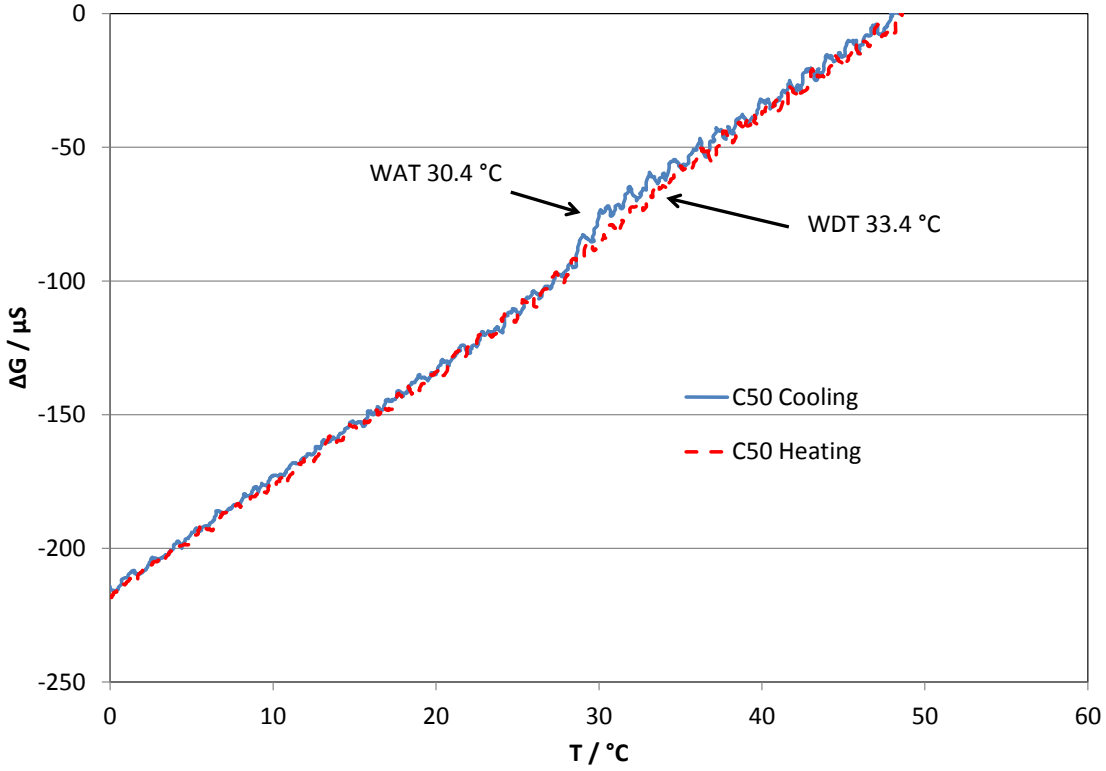

Figure 2.11. Plot of change in conductance (G) with temperature measured on cooling and heating binary C_{50}/C_{12} mixture of n-alkanes. Rate of temperature change 0.15 ºC per minute.

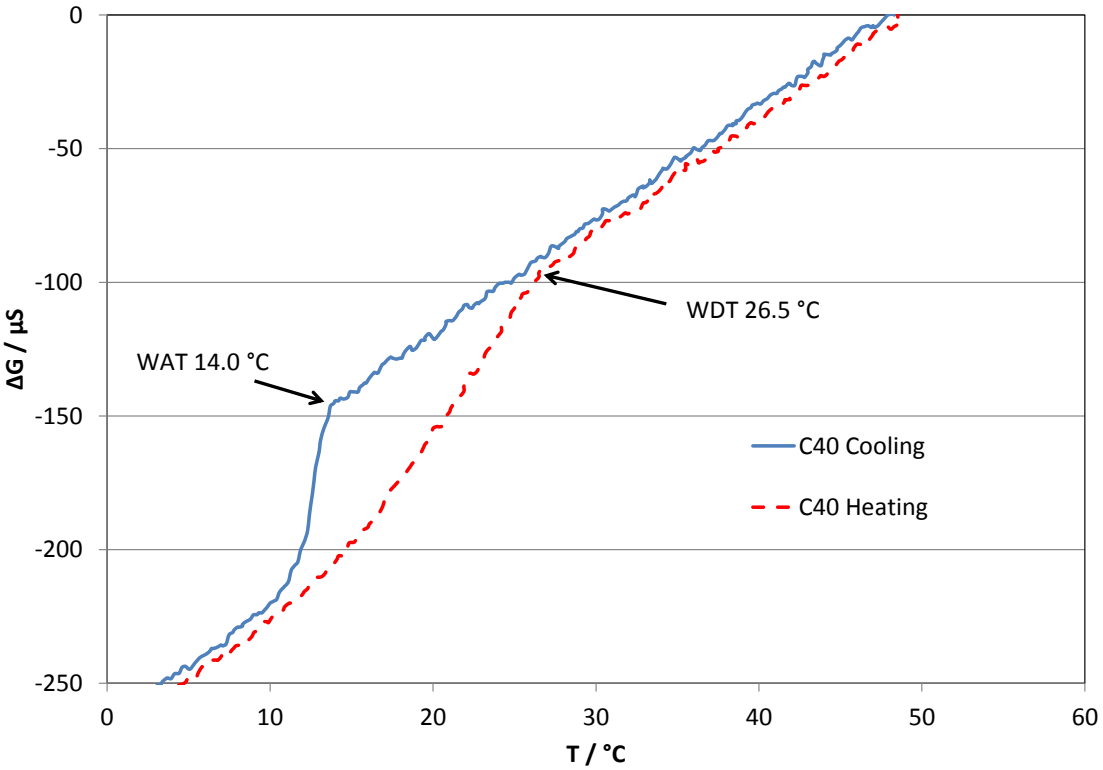

Figure 2.12. Plot of change in conductance (G) with temperature measured on cooling and heating binary C_{40}/C_{12} mixture of n-alkanes. Rate of temperature change 0.15 °C per minute.

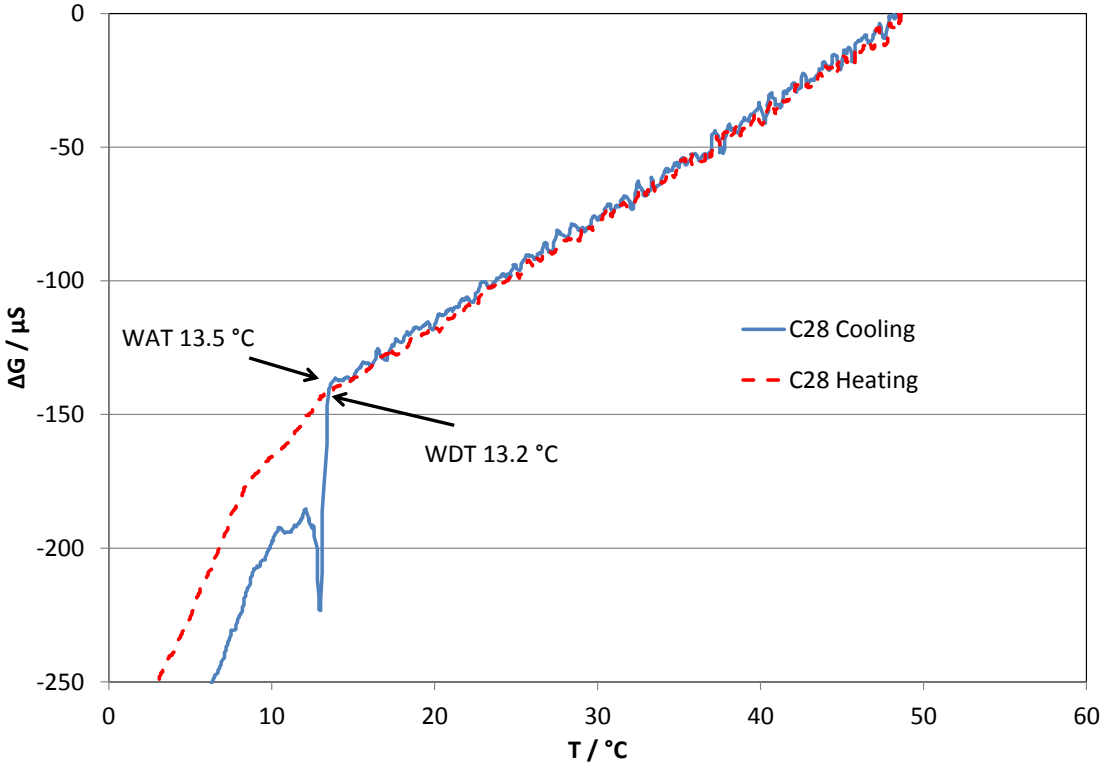

Figure 2.13. Plot of change in conductance (G) with temperature measured on cooling and heating binary C_{28}/C_{12} mixture of n-alkanes. Rate of temperature change 0.15 °C per minute.

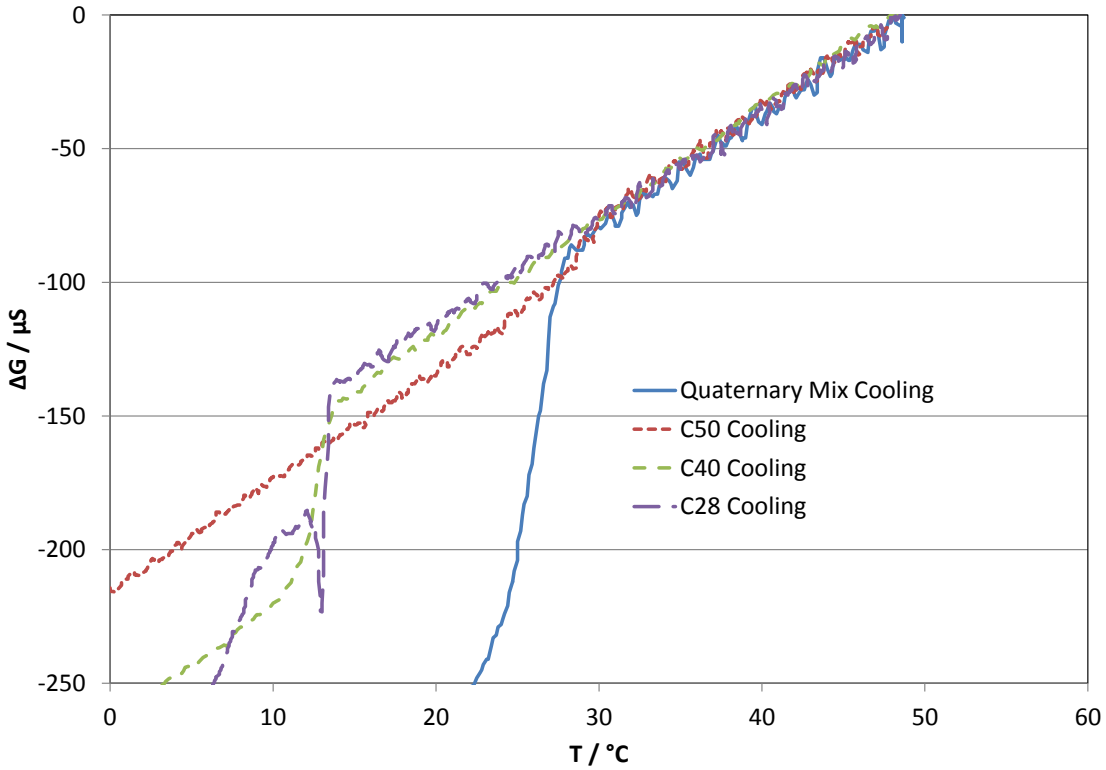

Figure 2.14. Plot of change in conductance (G) with temperature measured on cooling quaternary mixture of n-alkanes (Table 2.3) and the three binary mixtures C_{50}/C_{12}, C_{40}/C_{12} and C_{28}/C_{12}. Rate of temperature change 0.15 ºC per minute.

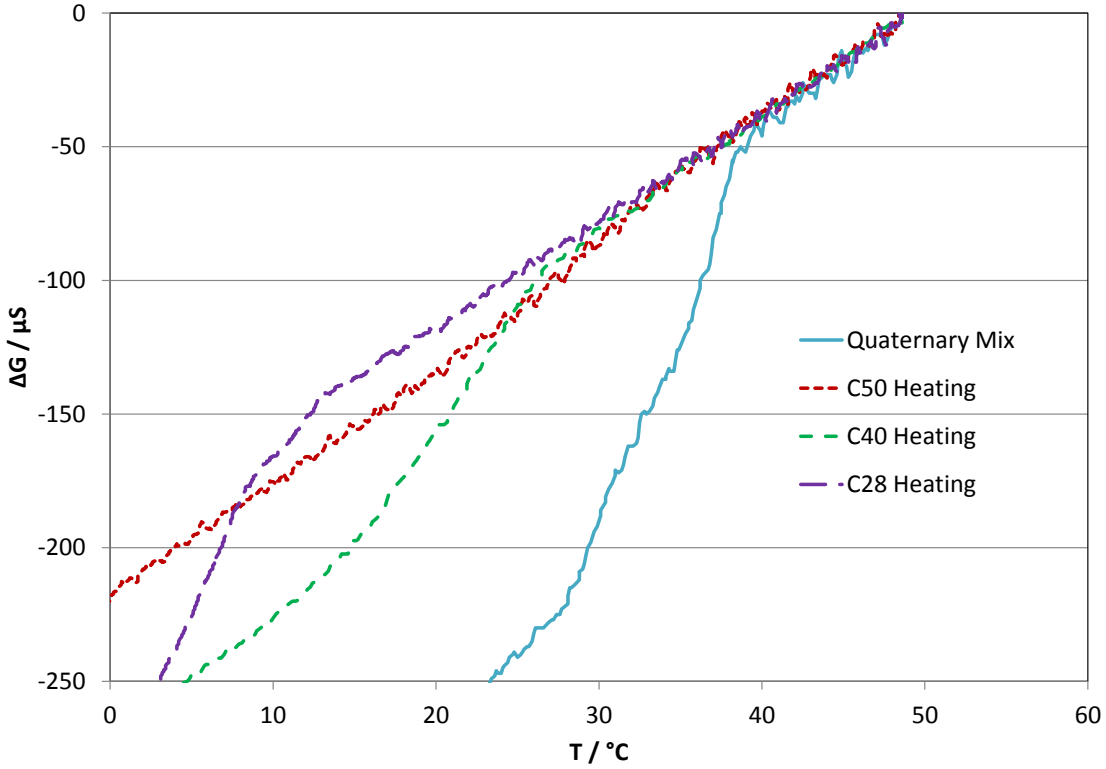

Figure 2.15. Plot of change in conductance (G) with temperature measured on heating quaternary mixture of n-alkanes (Table 10.3) and the three binary mixtures C_{50}/C_{12}, C_{40}/C_{12} and C_{28}/C_{12}. Rate of temperature change 0.15 ºC per minute.

2.5. WAT and WDT measurements at pressure

It is necessary to make WAT and WDT measurements for fluids under pressure in order to give data relevant to pipeline conditions. It is known that if there is no change in the fluid composition then increasing the pressure will increase the wax dissolution temperature [34]. In the case of a live oil, as the pressure is increased to the saturation pressure the composition of the liquid hydrocarbon will change as more of the light components are dissolved in the liquid. This will lead to a reduction in the wax dissolution temperature. Above the bubble point pressure where everything is liquid the composition will be constant as pressure increases. The aim of this work was to show that measurements could be made using the QCM at different pressures with stabilised oil and with a live oil.

The QCM, due to the materials of which it is composed, can be used at a wide range of pressures and temperatures. At Heriot-Watt it has been used to make measurements at pressures up to 3,000 bar and at temperatures up to 180 °C. NASA has been very active in exploiting the potential uses of QCM in space and missile applications, 500 references can be found on the U.S. Federal Science website http://www.science.gov/topicpages/q/quartz+crystal+microbalance.html#. QCM based detectors have been used at temperatures up to 430 °C [35]. The restricting factors are the pressure and temperature ratings of the cell within which the QCM is housed and of the electrical feedthroughs required to monitor RF and conductance of the QCM sensor.

2.5.1. Experimental equipment

A schematic of the experimental rig used for this study is shown in Figure 2.16. The rig is comprised of a windowed equilibrium cell, cryostat, rocking/pivot mechanism, and temperature/pressure recording equipment controlled by a PC.

The equilibrium cell (maximum effective volume of 100 ml) is comprised of a steel cylindrical sample chamber with sapphire windows at each end. The cell is mounted on a pivot frame that allows a rocking motion around a horizontal axis. Rocking of the cell, controlled by a compressed air drive system, provides mixing of sample fluids. For the experiments reported here, the cell was rocked through 180° degrees at a rate of 6 cycles per minute.

The rig has a standard working temperature range of –20 to +110 °C, with a maximum operating pressure of 517 bar. The system temperature is controlled by circulating coolant from a cryostat within a jacket surrounding the cell. The cryostat is capable of maintaining cell temperature stability to within < ±0.1 °C. The cell temperature is monitored by a platinum resistance thermometer (PRT) calibrated at regular intervals using a precision thermometer (reported accuracy of ±0.025 °C for the operating range). The cell temperature can be measured reliably to within ±0.1°C. The cell pressure is monitored by a pressure transducer with an accuracy of ±0.07 bar. Pressure and temperature are monitored and recorded by the PC through RS 232 outputs on the pressure and temperature readouts that are connected to serial ports on the PC. The cryostat is programmable, allowing temperature cycles to be carried out automatically.

A magnifying video camera and light source can be mounted at either end of the cell, allowing still images and/or video footage of contents to be captured during experiments. A QCM can also be mounted in the rig to allow for wax measurements to be conducted using the method described below.

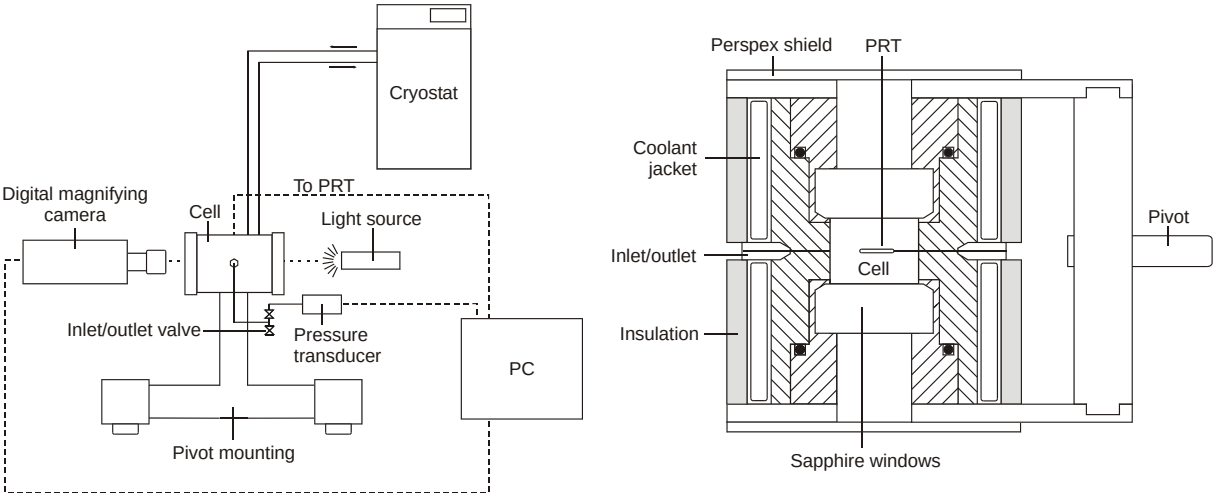

Figure 2.16. Schematic illustration of the visual rig experimental set-up and equilibrium cell (not to scale).

2.5.2. Experimental methods

In these tests WAT and WDT were measured using changes in QCM RF on cooling and heating the test fluids. An example of determination using data recorded during a test with a stabilised condensate sample is shown in Figure 2.17 below. As can be seen the RF reduces slowly as the sample is cooled, due to increases in density and viscosity. There is a sharp

change when wax appears. On heating the point at which the last wax is re-dissolved is less easy to identify precisely. In the test shown in Figure 2.17 the sample was continuously cooled and then heated at a slow rate of 13 °C per hour. In the tests reported in this section the temperature was step-cooled from a temperature above the WDT and then step-heated to find the WDT. The steps were 1 °C and the fluids were left to equilibrate for 0.5 hour at each step.

2.5.3. Test fluids

Tests at atmospheric pressure were conducted with a separator condensate sample with a composition as shown in Table 2.4. A live fluid was prepared by mixing 93.8 mass% (equivalent to 64.2 mole%) of the separator condensate with 6.2 mass% (equivalent to 35.8 mole%) natural gas. The composition of the live fluid is given in Table 2.5.

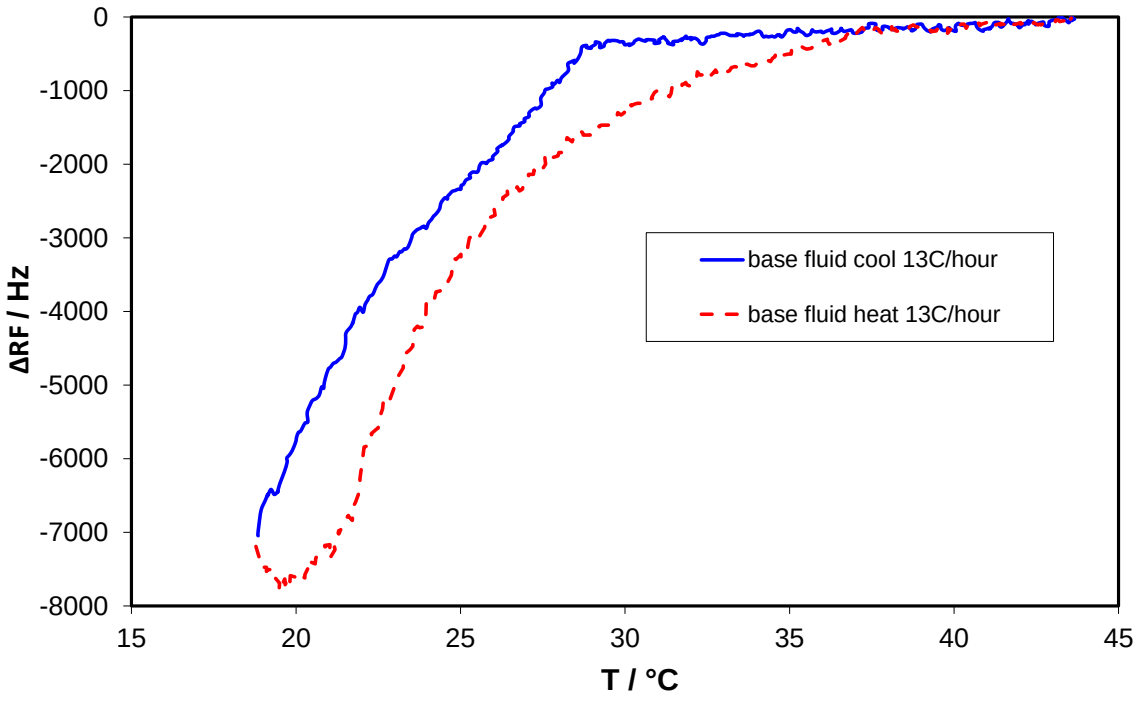

Figure 2.17. Plot showing measurement of WAT and WDT for a separator condensate sample using QCM RF versus temperature.

Table 2.4. Composition of separator condensate.

Component	Mass%	Mole%	Component	Mass%	Mole%
C_3	0.03	0.12	C_{11s}	5.77	6.07
iC_4	0.07	0.18	C_{12s}	4.95	4.75
nC_4	0.32	0.84	C_{13s}	4.58	4.09
iC_5	0.60	1.28	C_{14s}	4.93	4.10
nC_5	1.07	2.29	C_{15s}	4.45	3.39
C_{6s}	3.53	6.13	C_{16s}	3.74	2.69
C_{7s}	7.93	13.32	C_{17s}	3.23	2.18
C_{8s}	10.99	16.5	C_{18s}	3.34	2.10
C_{9s}	8.30	11.06	C_{19s}	2.94	1.76
C_{10s}	6.94	8.19	C_{20s}	22.31	8.98

Table 2.5. Composition of live fluid. Bubble point measured as 101 bar at 15 ºC.

Component	Mass%	Mole%	Component	Mass%	Mole%
CO_2	0.20	0.49	C_{10s}	6.51	5.26
N_2	0.31	1.16	C_{11s}	5.41	3.90
C_1	4.73	31.26	C_{12s}	4.64	3.05
C_2	0.58	2.03	C_{13s}	4.29	2.63
C_3	0.28	0.68	C_{14s}	4.63	2.63
iC_4	0.11	0.20	C_{15s}	4.18	2.18
nC_4	0.37	0.68	C_{16s}	3.51	1.73
iC_5	0.58	0.86	C_{17s}	3.03	1.40
nC_5	1.00	1.47	C_{18s}	3.13	1.35
C_{6s}	3.29	3.94	C_{19s}	2.76	1.13
C_{7s}	7.44	8.55	C_{20+}	20.92	5.76
C_{8s}	10.31	10.59			
C_{9s}	7.78	7.10			

2.5.4. Results

WATs and WDTs for the condensate measured using the QCM at different pressures are detailed in Table 2.6. WATs and WDTs for the live oil are shown in Table 2.7. The experimental data for the stabilised condensate and the live fluid are plotted in Figure 2.18. As can be seen from Figure 2.18, for the stabilised condensate, at all pressures, there is a significant difference between the WAT and WDT, on average 8 °C. The WDT, representing the wax phase boundary for the stabilised condensate shows, as expected a linear increase in temperature as pressure increases. In the case of the live fluid, as with the stabilised condensate there is a similar difference between WAT and WDT, also on average 8 °C. As expected the addition of the light components has the effect of shifting both the WAT and WDT to lower temperatures at each pressure. In addition the temperature shift increases up to the bubble point of the fluid (101 bar at 15 ºC), after which a linear trend of increasing

temperature with pressure is seen. The slope of the temperature/pressure line is steeper for the live fluid when compared to the separator condensate.

The results from these tests clearly show that the QCM can be used to measure accurately both WAT and WDT for hydrocarbon fluids at pressure for both stabilised and live fluids. The WDT data gives the wax phase boundary for the fluid which can be used for validation of thermodynamic models. When conducting tests with semi-transparent condensates it is possible to back up the QCM measurement for formation and dissolution of solids using visual observation. With visual observation there will be a minimum amount of solids that need to be present before a judgement can be made.

Table 2.6. WAT and WDT measured on the condensate (Table 2.4) at different pressures.

Pressure bar ±1	WAT °C ±1	Pressure bar ±1	WDT °C ±1
1	27	1	37
37	29	52	38
39	31	59	39
145	34	154	41
223	35	238	43
352	38	376	46
351	38	376	46

Table 2.7. WAT and WDT measured on live fluid (Table 2.5) at different pressures.

Pressure bar ±1	WAT °C ±1	Pressure bar ±1	WDT °C ±1
2	30	2	38
58	29	34	37
78	29	61	37
91	29	79	37
96	29	132	38
138	30	193	39
219	31	288	40
301	33	364	41

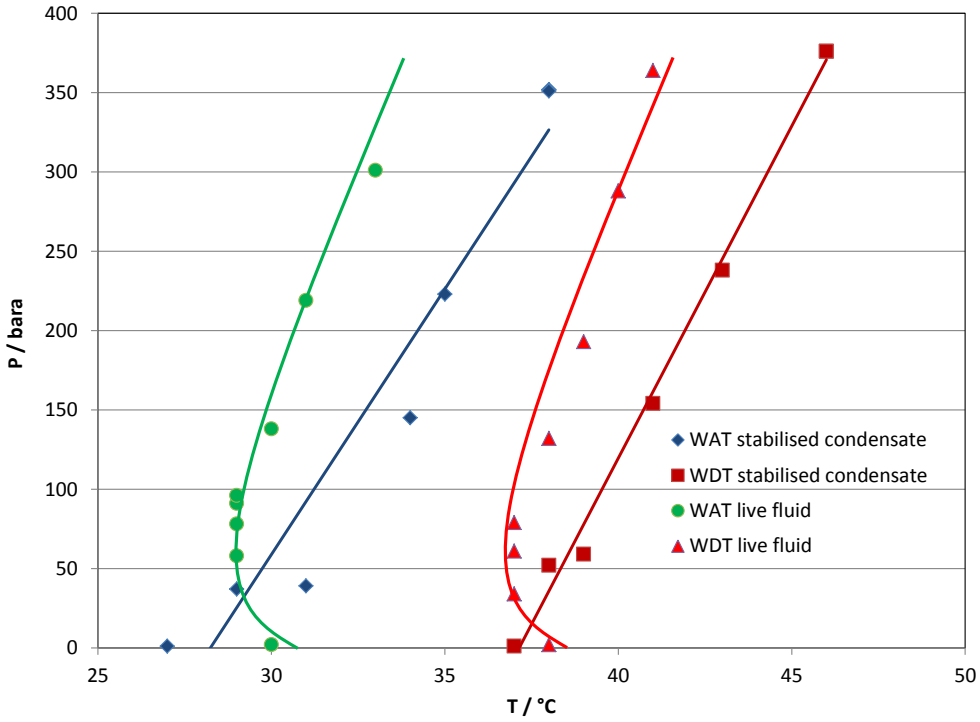

Figure 2.18. WAT and WDT measurements for stabilised condensate (Table 2.4) and live fluid (Table 2.5).

2.6. Temperature controlled QCM set-up

This section describes the development and validation of a set-up which enables the temperature of the QCM to be controlled, independently of the temperature of the bulk oil. This allows for the effect of temperature gradients at pipeline conditions to be investigated with regards to the tendency of wax to adhere to the cold pipeline walls.

2.6.1. Experimental equipment and methods

The concept was to use the capability of the QCM to measure adhesion of wax solids by reduction in RF in a set up similar to that used in cold finger studies. Essentially the oil is contained in a jacketed stirred vessel. A wax probe, which is comprised of a QCM cooled on one side and exposed to the oil on the other, is used to indicate wax deposition over time through measuring reductions in resonant frequency. The initial set up requires 30 ml of sample and can be used with different combinations of probe and bulk oil temperatures. The maximum pressure of the test cell is 100 bara. In each test the probe is lowered into the oil and cooled to a set temperature at which it is held for a set time. The probe is then heated to remove any wax that has been deposited before being cooled to the next set point. A schematic of the set-up is shown in Figure 2.19.

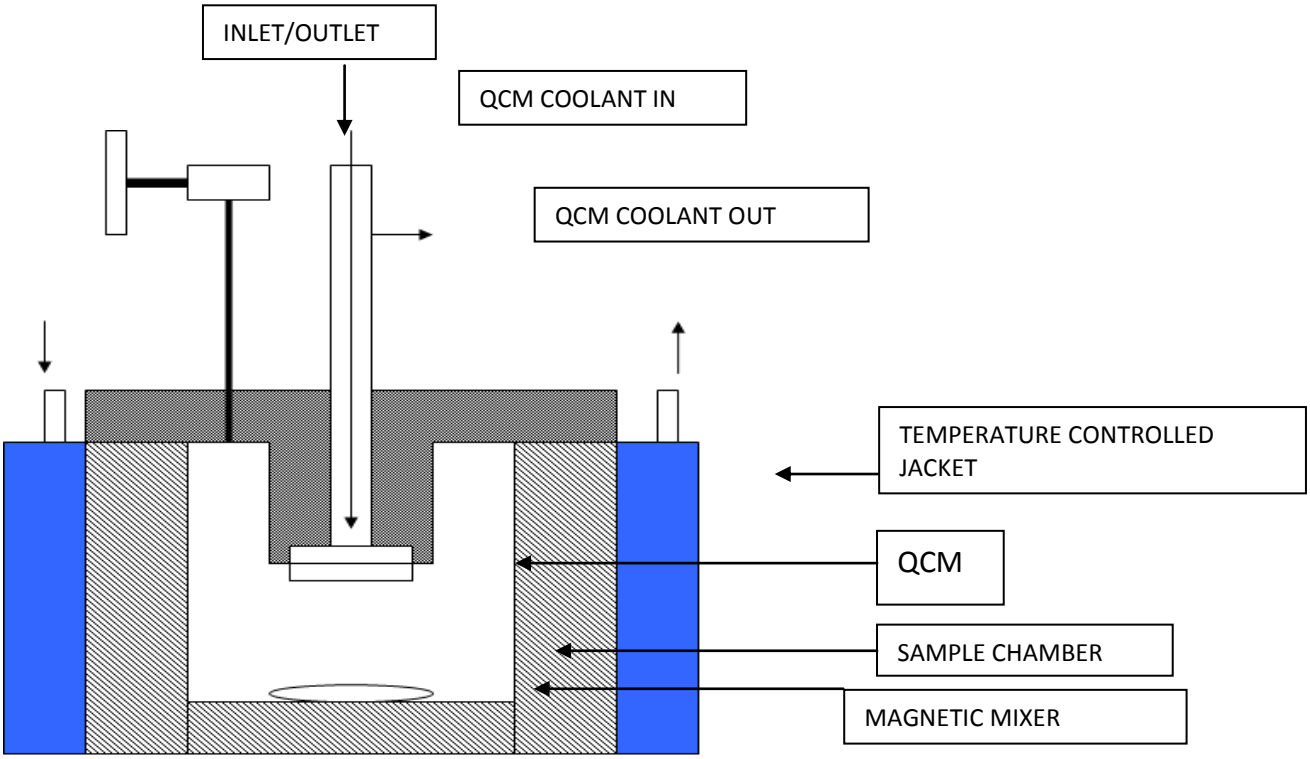

Figure 2.19. Schematic of temperature controlled QCM set-up.

2.6.2. Initial tests at atmospheric pressure

Initial tests were conducted with a stabilised crude oil of unknown composition. An example of data recorded for this oil when held at 40 ºC and different probe temperatures is shown in Figure 2.20. As can be seen from Figure 2.20 there is little wax deposited over time when the probe is at 27.5 ºC, whereas when the probe temperature is reduced to 25 ºC the rate of wax deposition increases significantly. This data coupled with realistic temperature gradients experienced in a pipeline may give an indication of the potential severity of problems caused by wax build up on pipeline walls.

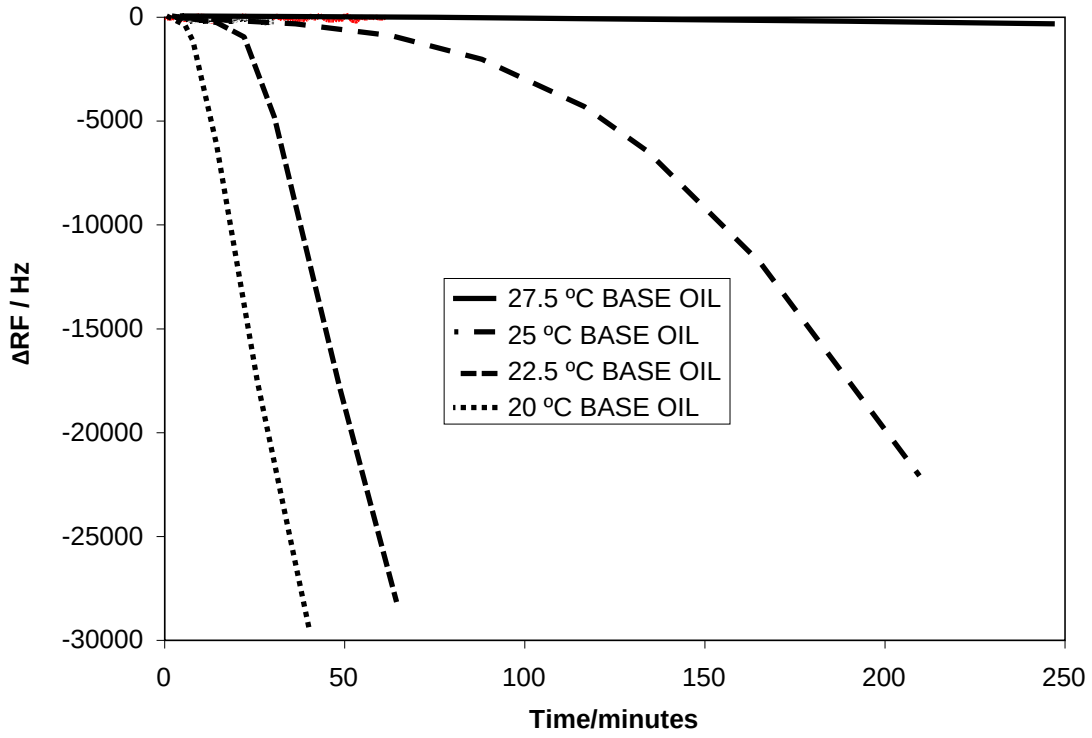

Figure 2.20. Example of data recorded for test with stabilised crude oil held at 40 ºC and different wax probe temperatures.

Further tests were conducted with an oil with a composition as shown in Table 2.8 with a measured WDT of 47 ºC. Tests were conducted with seven different oil temperatures, 50, 45, 40, 35, 30, 25 and 20 ºC. The results for each oil temperature and the four different QCM temperatures are plotted in Figures 2.21 through 2.27. In each plot the change in RF is the change in RF from the frequency recorded when the QCM had reached the set point temperature. As discussed previously the change in RF gives an indication of the amount of wax building up on the QCM surface.

The data for the first test with an oil temperature of 50 ºC (Figure 2.21) shows that with QCM temperatures of 45, 40 and 35 ºC there was little wax build up with time. With a QCM temperature of 30 ºC there is some wax adhering to the QCM. With an oil temperature of 50 ºC there is not expected to be wax present in the bulk oil as this temperature is above the WDT of the oil (47 ºC).

As seen in Figure 2.22 when the QCM temperature was at 45 ºC the wax build up was not significant at temperatures of 40 and 35 ºC. Wax build up was significant at temperatures of 30 and 25 ºC, being more rapid at 25 ºC compared to 30 ºC as might be expected. The results

for the test with an oil temperature of 40 ºC (Figure 2.23) are similar to the test at 45 ºC with little significant build up over time when the differential temperature between oil and QCM was 5 and 10 ºC and significant at 15 and 20 ºC. The most rapid build-up was seen at a differential temperature of 20 ºC. At oil temperatures of both 45 ºC and 40 ºC there would be expected to be wax solids present in the bulk oil.

In the test with an oil temperature of 35 ºC the amount of wax in the oil is expected to be significantly increased as the temperature is further inside the wax stability zone. The results, as shown in Figure 2.24, indicate significant wax build up at all QCM temperatures. The larger the difference in temperature between the oil and the QCM the more rapid was the build-up.

In the next test with an oil temperature of 30 ºC (Figure 2.25) the pattern is the same as for the previous two tests with regards to the QCM temperatures 5 and 10 ºC below the oil temperature. However it is different for QCM temperatures 15 and 20 ºC below the oil temperature. With the QCM 15 ºC below the oil temperature there is no increase in the rate of wax build up when compared to the results for the QCM 10 ºC below the oil temperature. With the QCM 20 ºC below the oil temperature the trend is reversed in that the amount of wax adhering to the QCM with time is less when compared with the results for the QCM at 10 and 15 ºC below the oil temperature. In the test with an oil temperature of 25 ºC (Figure 2.26) the trend is again different. The amount of wax adhering to the QCM increases for QCM temperatures between 5 and 10 ºC below the oil temperature, however it decreases for 15 and 20 ºC below the oil temperature. In the final test of this set with an oil temperature of 20 ºC (Figure 2.27) there is little significant wax build up at any of the four QCM temperatures.

Overall this initial set of results indicate that for this oil at oil temperatures of 50, 45, 40 and 35 ºC the trend is for more wax build up with time the greater the difference between the oil and QCM temperatures. At oil temperatures of 30 and 25 ºC the trend is different with the higher differential temperatures appearing to reduce the amount of wax build up. The final test, with the oil at 20 ºC, indicates that there was no significant build up at any of the four QCM temperatures.

The tests indicate that when there is little or no differential temperature between the QCM and the oil, the solids do not adhere to or build up on the QCM surface in significant quantities. When there is a significant differential then solids adhere to or build up on the QCM surface. The solids may be from two sources, new solids forming in the oil near the cold QCM surface and solids moving from the bulk oil to the QCM surface and adhering there, potentially adhering to other microcrystalline wax. The test with the oil temperature of 50 ºC shows that new solids are forming and adhering to the cold surface, as at this temperature there is not expected to be any solids in the bulk oil. The reasons for the change in trend for less wax build up with increasing differential temperature at oil temperatures of 30 and 25 ºC and the lack of wax build up for any of the QCM temperatures with an oil temperature of 20 ºC is interesting. It may be that wax solids are less free to move and adhere to the cold QCM surface due to the increasing viscosity of the oil. Hamouda et al. [36] concluded that molecular diffusion was the predominant mechanism when considering wax deposition on surfaces. In addition they proposed an empirical relation for estimating the diffusion coefficient (D). D is equal to a constant B divided by the viscosity. This clearly entails that at higher viscosities deposition is reduced. In addition the larger amount of wax solids present may mean that the solids present and any new solids formed are more likely to adhere to each other and not to the QCM surface. One other explanation is that a layer of gelled oil may form over the QCM surface, preventing further wax adhering. One point of relevance is that in previous research the idea of measuring pour point using a QCM was investigated. It was found that there was no clear change in RF when the oil gelled, becoming essentially a highly viscous medium. This suggests that the RF is not very sensitive to viscosity changes. It may be possible in further work to identify viscosity ranges at which different phenomena are observed in different oils.

Reviewing the results from the tests at atmospheric pressure shows that the conclusions with regard to wax deposition tendencies are in agreement with conclusions found in literature Sanjay et al. (1995) [37]. The work with inhibitors, described below, also shows that the QCM results are in keeping with results from a standard cold finger set-up.

Table 2.8. Composition of crude oil used in wax build up tests.

Component	Mole%	Component	Mole%	Component	Mole%
nC_{10}	6.27	nC_{21}	4.17	nC_{32}	0.79
nC_{11}	4.43	nC_{22}	3.32	nC_{33}	0.78
nC_{12}	7.51	nC_{23}	3.35	nC_{34}	0.49
nC_{13}	6.45	nC_{24}	4.33	nC_{35}	0.34
nC_{14}	6.77	nC_{25}	4.56	nC_{36}	0.22
nC_{15}	6.40	nC_{26}	2.82	nC_{37}	0.22
nC_{16}	5.24	nC_{27}	2.44	nC_{38}	0.20
nC_{17}	6.36	nC_{28}	3.30	nC_{39}	0.10
nC_{18}	3.55	NC_{29}	2.58	nC_{40}	0.11
nC_{19}	6.21	NC_{30}	1.58	nC_{41}	0.11
nC_{20}	3.71	nC_{31}	1.25	nC_{42}	0.06

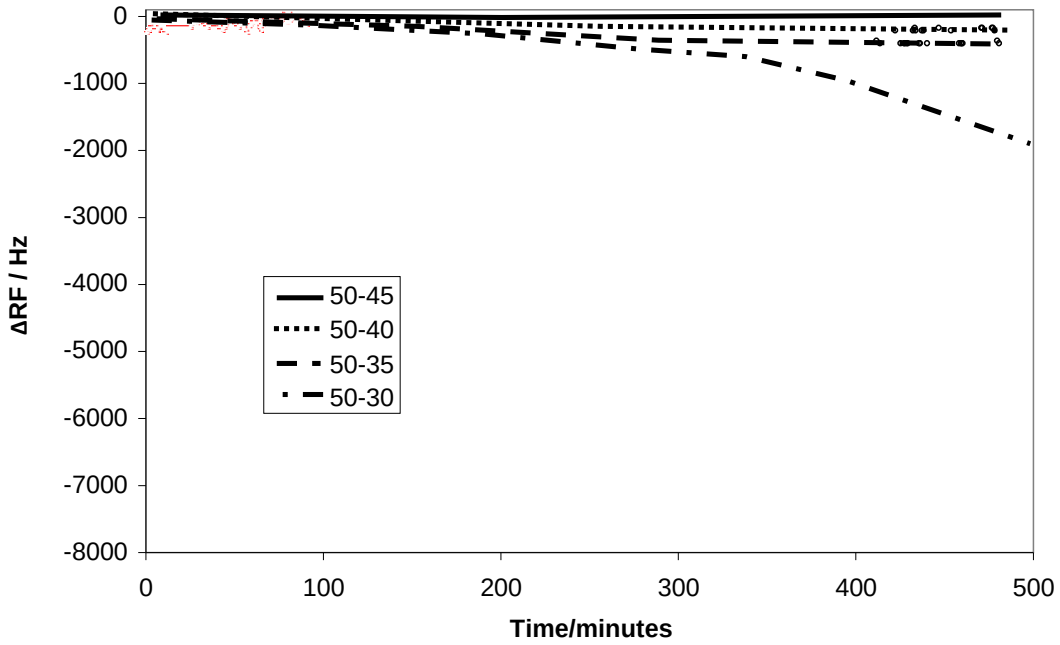

Figure 2.21. Plot showing resonant frequency changes with time in test with oil temperature of 50 ºC and QCM temperatures of 45, 40, 35 and 30 ºC.

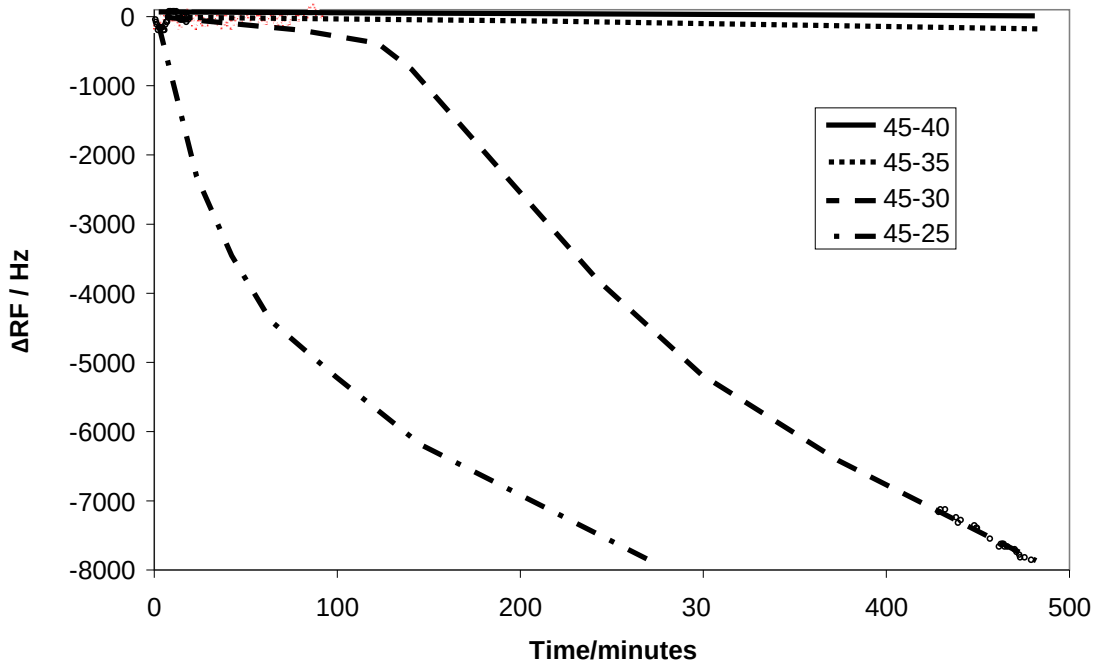

Figure 2.22. Plot showing resonant frequency changes with time in test with oil temperature of 45 ºC and QCM temperatures of 40, 35, 30 and 25 ºC.

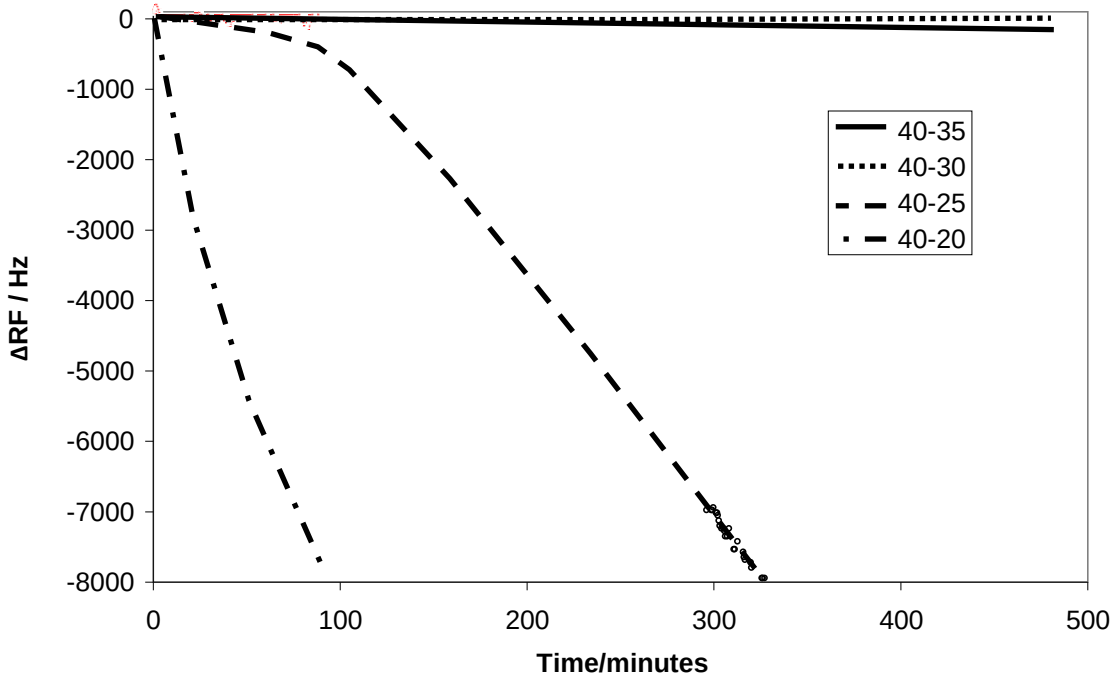

Figure 2.23. Plot showing resonant frequency changes with time in test with oil temperature of 40 ºC and QCM temperatures of 35, 30, 25 and 20 ºC.

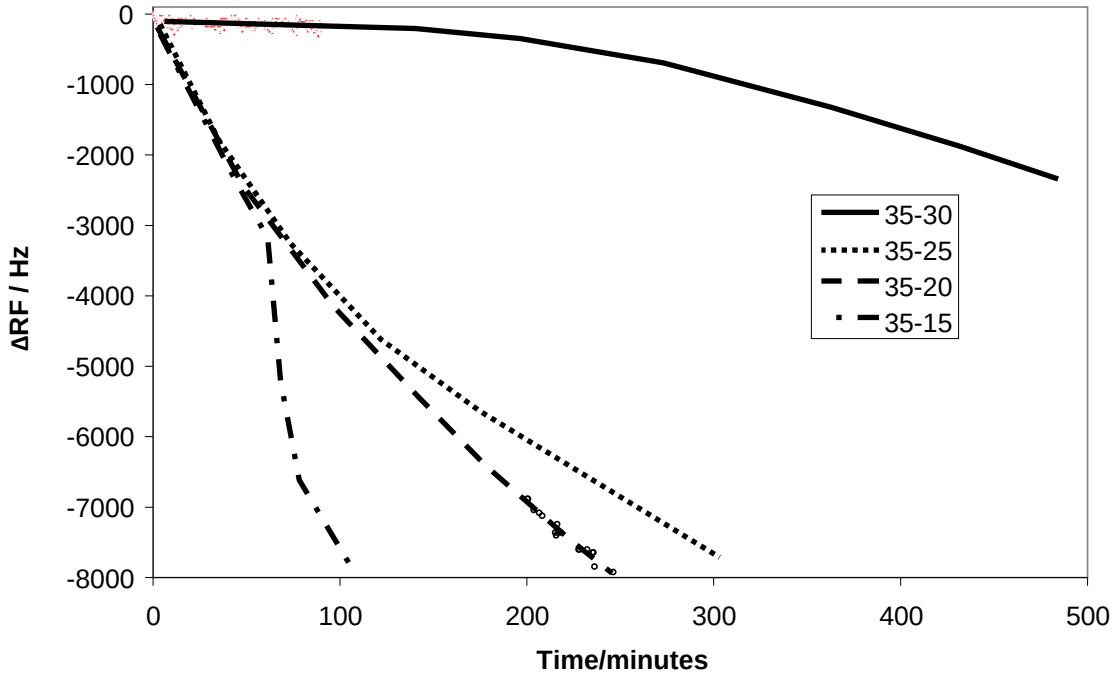

Figure 2.24. Plot showing resonant frequency changes with time in test with oil temperature of 35 ºC and QCM temperatures of 30, 25, 20 and 15 ºC.

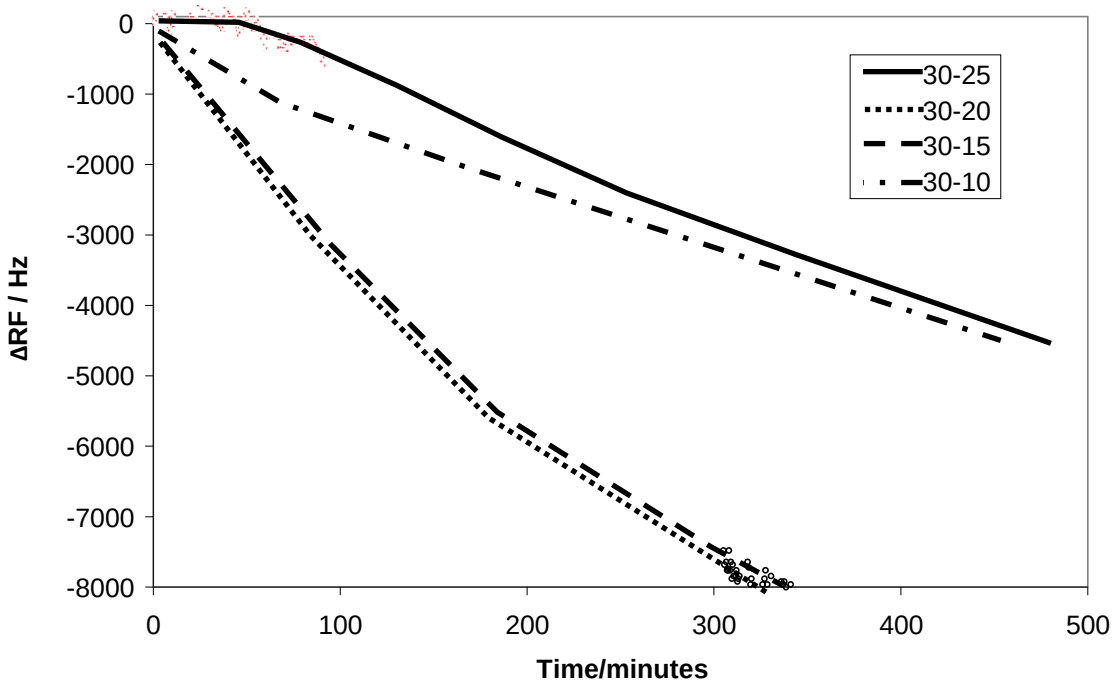

Figure 2.25. Plot showing resonant frequency changes with time in test with oil temperature of 30 ºC and QCM temperatures of 25, 20, 15 and 10 ºC.

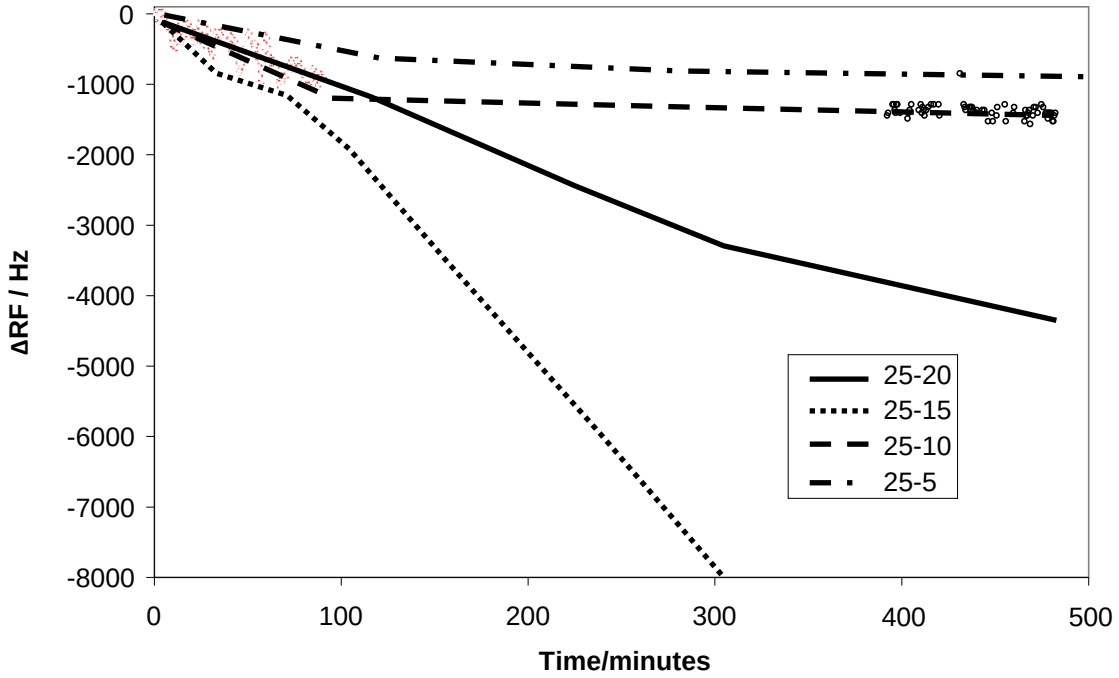

Figure 2.26. Plot showing resonant frequency changes with time in test with oil temperature of 25 ºC and QCM temperatures of 20, 15, 10 and 5 ºC.

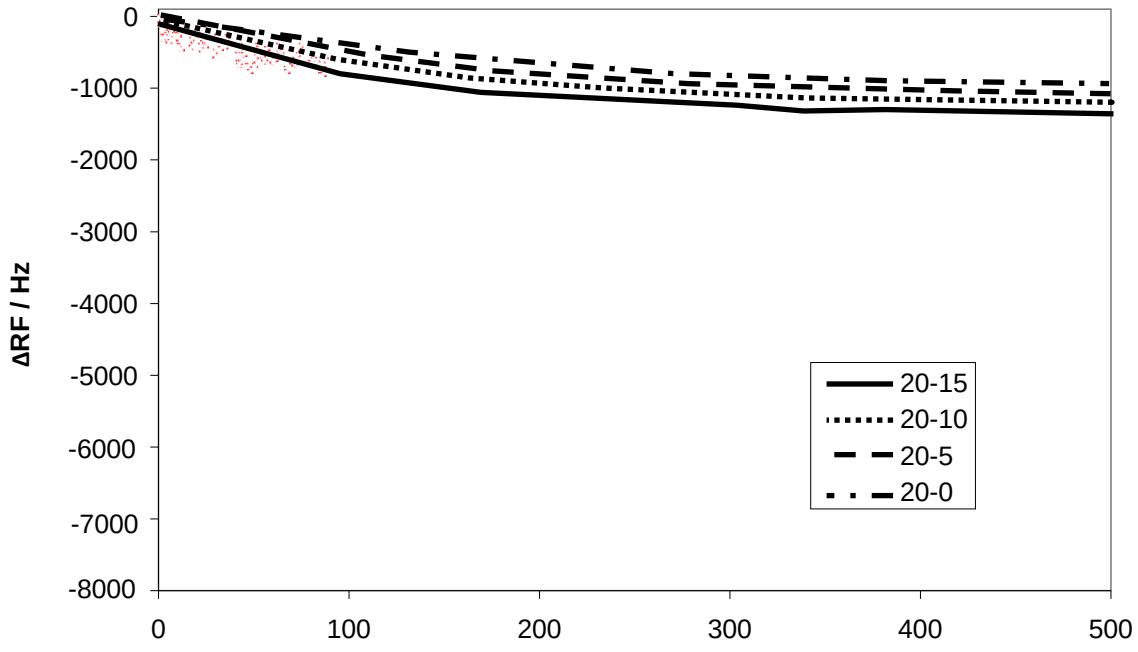

Figure 2.27. Plot showing resonant frequency changes with time in test with oil temperature of 20 ºC and QCM temperatures of 15, 10, 5 and 0 ºC.

2.6.3. Tests at pressure

In order to validate the cooled QCM set-up for measurements at pressure, tests were carried out at different pressures with a stabilised crude with a composition as given in Table 2.8. Tests were then conducted with the stabilised crude with natural gas with a composition as shown in Table 2.9.

Table 2.9. Natural gas composition

Component	Mole%
N_2	1.84
C_1	89.94
CO_2	0.91
C_2	5.32
C_3	1.45
iC_4	0.20
nC_4	0.21
iC_5	0.07
$(nC_5) + C_6^+$	0.06

2.6.3.1. Tests with stabilised crude

In these tests the QCM set-up was evacuated and then charged with a sample of stabilised crude. A piston cell with stabilised crude on one side of the piston and nitrogen on the other was connected to the set-up, the side with the oil side being connected to the cell. The cell pressure was changed by adding or withdrawing nitrogen from the piston vessel. In all of the tests the oil temperature was held at 30 ˚C and the QCM temperature was reduced from 65 ˚C to 25 ˚C in a time of 70 minutes (0.6 ˚C per minute). The QCM RF and temperature were recorded every 30 seconds. In each test the oil temperature and pressure remained constant.

Prior to starting tests at different pressures, three consecutive tests were conducted at the same pressure (1.9 bar) in order to assess the repeatability of the test results. Between each test the QCM temperature was increased to 65 ˚C for 1 hour prior to cooling. The results of these tests are shown in Figure 2.28. The initial RF at 65 ˚C was taken as the reference in order to calculate the ΔRF at each temperature. As can be seen from Figure 2.28 the results from the three tests were quite similar, indicating good repeatability.

Following the initial tests at 1.9 bar, five further tests were conducted at 9.0, 22.9, 43.2, 63.5 and 102.8 bar. The data are plotted together in Figure 2.29. As can be seen there is no

obvious trend with pressure, the highest rate of wax build-up is seen at the highest pressure (102.8 bar). Previous work measuring the WDT for fluids at different pressures showed that the WDT was not very sensitive to changes in pressure. Figure 2.30 shows a plot of WDT and pressure data for a synthetic mixture of hydrocarbons. As can be seen the WDT increases by around 1.5 ˚C for every 100 bar increase in pressure. Figure 2.18, above shows a similar trend for a stabilised condensate. This being the case there would not be expected to be significant changes in the amount of wax build-up between 1.9 and 102.8 bar.

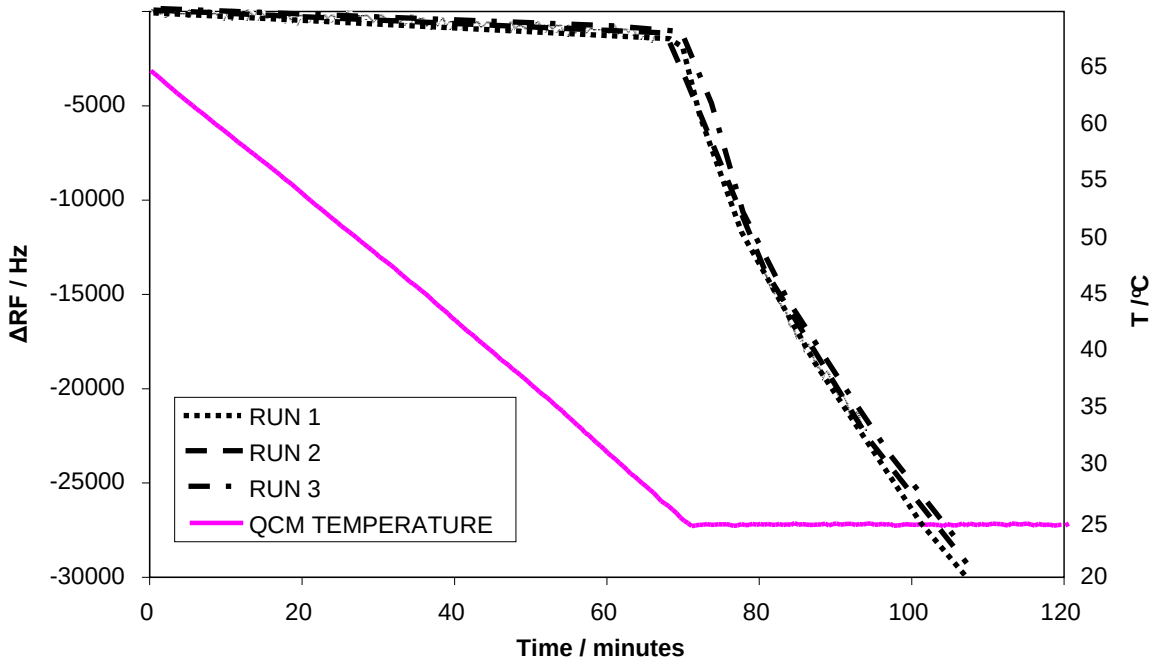

Figure 2.28. Plot showing the QCM ΔRF and temperature with time for three consecutive tests with stabilised crude (Table 2.8), oil temperature 30 ˚C.

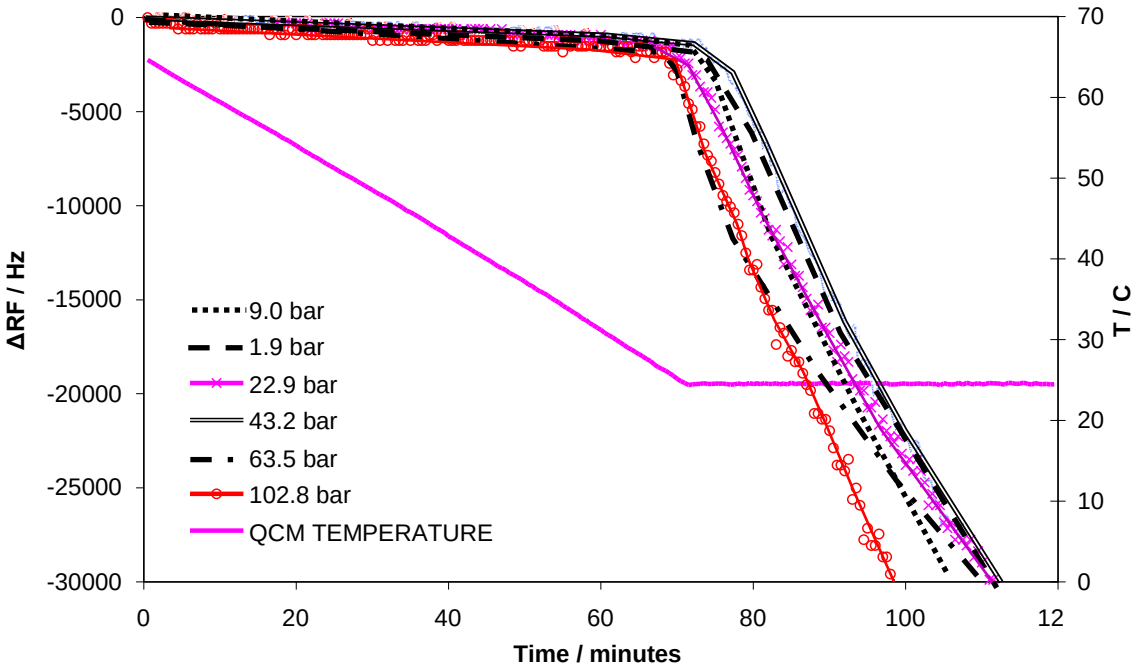

Figure 2.29. Plot showing the QCM ΔRF and temperature with time for five tests at different pressures with stabilised crude (Table 2.8), oil temperature 30 ˚C.

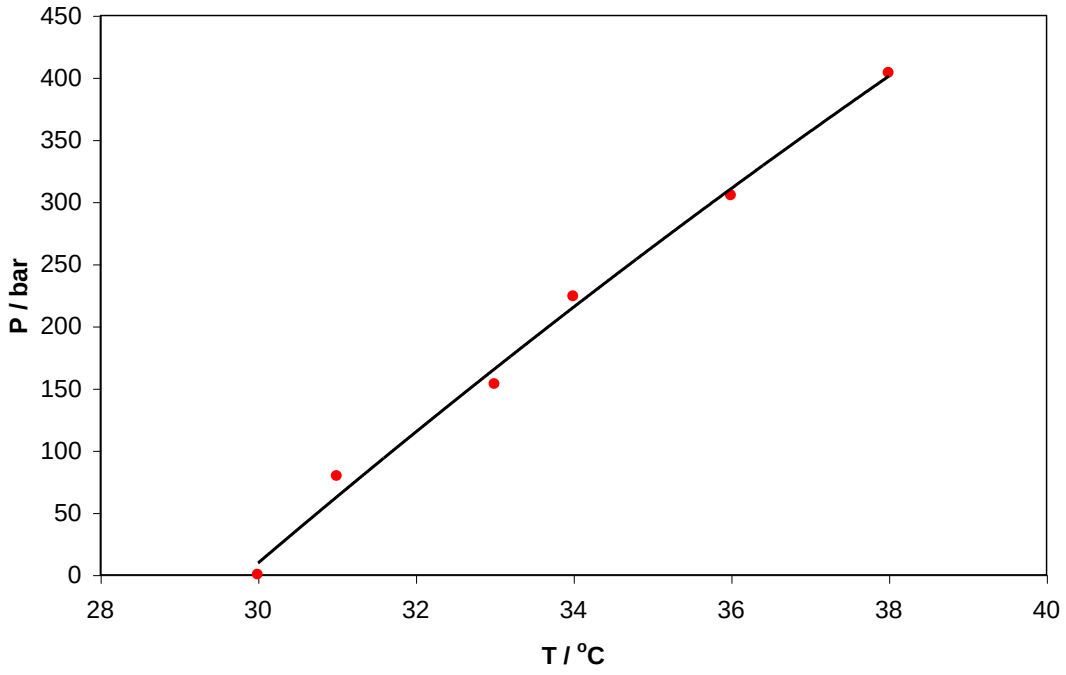

Figure 2.30. Plot showing experimental WDT measurements for a synthetic mixture of normal alkanes at different pressures, line fitted through experimental data.

2.6.3.2. Tests with stabilised crude and natural gas

Tests were conducted with natural gas at pressures of 8.6, 21.9, 42.0, 63.2, 83.2 and 100.3 bar. In all cases the oil temperature was kept at 30 ˚C. In the first test at 8.6 bar the QCM was cooled to a temperature of 25 ˚C as had been done with the test with no gas at 1.9 bar.

The amount of wax build-up with time was significantly less indicating that the addition of the gas had a strong effect. A second test was conducted, after reheating the QCM to 65 ˚C, this time reducing the QCM temperature to 23 ˚C. The data from the two tests are plotted along with the data for the test with no gas at 1.9 bar in Figure 2.31. As can be seen from Figure 2.31, the wax build-up with time as indicated by the ΔRF is similar for the tests with no gas and with gas where the QCM temperature was reduced to 23 ˚C.

In the second test with natural gas and a pressure of 21.9 bar the QCM temperature was reduced first to 25 ˚C then, after reheating to 65 ˚C, to 23 ˚C and finally to 22 ˚C. The data are plotted along with the data for the test with no gas in Figure 2.32. As can be seen from Figure 2.32 when the QCM temperature was reduced to 25 ˚C the wax build-up was significantly less with time compared to the case with no gas, as was seen in the previous test with natural gas at 8.6 bar. The wax build-up with time was slightly less compared to the test with no gas when the QCM temperature was reduced to 23 ˚C and faster when reduced to 22 ˚C.

For the tests with natural gas at 42.0, 63.2, 83.2 and 100.3 bar it was decided to conduct tests at different QCM temperatures, after reducing from 65 ˚C in order to find which temperature gave a similar wax build-up rate when compared to the test with no gas. The data recorded during these tests are shown in Figures 2.33 through 2.36. As can be seen the trend is for a lower QCM temperature to be achieved for the wax build-up rate with time to match the test with no gas.

In previous work the effect of adding light (C_1-C_4) components on the wax phase boundary was shown. As discussed in 2.5.4 above, the addition of light components not only will change the wax phase boundary, but the amount of wax solids at temperatures inside the wax phase boundary will also be changed.

The results from this series of tests may be attributed to less wax solids being present in the cell at 30 ˚C as the gas is added, due to the light components increasing the amount of solids that can be dissolved in the oil that is present. Figure 2.37 shows a plot of the estimated QCM temperature, based upon the recorded data, that would give the same wax build-up as that seen with no gas present (QCM 25 ˚C) and the predicted mole fraction of C_2 and C_3 in the liquid hydrocarbon at different test pressures. As can be seen from Figure 2.37,

as pressure increases, the amount of C_2 and C_3 increases, and the lower the QCM temperature has to be to produce the same wax build-up. It can also be seen that the rate of build-up is greater in the tests with gas present when the QCM temperature gives an equivalent build-up. This may be due to the increase in differential temperature or potentially the lower viscosity of the oil.

The results from the tests with the cooled QCM set-up at pressure show trends as expected, indicating that the equipment can be used to indicate wax deposition tendency at pressure. It is possible to increase the pressure rating of the equipment and the mixing capabilities so that measurements can be made up to higher pressures with different stirring rates, hence different shear rates. Although it is not possible to obtain exact values for the amount of wax deposited it may be possible to calibrate the system allowing for wax build-up to be estimated.

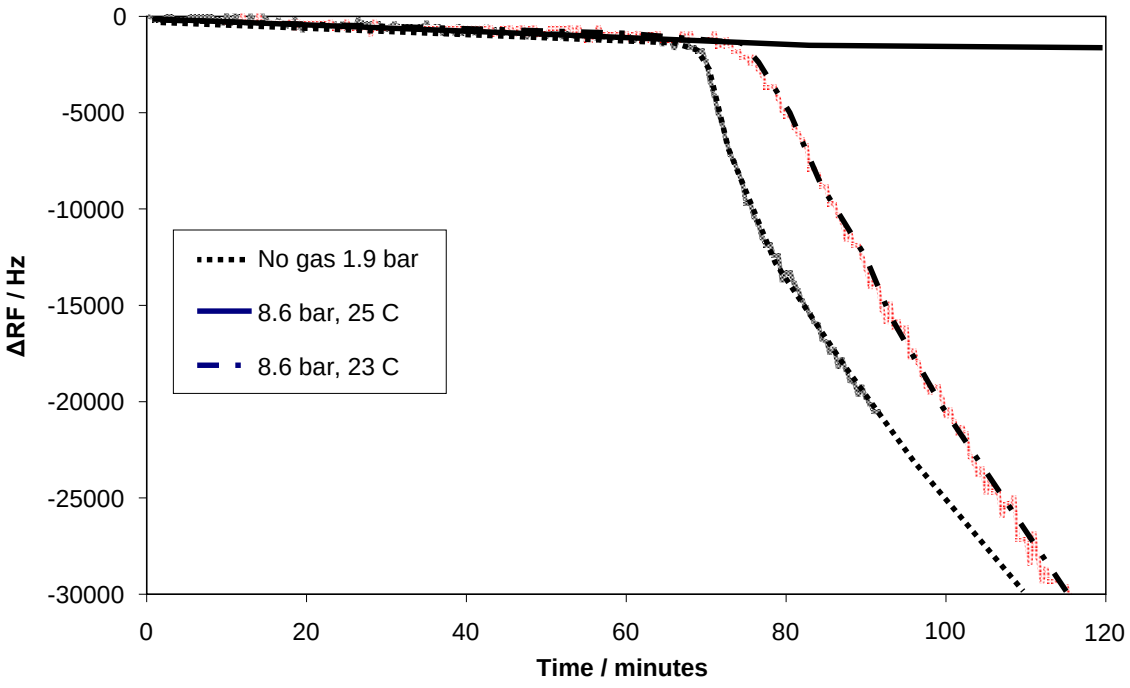

Figure 2.31. Plot showing QCM ΔRF with time for tests without (1.9 bar, 25 °C) and with natural gas (8.6 bar) and different QCM temperatures.

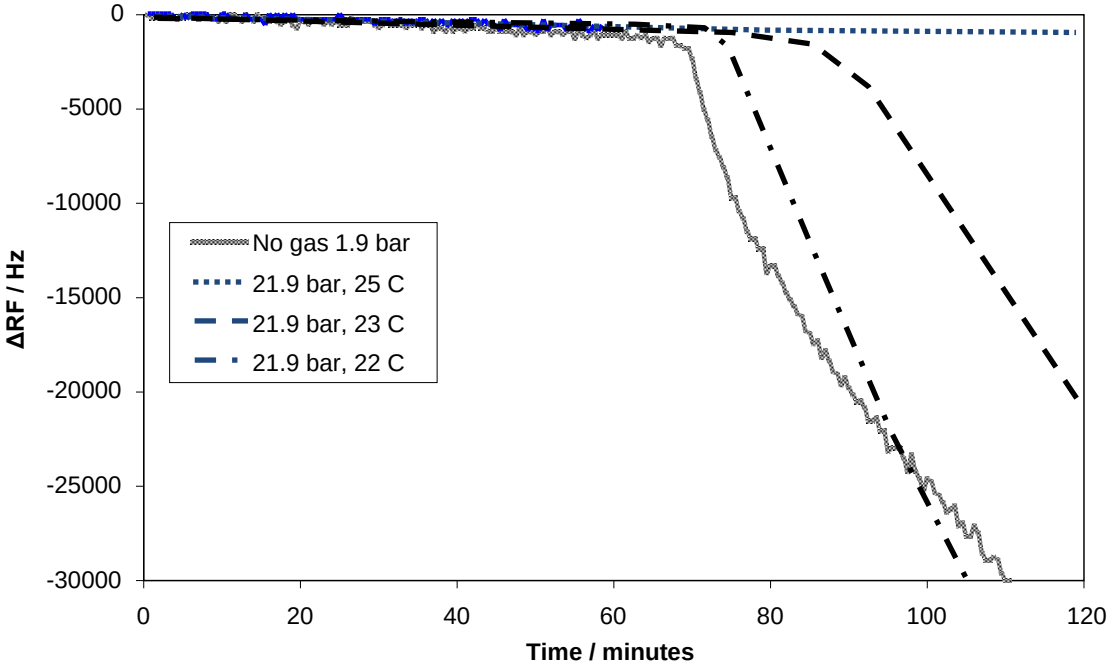

Figure 2.32. Plot showing QCM ΔRF with time for tests without (1.9 bar, 25 °C) and with natural gas (21.9 bar) and different QCM temperatures.

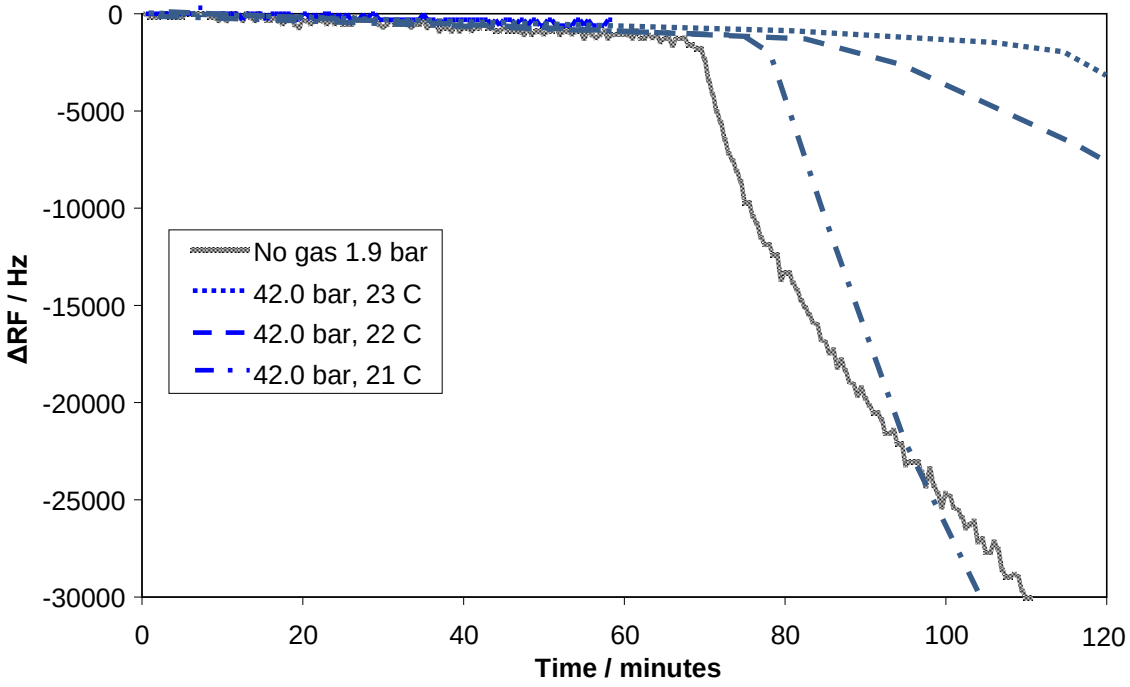

Figure 2.33. Plot showing QCM ΔRF with time for tests without (1.9 bar, 25 °C) and with natural gas (42.0 bar) and different QCM temperatures.

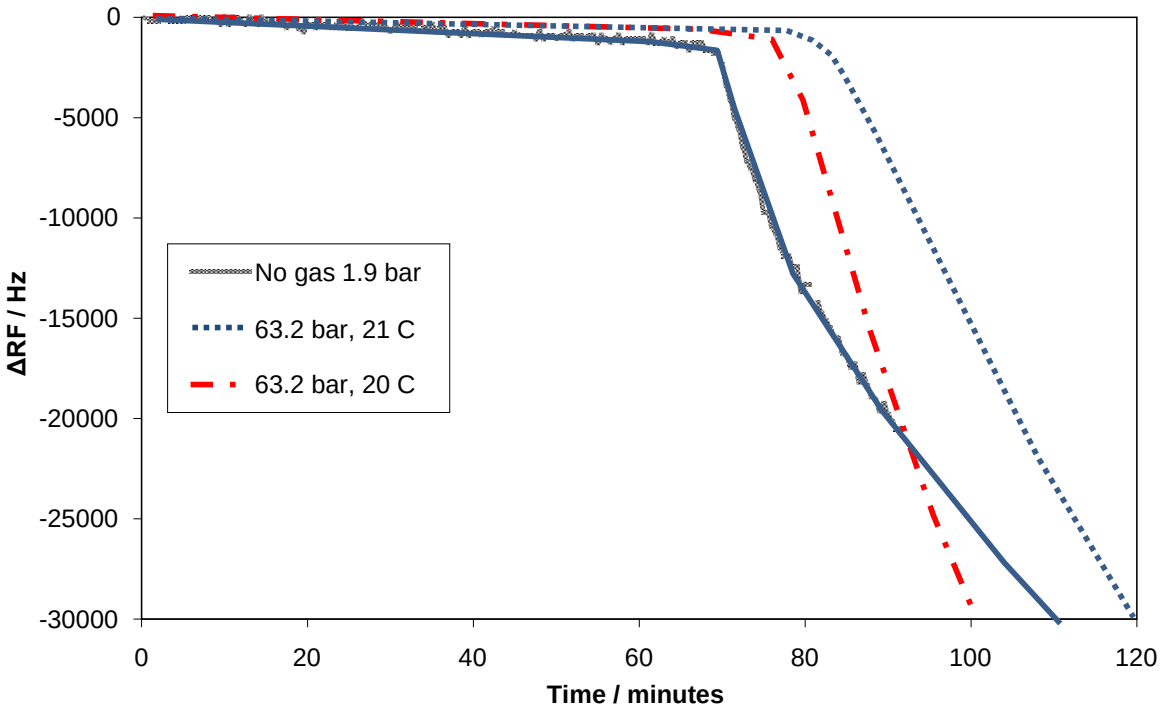

Figure 2.34. Plot showing QCM ΔRF with time for tests without (1.9 bar, 25 °C) and with natural gas (63.2 bar) and different QCM temperatures.

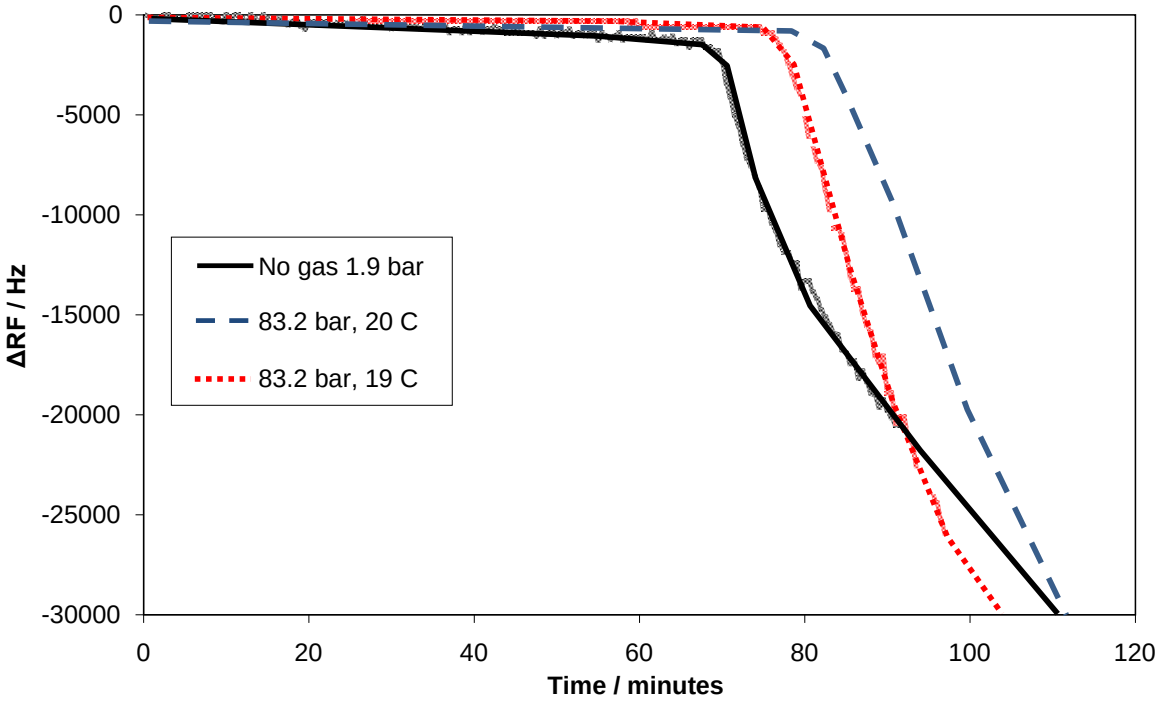

Figure 2.35. Plot showing QCM ΔRF with time for tests without (1.9 bar, 25 °C) and with natural gas (83.2 bar) and different QCM temperatures.

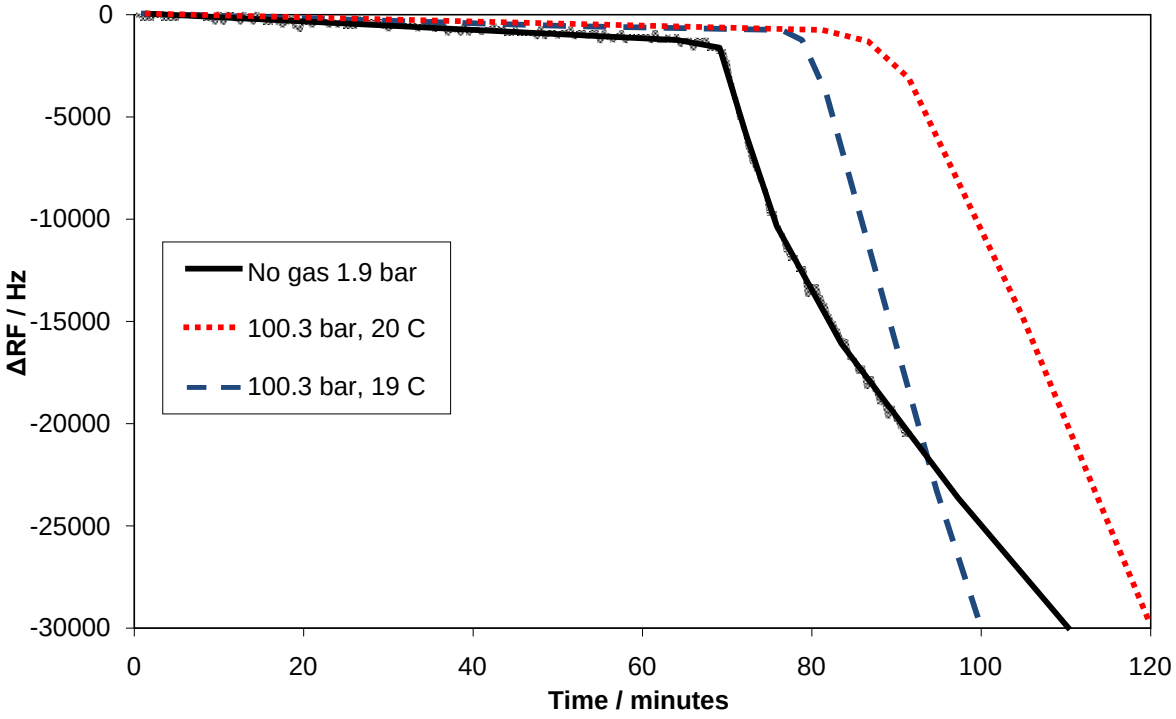

Figure 2.36. Plot showing QCM ΔRF with time for tests without (1.9 bar, 25 °C) and with natural gas (100.3 bar) and different QCM temperatures.

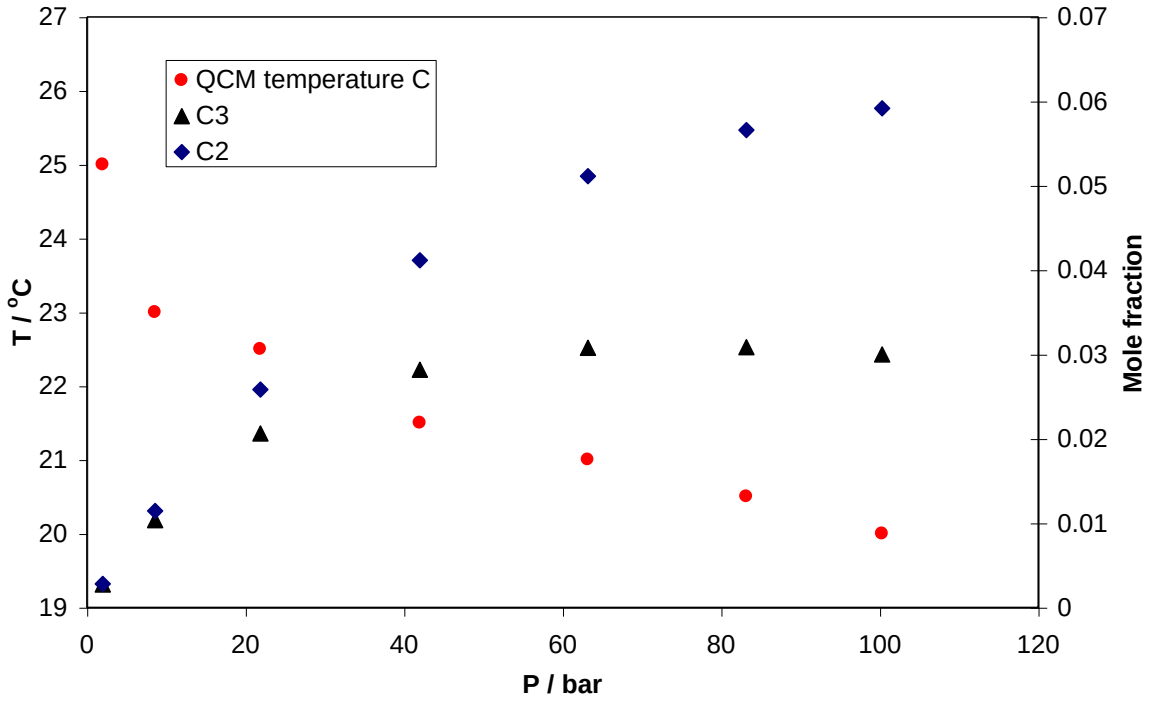

Figure 2.37. Plot showing QCM temperatures, from tests with gas at different pressures, required to match wax build-up for test with no gas along with the predicted mole fractions of C_2 and C_3 in the liquid hydrocarbon at different pressures.

2.7. Evaluation of developed equipment and methods for measurements with wax inhibitors.

As discussed in the introduction, wax inhibitors are commonly used to avoid flow assurance problems associated with wax formation such as adhesion to pipeline walls and gelling. As one of the main ways in which the inhibitors function is to co-crystallize with the wax [23], having the effect of reducing the adhesion tendency of the resulting solids, the QCM should be an ideal tool for inhibitor evaluation as it gives a direct measurement, through RF reduction, of adhesion tendency. In the next section initial validation tests are presented for inhibitor measurements using the atmospheric pressure QCM glass tube assembly (Figure 2.5) and the temperature controlled QCM set-up (Figure 2.19).

2.7.1. Tests with atmospheric pressure QCM glass tube assembly

Tests were carried out using an eight tube set-up. A stabilised crude of unknown composition was used and six inhibitors were tested. Each inhibitor was tested at two dose rates of 100 and 500 ppm by volume. QCM tests were conducted by cooling 5 ml test sample with no additive from 60 to 1 ºC at a rate of 0.5 ºC per minute and monitoring change in resonant frequency (RF) referenced to initial reading at 60 ºC. The samples were then reheated to 60 ºC for at least 30 minutes and chemical added before conducting the same cooling procedure. The WAT was measured at cooling rate of 0.5 ºC per minute. The WDT was measured at a slow heating rate of 0.08 ºC per minute. The pour point was measured by cooling sample tubes used in QCM measurements at cooling rate of 0.5 ºC per minute, using ASTM D 97 – 87 designation of pour point i.e. no movement when tilted for 5 seconds. The data from the QCM tests are plotted in Figures 2.38 through 2.49. The data for the oil is summarised in Table 2.10. The results from the QCM tests are represented by comparing the untreated and treated change in RF at 3 ºC (treated RF minus blank RF) hence a positive result means more solids adhering and negative less. The pour points are compared in similar manner positive meaning higher temperature than blank and negative lower.

Overall there is little difference in WAT in any of the oils with any of the additives. As can be seen from Figures 2.38 and 2.39 and Table 2.10 Dispersogen 4970 had a negative effect on both the wax adhesion tendency and the pour point. Dispersogen 4969 showed little improvement for both wax adhesion and pour point at 100 ppm, however a marked improvement at 500 ppm as seen in Figure 2.41 and the marked reduction in pour point

temperature. In the case of Dispersogen 5708 there was a negative effect at both dose rates from the QCM data but a positive result for the pour point at 500 ppm. It may be that at higher dose rates the wax adhesion tendency might also give a positive result. Dispersogen 5814 did not show any positive results for wax adhesion tendency or pour point. Dispersogen 5579 showed the best results for both dose rates from the QCM results, Figures 2.46 and 2.47, the improvement being better at the higher dose rate. The pour point measurements gave a positive result for both dose rates. In the case of Dispersogen 5725 there was no improvement seen in the QCM tests, however there was some improvement from the pour point results.

As can be seen from the QCM results it is clearly possible to identify the best performing inhibitors, and in addition if more dose rates are studied this can also be optimised. In some cases the pour point shows improvement not mirrored by the QCM data. One possibility is that in this oil the solids formed can separate from the bulk fluid and fall to the lower part of the sample tube. As they are no longer dispersed throughout the fluid it is difficult for the whole fluid to gel, especially the top layers. The solids that are formed through co-crystallisation with the inhibitor may still have a tendency to adhere to or build up on surfaces as shown from the QCM data.

As mentioned previously the potential for the QCM to be used as a means of identifying pour point was investigated. However it was found that there was no clear or repeatable change in RF seen when the fluid gelled.

Table 2.10. Results summary for oil with different inhibitors at two dose rates.

Oil WAT 31 ºC ±1 ºC, WDT 39 ºC ±1 ºC. Blank pour point 0 ºC.

	QCM data at 3 ºC ΔRF treated - ΔRF blank / KHz ±1		Pour point temperature treated – pour point temperature blank	
Dispersogen	100ppm	500ppm	100ppm	500ppm
4970	+8	+8	+8	+4
4969	-3	-26	0	-25
5708	+18	+4	+4	-10
5814	+4	-2	+4	-4
5579	-21	-52	-25	-19
5725	+1	+12	-14	-6

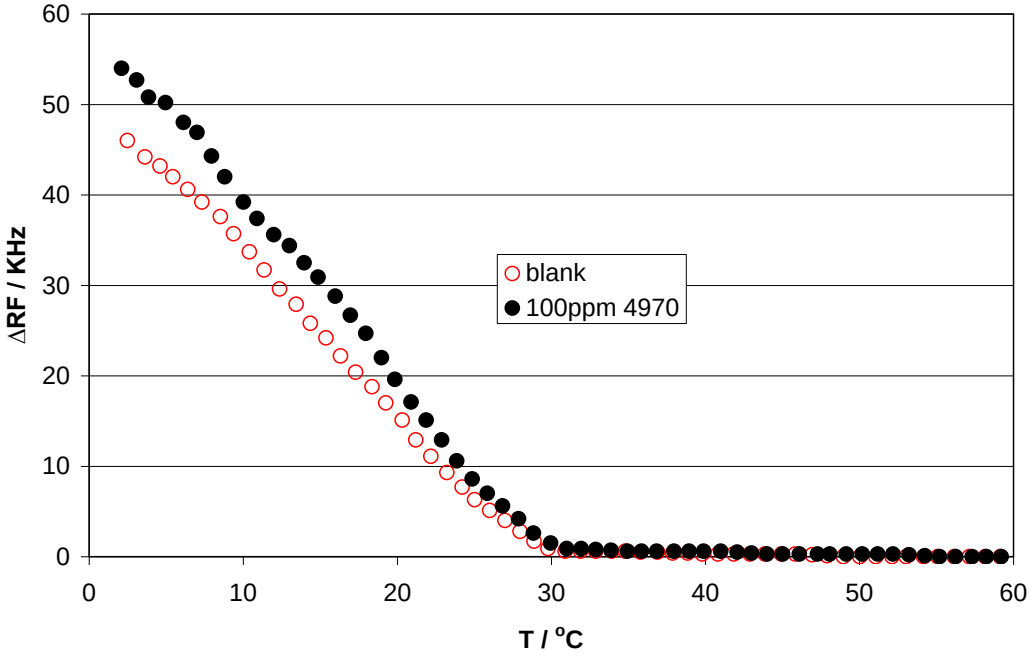

Figure 2.38. QCM data oil with 100ppm dispersogen 4970.

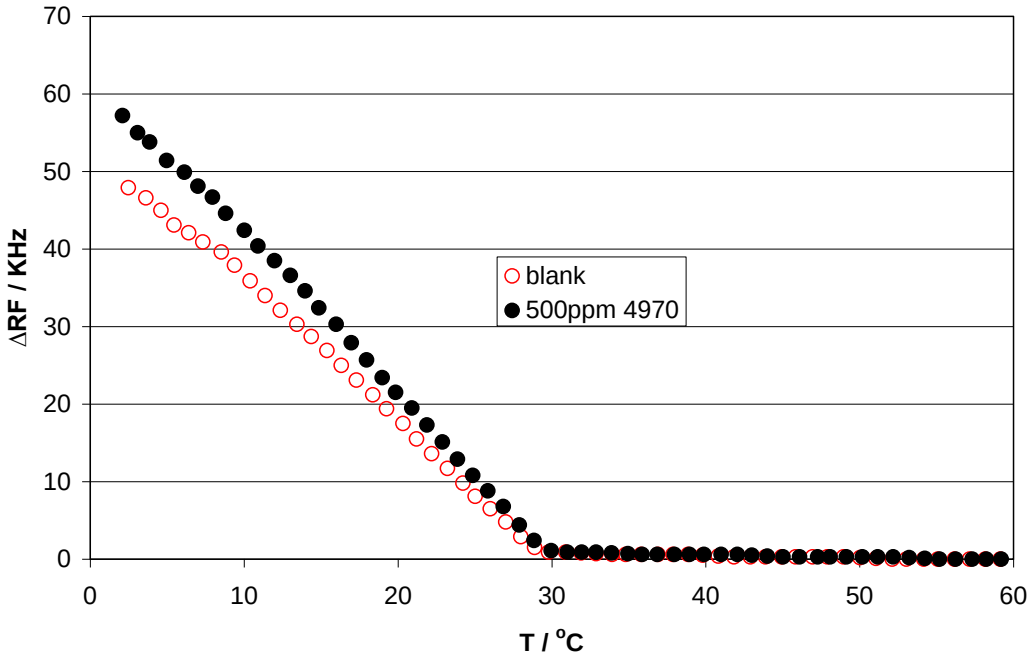

Figure 2.39. QCM data oil with 500ppm dispersogen 4970.

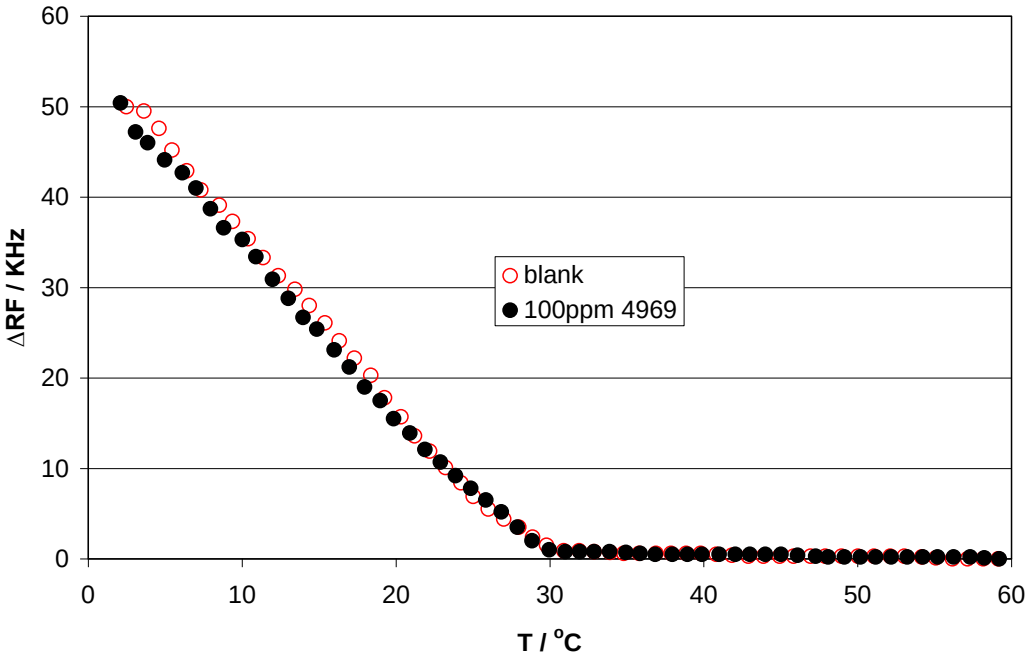

Figure 2.40. QCM data oil with 100ppm dispersogen 4969.

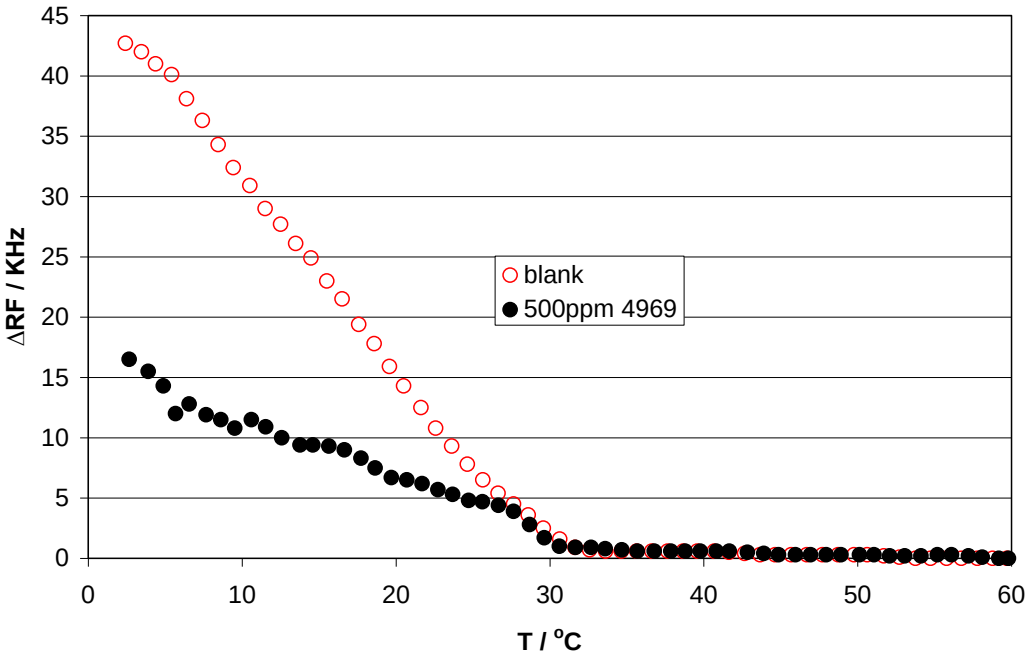

Figure 2.41. QCM data oil with 500ppm dispersogen 4969.

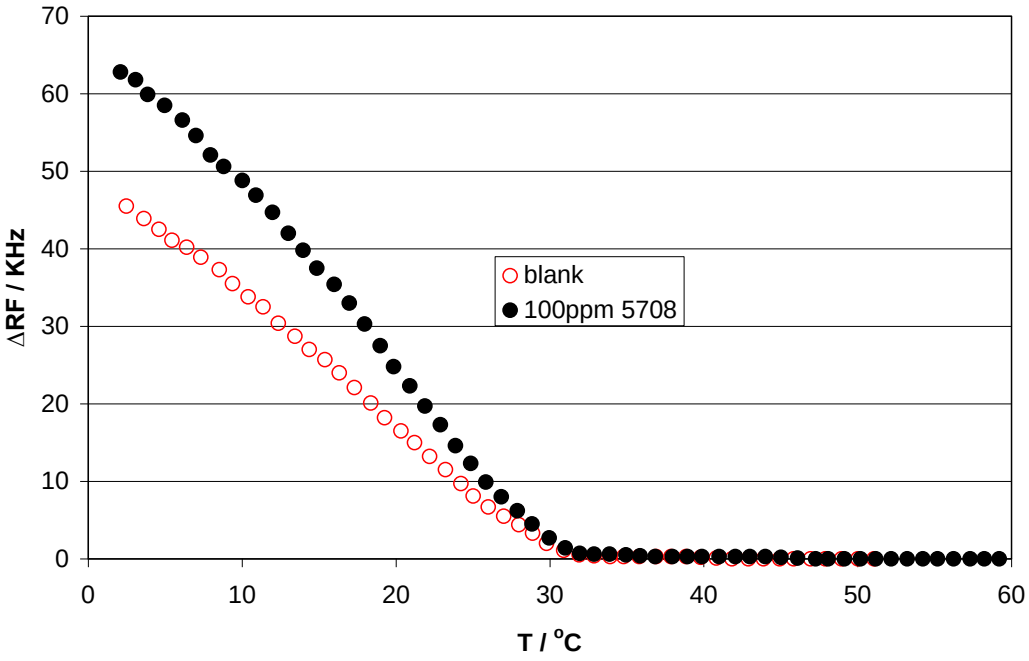

Figure 2.42. QCM data oil with 100ppm dispersogen 5708.

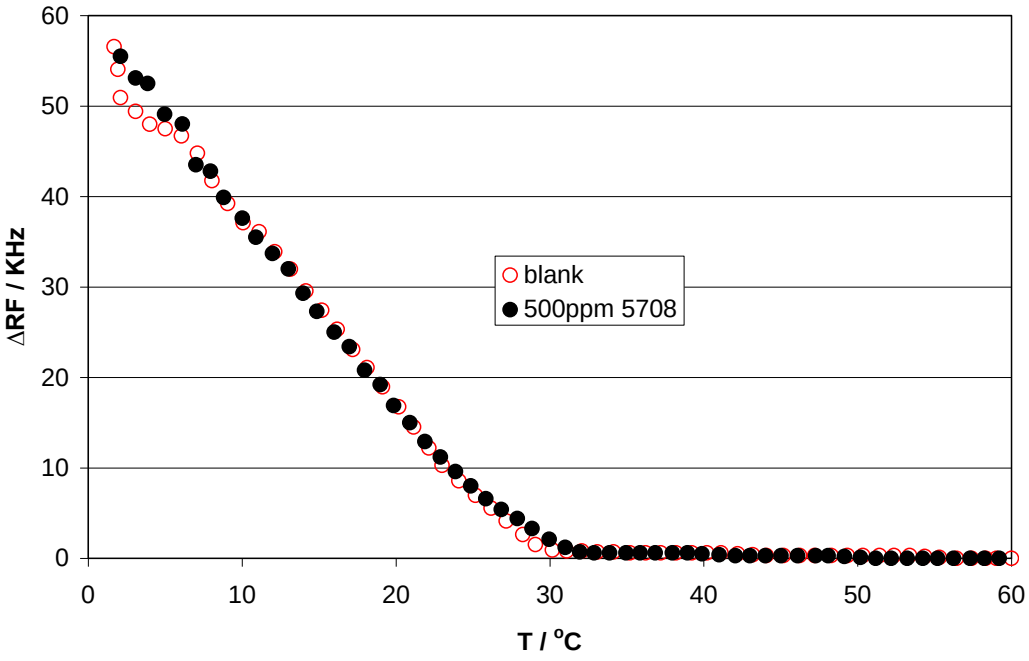

Figure 2.43. QCM data oil with 500ppm dispersogen 5708.

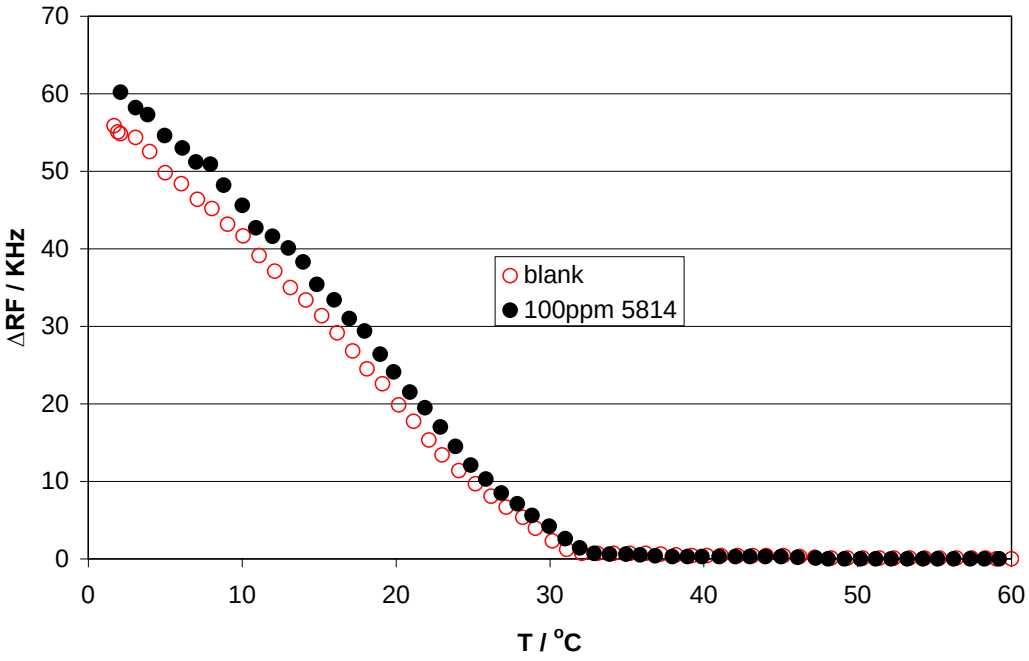

Figure 2.44. QCM data oil with 100ppm dispersogen 5814.

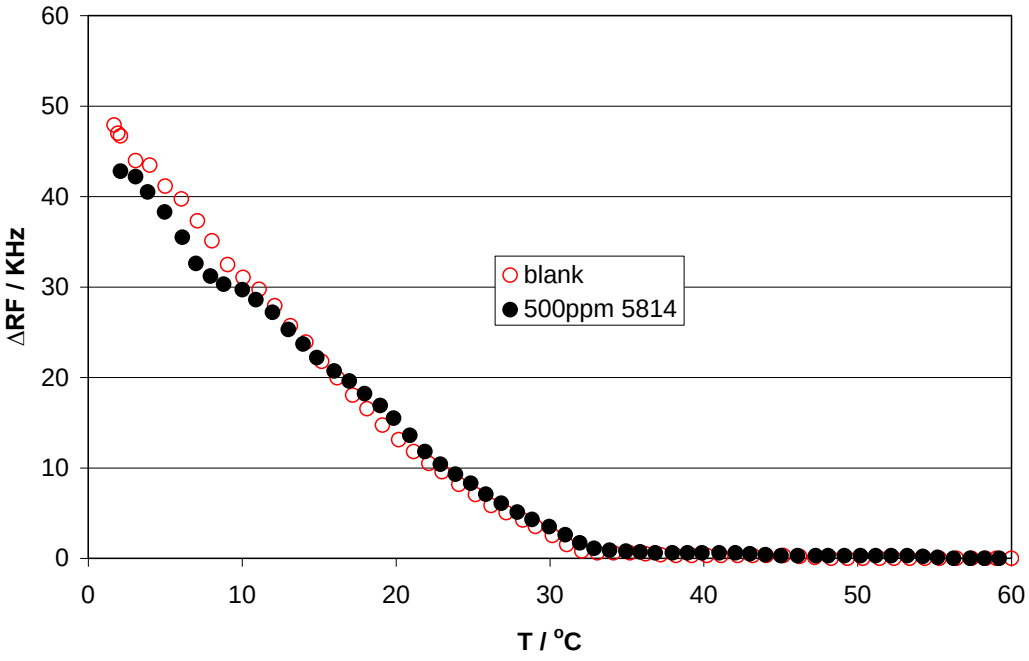

Figure 2.45. QCM data oil with 500ppm dispersogen 5814.

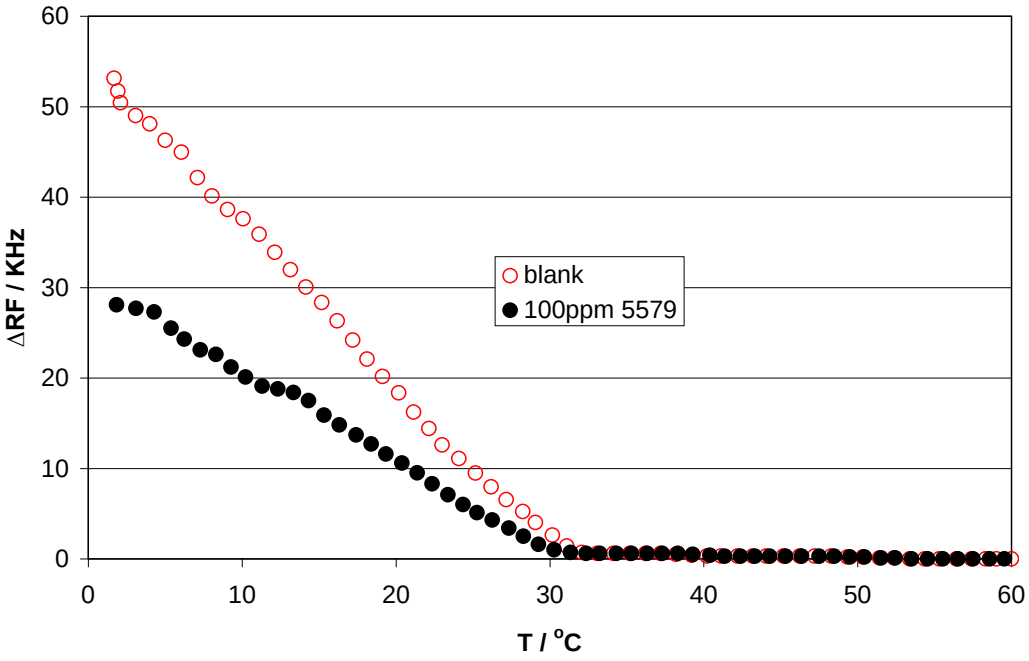

Figure 2.46. QCM data oil with 100ppm dispersogen 5579.

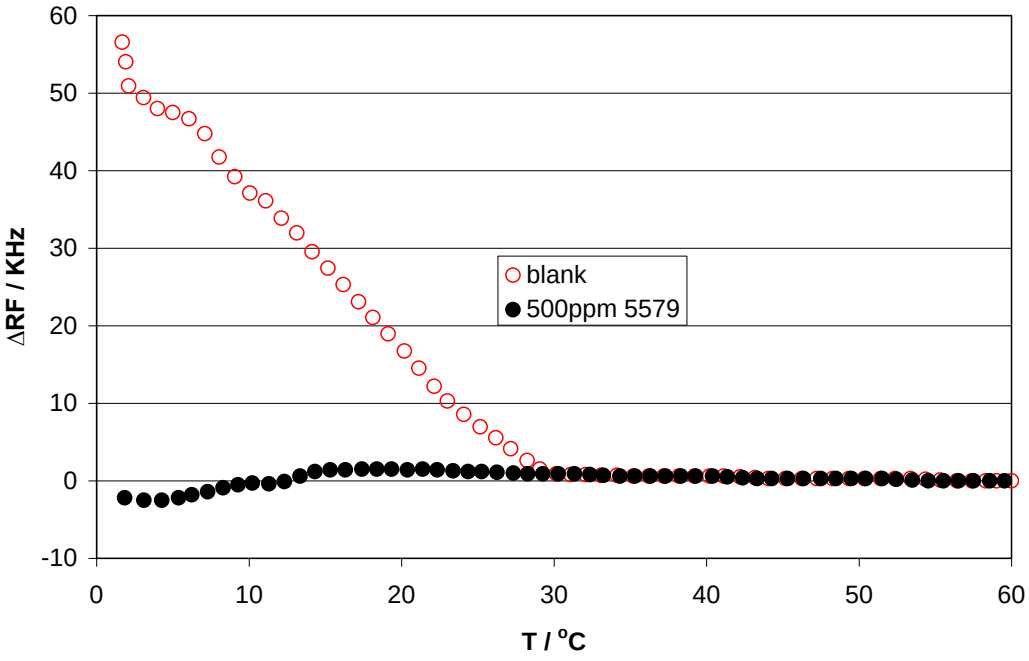

Figure 2.47. QCM data oil with 500ppm dispersogen 5579.

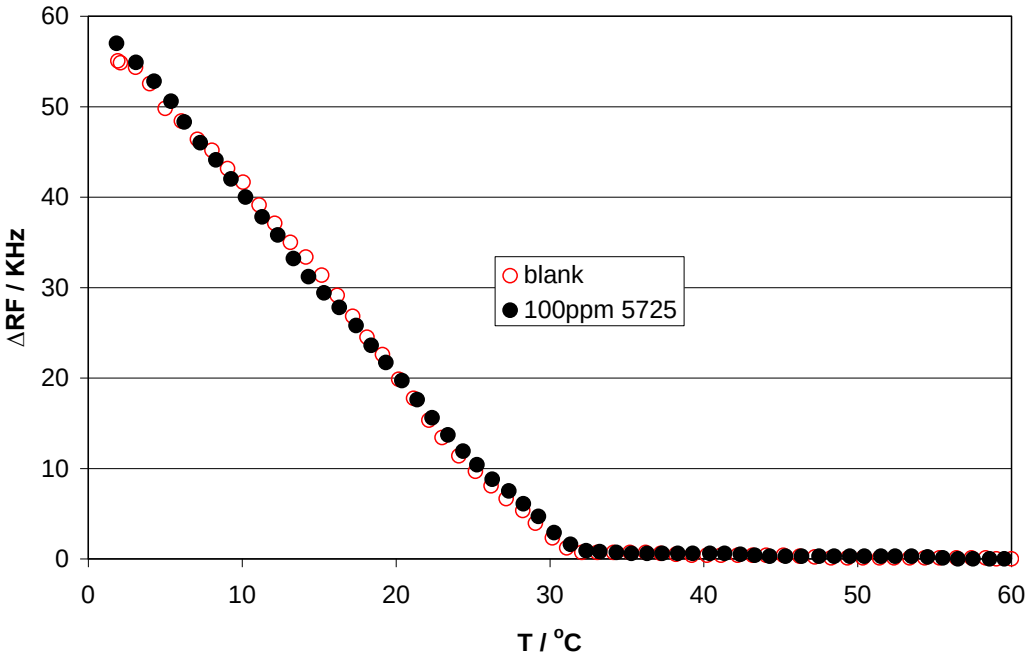

Figure 2.48. QCM data oil with 100ppm dispersogen 5725.

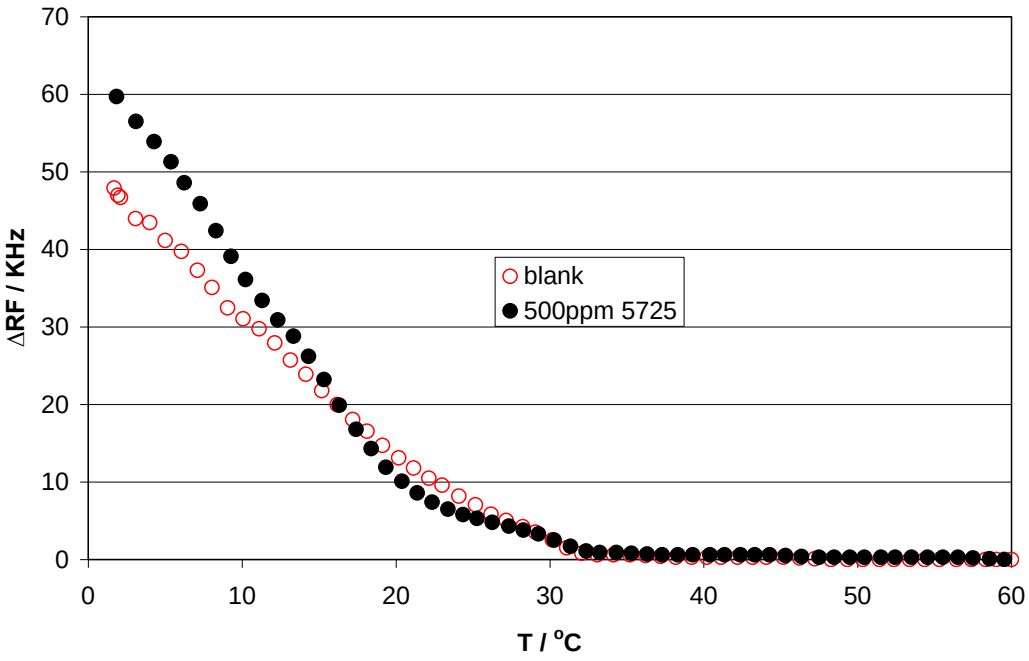

Figure 2.49. QCM data oil with 500ppm dispersogen 5725.

2.7.2. Tests with cooled QCM set-up

In order to validate the use of the cooled QCM set-up for evaluating wax inhibitors a series of tests was conducted with one oil and four inhibitors at two different dose rates. The results were then compared with results obtained using a standard cold finger apparatus. The test set-up was the same as that shown in Figure 2.19.

2.7.2.1. Test fluids

An oil with a composition as shown in Table 2.11 was used.

Table 2.11. Composition of stabilised crude used in QCM measurements. Asphaltene content 5.955 mass%. API 29.339.

Component	**Mass%**	**Mole%**	**Component**	**Mass%**	**Mole%**
Methane	<0.01	0.00	C_{35}	1.33	0.71
Ethane	<0.01	0.00	C_{36}	1.09	0.56
Propane	0.15	0.89	C_{37}	1.16	0.58
2-Methylpropane	0.11	0.50	C_{38}	0.92	0.45
n-Butane	0.36	1.62	C_{39}	1.08	0.51
2-Methylbutane	0.29	1.05	C_{40}	0.92	0.43
n-Pentane	0.35	1.27	C_{41}	0.80	0.36
Hexanes	1.16	3.52	C_{42}	0.84	0.37
Heptanes	2.50	6.53	C_{43}	0.83	0.36
Octanes	3.95	9.05	C_{44}	0.66	0.28
Nonanes	3.17	6.47	C_{45}	0.75	0.31
Decanes	3.50	6.44	C_{46}	0.62	0.25
C_{11}	2.96	4.96	C_{47}	0.63	0.25
C_{12}	2.63	4.04	C_{48}	0.62	0.24
C_{13}	2.99	4.24	C_{49}	0.65	0.25
C_{14}	3.01	3.97	C_{50}	0.53	0.20
C_{15}	2.99	3.68	C_{51}	0.54	0.20
C_{16}	2.59	2.99	C_{52}	0.42	0.15
C_{17}	2.73	2.97	C_{53}	0.57	0.20
C_{18}	2.60	2.67	C_{54}	0.60	0.21
C_{19}	2.70	2.63	C_{55}	0.47	0.16
C_{20}	2.30	2.13	C_{56}	0.47	0.16
C_{21}	1.92	1.69	C_{57}	0.44	0.14
C_{22}	2.16	1.82	C_{58}	0.45	0.14
C_{23}	1.84	1.48	C_{59}	0.49	0.15
C_{24}	1.81	1.40	C_{60}	0.37	0.11
C_{25}	1.72	1.28	C_{61}	0.46	0.14
C_{26}	1.75	1.25	C_{62}	0.32	0.10
C_{27}	1.89	1.30	C_{63}	0.42	0.12
C_{28}	1.71	1.13	C_{64}	0.34	0.10
C_{29}	1.65	1.06	C_{65}	0.36	0.10
C_{30}	1.63	1.01	C_{66}	0.35	0.10
C_{31}	1.56	0.93	C_{67}	0.32	0.09
C_{32}	1.36	0.79	C_{68}	0.31	0.08
C_{33}	1.33	0.75	C_{69}	0.32	0.09
C_{34}	1.17	0.64	C_{70}+	12.01	3.19

Information regarding the composition and use of each inhibitor is given below.

- 06-251 is a 22% blend of alykyresins and ethoxylated amines in aromatic hydrocarbon, primarily a wax dispersant.
- 06-252 is a 10% active Ethylene Vinyl Acetate polymer in aromatic solvent, primarily a wax inhibitor
- 06-253 is a 25% active high molecular weight copolymer in aromatic solvent, primarily a pour point depressant.
- 07-327, no information available.

2.7.2.2. Results from cooled QCM set-up

In the tests, all carried out at atmospheric pressure, the oil was held at 30 ºC and the probe was used at 20, 15, 10 and 5 ºC. Tests were run with the base fluid and four different inhibitors at two different dose rates of 300 and 500 ppm by volume.

Figure 2.50 shows the results for the base fluid at different temperatures. For each inhibitor the data is presented by comparing the base fluid with two inhibitor dose rates at each probe temperature. Figures 2.51 through 2.54 give the data for inhibitor 06-253. Figures 2.55 through 2.58 give the data for inhibitor 07-327. Figures 2.59 through 2.62 give the data for inhibitor 06-251. Figures 2.63 through 2.65 give the data for inhibitor 06-252. In the case of 06-252 there is no data presented for a probe temperature of 5 ºC because the solids build up was already high when the probe reached 5 ºC.

The data indicate the following:

- In tests with 06-253 the solids build up was reduced at all probe temperatures compared to the untreated oil. There was less solids build up when the dose rate was 500 ppm compared to 300 ppm.
- In tests with 07-327, at a dose rate of 300 ppm, the level of solid build up was reduced at all probe temperatures when compared to the untreated fluid. With a dose rate of 500 ppm the level of solids build up was reduced at a probe temperature of 20 ºC but increased at probe temperatures of 15, 10 and 5 ºC when compared to the untreated fluid.

- In tests with 06-251, at a probe temperature of 20 ºC, with a dose rate of 300 ppm the solids build up was less compared to the untreated fluid, however it was greater with 500 ppm. This was also the case with a probe temperature of 15 ºC. At 10 and 5 ºC both dose rates showed more solids build up compared to the untreated fluid. In all cases more solids build up was seen with 500 ppm compared to 300 ppm.
- In tests with 06-252, at a probe temperature of 20 ºC, with a dose rate of 300 ppm, the solids build up was less compared to the untreated fluid, however it was greater with 500 ppm. At 15, 10 and 5 ºC both dose rates showed more solids build up compared to the untreated fluid. In all cases more solids build up was seen with 500 ppm compared to 300 ppm.
- At a probe temperature of 5 ºC the least build up was seen with 07-327 at a dose rate of 300 ppm. The second least level of build-up was with 06-253 at a dose rate of 500 ppm.

Overall it would be interesting to compare the results from QCM tests with results from alternative equipment such as a rheometer giving viscosity and other properties of the fluids. In general the increase in viscosity does not have a significant effect on RF by comparison with solids adhering to the QCM surface. As discussed in Chapter 2, Page 16, conductance is mainly influenced by viscosity changes whereas RF is not changed significantly.

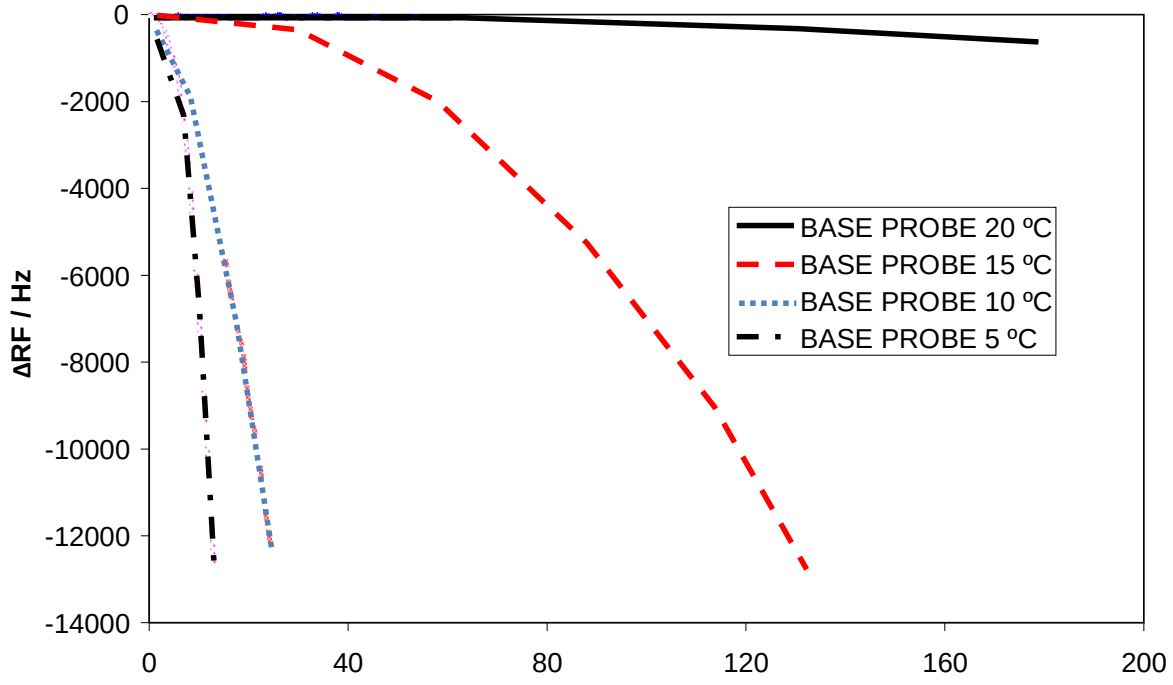

Figure 2.50. Data recorded for test with stabilised crude (Table 2.11) held at 30 ºC and different wax probe temperatures.

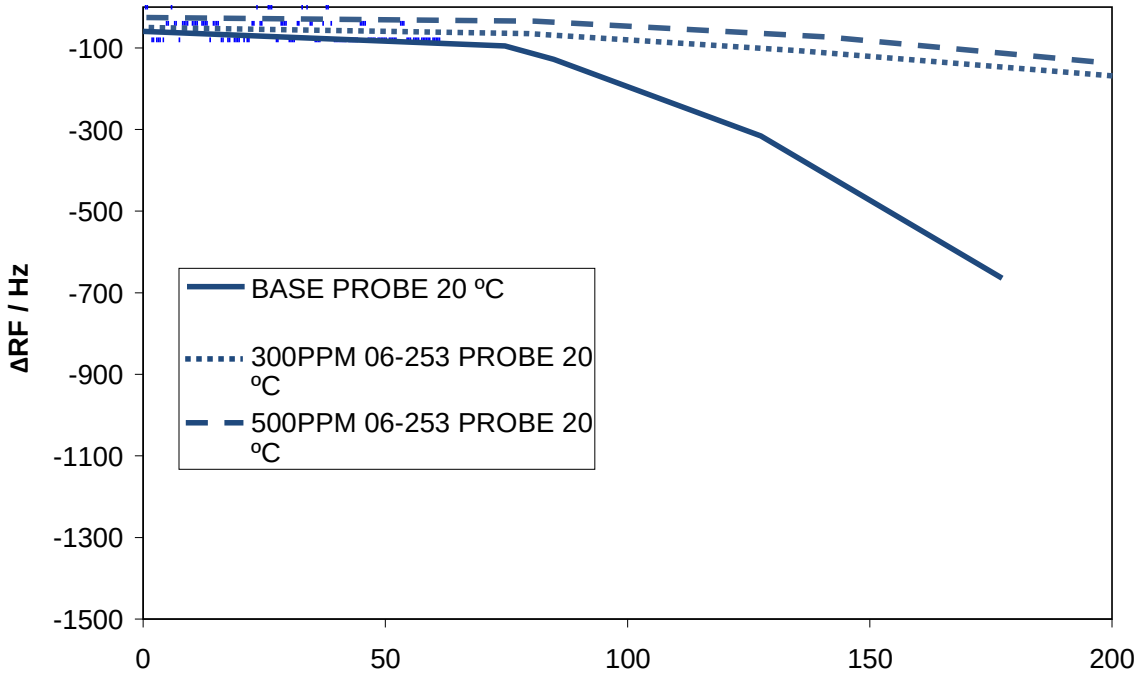

Figure 2.51. Data recorded for test with stabilised crude (Table 2.11) untreated and with 300 and 500 ppm of 06-253, oil held at 30 ºC, wax probe temperature 20 ºC.

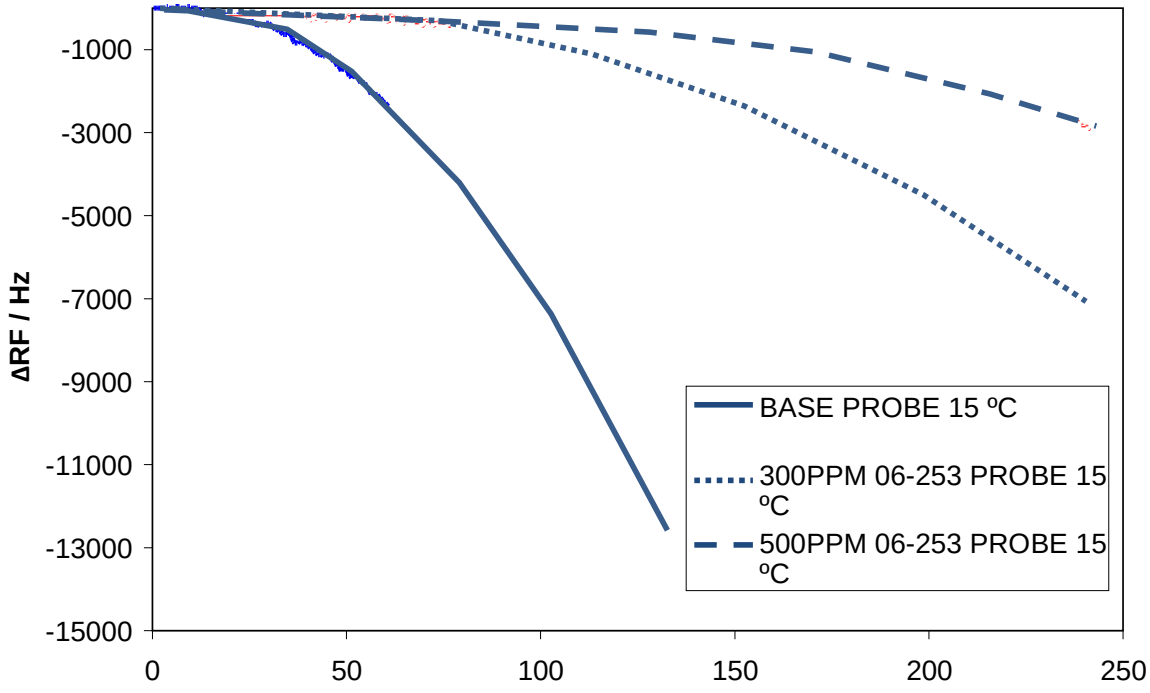

Figure 2.52. Data recorded for test with stabilised crude (Table 2.11) untreated and with 300 and 500 ppm of 06-253, oil held at 30 ºC, wax probe temperature 15 ºC.

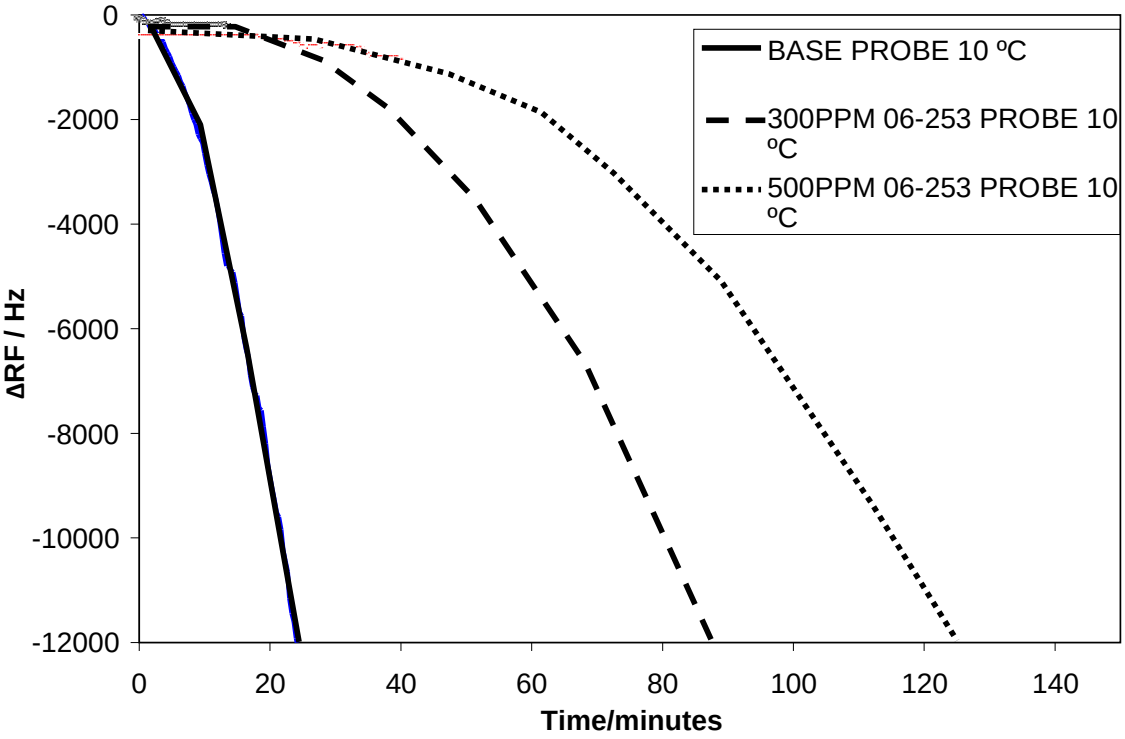

Figure 2.53. Data recorded for test with stabilised crude (Table 2.11) untreated and with 300 and 500 ppm of 06-253, oil held at 30 ºC, wax probe temperature 10 ºC.

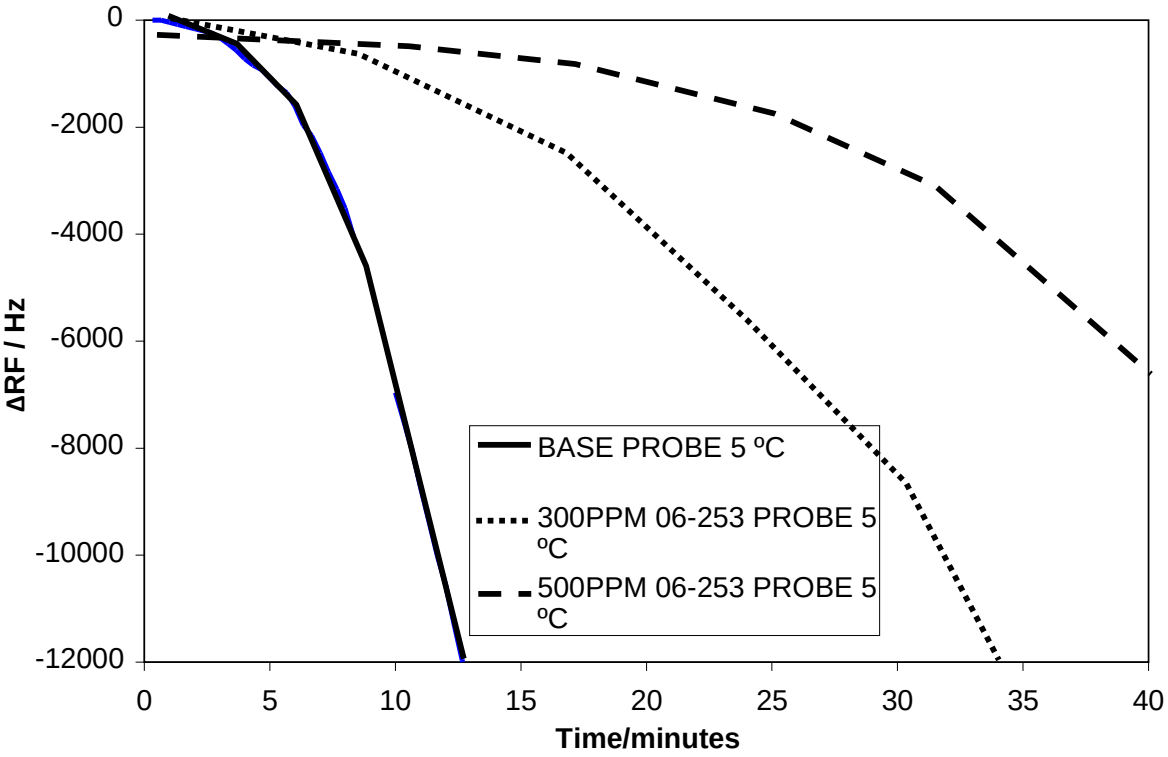

Figure 2.54. Data recorded for test with stabilised crude (Table 2.11) untreated and with 300 and 500 ppm of 06-253, oil held at 30 ºC, wax probe temperature 5 ºC.

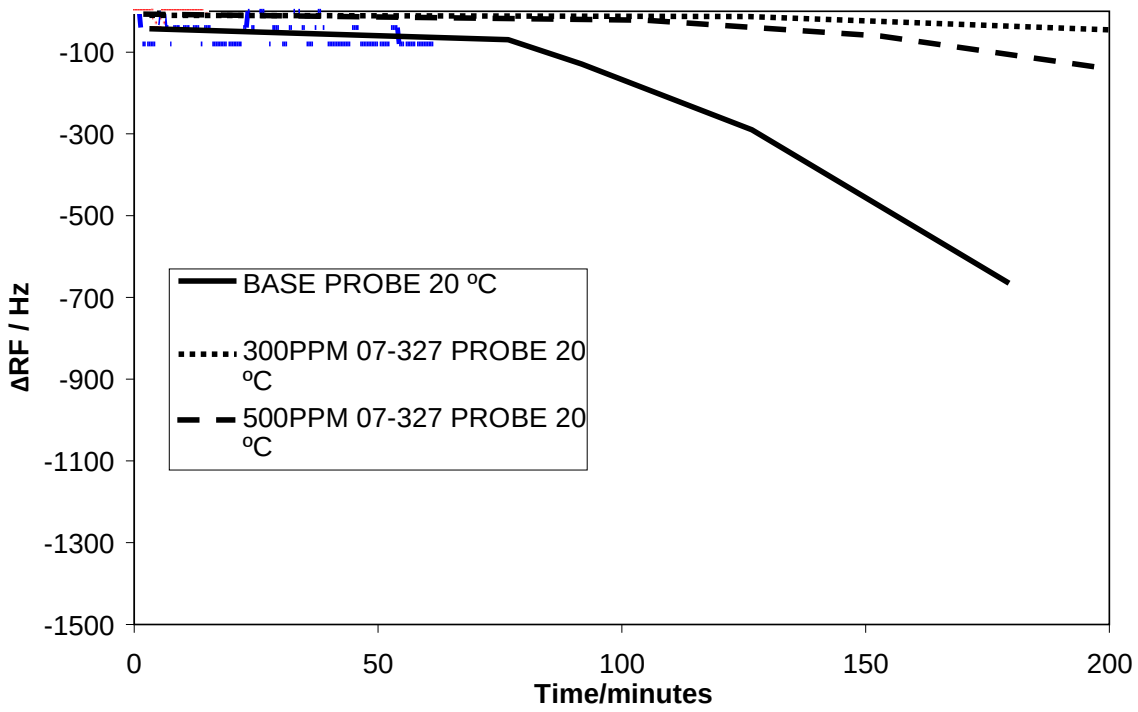

Figure 2.55. Data recorded for test with stabilised crude (Table 2.11) untreated and with 300 and 500 ppm of 07-327, oil held at 30 ºC, wax probe temperature 20 ºC.

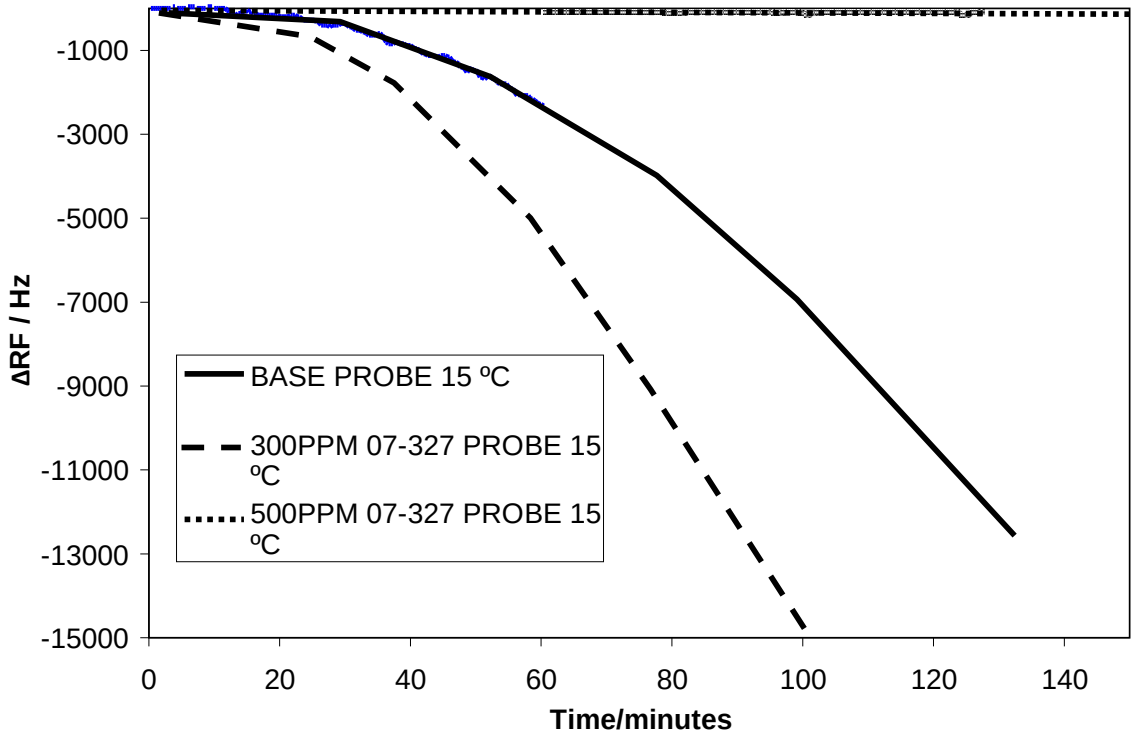

Figure 2.56. Data recorded for test with stabilised crude (Table 2.11) untreated and with 300 and 500 ppm of 07-327, oil held at 30 ºC, wax probe temperature 15 ºC.

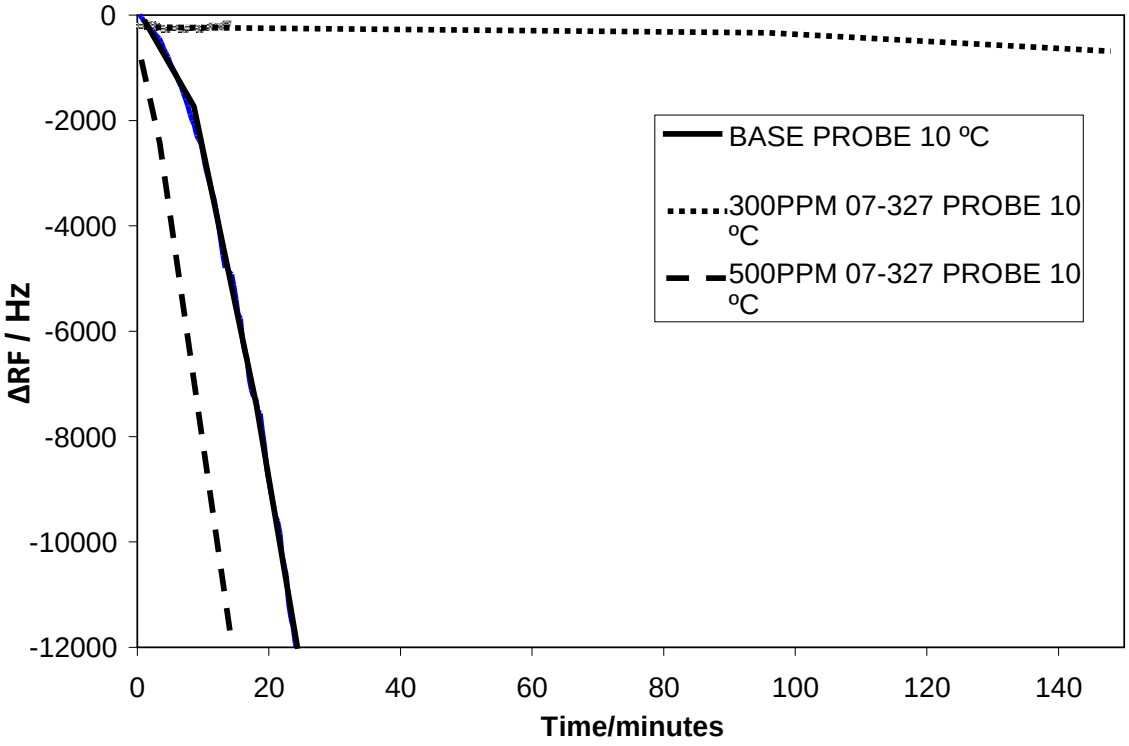

Figure 2.57. Data recorded for test with stabilised crude (Table 2.11) untreated and with 300 and 500 ppm of 07-327, oil held at 30 ºC, wax probe temperature 10 ºC.

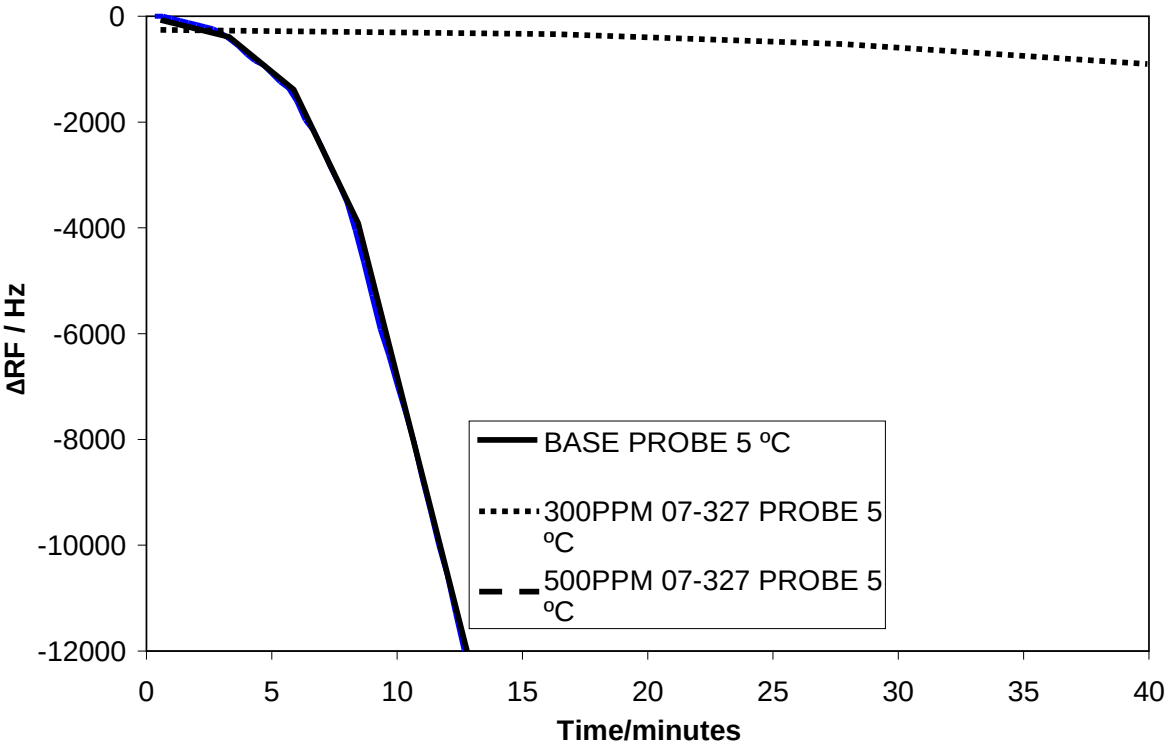

Figure 2.58. Data recorded for test with stabilised crude (Table 2.11) untreated and with 300 and 500 ppm of 07-327, oil held at 30 ºC, wax probe temperature 5 ºC.

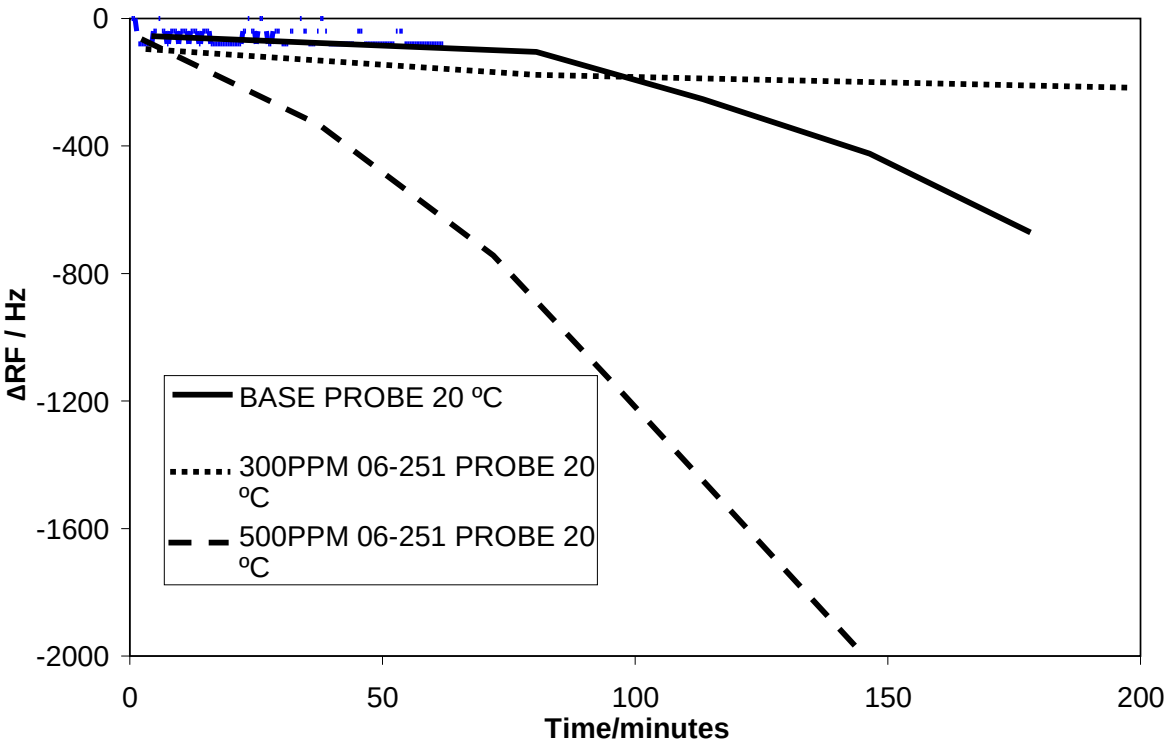

Figure 2.59. Data recorded for test with stabilised crude (Table 2.11) untreated and with 300 and 500 ppm of 06-251, oil held at 30 ºC, wax probe temperature 20 ºC.

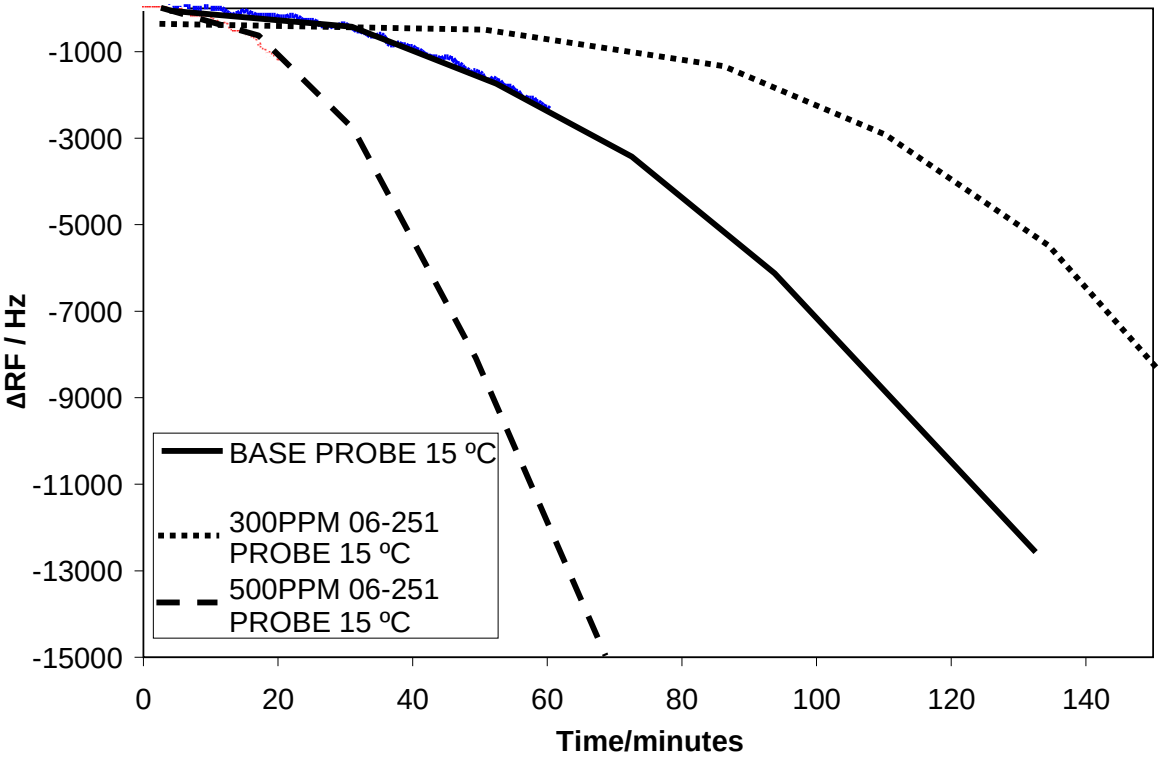

Figure 2.60. Data recorded for test with stabilised crude (Table 2.11) untreated and with 300 and 500 ppm of 06-251, oil held at 30 ºC, wax probe temperature 15 ºC.

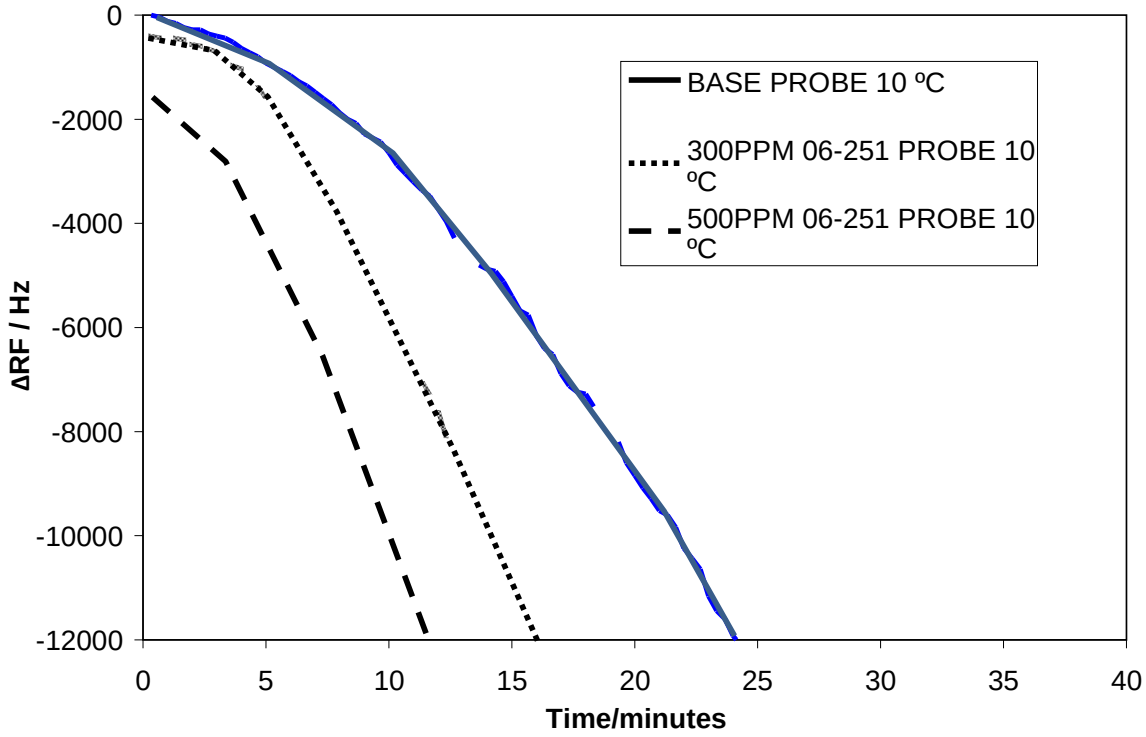

Figure 2.61. Data recorded for test with stabilised crude (Table 2.11) untreated and with 300 and 500 ppm of 06-251, oil held at 30 ºC, wax probe temperature 10 ºC.

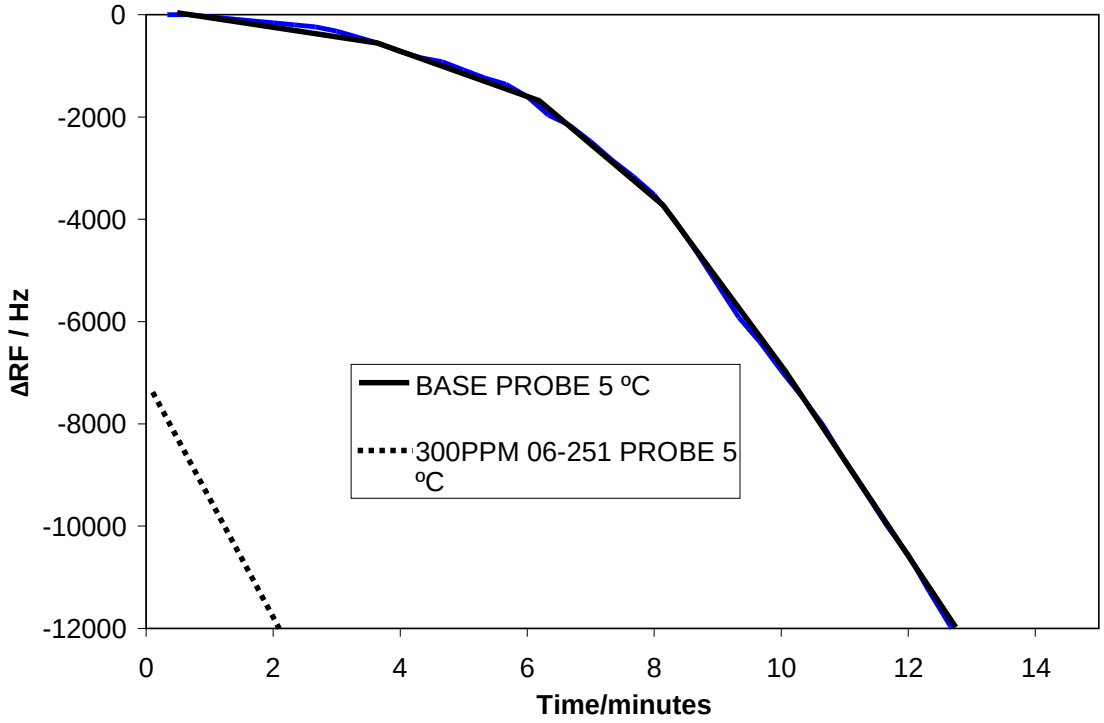

Figure 2.62. Data recorded for test with stabilised crude (Table 2.11) untreated and with 300 ppm of 06-251, oil held at 30 ºC, wax probe temperature 5 ºC (at 500ppm probe heavily loaded before set temperature reached).

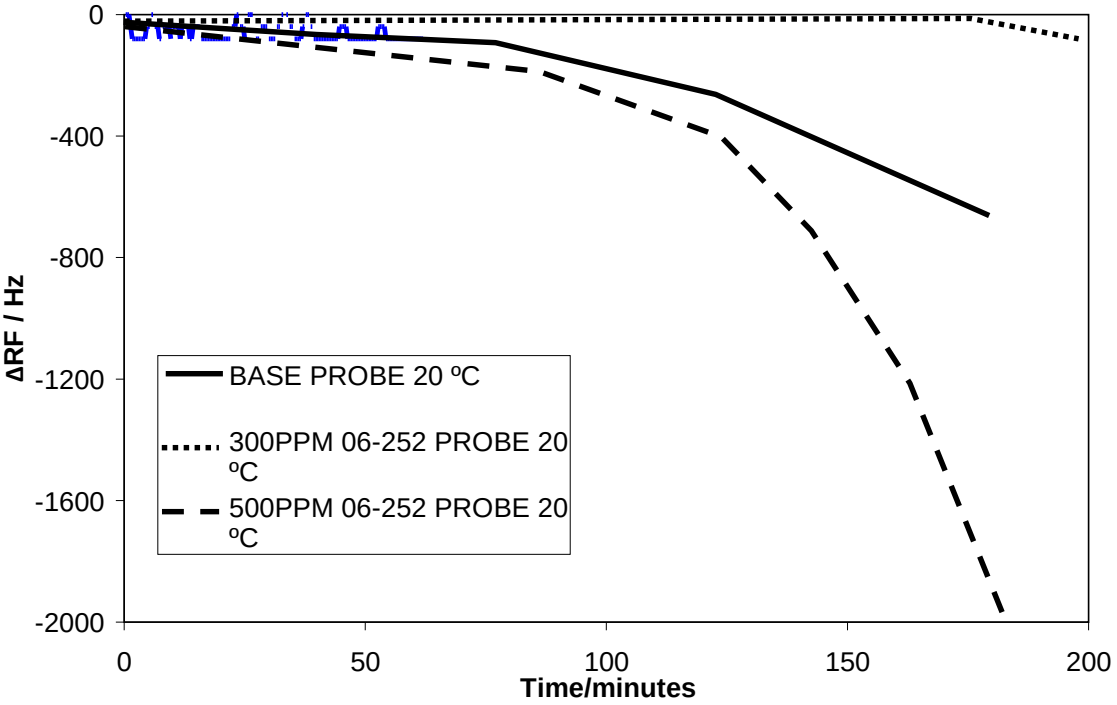

Figure 2.63. Data recorded for test with stabilised crude (Table 2.11) untreated and with 300 and 500 ppm of 06-252, oil held at 30 ºC, wax probe temperature 20 ºC.

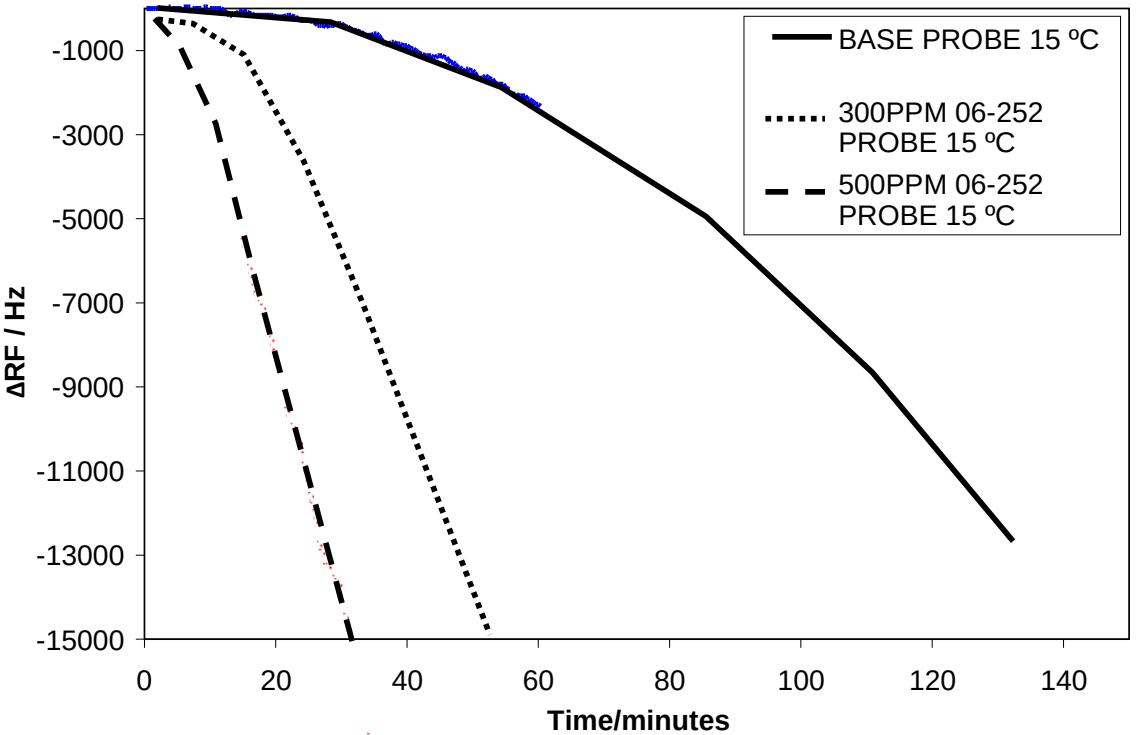

Figure 2.64. Data recorded for test with stabilised crude (Table 2.11) untreated and with 300 and 500 ppm of 06-252, oil held at 30 ºC, wax probe temperature 15 ºC.

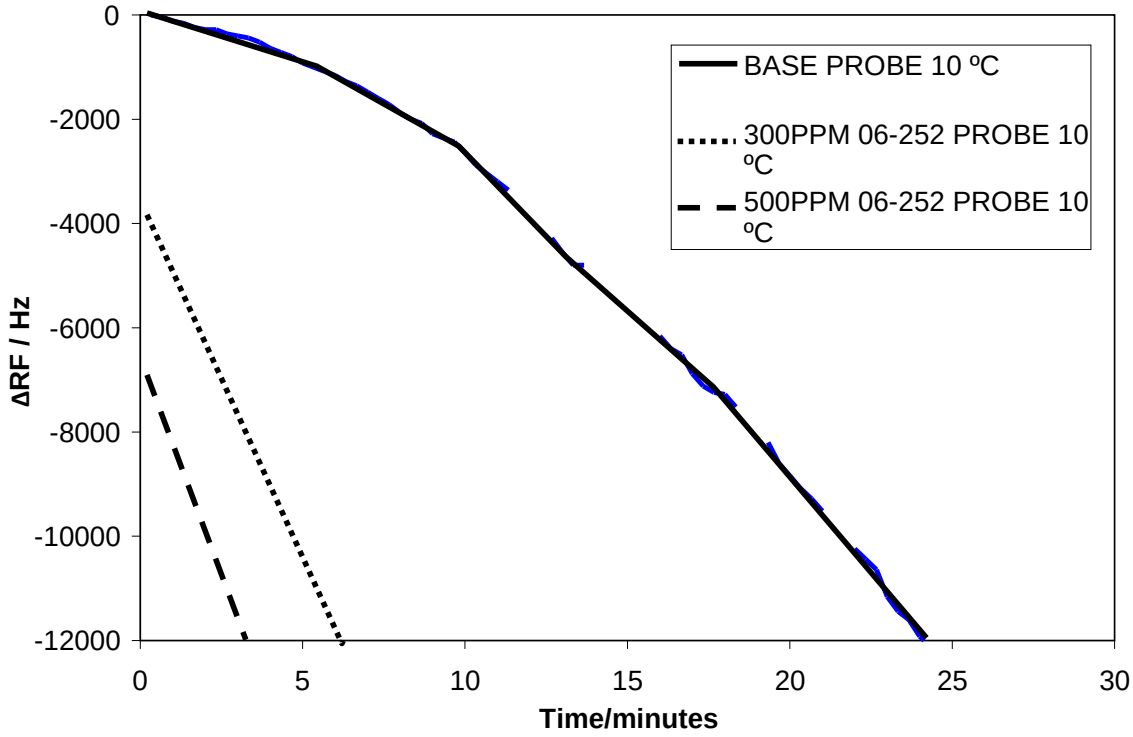

Figure 2.65. Data recorded for test with stabilised crude (Table 2.11) untreated and with 300 and 500 ppm of 06-252, oil held at 30 ºC, wax probe temperature 10 ºC.

2.7.3. Cold finger tests

Cold finger tests were conducted by another laboratory using the same oil and inhibitors in order to have independent verification of the experimental results. The apparatus, procedures and test results are given below.

2.7.3.1. Apparatus and procedure

The procedure is suitable for the evaluation of the performance of paraffin dispersants. It is based on the fact that the paraffin of a crude oil will deposit on a surface with a temperature below the Wax Appearance Temperature. Efficient paraffin dispersants will prevent paraffin crystals from depositing and will reduce the amount of paraffin sticking to the surface. Comparative determination of the mass of precipitated paraffins gained from treated and untreated crude oils allows the assessment of the effectiveness in form of a percentage of inhibition. This test is a comparative one so where possible inhibitors should be tested at the same time as small differences in test duration and test temperatures will have a large effect on percentage inhibition. It is usual to carry out each inhibitor/dosage rate combination in duplicate. It is usual for upper and lower temperatures to be provided by the project originator.

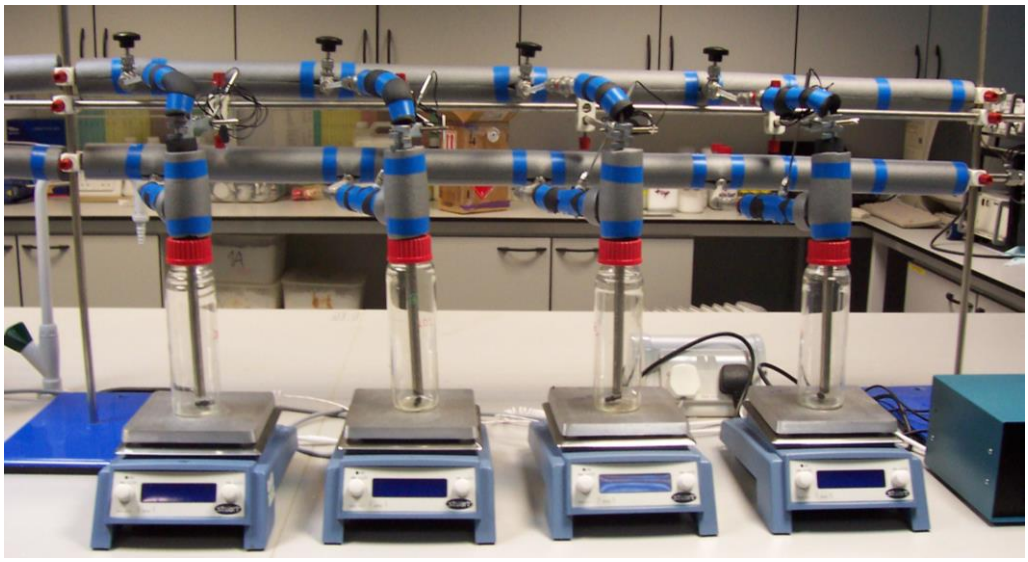

Figure 2.66. Picture of cold finger apparatus.

A picture of the cold finger apparatus is shown in Figure 2.66 above. The individual hot water baths are set to the upper test temperature (45 ºC) and the chiller bath set to the lower temperature (24 ºC). 250ml of treated or untreated crude oil is poured into the cold finger jar. The cold finger is then inserted and the cold finger cell placed into the individual hot water bath. The cells are left to equilibrate for half an hour. The cold fingers are then connected to the cooling bath and the system is left for 4 hours to allow the crude to deposit on the cold fingers. The coolant pump is then switched off and the cold finger removed from the crude. The deposition, which consists of paraffins and other components, can then be scraped off and washed with heptane into a pre-weighed round bottom flask. The solvent is removed using the Rotary Evaporator and the mass of the residue is determined. Percentage inhibition figures can be calculated, by comparing deposited weights of blank and dosed test runs.

2.7.3.2. Test results

The deposition of wax from the crude oil and the inhibition of this deposition was assessed using cold finger testing. The results, expressed as a percentage inhibition (100x(Mass-$Mass_{inh}$)/Mass), are presented in Table 2.12. and plotted in Figures 2.67 through 2.69.

Table 2.12. Summary of results from cold finger tests.

Treatment	Percentage inhibition %
WT 06-251 @ 100ppm	-11
WT 06-251 @ 300ppm	-7
WT 06-252 @ 100ppm	-94
WT 06-252 @ 300ppm	-106
WT 06-253 @ 100ppm	21
WT 06-253 @ 300ppm	34
WT 07-327 @ 50ppm	15
WT 07-327 @ 100ppm	21
WT 07-327 @ 200ppm	29
WT 07-327 @ 300ppm	30

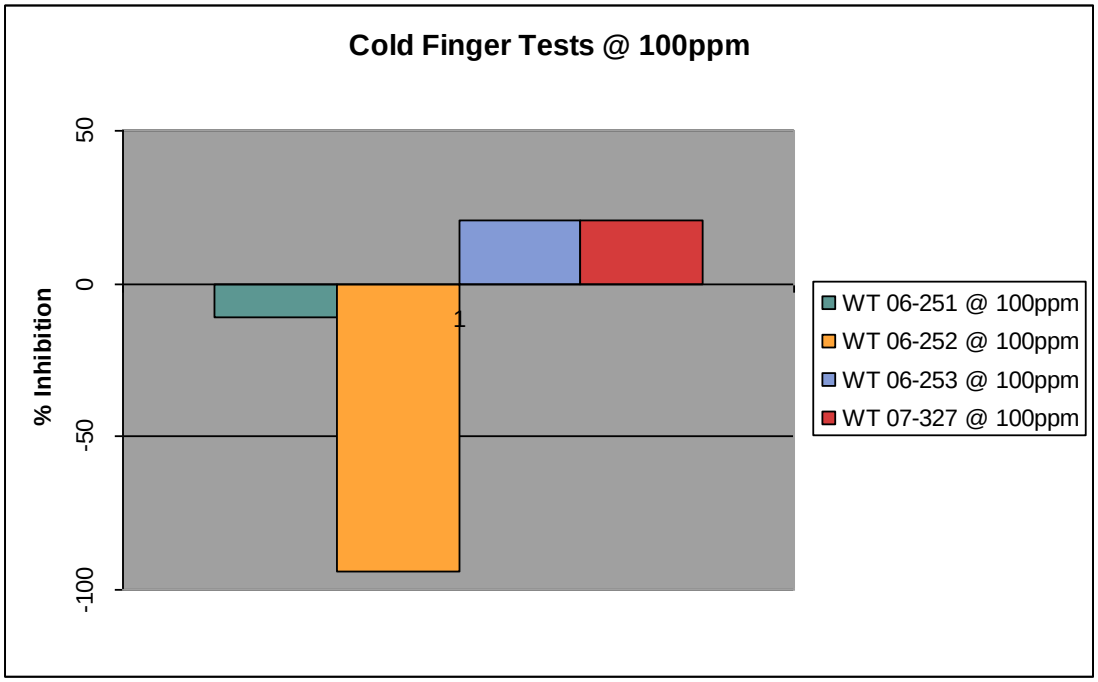

Figure 2.67. Percentage inhibition at 100ppm.

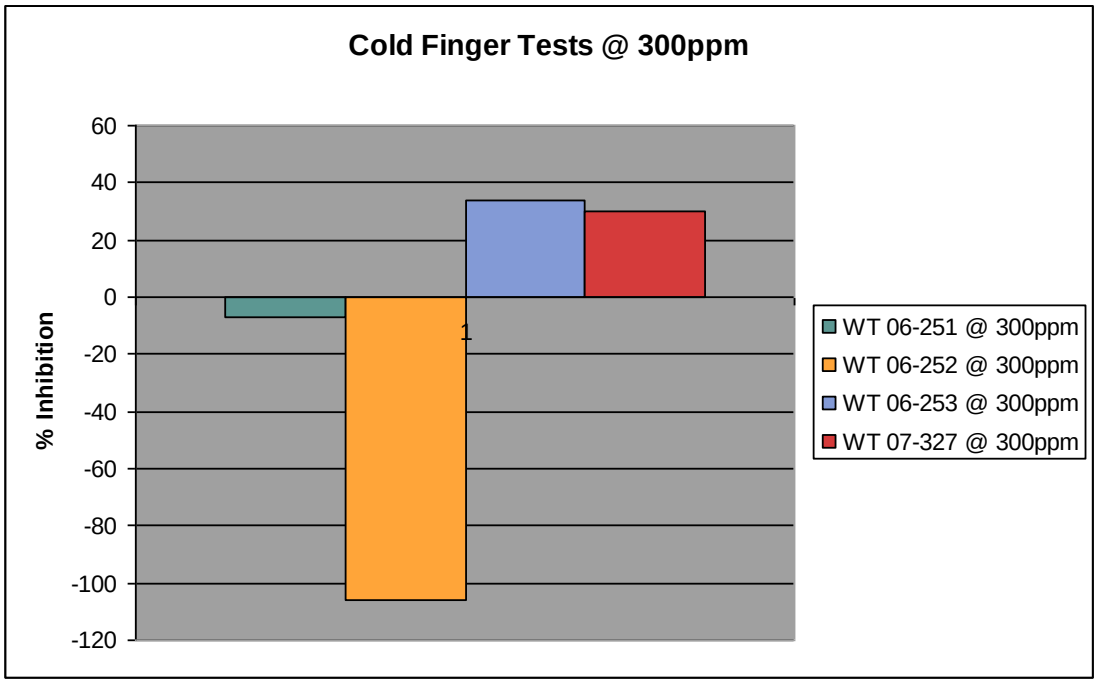

Figure 2.68. Percentage inhibition at 300ppm.

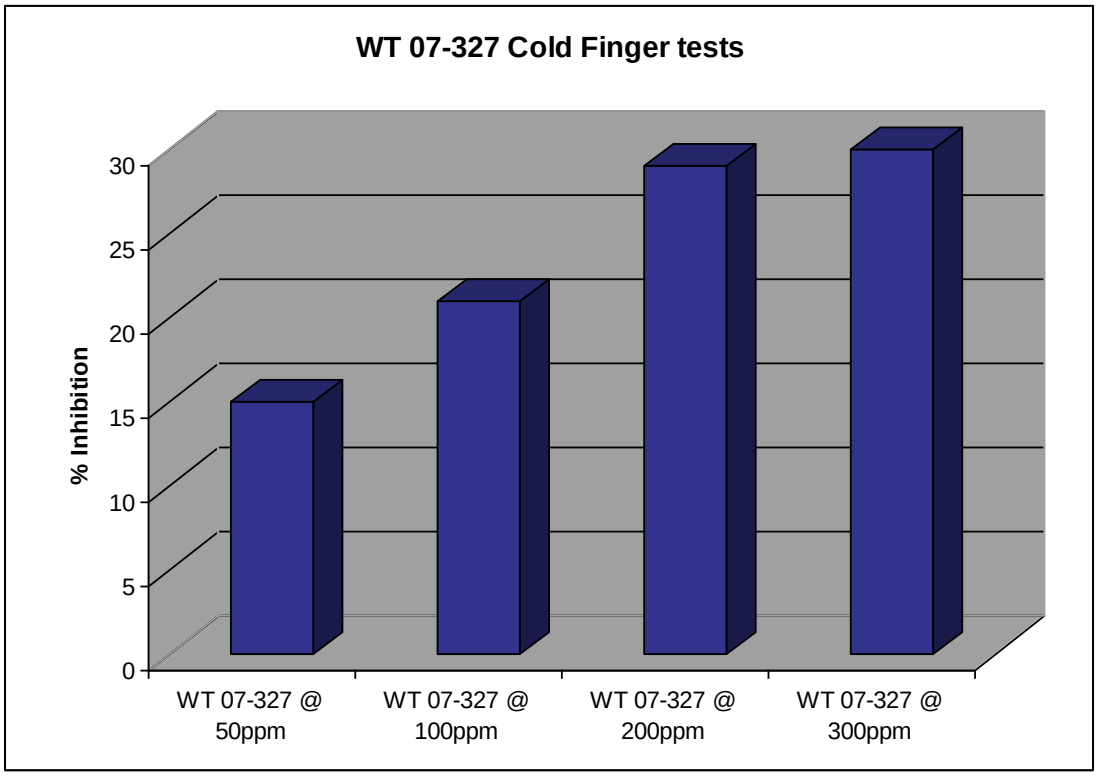

Figure 2.69. Percentage inhibition with WT 07-327.

2.7.3.3. Conclusions

The results of the cold finger testing show that the most effective product for treating the stabilized crude (Table 2.11) out of the products tested is 07-327 and 06-253, with both giving around a 30% reduction in deposited wax at a treatment rate of 300 ppm. The results also show that 06-251 and 06-252 have a negative effect on the wax deposition, i.e., increase the amount of wax, particularly 06-252.

If these results are compared to the QCM test data, it can be seen that the best two performing chemicals using both test methods were 07-327 and 06-253. It is also apparent that the negative impact of both 06-251 and 06-252 is observed in both test procedures. In addition the worst performing chemical 06-252 was the same for both data sets.

Overall these tests show that both QCM and cold finger tests give comparable results. The QCM method will clearly be better in terms of the amount of stabilized oil required (i.e., around 35 ml) which potentially could be recovered and reused. The cold finger set-up requires 250 ml per test and the fluid cannot be re-used i.e. heated and re-used with a different inhibitor dose rate. This is not useful in cases where the amount of fluid available for tests is limited. The QCM can give more information because many more parameters can be studied and results can be viewed during the test. This could have many useful features, e.g., early indication of the results, pattern of solid build-up as a function of time, etc. In the case of the cold finger only one value is obtained i.e. the amount of solids adhering to the cold surface and at the end of the test. The fact that the QCM tests can be run at different temperature gradients may help to find the most likely problem areas for a particular pipeline / oil scenario and then to optimize inhibitor type and dose rate to target the potential problem.

One important point is that the cooled QCM set-up can be used at pressure with live fluids. As shown in Section 2.6.3.2, the presence of light components (C_1 to C_4) has a significant impact upon the wax adhesion tendency, therefore it may be the case that the optimum dose rate of inhibitor based upon tests with stabilized crude could be too high. In **Chapter 3** the use of the QCM for evaluating inhibitors for a live fluid is presented.

2.8. Conclusions

The conclusions that can be made from the work presented in this chapter, aimed at developing and validating new equipment and approaches for tests with wax and wax inhibitors are as follows:

- Tests with synthetic fluids using the small volume (5 ml test fluid) QCM glass tube assembly showed that accurate measurements of WAT and WDT could be made. The fact that the generated data for the solubility of hexatriacontane agreed with literature data from three sources and predictions made using the Heriot-Watt Wax model HWWAX [33] confirms the accuracy of the measurements.
- The QCM method for measuring WAT and WDT values can be used for stabilised and live reservoir fluids at a wide range of P / T conditions.
- A temperature controlled QCM rig has been developed that can be used for making measurements of wax adhesion tendency at pipeline conditions, mimicking temperature gradients between oil and pipeline wall.
- The use of a multi-cell ambient pressure set-up to screen inhibitors at different dose rates has been demonstrated.
- The QCM method can give more information regarding inhibitor performance than pour point testing alone.
- The use of the temperature controlled QCM rig to screen inhibitors at different dose rates has been demonstrated. The results agreed with standard cold finger test results for the same fluid and inhibitors. The temperature controlled QCM set-up has distinct advantages in terms of the amount of fluid required, the information obtained and the capability to run tests at field conditions.
- It may be possible to use QCM test data to investigate the possibility of blending inhibitors to improve performance in cases where one inhibitor is not able to reduce wax adhesion across the whole range of conditions encountered at pipeline conditions.

It should be noted that to investigate the effect of shear stress on inhibitor performance would require tests using a rheometer or a flow loop. A QCM could also be used if embedded into the wall of a mixed autoclave cell.

2.9. References

[1] Holder G.A., and Winkler J., *Wax Crystallization form Distillate Fuels*, Journal of the Institute of Petroleum, Volume 51, Number 499, July (1965).

[2] Lundager Madsen, H.E., and Boistelle, R., *Solubility of Long-Chain n-Paraffins in Pentane and Heptane*, J. Chem. Soc., Faraday Trans. 1, **72**, 1078-1081, (1976).

[3] Roberts, K.I., Rousseau, R.W., and Teja, A.S., *Solubility of Long-Chain n-Alkanes in Heptane between 280 and 350 K*, J. Chem. Eng. Data, 39, 793-795, (1994).

[4] Ashbaugh, H. S., Radulescu, A., Prud'homme, R. K., Schwahn, D., Richter, D., and Fetters, L. J., *Interaction of paraffin wax gels with random crystalline/amorphous hydrocarbon copolymers*, Macromolecules 35, 7044–7053, (2002).

[5] Bhat, N.V. and A.K. Mehrotra, *Measurement and prediction of the phase behavior of wax-solvent mixtures: Significance of wax disappearance temperature*, *Industrial & Engineering Chemistry Research*, 43(12), 3451-3461 (2004).

[6] Rønningsen, H. P., Bjørndal, B., Hansen, A. B., and Pedersen, W. B, *Wax Precipitation from North Sea Crude Oils. 1. Crystallization and Dissolution Temperatures, and Newtonian and Non-Newtonian Flow Properties*, Energy Fuels 5, 895-907 (1991).

[7] Kok, M. V., Letoffe, J. M., Claudy, P., Martin, D., Garcin, M., and Volle, J-L. *Comparison of wax appearance temperature of crude oils by differential scanning calorimetry, thermosmicroscopy and viscometry*, Fuel, v.75 (7), p. 787-790, (1996).

[8] Mongure-McClure, T.G., Tackett, J.E., and Merrill, L.S., *Comparisons of Cloud Point Measurement and Paraffin Prediction Methods*, SPE Prod. & Facilities 14 (1), February (1999).

[9] Leontaritis, K. J., and Leontaritis, J. D., *Cloud Point and Wax Deposition Measurement Techniques*, In SPE International Symposium on Oilfield Chemistry, Houston, TX, February 5-7, 2003; Society of Petroleum Engineers Inc., (2003).

[10] Fogler, H., Singh, P., and Nagarajan, N., *Prediction of the Wax Content of the Incipient Wax-Oil Gel In a Pipeline: An Application of the Controlled-Stress Rheometer*, J. Rheol., 43 (6), 1437-1459 (1999).

[11] Elsharkawy, A. M., Al-Sahhaf, T. A., and Fahim, M. A., *Wax Deposition from Middle East Crudes*, Fuel, 79, 1047–1055 (2000).

[12] Wardhaugh, L. T., and Boger, D. V., *Flow Characteristics of Waxy Crude Oils: Application to Pipeline Design*, AIChE J. 37, 871–885 (1991).

[13] Jiang, Z., Hutchinson, J.M., and Imrie, C.T., *Measurement of the wax appearance temperatures of crude oils by temperature modulated differential scanning calorimetry,* Fuel 80, 367-371, (2001).

[14] Claudy, P., Letoffe, J. M., Neff, B., and Damin, B., *Diesel fuels: determination of onset crystallization temperature, pour point and filter plugging point by differential scanning calorimetry. Correlation with standard test methods,* Fuel, 65, 861–864 (1986).

[15] Hansen, A. B., Larsen, E., Pedersen, W. B., Nielsen, A. B., and Rønningsen, H. P., *Wax Precipitation from North Sea Crude Oils. 1. Precipitation and dissolution of wax studied by differential scanning calorimetry,* Energy Fuels 5, 914–923 (1991).

[16] Davidsen, S., and Hamouda, A., *Innovative Method To Determine The Wax Content And The Wax Precipitation Temperature Simultaneously For Crude Oils At Pipeline Pressures,* In SPE International Symposium on Oilfield Chemistry, Houston, TX, February 16-19, Society of Petroleum Engineers Inc., (1999).

[17] Kruka, V. R., Cadena, E. R., and Long, T. E., *Cloud-Point Determination for Crude Oils,* J. Pet. Technol., 681–687 (1995).

[18] Roehner, R. M., and Hanson, F. V., *Determination of Wax Precipitation Temperature and Amount of Precipitated Solid Wax versus Temperature for Crude Oils using FT-IR Spectroscopy,* Energy Fuels, 15, 756–763 (2001).

[19] Alex, R. F., Fuhr, B. J., and Klein, L. L., *Measurement of wax precipitation temperature and precipitated solid weight percent versus temperature by infrared spectroscopy,* Energy Fuels, 5, 866–868 (1991).

[20] Dantas Neto, A.A., Gomes, E.A.S., Barros Neto, E.L., Dantas, T.N.C., and Moura, C.P.A.M., *Determination of wax appearance temperature (wat) in paraffin/solvent systems by photoelectric signal and viscosimetry,* Brazilian Journal of Petroleum and Gas, V.3, n.4, pp. 149-157, (2009).

[21] Coutinho, A.P., and Daridon, J.L., *The Limitations of the Cloud Point Measurement Techniques and the Influence of the Oil Composition on Its Detection,* Petroleum Science and Technology, 23:1113-1128, (2005).

[22] Paso, K., Kallevik, H., and SjoBlom, J., *Measurement of Wax Appearance Temperature Using Near-Infrared (NIR) Scattering,* Energy Fuels, 23, 4988–4994 (2009).

[23] Manka, J.S., and Ziegler, K.L., *Factors Affecting the Performance of Crude Oil Wax-Control Additives*, SPE 67326, Presented at SPE Production and Operations Symposium, Oklahoma City, Oklahoma, 24-27 March (2001).

[24] Sauerbrey, Günter (April 1959), *Verwendung von Schwingquarzen zur Wägung dünner Schichten und zur Mikrowägung*, Zeitschrift für Physik 155 (2): 206–222.

[25] Stockbridge, C.D., *Vacuum Microbalance Techniques*, Plenum, New York, p. 5 (1966).

[26] T. Nomura and O. Hattori, *Determination of micromolar concentrations of cyanide in solution with a piezoelectric detector*, Anal. Chim. Acta, 115, 323–326 (1980).

[27] Kanazawa, K.K., and Gordon J.G., *The oscillation frequency of a quartz resonator in contact with a liquid*, Anal. Chim. Acta 175, pp. 99–105 (1985).

[28] Danesh, A., Todd, A.C., Tohidi, B., and Burgass, R., *Applicability of Oscillating Quartz Crystal in Measuring Fluid Properties in Laboratory or Downhole*, EPSRC research grant final report, ref No: GR/K63641, (1997).

[29] Burgass, R., Todd, A.C., Danesh, A., and Tohidi, B., *Dew Point and Bubble Point Measurement*, U.S. Patent Number 6,223,588 (1999).

[30] Burgass, R., Todd, A.C., Danesh, A., and Tohidi, B., *Clathrate Hydrate Dissociation Point Detection and Measurement*, U.S. Patent Number 6,298,724 (1999).

[31] Spates, J.J., Martin, S.J., Mansure, A.J., and Germer, J.W., *Cloud Point Determination Using a Thickness Shear Mode Resonator*, presented at the 210th Chemical Society National Meeting and Exposition, Chicago, IL, Aug. 20-24, (1995).

[32] Lichter, J.A., *Crystals and Oscillators*, Online book JL9113 Rev. C.

[33] Jennings, D.W., and Weispfennig, K., *Experimental solubility data of various n-alkane waxes: effects of alkane chain length, alkane odd versus even carbon number structures, and solvent chemistry on solubility*, Fluid Phase Equilibria 227, 27-35, (2005).

[34] Ji, H., Tohidi, B., Danesh, A., and Todd, A.C., *Wax Phase Equilibria: Developing a Thermodynamic Model Using a Systematic Approach*, Fluid Phase Equilibria, 216, 201-217 (2004).

[35] Pauly, J., Daridon, J-L., Sansot, J.M., and Coutinho, J.A.P., The pressure effect on the wax formation in diesel fuel, Fuel 82, 595-601, (2003).

[36] Du, X., Du, Y., and George, S.M., *In situ examination of tin oxide atomic layer deposition using quartz crystal microbalance and Fourier transform infrared*

techniques, Journal of Vacuum Science Technology, Volume 23, Issue 4, pp. 581-588 (2005).

[37] Hamouda, A.A., *Wax Deposition Mechanism Under High-Pressure and in Presence of Light Hydrocarbons*, SPE International Symposium on Oilfield Chemistry, New Orleans, L.A., U.S.A., March 2-5, (1993).

[38] Sanjay, M., Baruah, S., and Singh, K., *Paraffin Problems in Crude Oil Production and Transportation: A Review*, SPE Production and Facilities, Volume 10, Number 1, pages 50-54, (1995).

CHAPTER 3 - CASE STUDIES USING DEVELOPED QCM BASED EQUIPMENT AND METHODS FOR WAX MEASUREMENTS

3.1. Introduction

The main justifications for developing equipment and methods for making experimental measurements are that the data generated can be useful for both academic and industrial purposes and that it can improve or complement existing knowledge and capabilities. In order to gain acceptance it is a requirement to be able to prove through projects that the equipment can generate the required data. In this chapter three case studies are detailed. The first project relates to WAT and WDT measurements made for a recombined oil. The second project relates to WAT and WDT measurements made for a recombined condensate where the liquid hydrocarbon volume is low. The third case relates to a wax inhibitor study for a recombined oil using both the multi-cell QCM glass tube assembly and the temperature controlled QCM set-up.

3.2. Experimental WAT and WDT for a live oil using QCM technology

3.2.1. Introduction

The aim of this project was to measure WAT and WDT for a live oil at a range of pressures using QCM based equipment and procedures described in **Chapter 2**. In addition the WAT and WDT for flashed oil at atmospheric pressure was measured and the influence of cooling rate on the measured WAT of the flashed oil was assessed.

3.2.2. Experimental equipment

The windowed cell as described in **Chapter 2**, Section 2.5.1 was used in these tests.

3.2.3. Test fluids

The testing was conducted using a recombined black oil.

3.2.4. Experimental methods

The pressurised sample was heated to 70 °C and the pressure increased to 320 bara by reducing the oil sample volume injecting water below the piston installed in the sample vessel. The sample vessel was then rocked to mix the contents and allowed to stabilise for 24

hours. Single phase oil was transferred to the high pressure visual rig via a heated transfer line to give sufficient liquid phase in the cell to make the first WAT/WDT measurement.

The WAT was determined by reducing the cell temperature at a constant rate of 0.28 °C per minute whilst monitoring the RF and Conductance (G), at RF, of the QCM mounted within the test cell. As the temperature is reduced the viscosity and density of the liquid both increase leading to a reductions in both RF and G. The WAT is indicated by a sharp reduction in both RF and G on cooling as a result of solids adhering to the QCM combined with an increase in viscosity of the fluids in contact with the QCM. The change in RF is normally considered to be more sensitive to solids adhesion than viscosity increase as discussed in Chapter 2, Page 16. The repeatability of the WAT measurements was assessed by running the measurement twice for one of the tests as described in the results section below.

The WDT was measured by increasing the temperature step-wise allowing 30 minutes at each temperature for reaching equilibrium. As the wax solids melt from the QCM on heating, the RF and G increase. When all the wax has melted there is a distinct change in slope when RF is plotted with temperature. Experience has shown that using RF data to determine WDT gives a more easily identifiable point than using conductance data which tends to be more scattered on heating. After each WAT/WDT measurement more single phase oil was injected into the cell in order to make the next WAT/WDT measurement at a higher pressure.

At pressures below the bubble point of the oil no fluids were added or taken from the cell during the WAT/WDT measurements. At pressures above the bubble point a piston cell, containing single phase oil on one side of the piston and compressed gas on the other, was connected to the cell in order to keep the cell pressure relatively stable during the WAT/WDT measurements.

A sample of the single phase oil was flashed in a single stage from a pressure of 300 bara at 70 °C to atmospheric pressure/laboratory temperature (21 °C) and the stabilised liquid was transferred to an atmospheric pressure QCM set-up. Using this set-up the WAT and WDT were measured using the same procedure. In addition the WAT was measured at different cooling rates to assess the influence of this parameter on the measured value.

The bubble point of the single phase sample transferred to the test cell was measured by isochoric step-cooling in order to give a value to check against that measured by another laboratory.

3.2.5. Results

3.2.5.1. WAT/WDT measurements live and flashed oil

The RF and G data from all of the WAT and WDT measurements with the live oil at different pressures are presented in Figures 3.1 through 3.16. The data from the WAT/WDT measurements for the flashed oil are given in Figures 3.17 and 3.18. As can be seen from the WAT test plots the temperature at which both RF and G reduce sharply, as temperature is reduced, is easy to identify. The temperature is very repeatable as shown in Figure 3.5 where data from a repeat test (after reheating the test fluids) is shown. In the case of the WDT plots the RF data on heating does not give such a sharp change in slope at the WDT point compared to that seen in the WAT plots, however the break over point is still easy to identify. The reason for this is that on heating smaller amounts of heavier components remain on the QCM.

Table 3.1 presents the WAT and WDT measurements conducted with the live oil at different pressures along with the measurements with the flashed oil. Figure 3.19 shows a plot of the WAT and WDT measurements conducted with the live oil at different pressures along with the measurements with the flashed oil and the bubble point measurement. As can be seen there is a clear difference between the WAT and WDT measurements of around 20 °C at each pressure. In addition it can be seen that both WAT and WDT data follow similar trends, the temperature reducing with increasing pressure up to close to the saturation pressure and then increasing at higher pressures. This is as would be expected, below saturation pressure the increase in light components dissolved in the oil with increasing pressure, leading to a reduction in both WAT and WDT. Above saturation pressure the composition of the liquid remains unchanged hence the effect of pressure on the wax phase boundary is dominant leading to an increase in both WAT and WDT.

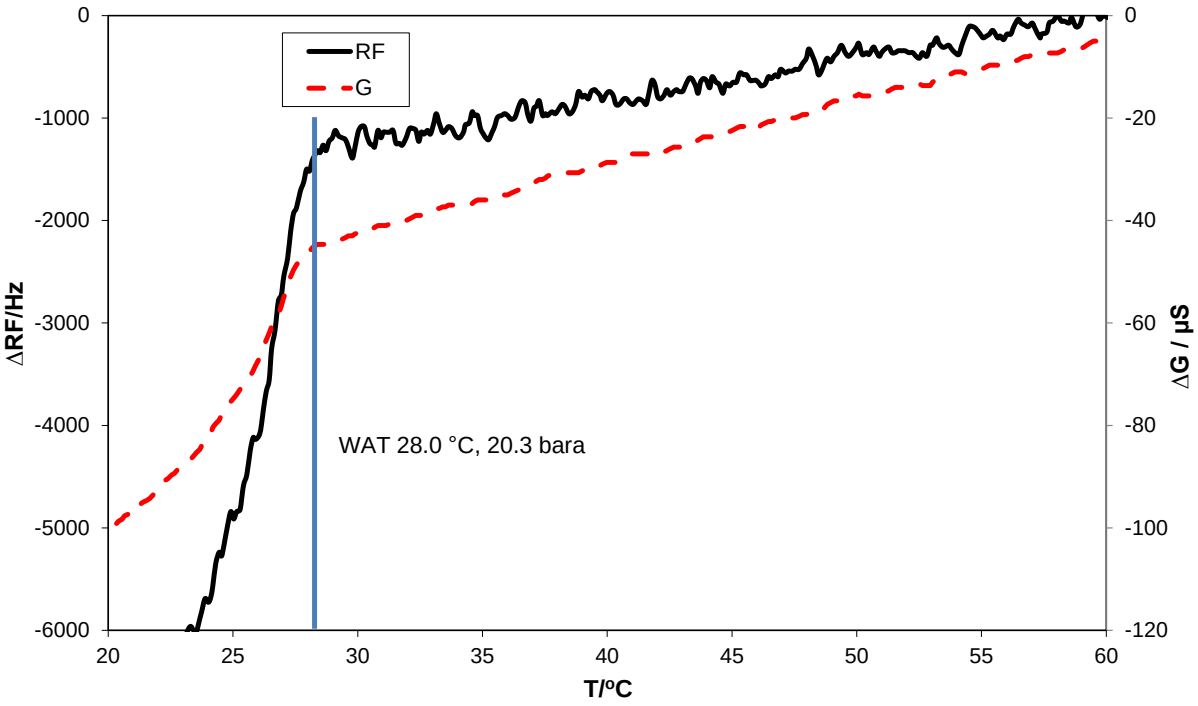

Figure 3.1. RF and G data with temperature for WAT test with live oil at a cooling rate of 0.28 °C per minute.

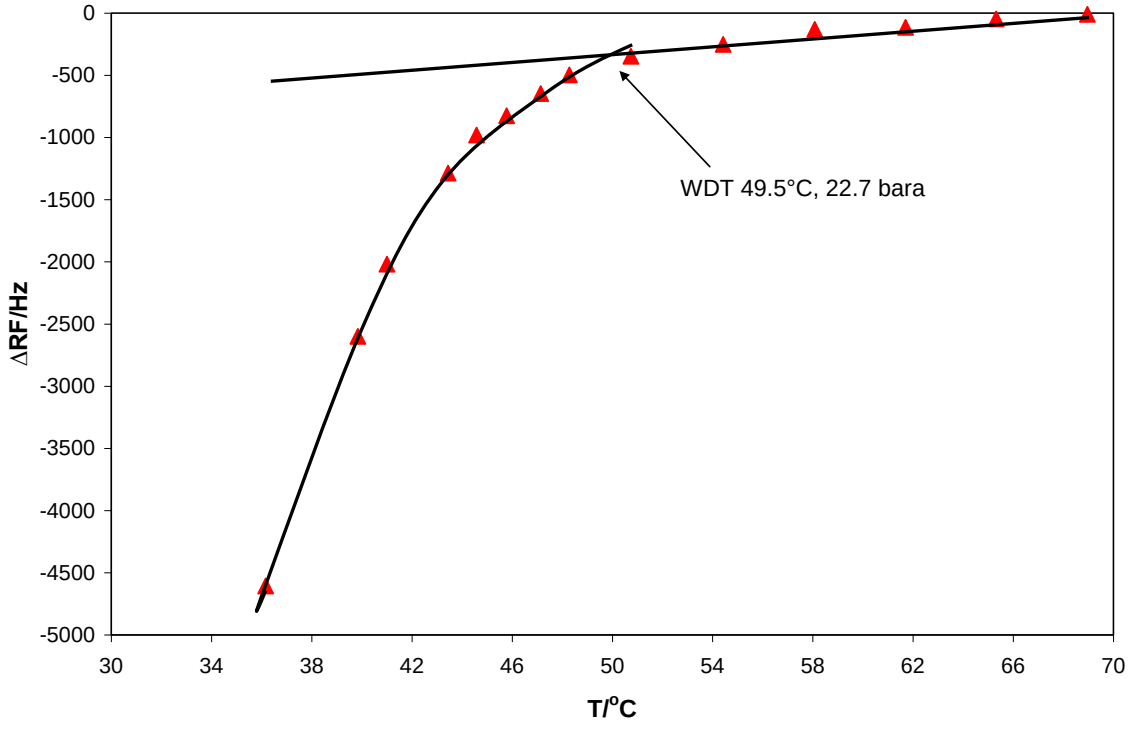

Figure 3.2. RF data with temperature for WDT test with live oil, step-heating allowing 30 minutes at each step for equilibrium.

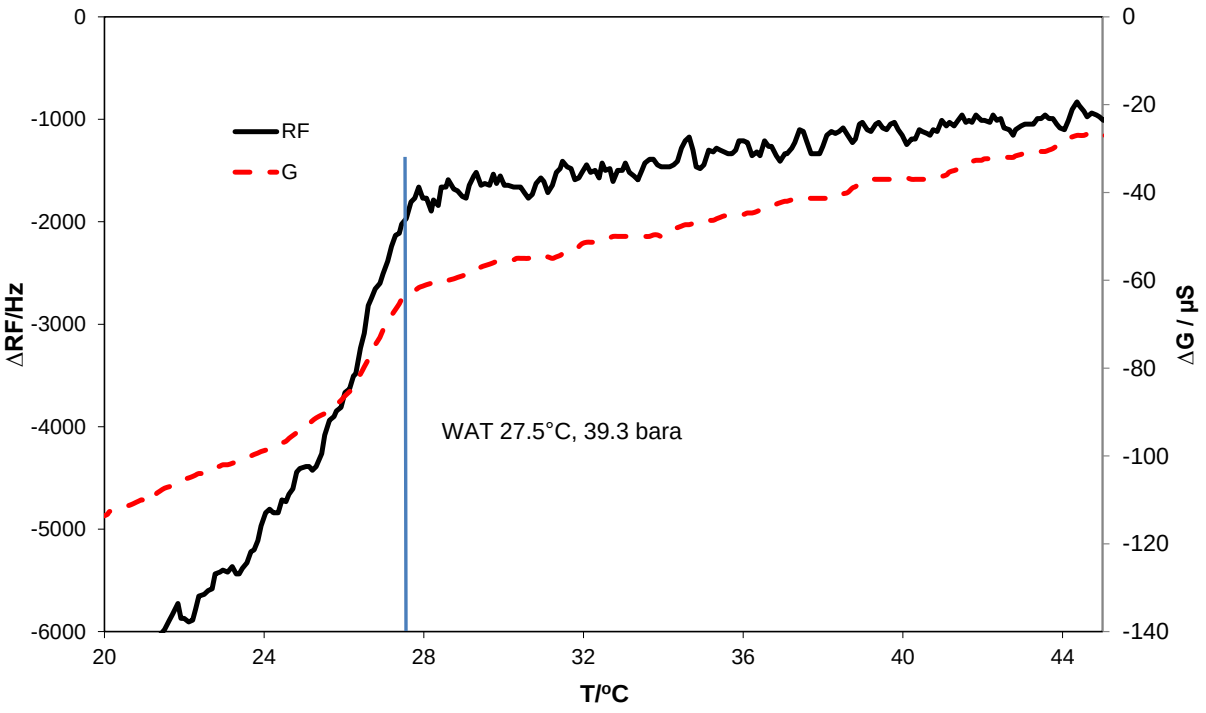

Figure 3.3. RF and G data with temperature for WAT test with live oil at a cooling rate of 0.28 °C per minute.

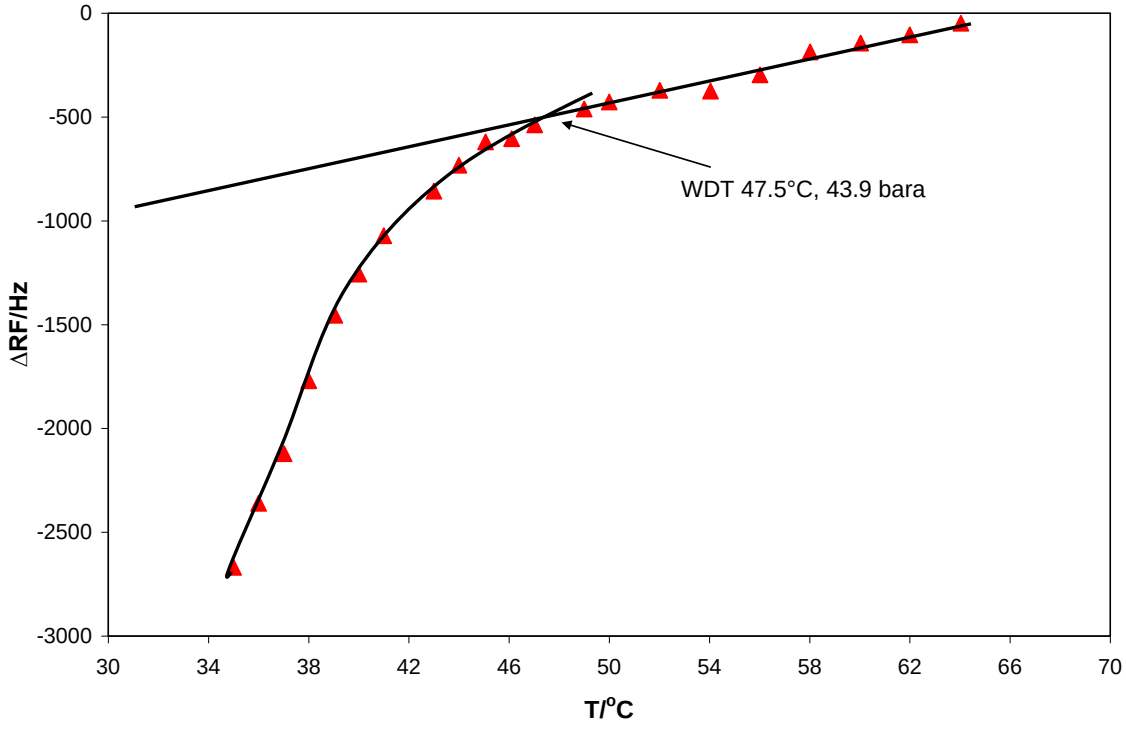

Figure 3.4. RF data with temperature for WDT test with live oil, step-heating allowing 30 minutes at each step for equilibrium.

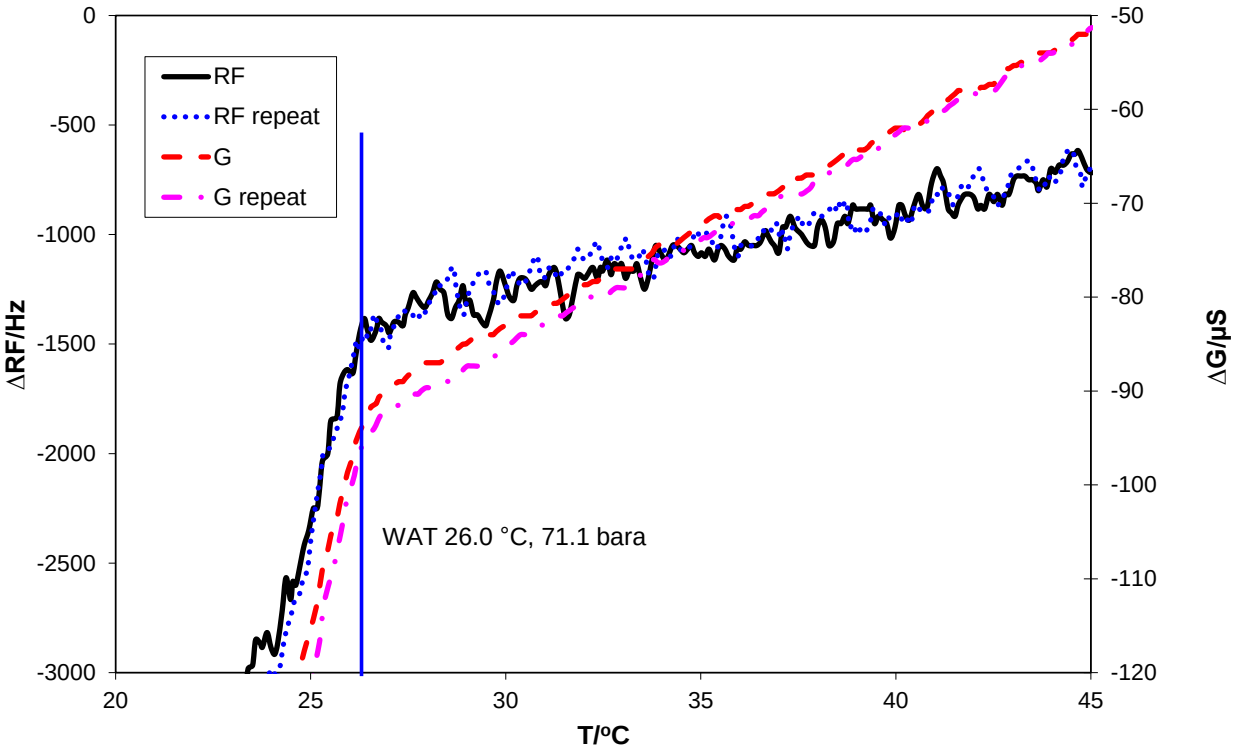

Figure 3.5. RF and G data with temperature for WAT test with live oil at a cooling rate of 0.28 °C per minute. Plot shows repeat cooling after heating to 70 °C.

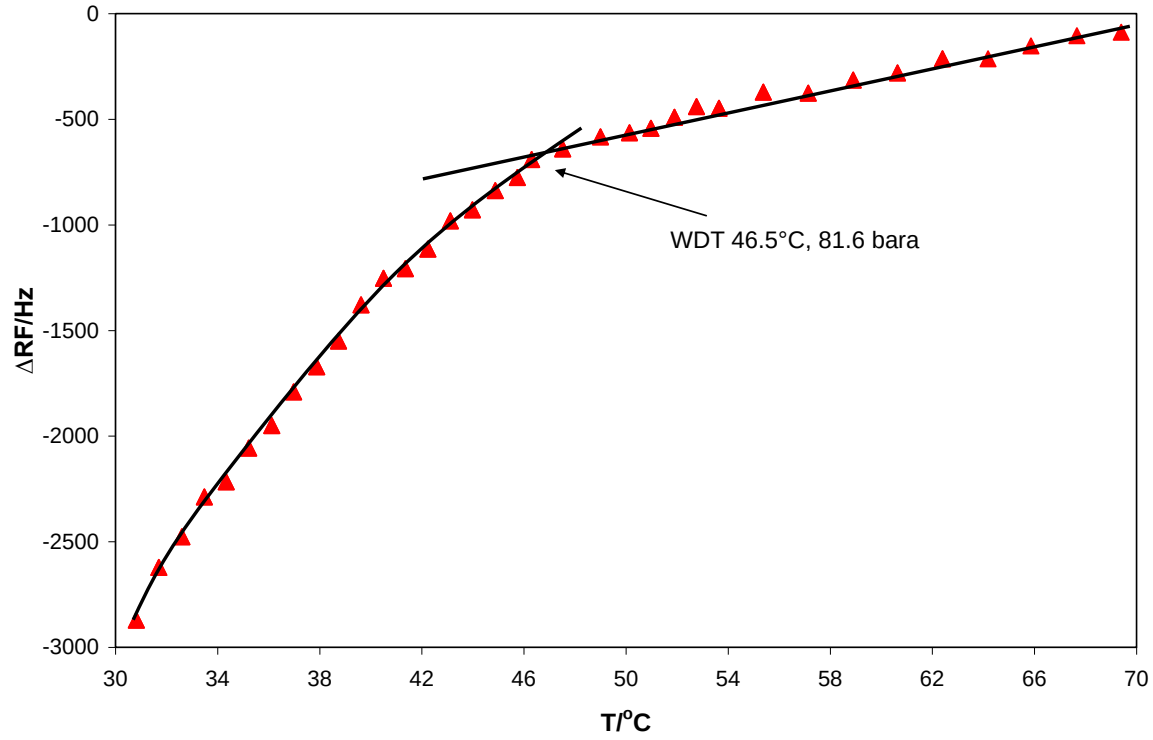

Figure 3.6. RF data with temperature for WDT test with live oil, step-heating allowing 30 minutes at each step for equilibrium.

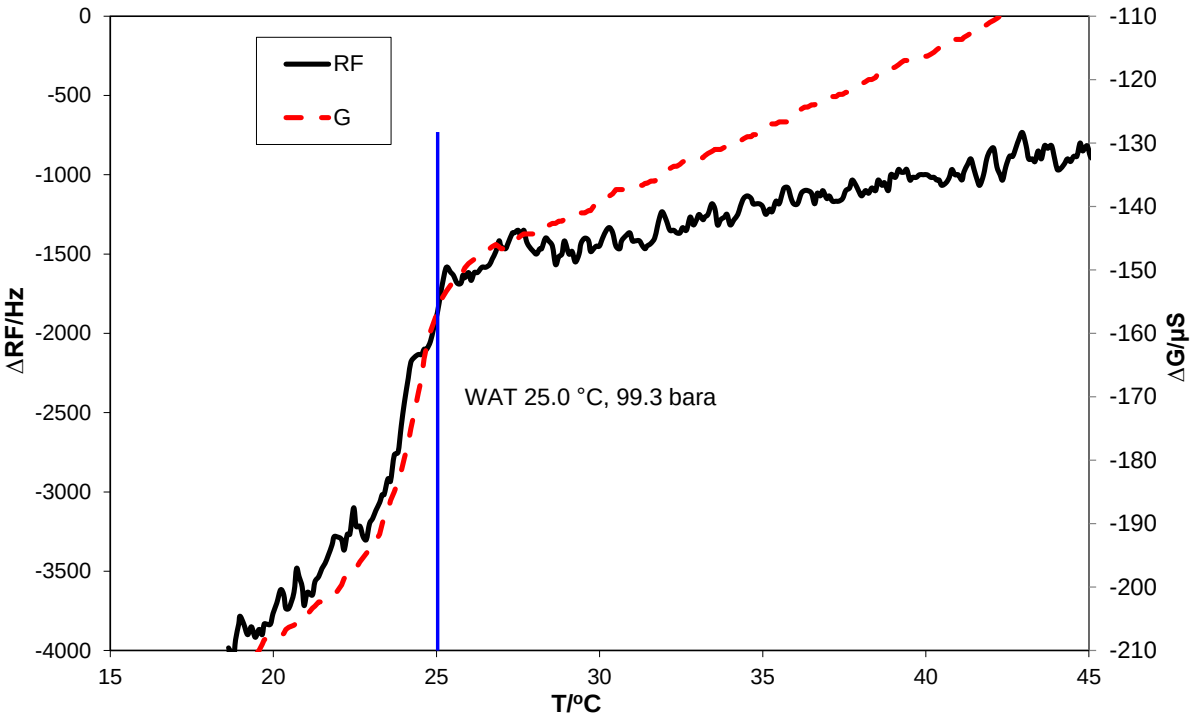

Figure 3.7. RF and G data with temperature for WAT test with live oil at a cooling rate of 0.28 °C per minute.

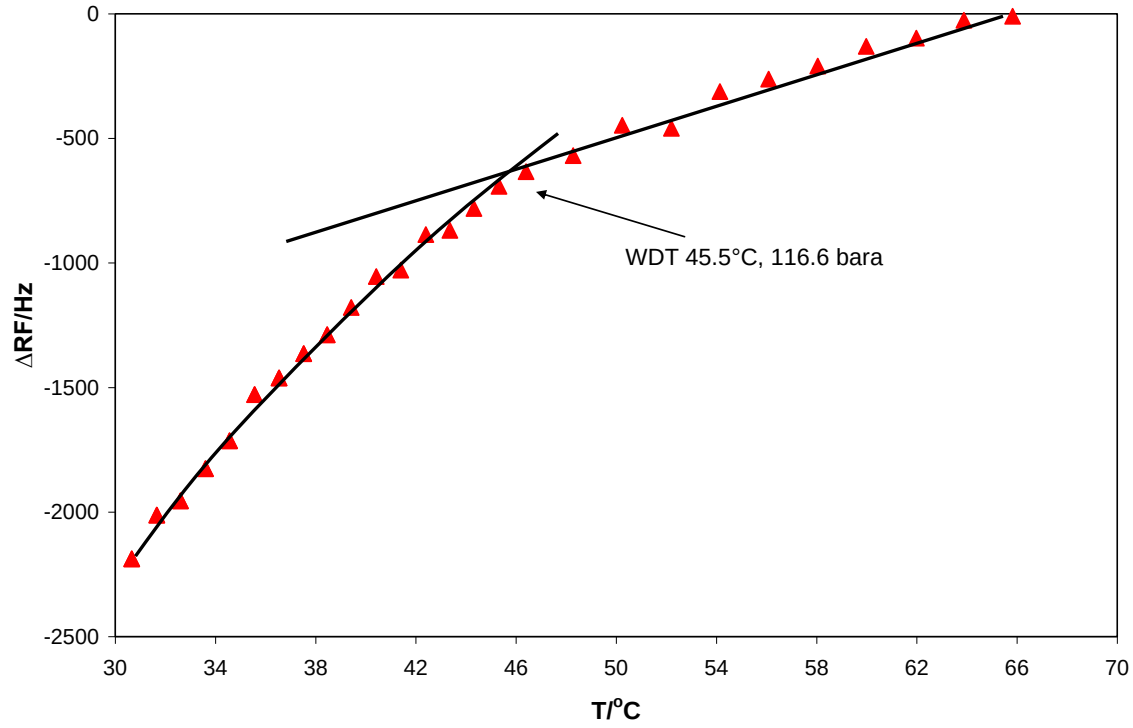

Figure 3.8. RF data with temperature for WDT test with live oil, step-heating allowing 30 minutes at each step for equilibrium.

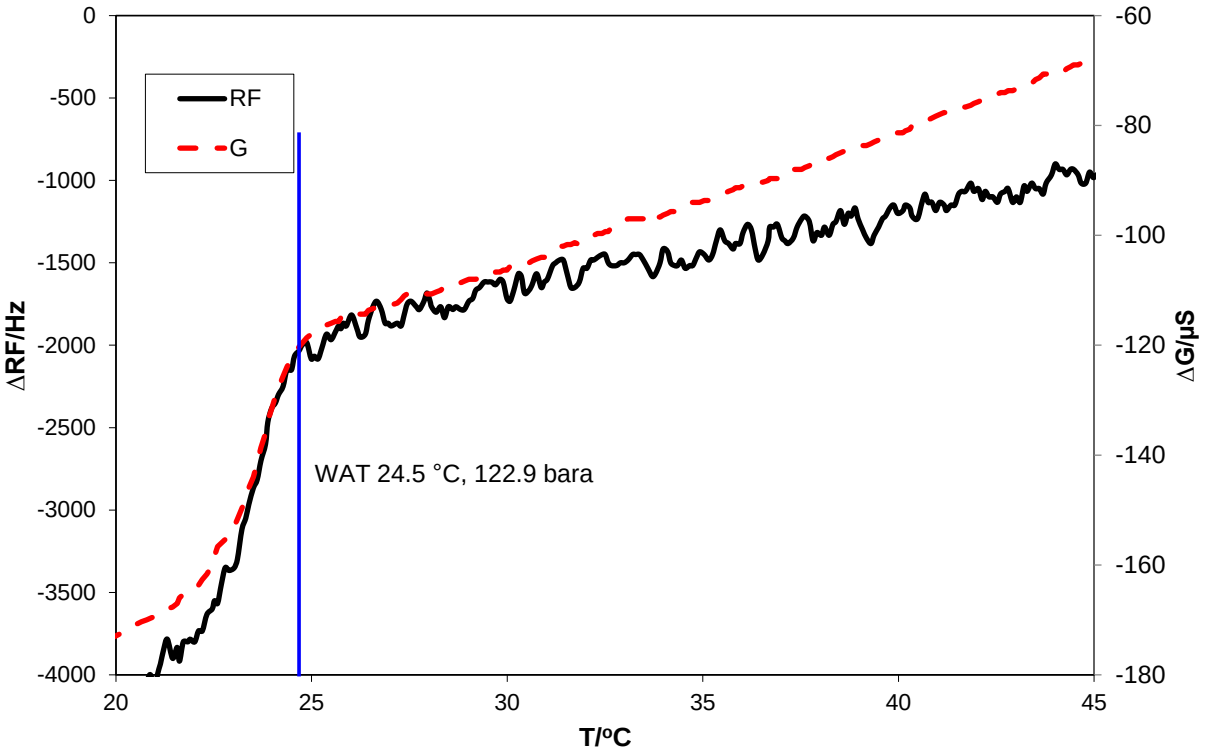

Figure 3.9. RF and G data with temperature for WAT test with live oil at a cooling rate of 0.28 °C per minute.

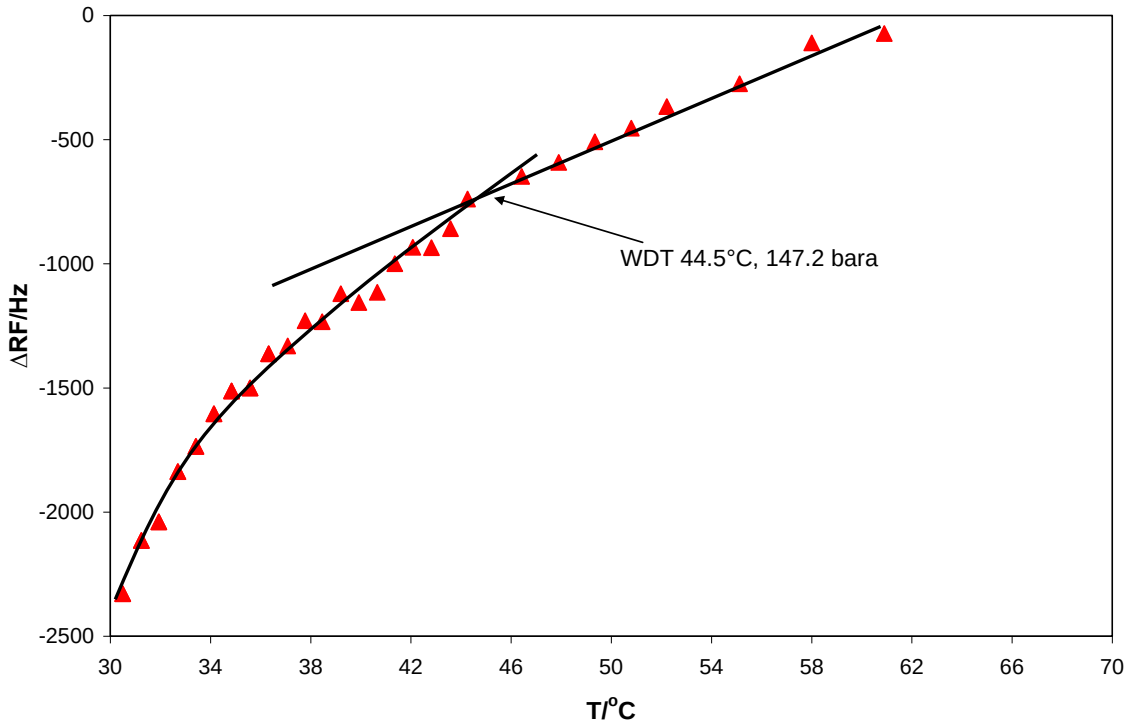

Figure 3.10. RF data with temperature for WDT test with live oil, step-heating allowing 30 minutes at each step for equilibrium.

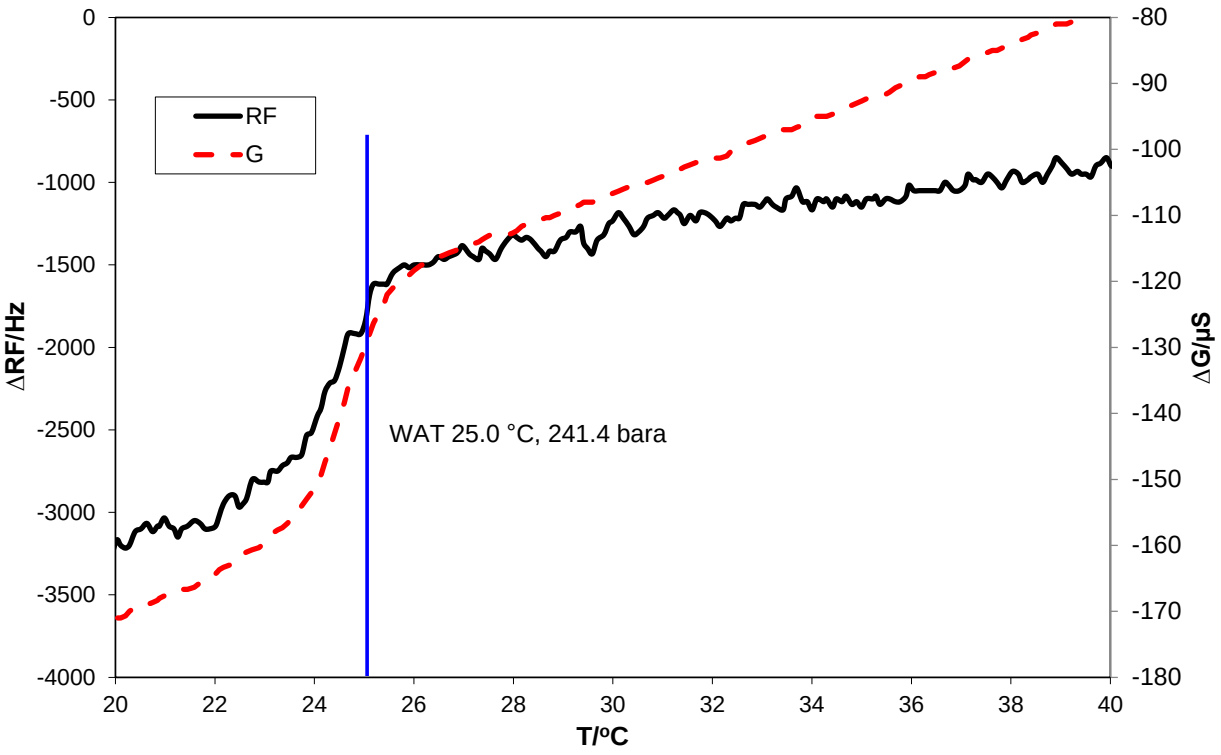

Figure 3.11. RF and G data with temperature for WAT test with live oil at a cooling rate of 0.28 °C per minute.

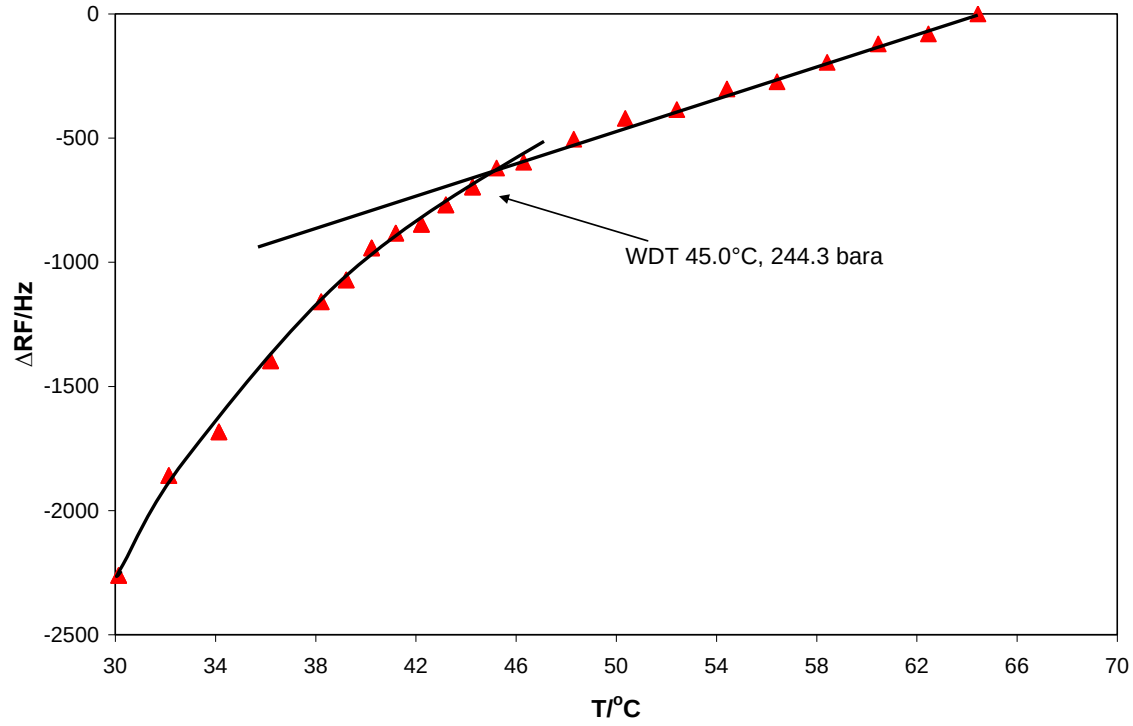

Figure 3.12. RF data with temperature for WDT test with live oil, step-heating allowing 30 minutes at each step for equilibrium.

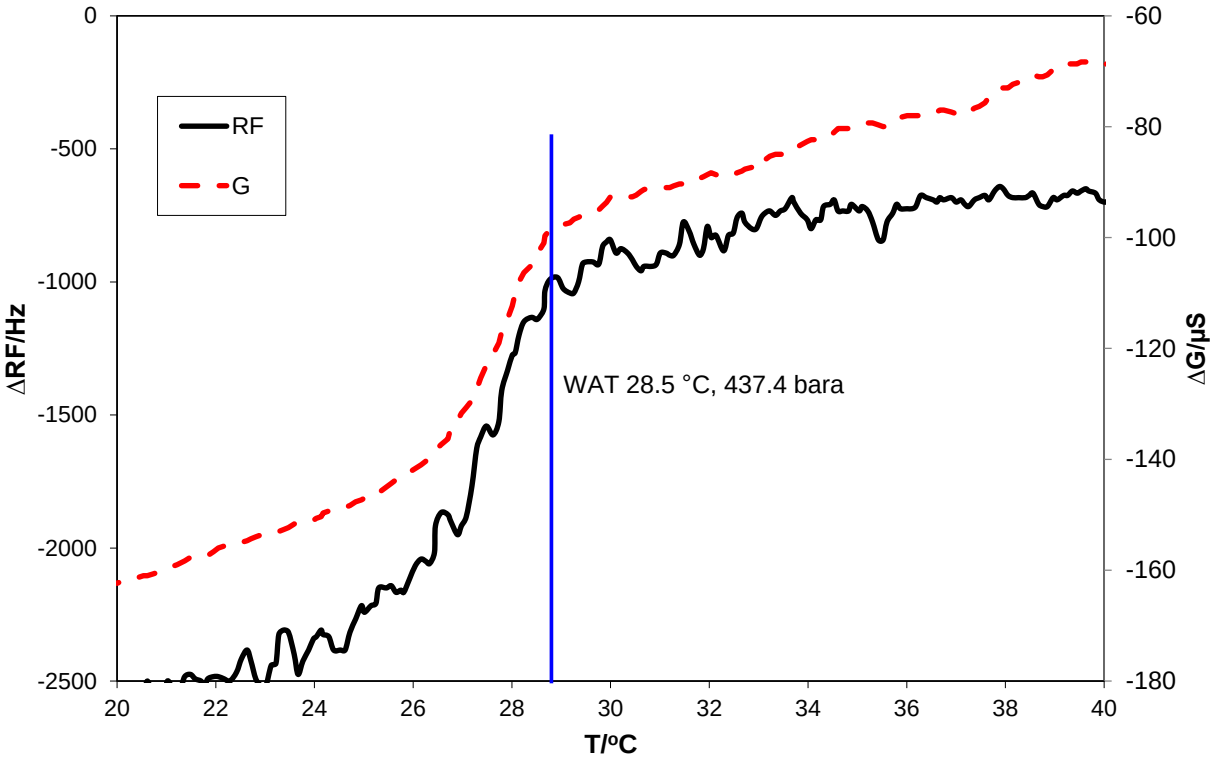

Figure 3.13. RF and G data with temperature for WAT test with live oil at a cooling rate of 0.28 °C per minute.

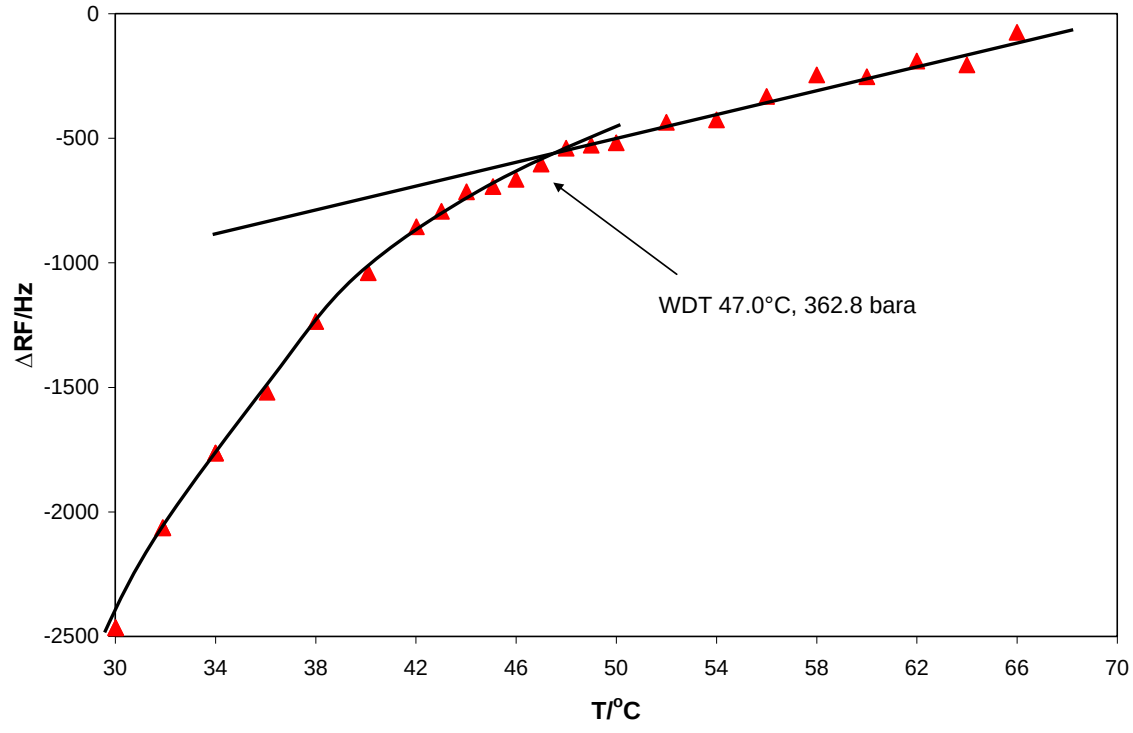

Figure 3.14. RF data with temperature for WDT test with live oil, step-heating allowing 30 minutes at each step for equilibrium.

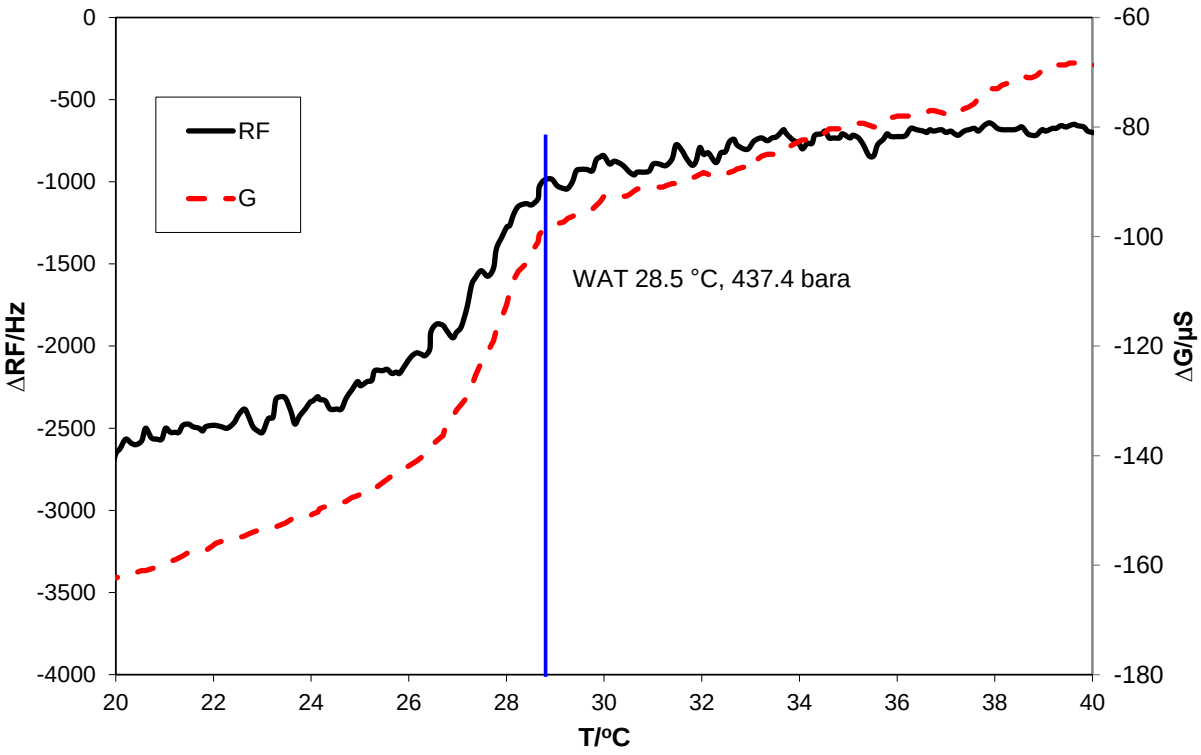

Figure 3.15. RF and G data with temperature for WAT test with live oil at a cooling rate of 0.28 °C per minute.

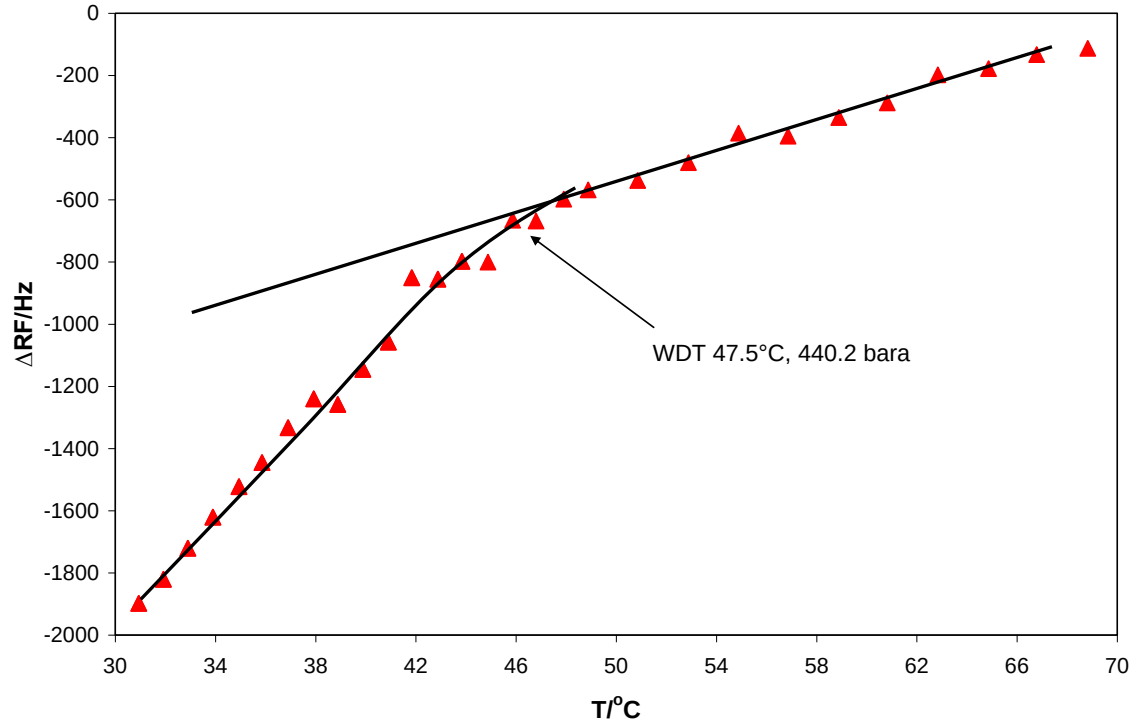

Figure 3.16. RF data with temperature for WDT test with live oil, step-heating allowing 30 minutes at each step for equilibrium.

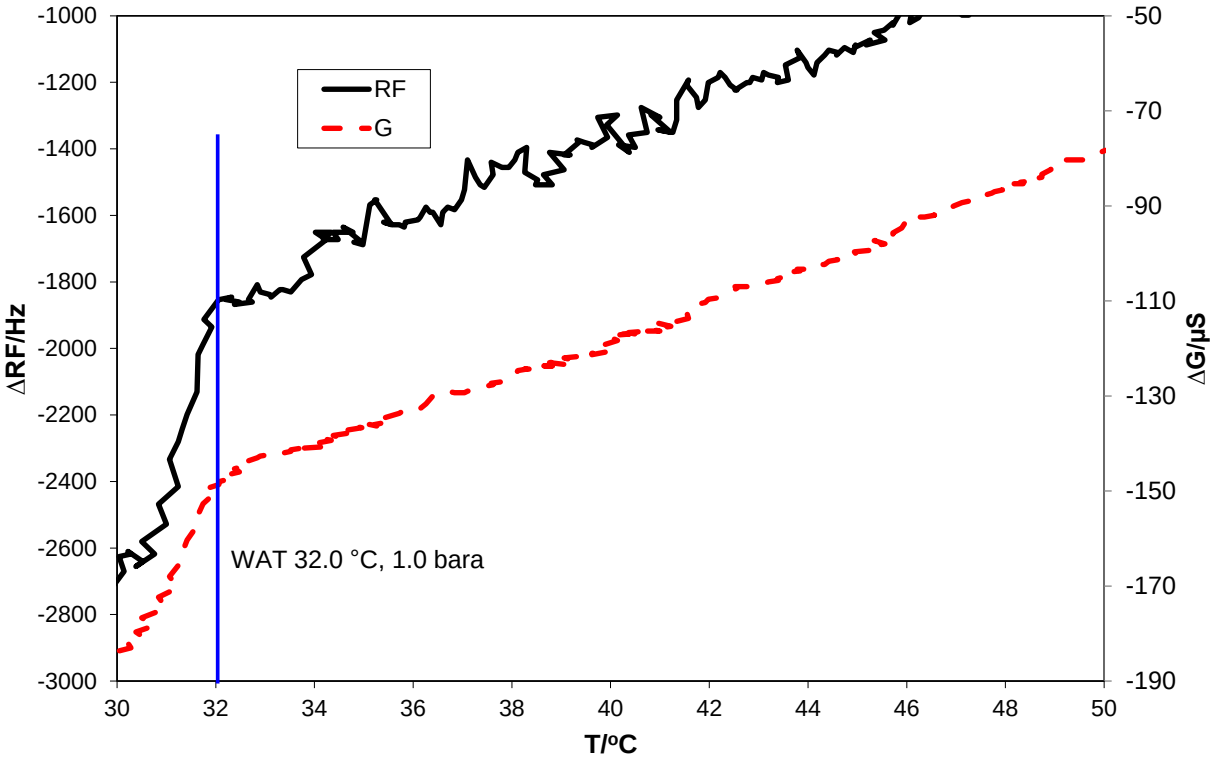

Figure 3.17. RF and G data with temperature for WAT test with flashed oil at a cooling rate of 0.28 °C per minute.

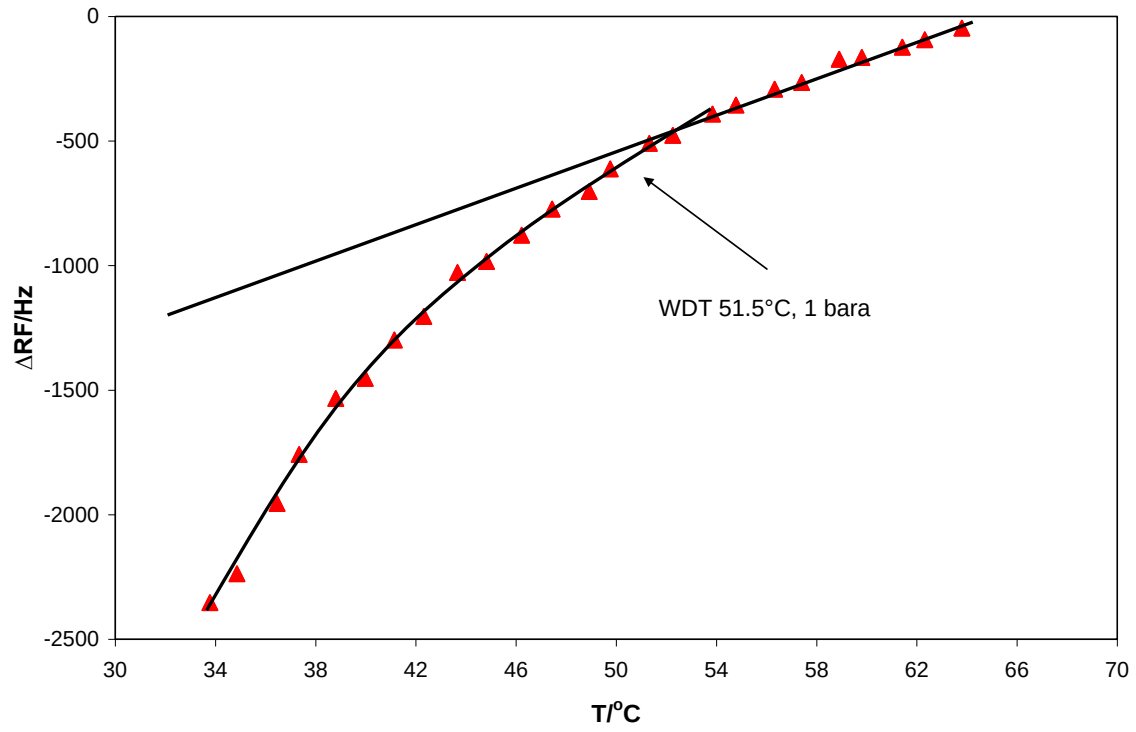

Figure 3.18. RF data with temperature for WDT test with flashed oil, step-heating allowing 30 minutes at each step for equilibrium.

Table 3.1. Summary of experimental WAT and WDT measurements conducted on live and flashed oil.

WAT		WDT	
Temperature °C ±0.5	Pressure bara ±0.3	Temperature °C ±0.5	Pressure bara ±0.3
32.0	1.0	51.5	1.0
28.0	20.3	49.5	22.7
27.5	39.3	47.5	43.9
26.0	71.1	46.5	81.6
25.0	99.3	45.5	116.6
24.5	122.9	44.5	147.2
25.0	241.4	45.0	244.3
27.5	361.3	47.0	362.8
28.5	437.4	47.5	440.2

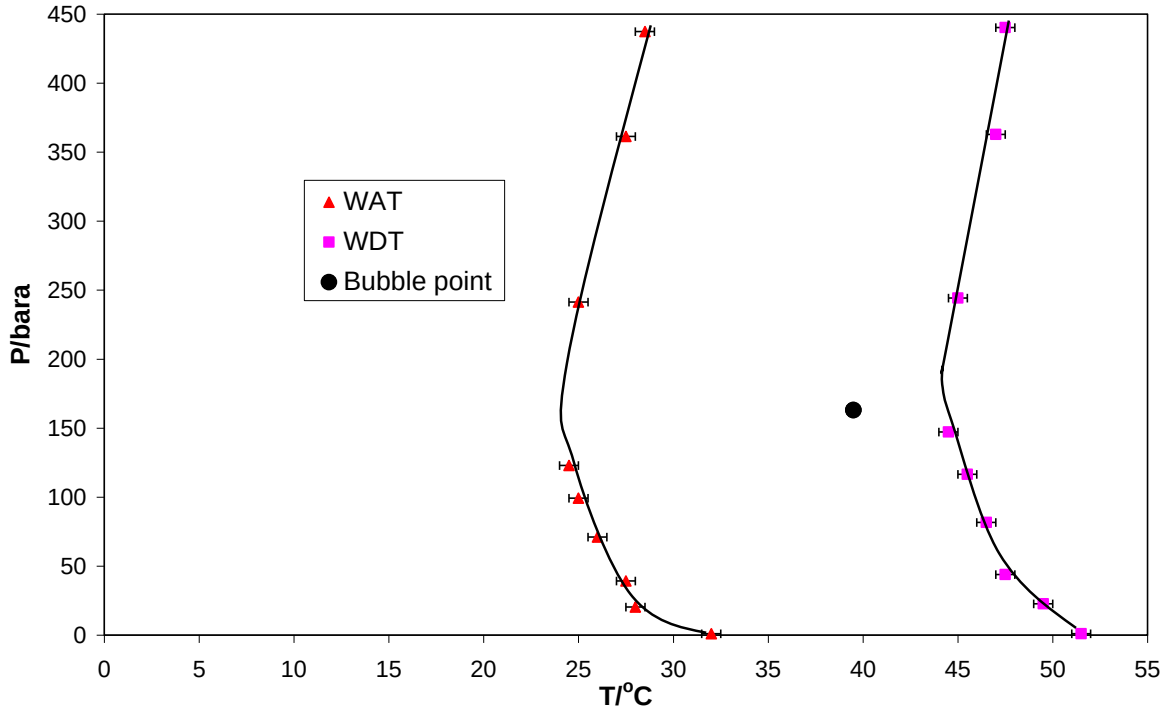

Figure 3.19. Plot showing experimental WAT and WDT measurements for live oil at different pressures along with data for flashed oil and experimental bubble point measurement (163.1 bara at 39.5 °C as shown in Figure-20). Lines fitted through experimental data.

3.2.5.2. Assessment of influence of cooling rate on WAT for flashed oil

In addition to the WAT test on the flashed oil at a cooling rate of 0.28 °C per minute two further tests were conducted at cooling rates of 0.14 and 0.07 °C per minute. The data is summarised in Table 3.2 below. As can be seen there is an increase in WAT with reducing cooling rate as might be expected. At a cooling rate of 0.07 °C per minute there is a 14 °C difference between the WAT and the WDT (51.5 °C) hence it is anticipated that only at very slow cooling rates would the WAT converge with the WDT.

Table 3.2. Measured WAT for flashed oil with different cooling rates.

Cooling rate °C per minute	WAT °C ±0.5
0.28	32.0
0.14	36.5
0.07	37.5

3.2.5.3. Bubble point measurement

As mentioned above, a bubble point measurement was made on the oil transferred from the original sample vessel to the visual test rig using isochoric step-cooling with continuous mixing. The equilibrium pressures and temperatures recorded on cooling the oil are plotted in Figure 3.20 and as can be seen the bubble point can be clearly identified. The measured value was 163.1 bara at 39.5 °C.

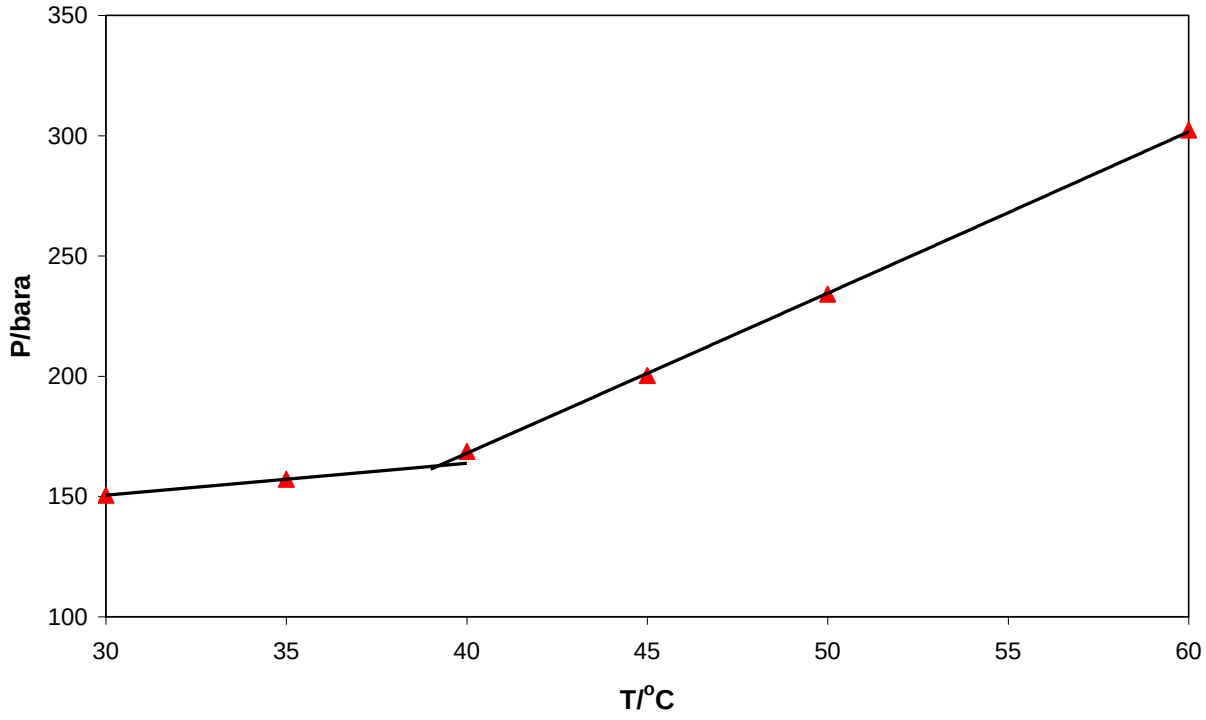

Figure 3.20. Plot of equilibrium pressures and temperatures from isochoric step-cooling bubble point test. Bubble point measured as 163.1 bara at 39.5 °C.

3.2.5.4. Discussion

The measurements made in this study gave the sponsors of the project data that could be used to validate their own internal test procedures which were based upon microscopy. Although the sponsor did not give details of their own measurements they indicated that the results from this test were in good agreement. The results from the WAT measurements at different cooling rates showed that only at very slow cooling rates will the WAT be close to the WDT.

3.3. Experimental investigation into the potential for measuring WAT and WDT for live condensates using QCM technology

3.3.1. Introduction

The aim of this project was to investigate the potential for measurement of WAT and WDT for live condensates at a range of pressures using the QCM based equipment and

procedures described in **Chapter 2**. In addition the WAT and WDT for the stabilised condensate used in this study were measured.

3.3.2. Experimental equipment

The experimental set-up is comprised of an equilibrium cell, cryostat, rocking/pivot mechanism, and temperature/pressure recording equipment controlled by a PC (Figures 3.21 and 3.22). The equilibrium cell is a piston-type variable volume (maximum effective volume of 300 ml) titanium cylindrical pressure vessel, mounted on a horizontal pivot with associated stand for pneumatic controlled rocking through 180 degrees. Rocking of the cell ensures adequate mixing of the cell fluids.

The rig has a working temperature range of –60 to 90 ºC, with a maximum operating pressure of 690 bar. The cell temperature is controlled by circulating coolant from a cryostat within a jacket surrounding the cell. The cryostat is capable of maintaining the cell temperature stability to within better than 0.05 ºC. To achieve good temperature stability, the jacket is insulated with polystyrene board, while connecting pipe work is covered with plastic foam.

The temperature is measured and monitored by means of a PRT (Platinum Resistance Thermometer) located within the cooling jacket of the cell. The cell temperature is measured with an accuracy of ± 0.05 ºC. A strain gauge pressure transducer with an accuracy of ± 0.3 bar was used to monitor pressure. Temperature and Pressure are monitored and recorded by the PC through an RS 232 serial port. The cryostat can be monitored and controlled via an interface connected to a serial port on the computer.

A QCM was mounted in the cell in such a way as to be immersed in liquid condensate present in the cell. In this set-up it was estimated that around 3 ml of liquid condensate is required to submerse the QCM.

The temperature probe is regularly calibrated against a platinum resistance probe that has a certificate of calibration issued in accordance with NAMAS Accreditation Standard and NAMAS Regulations. The pressure transducer is regularly checked for accuracy using a Budenberg dead weight tester.

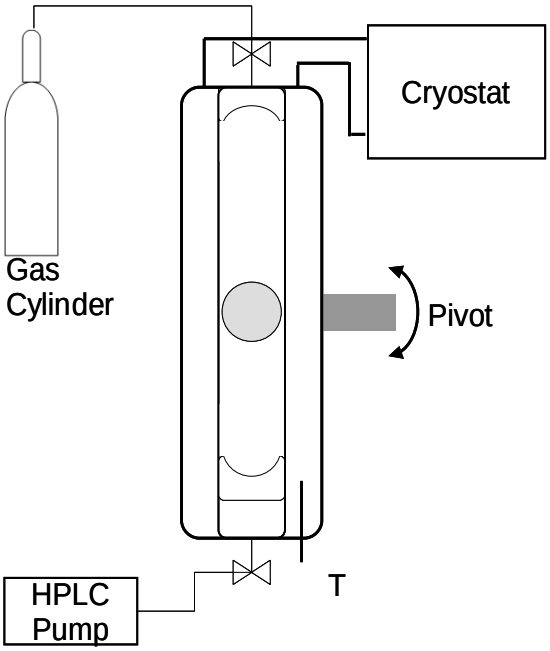

Figure 3.21. Schematic illustration of hydrate equilibrium rig used in this study, mixing ball shown was not used in this study.

Figure 3.22. Image of the hydrate equilibrium rig used in this study and associated data acquisition systems.

3.3.3. Test fluids

Stabilised condensate as supplied by the company sponsoring the work was used along with natural gas with a composition as shown in Table 3.3. The container of condensate was heated to 70 °C and mixed for three hours prior to taking a sub-sample for use in the experimental measurements.

Table 3.3. Natural gas composition.

Component	Mole%
N_2	2.24
C_1	88.06
CO_2	2.33
C_2	5.21
C_3	1.64
iC_4	0.16
nC_4	0.27
iC_5	0.04
nC_5	0.05

3.3.4. Experimental methods

The same methods for measuring WAT and WDT as described in Section 3.2.4 above were used in this study. An example of the data from a WAT measurement from this study is shown in Figure 3.23. An example of data for a WDT measurement from this study is given in Figure 3.24. As shown in Figure 3.24 changes in G were used to measure WDT in these tests as this was clearer than using changes in RF. A WAT/WDT measurement was also conducted for the stabilised condensate in order to give a reference point at atmospheric pressure with no gas present.

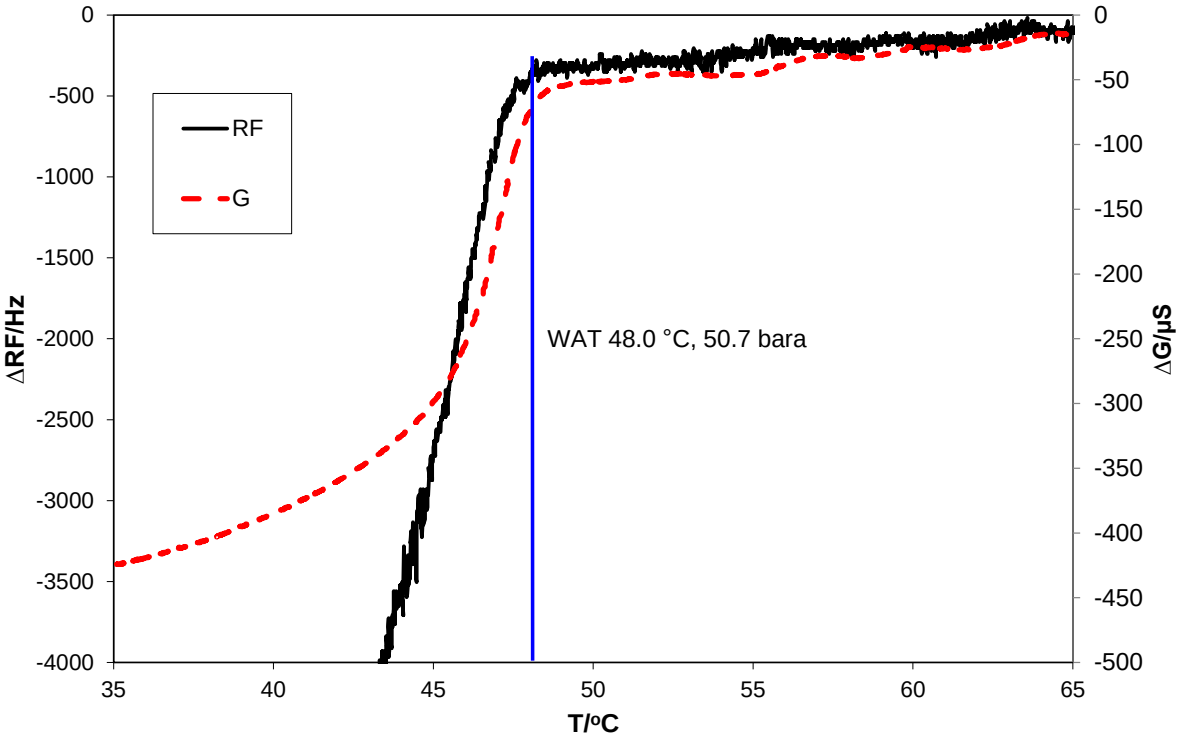

Figure 3.23. Example of RF and G data with temperature for WAT test with live condensate at a cooling rate of 0.15 °C per minute.

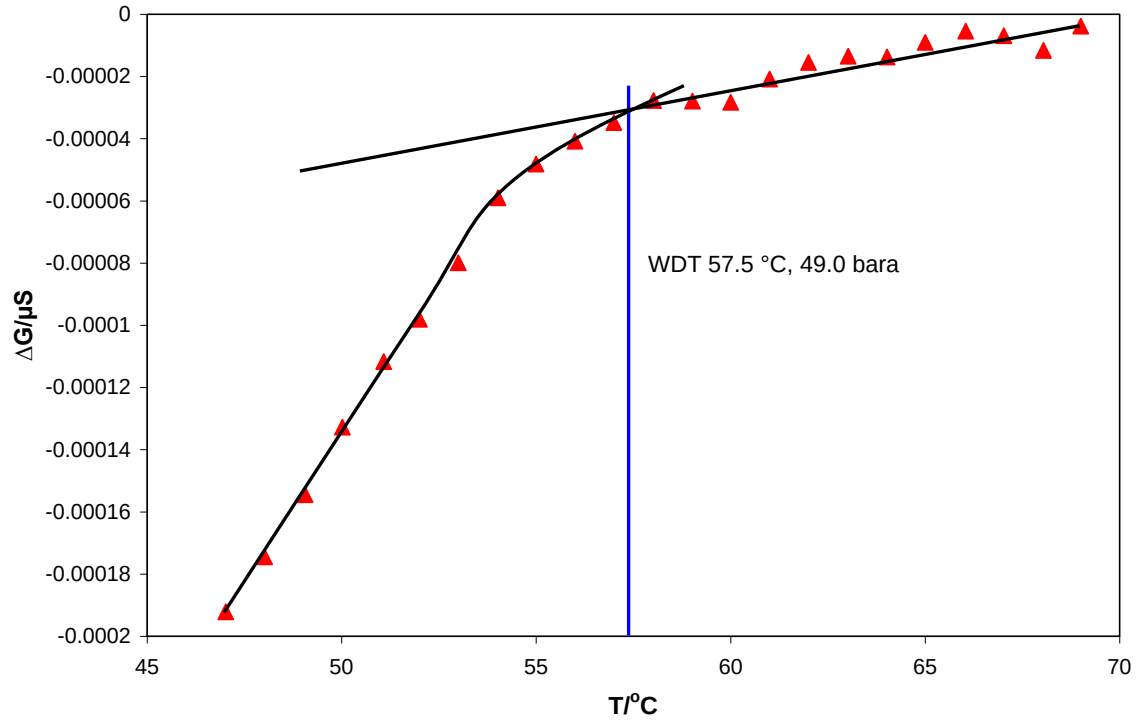

Figure 3.24. Example of G data with temperature for WDT test with live condensate, step-heating allowing 30 minutes at each step for equilibrium.

3.3.5. Results

Measurements were conducted with three different combinations of stabilised condensate and natural gas. The mass ratios of the natural gas to condensate for the three mixtures were 1.554, 2.247 and 3.695. The experimental measurements for the test with a ratio of 3.695 were erratic. The reason for this was most probably because there was not sufficient liquid phase present in the test cell to completely surround the QCM. Without visual observations it is not possible to confirm this, however it is the most likely explanation.

The experimental WAT and WDT measurements for the two mixtures with gas to condensate ratios are presented in Table 3.4. The WAT of the stabilised condensate at atmospheric pressure was measured as 50 °C (continuous cooling 0.15 °C per minute) and the WDT was 63 °C (step-heating). The data for the two fluids are presented together along with the data for the stabilised condensate at atmospheric pressure in Figure 3.25.

Table 3.4. Summary of experimental WAT and WDT measurements conducted on live condensates with different natural gas to condensate ratios.

	WAT		WDT	
natural gas to condensate ratio	Temperature °C ±0.5	Pressure bara ±0.3	Temperature °C ±0.5	Pressure bara ±0.3
1.554	45.0	46.8	57.5	49.0
	45.0	101.4	54.0	106.4
	44.5	153.6	54.0	163.8
	45.0	210.3	54.0	225.4
	47.5	261.8	56.0	285.7
2.247	48.0	50.7	59.0	52.4
	47.0	103.2	58.0	109.2
	45.5	156.0	55.5	166.3
	46.0	200.9	56.0	216.6
	47.0	271.3	55.0	291.1

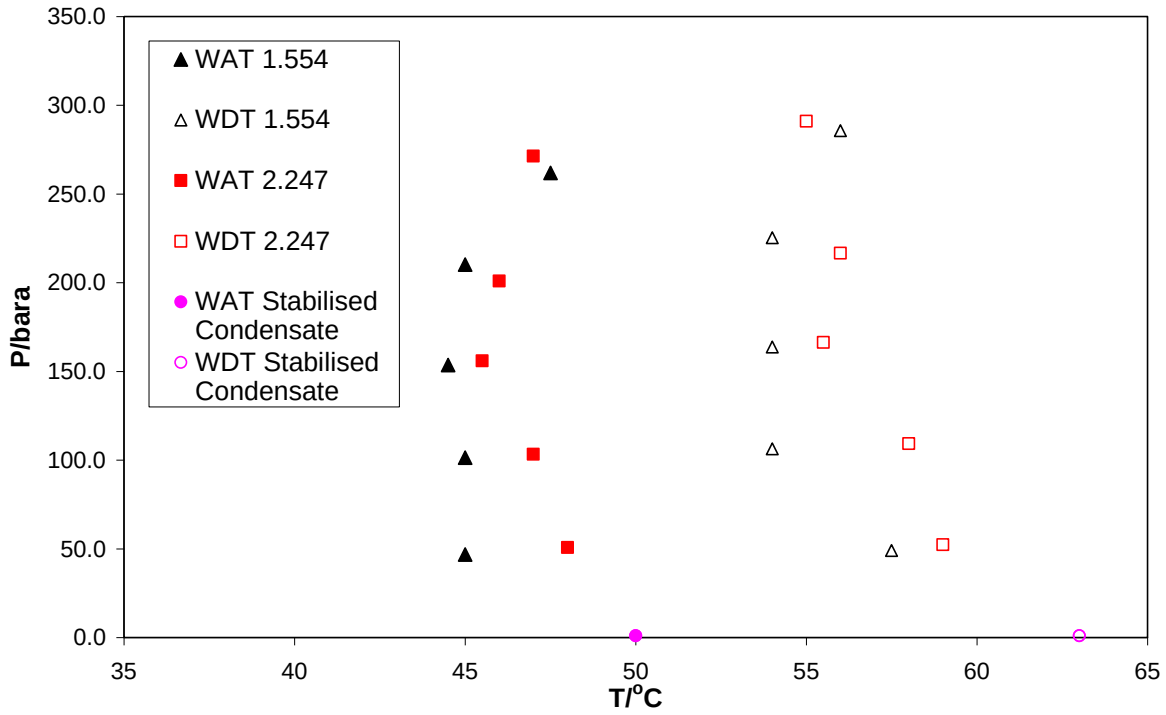

Figure 3.25. Summary of experimental WAT and WDT data for the two natural gas/condensate mixtures (gas to condensate ratios 1.554 and 2.247) along with the measured data for the stabilised condensate at atmospheric pressure.

3.3.6. Discussion

This study showed that the equipment and methods, based on QCM technology, could be successfully used to measure WAT and WDT for live condensates. The equipment was not designed for use with small volumes of condensate below approximately 3 ml, however it is considered possible that equipment could be designed to allow for measurements with volumes of condensate of as little as 0.5 ml.

The experimental data show that, as with measurements on most real fluids, there is a significant difference between the WAT and the WDT. As with other fluids it is expected that the slower the cooling rate the higher the WAT will be. In one test with the test fluid with a gas to condensate ratio of 1.554 the WAT was measured as 45 °C at a cooling rate of 0.15 °C per minute and 49 °C at a cooling rate of 0.03 °C per minute.

The data also show that there is a difference between the two fluids tested in this study in that for the tests with a higher gas to condensate ratio both WAT and WDT are measured to be at higher temperatures at pressures up to around 250 bar, most probably reflecting changes in the composition of the liquid condensate present in the cell and in contact with the QCM.

The higher gas ratio would be expected to lead to lighter components being removed from the liquid hydrocarbon phase thus leading to a heavier fluid with a higher WDT.

3.4. Comparison of wax inhibitor performance for 5 commercial products with oil from North Sea field using QCM technology

3.4.1. Introduction

The aim of this work was to conduct an experimental study to compare the performance of 5 different wax inhibitors supplied by different suppliers with oil from a North Sea Field. Tests were conducted using two QCM based experimental set-ups, the multi-sample atmospheric pressure set-up and the pressurised single sample set-up.

3.4.2. Experimental equipment

The multi-sample set-up is comprised of eight 15 ml glass test tubes, each having a QCM suspended within them. The tubes are submersed in a temperature controlled bath. The temperature of the bath is measured using a Platinum Resistance Probe suspended in the bath. The Resonant Frequencies (RF) of the QCMs are measured using an Impedance Analyser and recorded using a PC. The temperature controlled QCM set-up as described in **Chapter 2**, Section 2.6.1 was used in this work.

3.4.3. Experimental Methods

In the tests with the multi-sample set-up the tubes were loaded with stabilised crude with or without different concentrations of different inhibitors. The temperature was set to 55 °C, above the WAT of the fluid, the temperature was then reduced to 3 °C at a rate of 0.23 °C per minute. During this process the RF of the QCMs were continuously monitored. In the first set of tests with an inhibitor concentration of 300 ppmv the pour point of the test fluids was also measured in the 15 ml sample tubes. For this purpose the bath temperature was reduced to a minimum of -20 °C. The ASTM D97 - 87 definition of the pour point, "no movement of the fluid when the tube is held horizontal for 5 seconds", was used.

For the tests in the pressurised set-up, the stabilised crude was combined with pure components C_1 to C_4, N_2 and CO_2, to give a recombined oil with a composition similar to that provided by the company sponsoring the work. The clean dry evacuated test cell was

pressurised to 400 psia with the recombined oil without or with inhibitor. The temperature of the sample chamber was held at 30 °C. The temperature of the QCM was reduced from 35 °C to 17 °C at a rate of 0.5 °C per minute. The temperature was then maintained at 17 °C for the remainder of the test. The QCM RF was continuously monitored.

3.4.4. Test fluids

A stabilised crude from a North Sea Field was used in all tests, along with five inhibitor samples, as detailed in Table 3.5 below. As indicated above for the tests with the pressurised QCM set-up, the stabilised crude was combined with pure components C_1 to C_4, N_2 and CO_2, to give a recombined oil with a composition similar to that provided by the company sponsoring the work. All of the inhibitors were dosed by ppm based on the volume of stabilised crude.

Table 3.5. Details of wax inhibitors compared in this study.

Supplier	Product name
Baker Petrolite	PAO85433
Champion Technologies	Flexoil WM-1840-F1
Clariant	Provisional Waxtreat DF 12571
M-I Swaco	PI-7393
NALCO	NALCO® EC6592A

3.4.5. Test results

3.4.5.1. Multiple sample QCM set-up

In the first instance the inhibitors were tested at a concentration of 300 ppmv. The results were somewhat scattered with none of the inhibitors showing any improvement compared to the blank untreated sample. During this test the pour points of the samples were measured by reducing the bath temperature to a minimum of -20 °C. The results from these measurements are given in Table 3.6 below. As can be seen all of the inhibitors reduced the pour point of the oil, compared to the untreated oil. In the cases of PAO85433 and Flexoil WM-1840-F1 the pour point was not reached at -20 °C.

Table 3.6. Measured pour point temperatures for oil without and with 300 ppmv of different inhibitors.

Test fluid	Pour point temperature °C ±2
300 ppmv PAO85433	<-20
300 ppmv Flexoil WM-1840-F1	<-20
300 ppmv Waxtreat DF 12571	-7
300 ppmv PI-7393	-15
300 ppmv NALCO® EC6592A	9
No inhibitor	11

Following the test at 300 ppmv measurements were conducted at 600 and 1000 ppmv. The RF changes with temperature for the QCMs, from the two tests, are shown in Figures 3.25 and 3.26. As can be seen there are clear differences between the inhibitors. In both tests PAO85433 and Flexoil WM-1840-F1 show the least reduction in RF, indicating less tendency of wax to adhere to or build up on the QCM surface (Chapter 2, Page 16). The RF for these two samples shows a small increase at lower temperatures, possibly as a result of density and viscosity changes in the fluid surrounding the QCM. This may be due to lighter components, not taking part in wax formation surrounding the QCM. The order in terms of which inhibitor has the best effect, in terms of least RF reduction is similar between the two tests with different concentrations, apart from PI-7393 which is markedly better at 1000 ppmv than at 600 ppmv.

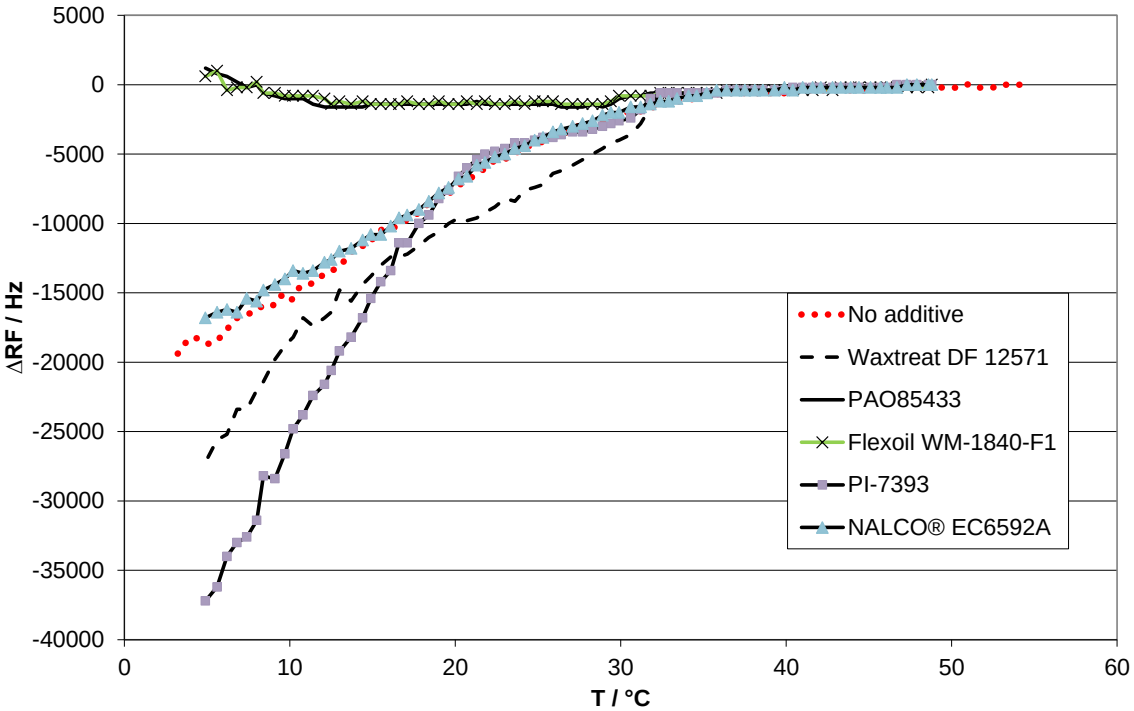

Figure 3.25. Plot showing changes in RF with temperature in test with stabilised crude without and with 600 ppmv of 5 different wax inhibitors.

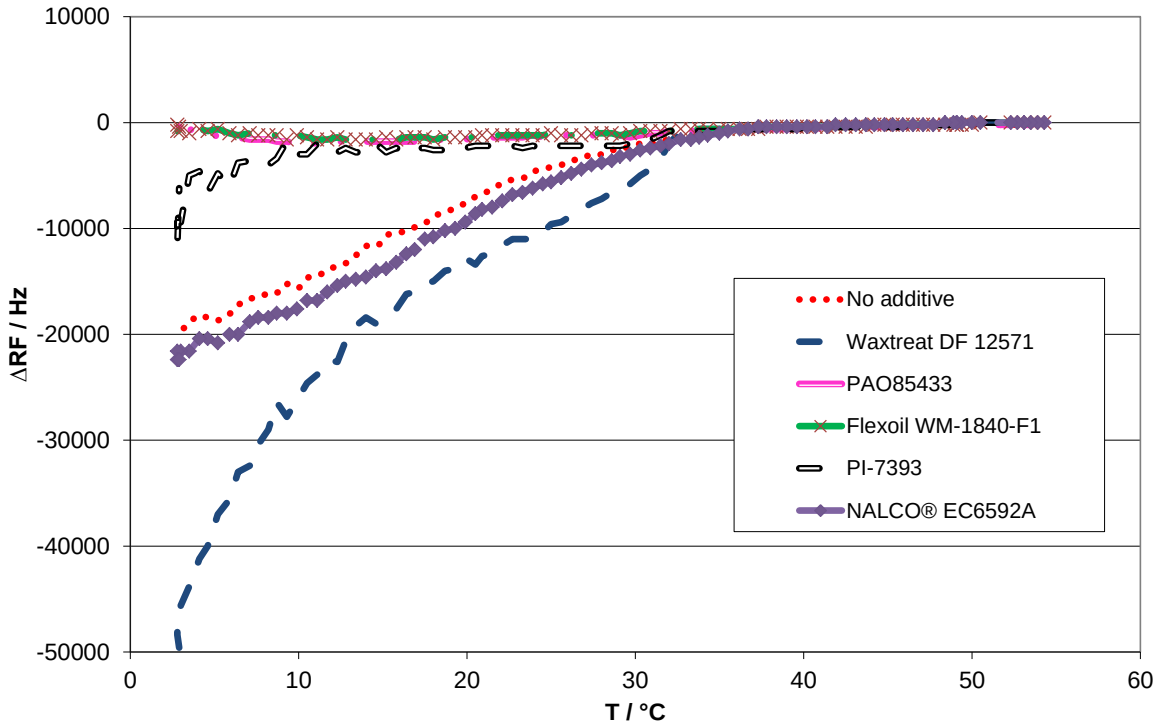

Figure 3.26. Plot showing changes in RF with temperature in test with stabilised crude without and with 1000 ppmv of 5 different wax inhibitors.

3.4.5.2. Pressurised cooled QCM set-up

The RF data with time, recorded during the tests with the recombined oil at 400 psia are shown in Figure 3.27. Tests were conducted with the recombined oil with no additive and with 600 ppmv of the different inhibitors. In these test the QCM temperature (shown in red solid line) was reduced from 35 to 17 °C at a rate of 0.5 °C per minute whilst the cell jacket temperature was kept at 30 °C. As can be seen, apart from in the test with NALCO® EC6592A, there was little reduction in RF before the QCM temperature reached 17 °C. It can also be seen that there were clear differences in the wax adhesion tendency between the different inhibitors. In the cases of PI-7393 and NALCO® EC6592A the RF reduction is greater than the recombined oil with no additive. At the conditions used in this test and the dose rate of 600 ppmv, Flexoil WM-1840-F1 performed best in terms of reducing RF reduction and therefore wax adhesion tendency. The differential temperature between the oil and QCM is much greater than would be expected at the pipeline wall in the field, however it allows for clear differentiation between the performances of the inhibitors. Optimising the dose rate of the inhibitor could be done using realistic predicted temperature gradients.

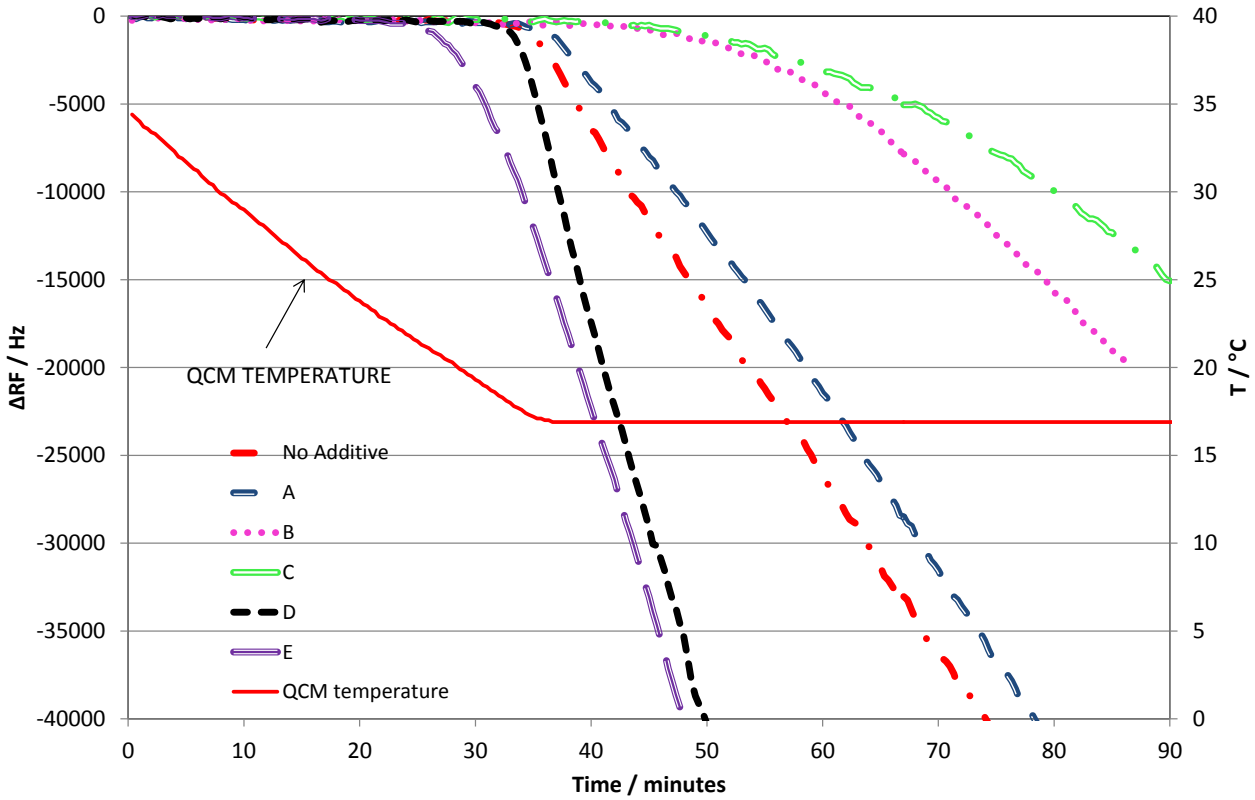

Figure 3.27. Plot showing changes in RF with time in test with recombined oil at 400 psia without and with 600 ppmv of 5 different wax inhibitors. Oil temperature 30 °C, QCM temperature is shown with the red solid line.

3.4.6. Conclusions

From the experimental data presented in this work the performance of the inhibitors can be ranked in terms of capability to reduce wax adhesion tendency and pour point, as presented in Table 3.7 below (1 to 5 meaning the best to the worst). As can be seen the Champion (Flexoil WM-1840-F1) and Baker Petrolite (PAO85433) inhibitors were the best performing for these tests at the tested concentrations. The Champion (Flexoil WM-1840-F1) product was best at 600 ppmv when tested at live-pressurised conditions.

Table 3.7. Rankings for 5 wax inhibitors based upon 4 tests.

Supplier	Product name	600 ppmv inhibitor, static QCM test, atmospheric pressure	1000 ppmv inhibitor, static QCM test, atmospheric pressure	600 ppmv inhibitor, mixed, pressurised QCM test	300 ppmv, pour point measured in 10 ml tubes cooled at atmospheric pressure
Champion	Flexoil WM-1840-F1	1=	1=	1	1=
Baker Petrolite	PAO85433	1=	1=	2	1=
Clariant	Waxtreat DF 12571	4*	5*	3	4
Mi Swaco	PI-7393	5*	3	4*	3
Nalco	NALCO® EC6592A	3	4	5*	5

*Denotes greater wax adhesion tendency than blank untreated oil.

3.5. Conclusions

The three separate case studies presented in this chapter show how the QCM based equipment has been used to provide information on WAT and WDT values for a live oil and a condensate. In addition to enable selection of inhibitors based upon performance at both atmospheric and pressurised conditions. It is hoped that further studies will be conducted enabling the equipment and methods to become accepted as a reliable option for improving or complimenting existing technologies.

CHAPTER 4 - DEVELOPMENT OF QCM BASED EQUIPMENT AND METHODS FOR ASPHALTENE MEASUREMENTS

4.1. Introduction

Asphaltenes are commonly identified as the part of reservoir fluids that are insoluble in n-alkanes such as n-pentane and n-heptane but soluble in toluene [1-3]. They are high molecular weight components, average ~750 g/mol, made up of carbon and hydrogen in an approximate 1 to 1.2 ratio. They typically contain a small percentage of other atoms, known as heteroatoms such as sulphur, nitrogen, oxygen, vanadium and nickel. Across the range of reservoir fluids the asphaltene content can vary from barely measureable to ~20% in some heavy oils. The asphaltenes are stable, i.e. part of the reservoir fluid, at the original reservoir conditions, however changes in pressure, temperature and composition that occur throughout the production process can cause them to separate out [4]. The separated asphaltenes can adhere to surfaces within the reservoir and in pipelines, production and processing facilities leading to flow assurance problems such as reduction in reservoir permeability and in severe cases pipeline restriction and potentially blockage. If allowed to build-up, by their nature, asphaltene deposits can be difficult to remove leading to very costly procedures and loss of production.

Problems associated with asphaltenes during production and processing are widespread [5-7] including Aegean Sea, Venezuela, Algeria, North Sea and Gulf of Mexico. Asphaltene problems are most commonly associated with lighter oils which contain lower levels of asphaltenes. In heavier oils with larger amounts of asphaltenes problems may not be encountered because the asphaltenes are less likely to adhere to surfaces. This may be similar to wax, where deposition is reduced or eliminated due to a significant reduction in the diffusion coefficient in higher viscosity oils [8]. Asphaltene problems may increase as reservoir pressures reduce in later production life and due to the increasing interest in CO_2 injection. Increasing the CO_2 content of an oil is well known to lead to asphaltene precipitation. Asphaltene problems can also occur with mixing of fluids from different locations or indeed any procedures that result in changes in fluid composition such as solvent treatments.

The role of resins in asphaltene stability has been well documented [9], considering them to be dispersed in resin-coated inverse micelles, however there are some disagreements regarding this view [10]. The asphaltene to resins ratio is often seen as a key parameter for determining asphaltene stability in different fluids. There are a number of approaches that have been considered for modelling asphaltene deposition such as solubility, solid, colloidal and association EOS models. The different views on the composition of asphaltenes, their relationship with the fluid and how best to model their behaviour suggests that there is further work required to gain a better understanding of asphaltene related problems.

Avoiding or alleviating problems associated with asphaltenes is clearly an important topic in Flow Assurance. Clearly one approach is to avoid P / T conditions at which asphaltene deposition is known to occur, however this might have too much bearing on production levels. Keeping temperature high through insulation or heating is costly. Periodic removal of asphaltenes, based upon knowledge of build-up rate, using solvents or mechanical means can be another option. There are a significant number of additives that have been found to reduce asphaltene deposition, essentially by keeping the asphaltene from separating from the oil. It would be a large undertaking to assimilate a list of all of the different chemicals that have been documented. A few are dodecyle resorcinol, nonylphenol, oil-soluble polymeric dispersants, oxazolines derivative of poly alkyl or poly akenyl N-hydroxyalkyl and ester and ether reaction products [11-13]. Their mode of action is reported to be to adhere to asphaltene particles, keeping them in suspension, in essence replacing the resins. These asphaltene inhibitors are commonly injected downhole or into the near well-bore area by means of squeeze treatments to reduce formation damage. They can work at low dose rates ~ 50 ppm and are clearly an attractive option from an economic point of view.

If asphaltene is considered to be a potential Flow Assurance issue then the first information that will be required is the asphaltene deposition envelope. This gives knowledge of the P / T conditions at which asphaltenes are likely to precipitate. As mentioned above different models can be used to predict asphaltene stability. There are a number of different experimental approaches that can be used to measure the point at which asphaltenes precipitate, including NIR spectroscopy, laser light scattering, microscopy, conductivity, filtration, capillary flow and vapour pressure osmometry [8, 14-18]. One approach is to make measurements of asphaltene stability on stabilised oil samples and use this information as an input to a predictive model along with other parameters such as oil

composition and balance of saturates, aromatics, resins and asphaltenes. Stability is commonly measured by injecting n-alkanes such as pentane and heptane into the oil at a continuous slow rate and detecting the point at which asphaltenes precipitate using different detection methods. In some cases the technique requires the oil to be diluted with toluene to make it more transparent. Ultimately it would be better to have some points measured at field conditions on real reservoir fluids. The best option is to have a relatively uncontaminated downhole sample. If this is not available then a recombined reservoir fluid is the next best option. Measurements can then be made by simulating the P / T changes that will occur in the field and detecting the onset of asphaltene deposition. Clearly tests with live fluids are considerably more costly both in terms of the fluid requirements, if a downhole sample is used, and high pressure PVT equipment that is needed.

A recent proposal is to titrate a sample of oil with different n-alkanes to obtain an ASphaltene InStability Trend (ASIST) [10]. The trend is a linear relationship between the asphaltene onset solubility parameters and the square-root of n-alkane nonsolvent molar volumes. It is considered that ASIST can be used along with other parameters to predict the onset of asphaltene precipitation for the live fluid during depressurisation [19].

Once the asphaltene deposition envelope has been established it would be ideal to know the scale of the potential problem in the field in terms of the rate of build-up of asphaltene. The rate of build-up is more difficult to obtain from an experimental point of view in the laboratory. It is also difficult to predict the effects of a variety of parameters at field conditions such as shear rate on asphaltene deposition and build-up.

If asphaltene inhibitors are considered to be the best approach then some screening and dose rate optimisation is required. As with measuring asphaltene onset, tests are often conducted on stabilised samples in the first instance, assessing the asphaltene onset and amount of deposition for additised samples using pentane or heptane titration. Following on from that, measurements using high pressure equipment can be used to confirm that the inhibitor will be successful at reducing deposition at field conditions.

As discussed in **Chapter 2** the ability of a QCM to detect small amounts of deposited material and its build-up in hydrocarbon fluids at atmospheric pressure and at high P / T conditions make it a good candidate for asphaltene studies. Actual deposition and the amount

of deposition could be considered as the most important parameters in assessing asphaltene problems. In addition it should also be useful for assessing the effect of inhibitors on asphaltene deposition. A recent report indicates that inhibitors selected upon the basis of their ability to disperse and reduce flocculation of asphaltenes are not effective at reducing deposition and build-up [20]. As with wax measurements, QCM technology may help to improve understanding and compliment other experimental approaches. This chapter presents initial work that has been done to investigate the potential use of QCM technology for asphaltene studies and in **Chapter 5** two case studies are presented using the developed equipment and methods. The initial work is divided into atmospheric pressure heptane titrations and high pressure tests.

4.2. Heptane titration tests

The colloidal stability of asphaltenes can be estimated using three Heithaus compatibility parameters according to ASTM D6703 – 07. In this procedure asphaltenes are diluted with toluene in three different ratios. The three solutions are then titrated with a solvent such as isooctane or heptane that will promote flocculation or asphaltene precipitation. The point of flocculation is measured by continuously circulating the solution through a spectrophotometer. From the dilution ratio of asphaltene to toluene and the amount of solvent injected to initiate flocculation the three Heithaus compatibility parameters are calculated. These are P_a the peptizability of asphaltenes, P_o the peptizing power of maltenes and P the overall compatibility of the system. There are different methods available for measuring the onset of asphaltene flocculation or precipitation, apart from the spectrophotometer, such as NIR spectroscopy and light scattering.

As discussed in the introduction the same titration method is used with either diluted or undiluted oil samples to find the point at which asphaltenes flocculate or precipitate in terms of the ratio of “ml” of solvent to “g” of oil. Titrations with different n-alkanes can be used to give the ASIST for different oils. In addition titrations can be conducted with the oil samples with additives in order to evaluate their performance.

4.2.1. Experimental equipment

The experimental equipment is comprised of a jacketed beaker which is sited on a magnetic mixer within which a QCM sensor is mounted. The jacketed beaker is connected to

a constant temperature circulator in order to control the temperature of the test fluids. An HPLC pump is used to inject heptane at a constant flow rate into the jacketed beaker. The RF and conductance at RF of the QCM sensor is measured using an Impedance Analyser and recorded using a PC. A schematic of the experimental equipment is shown in Figure 4.1 below.

4.2.2. Experimental method

In the first instance a weighed sample of oil is loaded into the jacketed beaker. In these tests the temperature of the beaker was maintained at 15.5 °C. After the oil has been mixed for 10 minutes the QCM sensor is inserted into the oil. Once the QCM RF is stable heptane is injected either step-wise or at constant rate. The test fluids are continuously mixed throughout the measurement. The QCM RF and G at RF are continuously monitored and recorded.

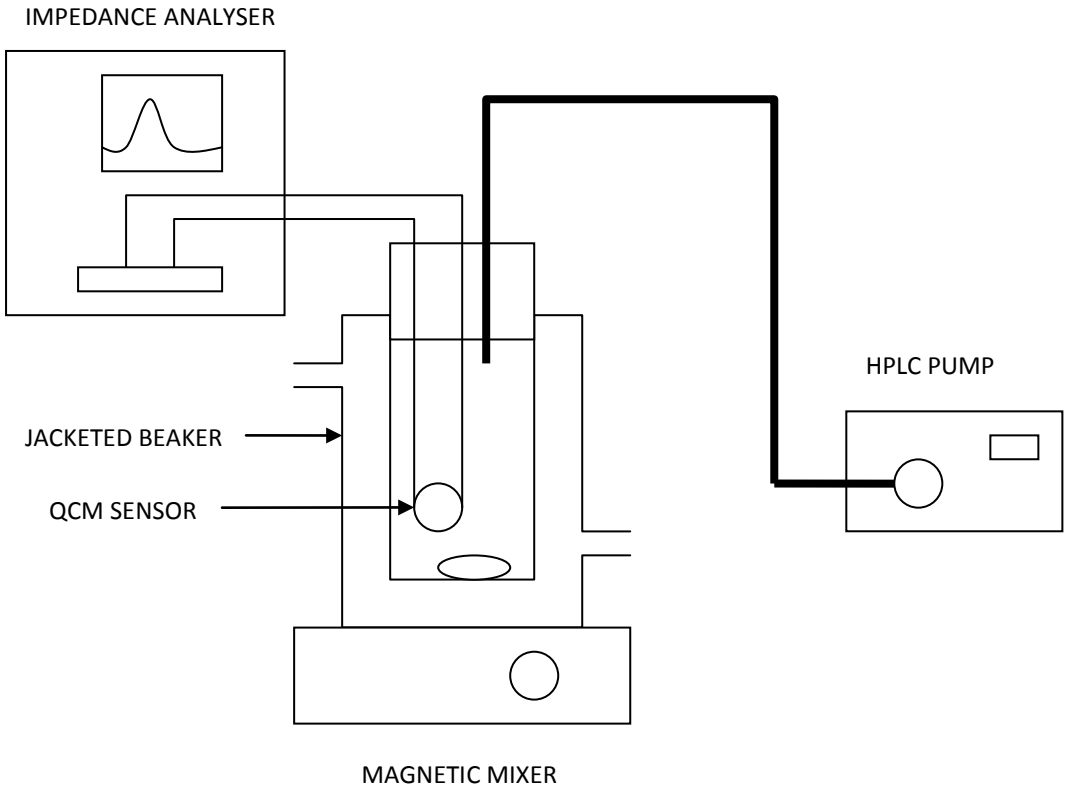

Figure 4.1. Schematic of experimental equipment used to make asphaltene precipitation measurements.

4.2.3. Results

Three different scenarios were investigated in the first instance, step-wise injection of heptane into a sample of stabilised crude, continuous injection of heptane into a sample of stabilised crude and continuous injection of heptane into a solution composed of toluene with separated dried asphaltenes.

4.2.3.1. Step-wise injection of heptane into stabilised crude

An example of the results from a test with a stabilised North Sea oil with an unknown composition is shown in Figure 4.2. Figure 4.2 shows the results in terms of changes in RF and G at RF versus ml heptane / g oil. In this test at least 20 minutes was given at each step. As can be seen from Figure 4.2 both RF and G at RF increase as heptane is added up to a point, ~1.03 ml heptane/g oil, where both decline sharply. The increasing RF and G at RF is associated with reductions in the density and viscosity of the tests fluids surrounding the QCM and the point at which they decline can be associated with asphaltene adhering to the QCM surface. This shows that the QCM can be used to measure the point at which asphaltenes come out of solution and adhere to the QCM.

To confirm that asphaltenes are adhering to the QCM surface the QCM was washed with heptane and dried and the RF was measured. This process was repeated but with toluene. The RF after being washed with toluene was significantly lower as expected due to the removal of asphaltenes by the toluene and not by heptane. In this test the time given at each step was not sufficient for the RF and G at RF to stabilise at the steps after these values had started to decline. Allowing more time would possibly increase the ease with which the asphaltene precipitation point can be identified from the plotted data.

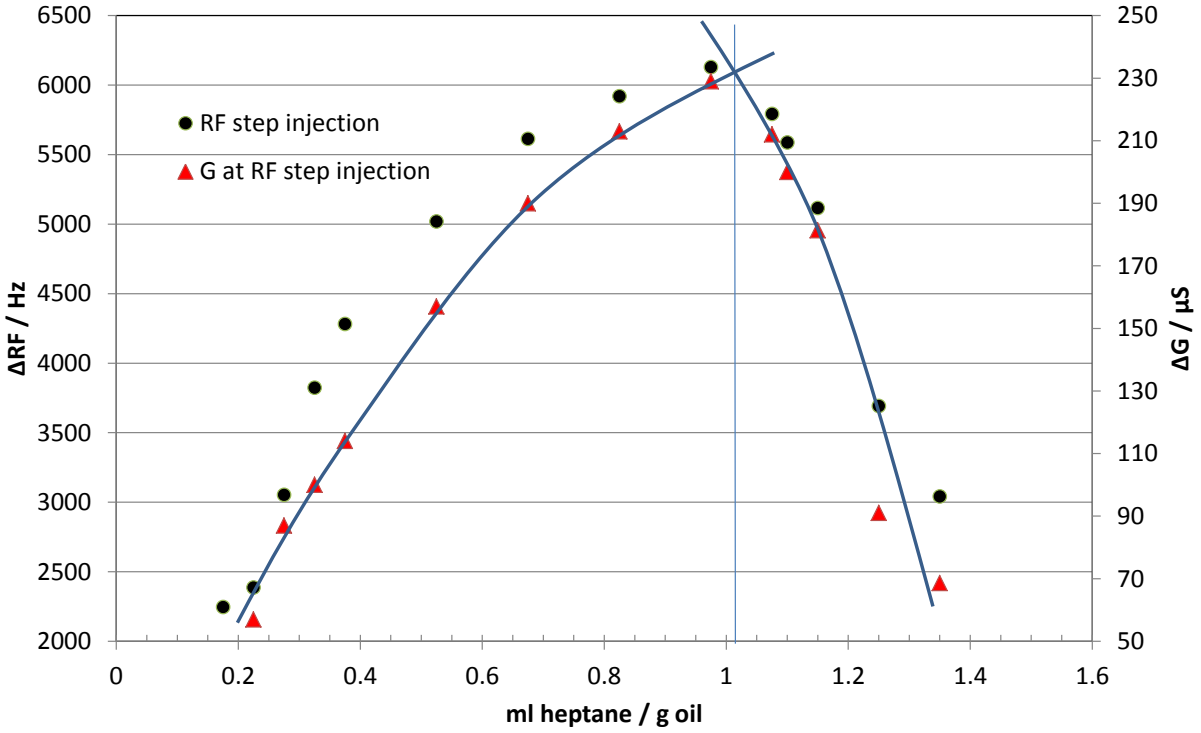

Figure 4.2. Changes in RF and G at RF on step-wise injection of heptane into sample of stabilised North Sea oil. Test temperature was 20 °C.

4.2.3.2. Continuous injection of heptane into stabilised crude

A test was conducted with the same oil as used in the test above. In this case the heptane was injected into the oil at a constant rate of 0.01 ml per minute. The test results are shown in Figure 4.3 along with the results from the test with step-wise injection. As can be seen from Figure 4.3 the point at which the RF and G at RF decline is at a higher volume of heptane injected per ml of oil. In addition the point is less clear. In order to make it clearer it is necessary to plot only the values close to the break over point as shown in Figure 4.4.

The differences in the amount of heptane per g of oil between the test with step-wise and continuous injection may be due to the system not achieving equilibrium with continuous injection. Another possibility is that the sharper increase in the amount of heptane present at each step in the step-wise injection may lead to localised instability and asphaltenes coming out of solution. More work is required to investigate these differences. It should be noted that in ASTM D6703 – 07 the solvent flow rate is 0.5 ml per minute with a sample of similar size to that used in the tests presented in this work. It might be suggested that a step-wise

injection approach would be better at giving a more accurate value for ml of heptane per g oil than continuous injection as the system is given time to reach equilibrium.

Example plots from commercially available equipment based upon detecting asphaltene onset using changes in light transmittance are shown in Figure 4.5. No information is available on the size of oil sample or the rate of injection. The shape of the plots is similar to those generated using continuous injection with the QCM (Figure 4.3). The manufacturer identifies two points, a point where there is a change in slope, named the flocculation point as shown in Figure 4.5, and a second point named the precipitation point where the transmittance begins to decline. It would be interesting to see the results of a test conducted with step-wise injection of heptane using this same equipment.

The main point to be taken from these tests is that the QCM is a good option for identification of the amount solvent required per g of oil to start asphaltene precipitation.

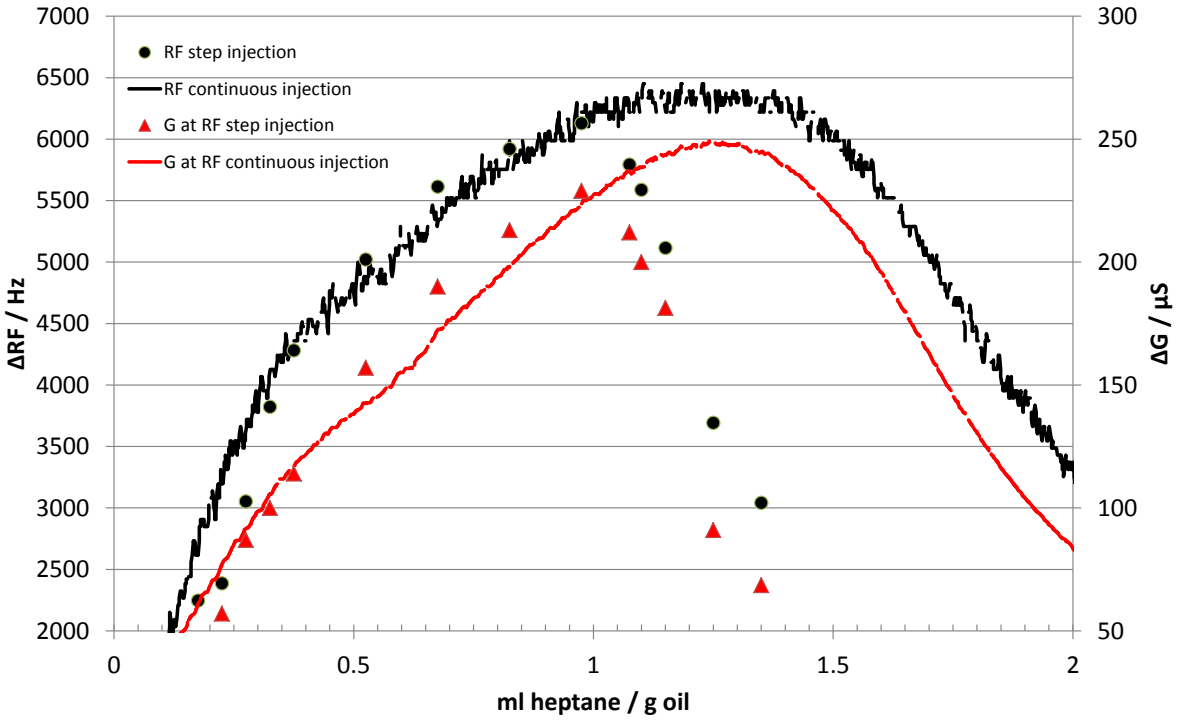

Figure 4.3. Changes in RF and G at RF on step-wise and continuous injection of heptane into sample of stabilised North Sea oil. Test temperature 20 °C.

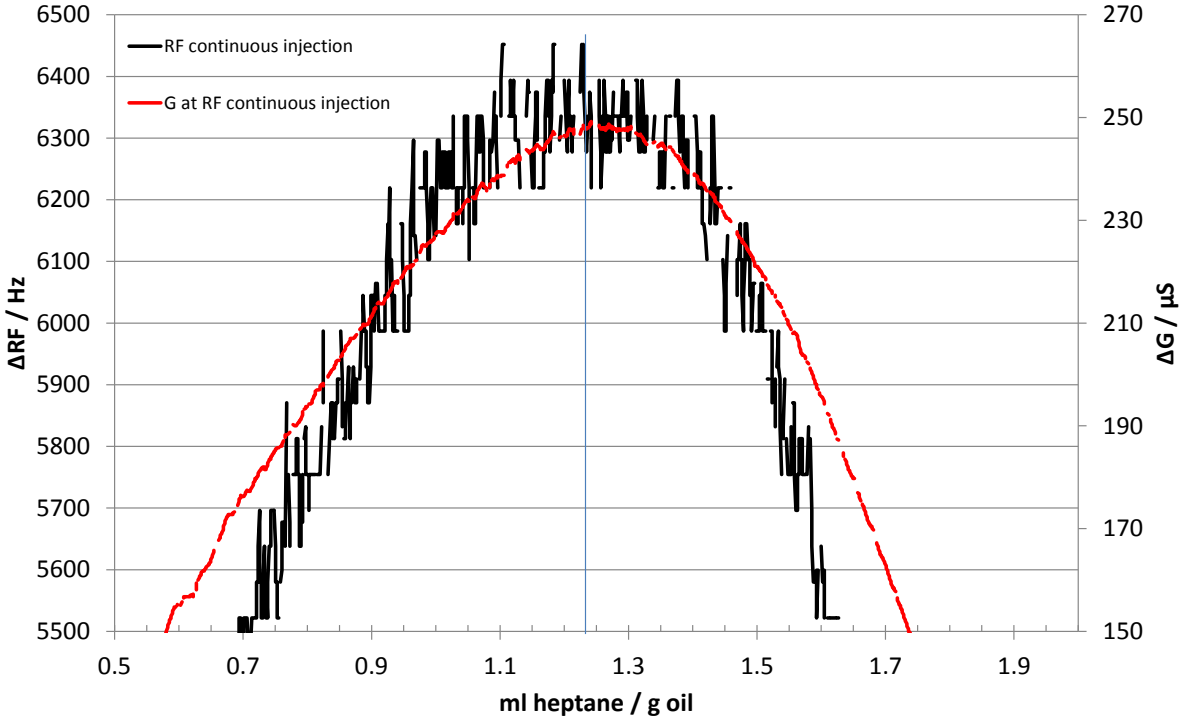

Figure 4.4. Changes in RF and G at RF on continuous injection of heptane into sample of stabilised North Sea oil. Test temperature 20 °C.

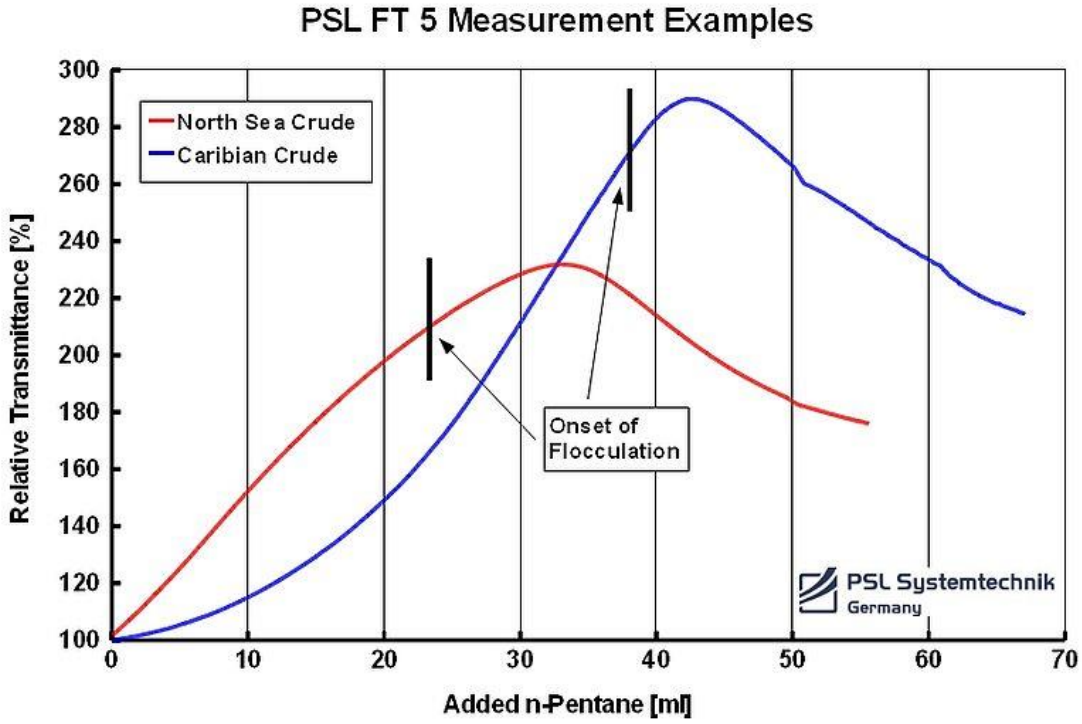

Figure 4.5. Example plot available from PSL Systemtechnik Germany for tests using a Flocculation Titrimeter.

4.2.3.3. Continuous injection of heptane into a toluene/asphaltene solution

In order to find if the QCM set-up could be used as an alternative for detection of asphaltene onset in ASTM D6703 – 07, tests were carried out with a solution composed of a small sample of asphaltenes dissolved in toluene. An example of the data from one test is shown in Figure 4.6. In this test the heptane was injected at a rate of 0.01 ml per minute. As can be seen from Figure 4.6 the RF is stable as heptane is injected, in the first instance. This is due to the fact that the density and viscosity of the overall solution will not change very significantly as a result of adding heptane, the density and viscosity of both heptane and toluene being similar. There is some change in G at RF but not as marked as the changes seen in the tests with stabilised oil (Figures 4.2 and 4.3). It is clear from Figure 4.6 that the point at which asphaltene precipitates can easily be identified from a marked decline in RF and G at RF. This work clearly shows that the QCM set-up can be used as an asphaltene onset detection method in ASTM D6703 – 07. In addition it can be used to generate data required to determine the ASIST for different oil samples.

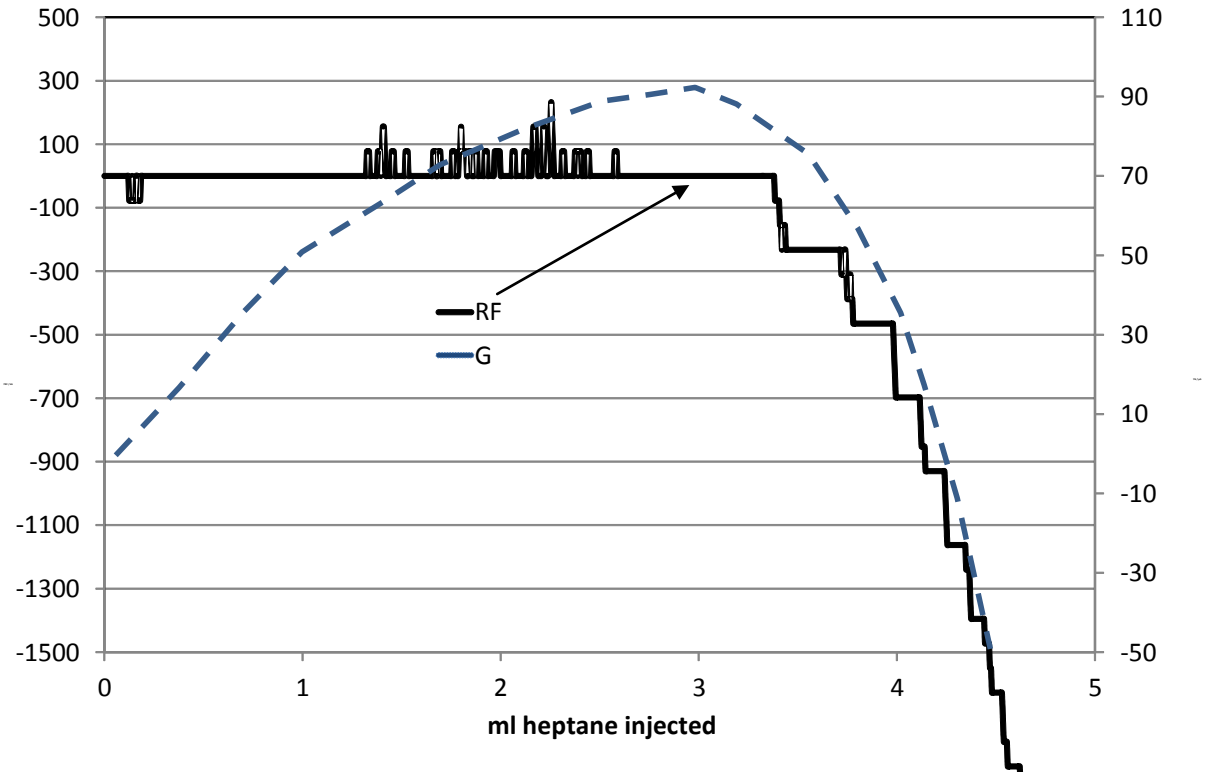

Figure 4.6. Changes in RF and G at RF on continuous injection of heptane into a toluene/asphaltene solution. Test temperature 20 °C.

4.3. Gas injection tests

Initial tests were conducted to evaluate the use of QCM based equipment to measure asphaltene precipitation for live fluids and in addition assess the effect of asphaltene inhibitors at these conditions.

4.3.1. Experimental equipment

The tests were carried out using the rocking visual cell as detailed in **Chapter 2**, Section 2.5.1.

4.3.2. Test fluids

A stabilised North Sea oil with an unknown composition was used. Natural gas with a composition as shown in **Chapter 2**, Table 2.9 was used.

4.3.3. Experimental methods

Stabilised oil was injected into the clean dry cell. The cell temperature was held at 55 °C throughout the test. This was at a temperature higher than the WDT of the fluid to prevent wax coming out of solution during the test. Gas was injected into the cell step-wise. At each step the cell was rocked to achieve mixing of the test fluids and achieve equilibrium. The QCM RF was recorded and once the value was found to be constant further gas was injected.

4.3.4. Results

Figure 4.7 below compares asphaltene onset pressure (AOP) and amount of asphaltene deposition, seen by reduction in Resonant Frequency RF for a real fluid on gas injection, without and with asphaltene inhibitor present. As can be seen from Figure 4.7 as gas is injected the RF increases as expected due reductions in the density and viscosity of the oil. At a certain pressure the RF begins to decline, associated with asphaltenes adhering to the surface. The presence of asphaltenes was confirmed by taking pictures of the surface of the springs holding the QCM after removal from the test cell at the end of the test and cleaning with heptane. Figure 4.8 shows the asphaltenes from a test with the oil with no inhibitor present. It can be seen from Figure 4.7 that in the test with inhibitor present the pressure at which asphaltenes adhere to the QCM surface is higher, meaning that it appears to reduce deposition. Figure 4.9 shows an image of the asphaltenes adhering to the surface of the

springs in the test with inhibitor present and as can be seen the deposits are markedly smaller compared to those seen without inhibitor present.

The results clearly show the capability of the technique to measure accurately asphaltene onset using non-visual means and to assess inhibitor performance at realistic live conditions.

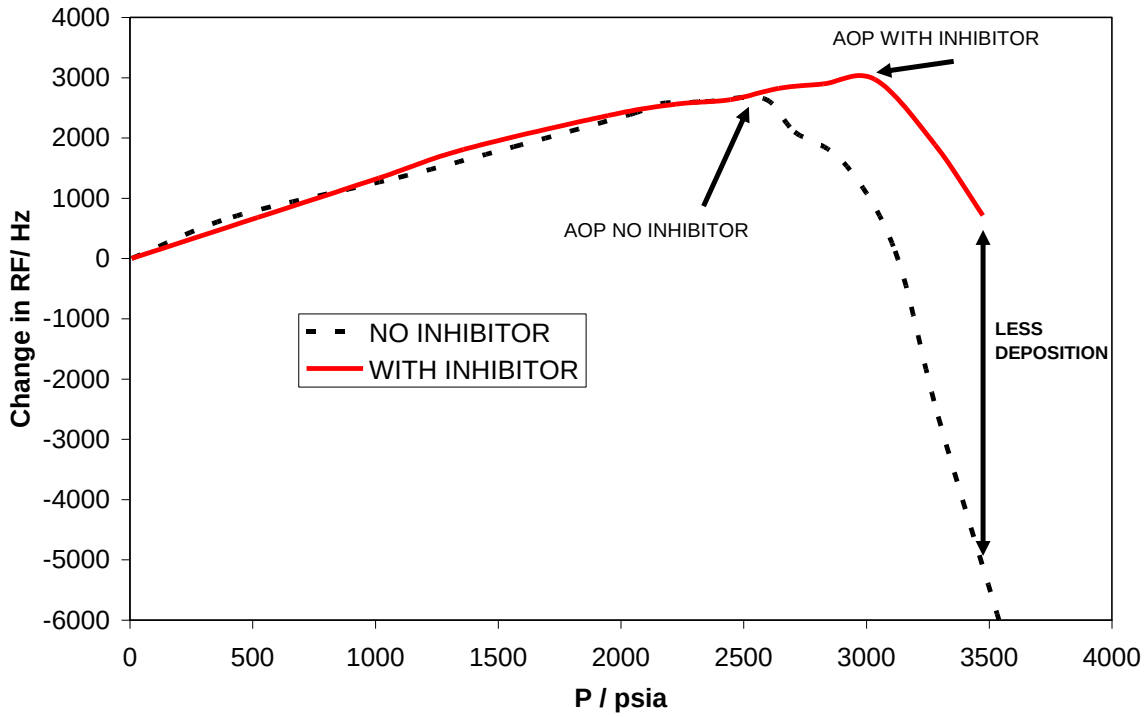

Figure 4.7. Plot showing measurement of AOP in a live fluid on gas injection for oil without and with asphaltene inhibitor added. Lines fitted through experimental data points.

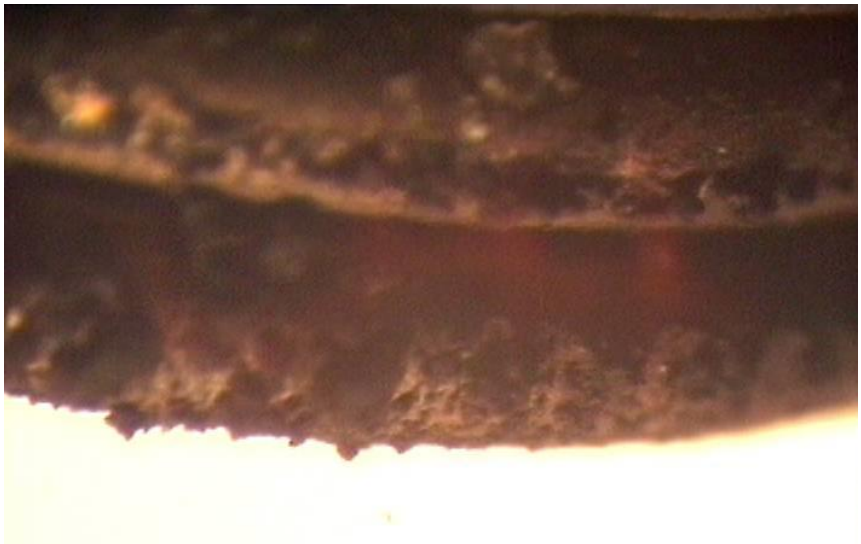

Figure 4.8. Picture of asphaltenes deposited onto surface of QCM retaining spring in test with no asphaltene inhibitor, QCM data as shown in Figure 4.7 above. Approximately 150 times magnification.

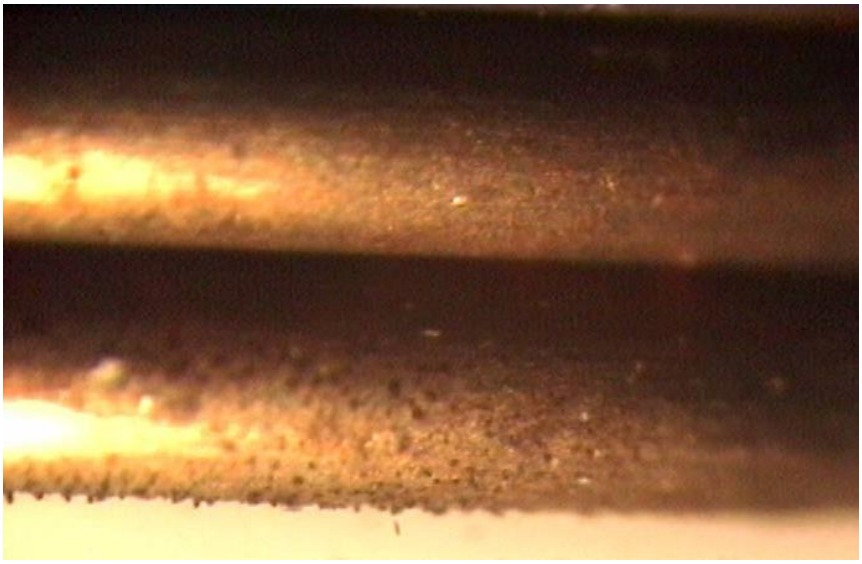

Figure 4.9. Picture of asphaltenes deposited onto surface of QCM retaining spring in test with asphaltene inhibitor, QCM data as shown in Figure 4.7. Approximately 150 times magnification.

4.4. Conclusions

The results from the work presented in this chapter, aimed at developing and validating QCM based equipment for asphaltene measurements are as follows:

- The heptane titration tests showed that the QCM can be used to measure the onset of asphaltene precipitation and adhesion for stabilised crude oils. This makes the method applicable for use in ASTM D6703 – 07 and for the stock tank oil titrations required for the ASIST method of assessing asphaltene onset in live fluids.
- The difference between the asphaltene onset, in terms of the amount of heptane injected per g oil, between tests with step-wise and continuous injection suggests that more research is required to optimise procedures. In addition it suggests that the true point of asphaltene may not be correctly measured in tests with continuous solvent injection. It may be that as for other cases where a new solid is formed some degree of super saturation is required before the new phase forms and therefore onset measurements could be stochastic. If this is the case then step wise measurement of melting or disappearance temperature is the only means of measuring the true point of thermodynamic equilibrium required for development and validation of thermodynamic models.

- The tests at pressure show that QCM based equipment can be used to measure the asphaltene onset conditions in live fluids at high pressure/high temperature conditions. The high sensitivity of the QCM to very small amounts of deposition may make it more sensitive than some other experimental methods for detecting asphaltene onset conditions.
- The tests comparing live oil without and with inhibitor indicate that the effectiveness of the inhibitor at reducing deposition can be evaluated. As reducing the deposition of asphaltenes on surfaces is arguably the most important aim of inhibitor injection, QCM could be considered as the best option for inhibitor screening and optimisation. Although not investigated in this work it is expected that inhibitor evaluation can also be conducted for stabilised oil with solvent injection.

In general there are fewer avenues to validate the accuracy of QCM based measurements for asphaltenes when compared to those for wax measurements. In the case of wax measurements there is literature data available for synthetic mixtures and in the case of wax inhibitors it was possible to run a parallel study with another laboratory. For asphaltenes it would be better to run further tests to validate the developed equipment and methods, preferably by conducting parallel studies with other laboratories. One study was conducted on a downhole sample in which, on isothermal depressurisation no asphaltene precipitation had been found by a service laboratory using laser scattering and microscopy. Using QCM no deposition was found, thus in agreement. This study is not shown in Chapter 5 as it was complicated by the presence of barite drilling mud and mercury in the downhole sample. As with the wax equipment and methods it is not suggested that QCM based equipment is better than, or can replace the equipment and methods currently in use, rather that it can be used to complement existing technologies and that it may be useful as a research tool to investigate some aspects of asphaltene behaviour.

Two case studies where QCM based equipment has been used for specific investigations are presented in **Chapter 5**.

4.5. References

[1] Mitchell, D.L. and Speight, J.G. 1973. *The solubility of asphaltenes in hydrocarbon solvents*. Fuel 52 (2): 149-152.

[2] Speight, J.G., Long, R.B., and Trowbridge, T.D. 1984. *Factors influencing the separation of asphaltenes from heavy petroleum feedstocks*. Fuel 63 (5): 616-620.

[3] Joshi, N.B., Mullins, O.C., Jamaluddin, A. et al. 2001. *Asphaltene Precipitation from Live Crude Oil.* Energy Fuels 15 (4): 979-986.

[4] Leontaritis, K.J., Asphaltene Deposition: *A Comprehensive Description of Problem Manifestations and Modeling Approaches*. Presented at the SPE Production Operations Symposium, Oklahoma City, Oklahoma, USA, 13-14 March. SPE-18892-MS.

[5] Haskett, C.E, Polumbus, E.A, and Tartera, M., *A Practical Solution to the Problem of Asphaltene Deposits-Hassi Messaoud Field, Algeria,* Journal of Petroleum Technology, Volume 17, Number 4, 387-391, April (1965).

[6] Lichaa, P.M., *Asphaltene Deposition Problem in Venezuela Crude,* Can. PTJ. Oil Sands, 609-624, (1997).

[7] Kokal, S.L., and Sayegh, S.G., *Asphaltenes: the Cholesterol of Petroleum,* SPE paper 29787, presented at the SPE Middle East Oil Show in Bahrain, March 11-14, (1995).

[8] Escobedo, J., and Mansoori, G.A., *Heavy-organic particle deposition from petroleum fluid flow in oil wells and pipeline,* Pet.Sci. 7:502-508 (2010).

[9] Golczynski, T. S., and Kempton, C.K., *Understanding Wax Problems Leads to Deepwater Flow Assurance Solutions,* World Oil®, March 2006 Issue pages D-7-D-10.

[9] Goual, L., and Firoozabadi, A., Effect of Resins and DBSA on Asphaltene Precipitation from Petroleum Fluids, AIChE Journal, Vol. 50, No. 2, (2004).

[10] Buckley, J.S., Wang, J.X., and Creek, J.L., *Solubility of the Least Soluble Asphaltenes,* Chapter 16 in *Asphaltenes, Heavy Oils and Petroleomics*, O. Mullins, E. Sheu, A. Hammami, and A. Marshall, eds., Springer (2007) 401-437.

[11] Allenson, S. and Walsh, M. 1997. *New Chemicals and Treatment Methods that Prevent Asphaltene Deposition Problems Found in Oil Production*. Proc., IBC U.K. Conference, Aberdeen.

[12] Ammar M. Abdel Ghaffar, Khalid I. Kabel, Reem K. Farag, N. E. Maysour, Magdy A. H. Zahran., *Synthesis of poly(dodecyl phenol formaldehyde)*-b-*poly(oxypropylene)*

block copolymer, and evaluation as asphaltene inhibitor and dispersant, Research on Chemical Intermediates January 2015, Volume 41, Issue 1, pp 443-455.

[13] Villano L. D, Kommedal, R., Fijten, M. W. M., Schubert, U. S., Hoogenboom, R., and Kelland, M. A., *A Study of the Kinetic Hydrate Inhibitor Performance and Seawater Biodegradability of a Series of Poly(2-alkyl-2-oxazoline),* Energy & Fuels 2009, 23, 3665–3673.

[14] Oliensis, G.L.. In: ASTM, Proceedings. of the 36th Annual Meeting, Chicago 33, Part II, p. 715 (1933).

[15] Hotier, G. and M. Robin, *Effects of different diluents on heavy oil products: measurement, interpretation, and a forecast of asphaltene flocculation,* Revue de l'IFP 38, 101 (1983).

[16] Fotland, P., H. Anfindsen, and F.H. Fadnes. *Detection of asphaltene precipitation and amounts precipitated by measurement of electrical conductivity,* Fluid Phase Equilibria 82, 157 (1993).

[17] Jamaluddin, A.K.M., N. Joshi, M.T. Joseph, D. D'Cruz, B. Ross, and J. Creek et al. *Laboratory Techniques to Measure Thermodynamic Asphaltene Instability* Paper # 2000–68. In: Canadian International Petroleum Conferences (2000).

[18] Yarranton, H.W., Alboudwarej, H., and Jakher, R., *Investigation of Asphaltene Association with Vapor Pressure Osmometry and Interfacial Tension Measurements,* Ind. Eng. Chem. Res., *39,* 2916-2924 (2000).

[19] Wang, J.X. and J.S. Buckley. *An Experimental Approach to Prediction of Asphaltene Flocculation, In:* SPE 64994, Oilfield Chem. Symposium, Houston (2001).

[20] Montesi, A., Pinnick, R., Subramanian, S., Wang, J., and Creek, J., *Asphaltene Management in GOM DW Subsea Development,* Offshore Technology Conference, Houston, Texas, U.S.A., 2-5 May (2011).

CHAPTER 5 - CASE STUDIES USING DEVELOPED QCM BASED EQUIPMENT AND METHODS FOR ASPHALTENE STUDIES

5.1. Introduction

As with the work with wax the main justifications for developing equipment and methods for making experimental measurements are that the data generated can be useful for both academic and industrial purposes and that it can improve or complement existing knowledge and capabilities. Again as with the work with wax, in order to gain acceptance it is a requirement to be able to prove through projects that the equipment can generate the required data. In this chapter two case studies are detailed. The first project relates to a short study where ambient pressure heptane injection was used to find if mixing of oil from two fields would have any effect upon the stability of asphaltenes. The second study was aimed at finding if asphaltene deposition was likely at P/T conditions experienced in the field for an oil and to evaluate the use of an asphaltene inhibitor at different concentrations.

5.2. Determination of asphaltene deposition using heptane titration

5.2.1. Introduction

Heptane titration tests were conducted on three stabilised crude oil samples labelled Andrew 25/Tay 75, Andrew 50/Tay 50 and Andrew 75/Tay 25. The aim of the tests was to find if there was any incompatibility, in terms of effect on asphaltene stability when mixing fluids from two fields, namely Andrew and Tay.

5.2.2. Experimental equipment

Details of the experimental equipment are given in Chapter 4, Section 4.2.1.

5.2.3. Experimental methods

Section 4.2.2 in Chapter 4, gives details of the experimental methods. In the tests in this work the temperature was set at 15.5 °C. Heptane was injected at a constant rate of 0.18 ml per minute. An example for the Andrew 25/Tay 75 sample is shown in Figure 5.1 below. At the end of the test the presence of asphaltenes on the QCM surface was confirmed by measuring the QCM RF after washing with heptane and subsequently after washing with

toluene. A significant increase in RF was seen after washing with toluene indicating the presence of asphaltenes.

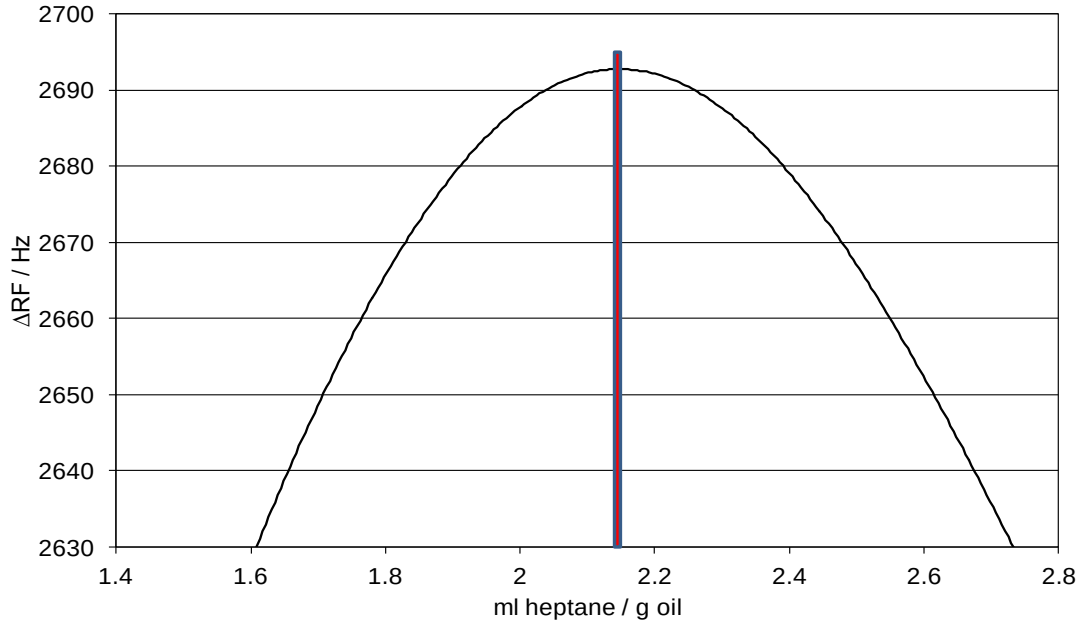

Figure 5.1. Plot showing changes in RF versus ml of heptane injected per g of stabilised crude recorded during test with Andrew 25/Tay 75 sample. Lines fitted through raw experimental data. As can be seen there is a clear change in slope at close to 2.2 ml heptanes per g of oil, indicating the onset of asphaltene deposition. Test temperature 15.5 °C.

5.2.4. Test fluids

The stabilised crude oil samples were supplied by the company sponsoring the work and labelled Andrew 25/Tay 75, Andrew 50/Tay 50 and Andrew 75/Tay 25. Heptane with a stated purity of 99+% was used in the tests.

5.2.5. Results

The results from the test with the three samples are shown in Table 5.1 below. It can be concluded from the tests that the asphaltene stability as measured by the "ml" of heptane per "g" oil is similar for the different mixtures of oil from the Andrew and Tay fields. The 50/50 mix is slightly lower showing a small degree of incompatibility between the fluids.

Table 5.1. Results from asphaltene onset tests using heptane titration at a test temperature of 15.5 °C.

Sample	**ml heptane per g oil ±0.1**
Andrew 25/Tay 75	2.2
Andrew 50/Tay 50	1.9
Andrew 75/Tay 25	2.3

5.3. Asphaltene deposition tendency evaluation for recombined North Sea reservoir fluid and inhibitor evaluation

5.3.1. Introduction

The aim of this work was to carry out an experimental study to evaluate asphaltene deposition tendency for a recombined North Sea reservoir fluid, without and with asphaltene inhibitor, at temperatures and pressures similar to those between bottom hole (BH) and top hole (TH) values, based upon field data.

Firstly an initial test was conducted to find if asphaltene deposition was detected. As this initial test showed that asphaltene deposition was occurring, further tests were conducted to evaluate the performance of an asphaltene inhibitor already in use in the field, at different concentrations. This work details the experimental equipment, experimental methods, test fluids and results from this study.

5.3.2. Experimental equipment

The experimental equipment is the same as that used in the wax study detailed in Chapter 3, Section 3.3.2.

5.3.3. Experimental methods

In this study the clean, dry, evacuated cell was charged with sufficient quantity of the test fluid to give the desired pressure at the starting temperature, with an initial volume of close to 50 ml. The QCM RF was monitored for a period of at least 4 hours prior to changing the temperature and pressure to the next set point. The volume was adjusted by releasing or injecting confining fluid behind the moving piston in the test vessel, in order to achieve the desired pressure.

5.3.4. Test Fluids

A sample of stabilised crude oil was supplied by the company sponsoring the work. A measured quantity of this oil was combined, gravimetrically, with pure components $C_1 – C_9$, CO_2 and N_2 in order to achieve a recombined reservoir fluid with a composition close to that given in a PVT report on fluids from the relevant reservoir.

The asphaltene inhibitor was supplied by the chemical company providing the product being used in the field. In the tests to evaluate the performance of the inhibitor the product was combined with the recombined oil on a mass basis to give the desired ppm concentration.

5.3.5. Test results

5.3.5.1. WAT/WDT

Prior to starting the tests both WAT and WDT were measured for a sample of the stabilised crude oil using an ambient pressure QCM set-up. This was carried out in order to establish if any of the solids detected during the subsequent asphaltene tests might be wax. A plot of the recorded data in terms of ΔRF with temperature on continuous cooling and continuous heating at a constant rate of 15 °C per hour is shown in Figure 5.2. As can be seen the WAT (37 °C) can be clearly identified where the RF reduces sharply on cooling. The WDT can be taken as the temperature at which the RF measured on heating matches that measured on cooling, indicating that all of the wax that had adhered to the QCM surface had been re-dissolved. As can be seen the WDT (45 °C) is less easy to identify precisely. The measured WAT/WDT values matched with values for fluids from the same reservoir previously reported by another laboratory.

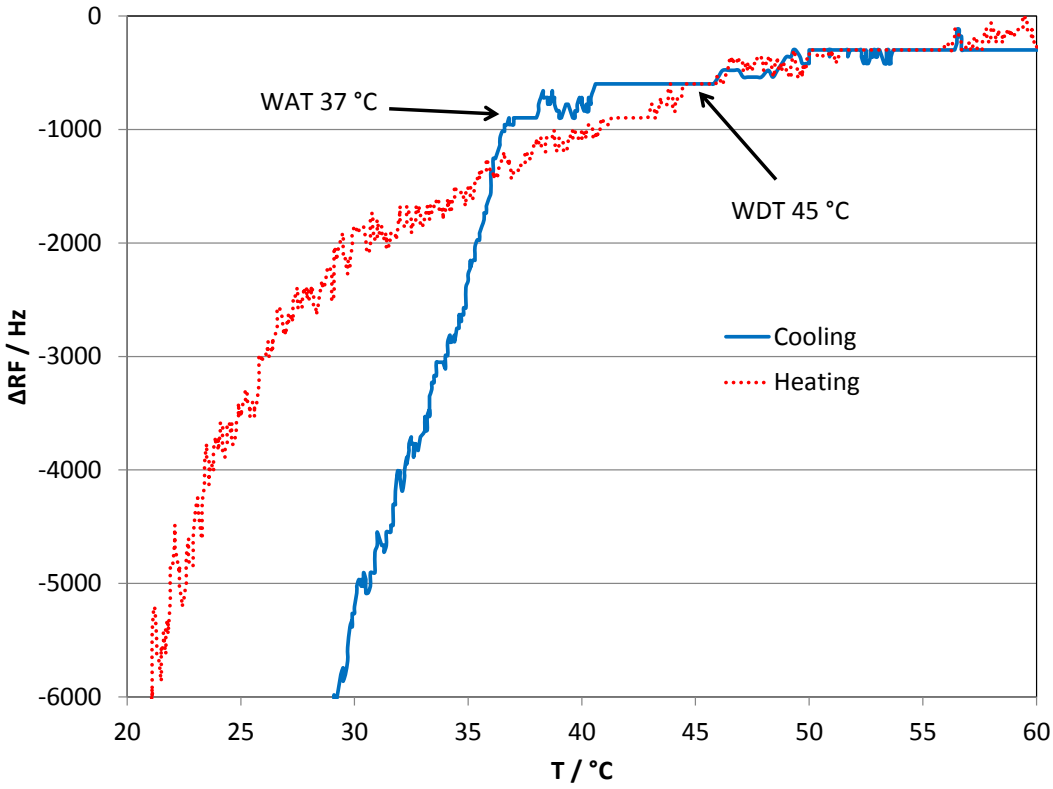

Figure 5.2. Plot of ΔRF with temperature on continuous cooling and continuous heating at a constant rate of 15 °C per hour, from test with stabilised crude.

5.3.5.2. Asphaltene tests with no inhibitor

The initial asphaltene test with no inhibitor was conducted at the temperatures and pressures shown in Table 5.3. As shown in Table 5.3, at each T/P the RF was seen to be declining or rising, indicating deposition or loss of solids from the QCM surface. Examples of the recorded data in terms of ΔRF with time for both outcomes are plotted together in Figure 5.3. As can be seen in Figure 5.3 the RF initially changes rapidly due to the changes in pressure and temperature prior to showing either a continuous decline or continuous increase with time. As shown in subsequent tests with inhibitor, part of the changes in RF at conditions where solids deposition was found, can be attributed to solids deposition taking place. Following the six planned T/P steps the sample pressure was increased to 402 bara, close to the initial reservoir pressure at 104 °C, in order to check that asphaltene deposition was not occurring at these conditions. Finally the T/P was set to 77 °C at 153 bara for a period of 48 hours in order to build up sufficient solids for subsequent visual observations.

As can be seen from Table 5.3 for the first four P/T steps the RF was seen to decline indicating solids deposition. These conditions were all above the fluid saturation pressure. The saturation pressure could not be measured accurately with the QCM equipment used in this study, however from the recorded P, T and estimated volumetric data it was close to 145 bara at between 77 and 68 °C. At the P/T conditions of 111 bara/68 °C, 70 bara/59 °C, 36 bara/50 °C and 402 bara/104 °C the RF was seen to rise indicating loss of solids from the QCM.

Following the last P/T step the QCM was removed from the set-up and washed with heptane. Images of the surface of the QCM, taken using a digital magnifying camera, are shown in Figures 5.4 and 5.5 and as can be seen there are black solids present on the surface. The QCM was then washed with toluene by way of indicating that the solids were mainly asphaltenes. This is based upon the operational definition of asphaltenes being insoluble in heptane and soluble in toluene. Figure 5.6 shows the surface after this washing. As can be seen the toluene removed the black deposits.

Table 5.3. Summary of test T and P steps used for asphaltene tests along with observation from RF data.

T / °C ±0.2	P / bara ± 1	Direction change in RF
104.0	278	Negative
95.0	236	Negative
86.0	195	Negative
77.0	153	Negative
68.0	111	Positive
59.0	70	Positive
50.0	36	Positive
104.0	402	Positive
77.0	153	Negative

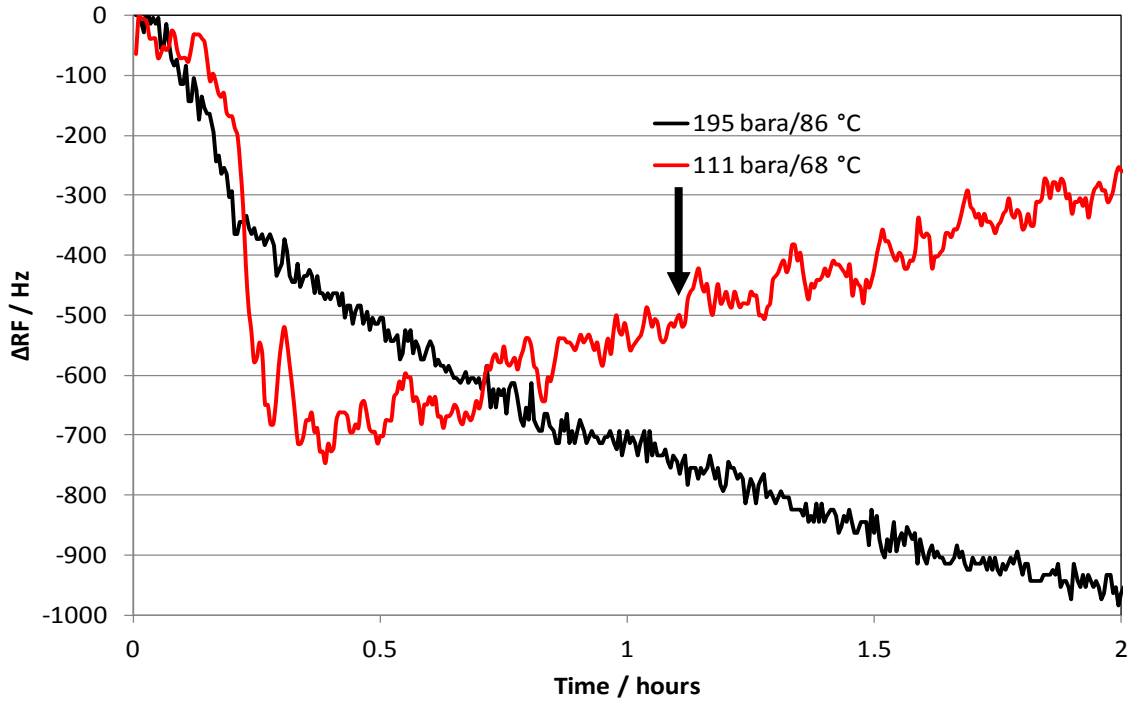

Figure 5.3. Plot showing changes in RF on changing the sample P/T conditions. The P/T shown are the conditions that were set following completion of the previous steps i.e. 236 bara/95 °C for the 195 bara/86 °C data and 153 bara/77 °C for the 111 bara/68 °C data. As shown in the figure changing the conditions from 236 bara/95 °C to 195 bara/86 °C resulted in a reduction in RF, indicating an increase in the amount of deposition. However, changing the system conditions from 153 bara/77 °C to 111 bara/68 °C resulted in an increase in RF, indicating a reduction in the amount of deposits (i.e., re-dissolve).

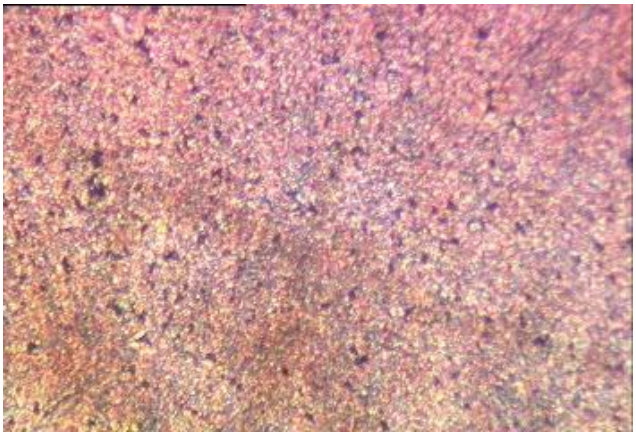

Figure 5.4. Digital image of QCM surface after washing with heptane.~120 times magnification. Dark spots are observed on the QCM surface, i.e., the deposits are not soluble in heptane.

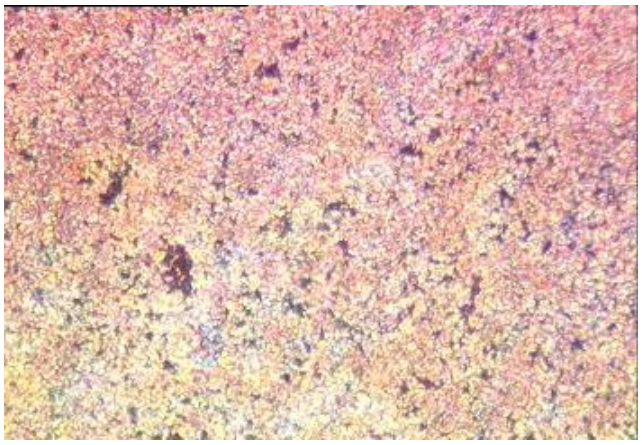

Figure 5.5. Digital image of QCM surface after washing with heptane. ~120 times magnification. Dark spots are observed on the QCM surface, i.e., the deposits are not soluble in heptane.

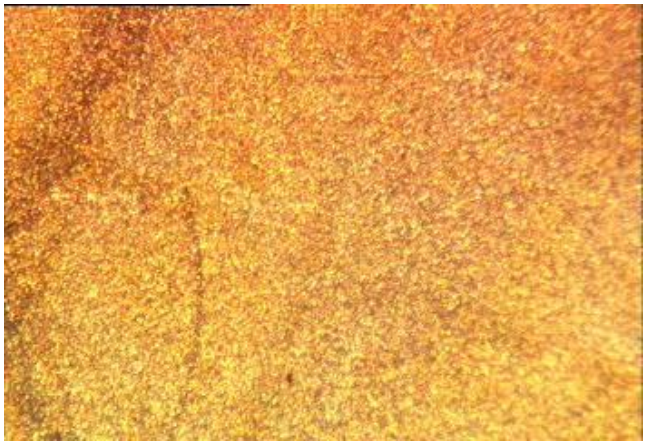

Figure 5.6. Digital image of QCM surface after washing with toluene. ~120 times magnification. No dark spots are observed on the QCM surface, i.e., the deposits are soluble in toluene.

5.3.5.3. Tests to evaluate performance of asphaltene inhibitor

As the initial tests indicated that asphaltenes were being deposited on the QCM surface at wellbore temperatures and pressures, further tests were conducted to evaluate the performance of an asphaltene inhibitor currently being injected, namely FLOTREAT DF 3167. In these tests an initial test with no inhibitor was run followed by three further tests conducted in exactly the same way with different concentrations of inhibitor present. In the first instance the QCM RF was monitored with time at a pressure of 402 bara and a temperature of 95 °C. At these conditions the RF was stable indicating that no solids deposition was occurring. The P and T were then reduced, over a period of close to 30 minutes, to 153 bara at 77 °C, thus passing through the conditions at which asphaltene deposition had been detected in the initial test.

The results in terms of RF reduction with time from the four tests, without inhibitor and with different concentrations of inhibitor, are plotted together in Figure 5.7. As can be seen there is a marked difference in the plotted data between the test without inhibitor and those with inhibitor present. The two main changes are firstly the reduction in the change in RF during the first 30 minutes of the test, when the P and T conditions were being changed, in the tests with inhibitor present compared to the test with no inhibitor.

The second observation is that the reduction in the rate of RF reduction seen in the tests with inhibitor present after the first 30 minutes of the test. It can also be seen that the most marked effect of the inhibitor is seen in the test with 11 ppm, with less benefit in terms of reducing deposition being seen as the concentration was increased to 61 ppm.

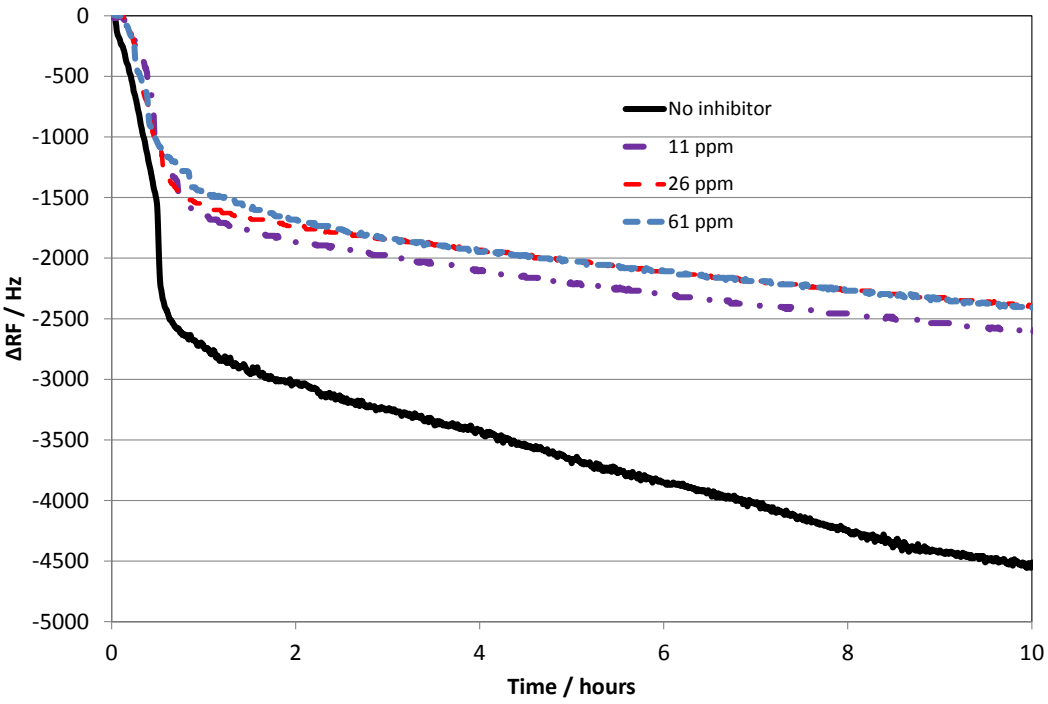

Figure 5.7. Plot showing changes in RF on changing the sample P/T conditions from 402 bara/95 °C to 153 bara/77 °C without and with different concentrations of asphaltene inhibitor.

5.3.5.4. Conclusion/discussion

Based on the tests conducted in this study on a re-combined sample the following conclusions can be drawn:

- The initial QCM results indicated that at the P/T conditions 278 to 153 bara/104 to 77 °C (above saturation P/T) solids were adhering to the QCM surface.
- The initial QCM results indicated that at the P/T conditions 111 to 36 bara/68 to 50 °C (below saturation P/T), and at 402 bara (close to initial reservoir pressure) at 104 °C, solids were being lost from the QCM surface.
- The pictures of the QCM surface after washing with heptane show small deposits of black solids over all the QCM surfaces. The removal of the solids by washing with toluene indicates that the solids are mainly asphaltenes.
- The tests without and with different concentrations of inhibitor indicated that asphaltene deposition was occurring both, rapidly, as the P and T were being reduced, and less rapidly over time.
- The tests with inhibitor showed that the inhibitor had a marked influence upon the amount of solids deposited as the P and T were being reduced and the rate of subsequent deposition over time.

- The effect of the inhibitor was most marked at a concentration of 11 ppm with less benefit, in terms of reducing solids deposition being seen at concentrations up to 61 ppm. Although not directly comparable this is in agreement with the data reported by another laboratory, regarding the performance of the same asphaltene inhibitor with stabilised oil from the same field, showing that the most benefit from the inhibitor was found for the test with 11 ppm.

From discussions with the sponsor an important question is; what is the likely rate of asphaltene deposition in tubing when no inhibitor is present? As these initial tests were conducted at static conditions, it would be ideal to conduct tests with different shear rates to find how this influences the rate of deposition. This could be done using a device equipped with a magnetic mixer and QCM embedded in the wall of the chamber containing the test fluids.

As mentioned earlier, the above tests were conducted on a re-combined sample in the absence of a downhole sample. This could have an impact on the results obtained in this study.

5.4. Conclusions

The first case study presented in this chapter shows that using the QCM in heptane titration testing allows for comparison of asphaltene stability in fluids composed of different blends of reservoir fluids.

The second case study shows that the QCM based equipment can be used to detect deposition of asphaltenes in live reservoir fluids. As discussed in **Chapter 2** a QCM itself has been used at pressures up to 3,000 bara and 430 °C hence with suitable constructed vessels it is possible to make measurements at any realistic reservoir conditions. The second case study also showed how the set-up can be used to evaluate inhibitor performance in terms of reducing asphaltene deposition and also to optimise inhibitor dose rate at field conditions.

One interesting observation from the second case study was that, as shown in Figure 5.3, there were two trends depending upon P/T conditions, either reducing RF indicating

asphaltene deposition or decreasing RF indicating asphaltene dissolution. The reversibility of asphaltene precipitation/flocculation/deposition has been the subject of a significant number of publications [1-3] and is considered to be an important issue. Some studies have focussed upon the reversibility of asphaltene precipitation induced by heptane titration, however it could be argued that reversing the process by adding toluene for example is not strictly correct as the original fluid composition is markedly changed. Hammami et al. [1] showed at least partial reversibility in tests using an experimental set-up comprised of a PVT cell equipped with a laser detection system for asphaltene detection. In these tests they carried out isothermal depressurisation/re-pressurisation tests and showed an increase in light transmittance on re-pressurisation indicating asphaltene dissolution. The results from this study indicate that the asphaltenes are dissolving at P/T conditions below saturation pressure and that from the rate of RF change with time (Figure 5.3) at a similar rate at which they were being deposited. Clearly this is the result from only one study and it would be interesting to conduct a more systematic study by conducting step-wise isothermal depressurisation/re-pressurisation tests at a range of temperatures from a starting temperature outside the asphaltene deposition envelope to close to the WDT (Wax Disappearance Temperture) of the fluid. In addition the reverse of deposition in porous media could be studied in terms of evaluating the effectiveness of different treatment procedures such as solvent injection aimed at removing asphaltene deposits.

5.5. References

[1] Hammami, A., Phelps, C.H., Monger-McClure, T., and Little, T.M., *Asphaltene Precipitation from Live Oils: An Experimental Investigation of Onset Conditions and Reversibility*, Energy & Fuels, 14, 14-18 (2000).

[2] Juyal, P., Ho, V., Yen, A., and Allenson, S.J., *Reversibility of Asphaltene Flocculation with Chemicals,* Energy Fuels, 26, 2631−2640 (2012)

[3] Peramanu, S., Singh, C., Agrawala, M., and Yarranton, H.W., *Investigation on the Reversibility of Asphaltene Precipitation*, Energy & Fuels, *15*, 910-917 (2001).

CHAPTER 6 - APPLICATION OF QCM BASED EQUIPMENT AND METHODS FOR HYDRATE MEASUREMENTS, IDENTIFICATION OF SOLIDS FORMING IN A DEW POINTING AND MERCAPTAN REMOVAL UNIT, DETECTING DEPOSITION OF DIESEL PERFORMANCE ADDITIVES AND EVALUATION OF ANTI-DEPOSITION COATINGS FOR SCALE AND WAX

6.1. Introduction

Hydrates are often lumped together with wax, asphaltenes, scale and napthenates as major Flow Assurance issues. Hydrates are formed when water and the hydrate forming molecules present in reservoir fluids are mixed at favourable P/T conditions [1]. The hydrate forming molecules become trapped in cages formed from water molecules and the resultant solid can restrict pipelines, form plugs blocking lines and increase the viscosity of oil/water mixtures. The hydrate forming molecules require to be of a size such that they can fit into the cages formed from the water molecules. In brief there are three hydrate structures commonly associated with hydrate formation in oil and gas systems, these are Structure I, Structure II and Structure H. The molecules present dictate the hydrate structure that is formed. Components such as methane, ethane and carbon dioxide are Structure I formers, propane and iso-butane Structure II formers and 2,2-dimethylbutane and methyl-cyclopentane along with a help gas such as methane are Structure H formers [2].

In order to deal with potential hydrate problems the first information required is the hydrate stability zone (HSZ) for the combination of hydrocarbon and aqueous phase present. With this knowledge the best strategy can be decided upon. If the planned operating conditions are inside the hydrate stability zone then there are a number of options. The pressure could be reduced to a point outside the HSZ. Heating and or insulation could be considered to keep the temperature higher than the HSZ at operating pressure or a combination of the two. Inhibitors such as ethylene glycol, methanol and ethanol can be injected in order to shift the HSZ to lower temperatures at each pressure. Kinetic hydrate inhibitors can be injected in order to shift the HSZ and within certain limits to reduce the rate

of hydrate formation [3]. Anti-agglomerants can be added to prevent hydrate solids agglomerating and forming larger pieces thus reducing the likelihood of blockages [4].

Whatever strategy is considered it is necessary to be able to accurately predict the HSZ and the effect of inhibitors on it. This is done using either a simple correlation or a thermodynamic model. There are a number of different thermodynamic models and equation of state (EoS) options that can be used. A thermodynamic model has been developed at Heriot-Watt over the past 28 years. A commercial version of the model named HydraFLASH® is available from the Heriot-Watt spin out company Hydrafact Ltd. A systematic approach has been taken, using physical property data to develop the model and accurately measured hydrate dissociation point data to validate the model. The most commonly used method for measuring hydrate dissociation points is isochoric step-heating. This method can be time consuming, however if certain guidelines are not adhered to then the data can be incorrect [5]. There are a number of other options available such as visual, Cailletet, Raman Spectroscopy and high pressure DSC [1]. The use of QCM based equipment to measure hydrate dissociation points is described in this chapter.

Solids formation causes problems throughout oil and gas production facilities. In most cases identification of the solids is not difficult, however in some cases it is not clear. Through measurements of parameters such as formation and melting points and solubility in different media, QCM based equipment can not only help to identify the solids but also enable screening and optimisation of solids removal strategies. In this chapter the identification of solids, using QCM, forming in a dew pointing and mercaptan removal unit is described.

In diesel engines fuel injection pressure plays an important role in better atomisation of injected fuel allowing a more complete burn, helping to reduce emissions [6]. The drive towards reducing emissions and improving economy has pushed up injector pressures in excess of 40,000 psi [7]. Problems with blocked injectors have increased [8] and the cause of these problems has been associated with different types of fuel and performance additive combinations at such high pressure conditions. In this work the development of equipment and methods to investigate deposition problems at pressures up to 40,000 psi and temperatures up to 90 °C is presented.

An attractive option for reducing problems associated with solids deposition is to develop anti-depositional coatings. QCM based equipment can be used to evaluate the performance of anti-depositional coatings at laboratory scale. Due to the sensitivity of the QCM to mass deposition only small amounts of test fluids are required and large numbers of coatings can potentially be screened. In this chapter the use of QCM in comparing the performance of different coatings for their anti-depositional properties in relation to scale and wax is described.

6.2. Hydrate Measurements

The initial idea behind the development of the use of QCM based equipment for hydrate measurements was that as only a small droplet of aqueous phase in contact with the QCM surface would be sufficient to enable both detection of hydrate formation and dissociation then equilibrium times would be short allowing for a rapid and accurate means of making hydrate measurements. In the isochoric step-heating method, depending upon the system being studied, it can take between 3 and 10 days to measure one dissociation point, whereas with QCM this can potentially be reduced to only a few hours. In the work presented here the measurement of hydrate dissociation points using QCM is described.

In cases where volatile inhibitors such as methanol and ethanol are being used to inhibit hydrate formation the amount of inhibitor that goes to the vapour and liquid hydrocarbon phases is significant. It is necessary to be able to accurately predict the phase distribution in order to ensure that the inhibitor injection rate is sufficient to prevent hydrate formation in the aqueous phase at operating conditions. It is the case at present that there are significant differences between predictions from different thermodynamic models. In order to find which model and which EoS options are giving the most reliable predictions, accurate and reliable experimental data is required. In a system with a low aqueous fraction knowledge of the amount of both water and methanol or ethanol that is present in the vapour phase is important, allowing calculation of the inhibitor concentration in the aqueous phase. The water content can be reliably obtained using Tuneable Diode Laser Absorption Spectroscopy (TDLAS) based equipment as described in this Chapter. The amount of methanol or ethanol in the vapour phase can be measured using Gas Chromatography (GC). The GC approach will have problems where components such as propane elute at close to or at the same time as

methanol or ethanol. As these components are commonly present in reservoir fluids this may make accurate measurements difficult with conventional GC columns.

One possibility is to have a large vapour volume in equilibrium with a small aqueous volume in contact with a QCM and to measure the dissociation point of the aqueous phase on the QCM. The dissociation point will indirectly give the concentration of inhibitor in the aqueous phase and knowing the initial composition of the aqueous phase and the water content of the vapour phase then the inhibitor concentration in the vapour phase can be inferred. Initial work using this approach is described below.

6.2.1. Experimental equipment

Two experimental set-ups were used in this work. The first is the high pressure visual rig as described in **Chapter 2**, Section 2.5.1 with a QCM mounted inside.

The second rig is comprised of a 414 bar rated 9 litre jacketed cell within which a QCM is mounted. A schematic of the rig is shown in Figure 6.1. The cell is fitted with a magnetic mixer and a piston. The QCM is mounted in such a way as to allow for small amounts of aqueous solution to be introduced onto its surface using an HPLC pump. An Impedance Analyser is used to measure the resonant frequency RF of the QCM.

Water content measurements were made using a Yokogawa TDLAS and a flow meter. A back-pressure regulator is sited between the TDLAS and the flow meter. The Yokogawa TDLAS, pictured in Figure 6.2, can measure water content up to 3000 ppmV. It has two detectors with different ranges up to 100 ppmV and up to 3000 ppmV. The stated accuracy is ±1% of the relevant range. The Yokogawa TDLAS requires to be operated with gas flowing through at 50 °C and 0.34 barg, a schematic of the set-up is shown in Figure 6.3.

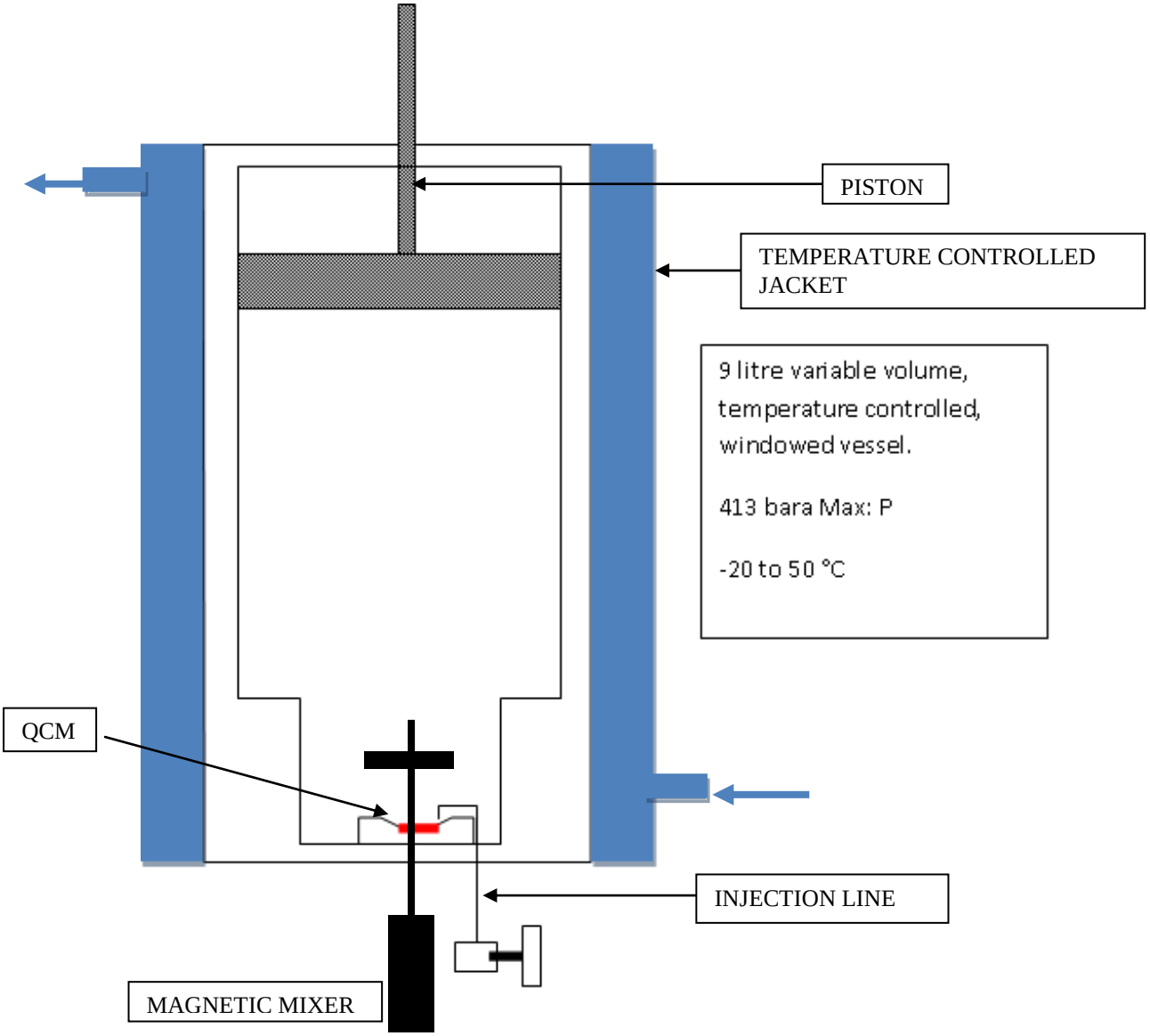

Figure 6.1. Schematic of large variable volume rig fitted with a QCM.

Figure 6.2. Picture of Yokogawa TDLAS.

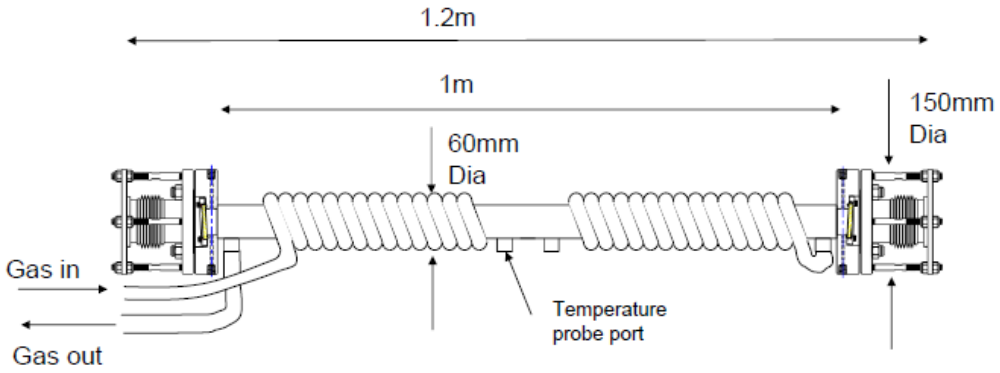

Figure 6.3. Schematic of Yokogawa TDLAS set-up.

6.2.2. Experimental methods

6.2.2.1. Hydrate dissociation point

For hydrate dissociation point measurements a droplet of water (~0.1 ml) was placed upon the QCM surface as shown in Figure 6.4. The cell was then evacuated and charged with ethane. The temperature was reduced below 0 °C to form ice. Ice formation resulted in severe damping of the QCM oscillation and no RF was detectable. The temperature was then increased above 0 °C, at which point the ice melted and hydrates formed immediately. The temperature was then increased step-wise whilst monitoring both resonant frequency (RF) and conductance (G). The dissociation point can be identified by a distinct change in the slope of both RF and G. An example of changes in resonant frequency (RF) and conductance (G) with temperature of the QCM in one test is shown in Figure 6.5.

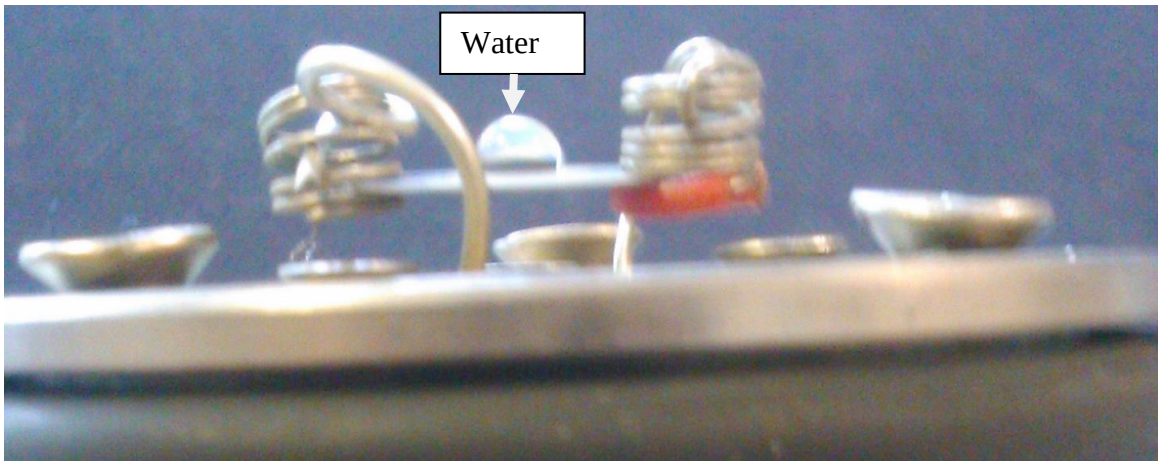

Figure 6.4. Water droplet on QCM surface.

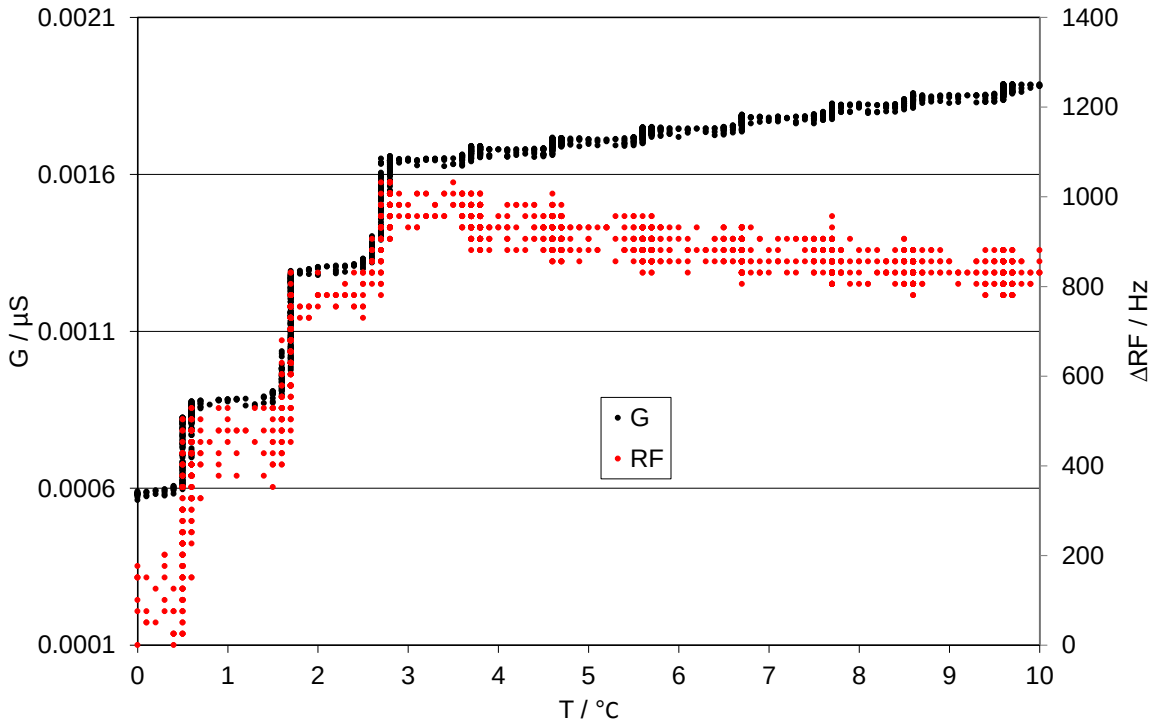

Figure 6.5. Plot showing measurement of hydrate dissociation point using changes in G and RF with temperature for test large volume rig fitted with QCM.

6.2.2.2. Large variable volume rig

In the measurements presented in this report the large cell was charged with methane, following which a small measured volume of an aqueous methanol solution was injected onto the surface of the QCM mounted inside the cell. After equilibration at 20 °C the temperature was reduced to form hydrates and then increased step-wise to measure the dissociation point of the hydrate that had formed. The idea was to find if the loss of methanol from the aqueous phase could be inferred from the apparent difference between the measured dissociation point and that calculated, assuming no loss of methanol from the aqueous phase. As with measurements using the QCM in the visual cell the dissociation point can be determined from the break over point in both RF and G trends.

6.2.3. Test fluids

The methane and ethane used were research grade 99.995% pure. The methanol was 99+% pure and deionised water was used to make aqueous solutions.

6.2.4. Results

Ethane

The measured dissociation points for simple ethane hydrates using the QCM technique are given in Table 6.1 and shown in Figure 6.6 along with data from literature and predictions made using HydraFLASH®. As can be seen the agreement between the data measured using QCM technique is in good agreement with the data from literature and the model predictions, demonstrating the reliability of the technique.

Table 6.1. Experimental dissociation points for simple ethane hydrates made using QCM technique.

T °C ±0.1	P bara ±0.4
5.4	9.1
10.0	16.0
14.1	30.9

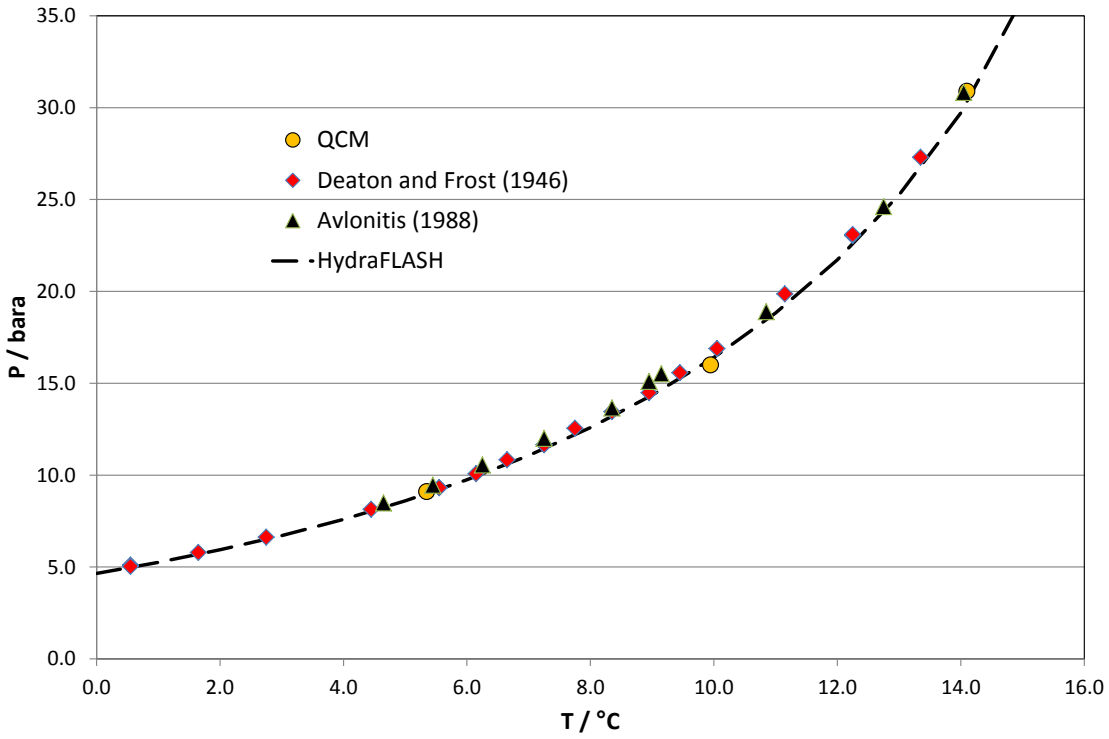

Figure 6.6. Experimental dissociation points for simple ethane hydrates made using QCM technique along with literature data [9, 10] and the predicted hydrate phase boundary for simple ethane hydrates.

Methanol loss

Measurements of the hydrate dissociation point of small aqueous phases were measured for methane with aqueous 15 mass% methanol at different pressures. In addition the water

content of the methane was measured at the measured hydrate T/P conditions using the Yokogawa TDLAS. The aqueous mole% of the feed at the start of the test, the measured dissociation point and the measured water content are given in Table 6.2. Table 6.2 also gives the predicted water content and the predicted methanol content of the aqueous phase at the dissociation conditions. As can be seen from Table 6.2 the measured water contents are in good agreement with the predicted values. Figure 6.7 shows that the experimental dissociation points are in good agreement with that predicted, based upon the predicted methanol content of the aqueous phase after loss of both water and methanol to the vapour phase.

A second set of tests was conducted with a 25 weight% methanol solution and two different aqueous contents at initial test conditions. As with the first set of tests the experimental and predicted data are tabulated in Table 6.3 and plotted in Figure 6.8. As can be seen from Table 6.3 the experimental and predicted water content values at hydrate dissociation conditions are in good agreement. Figure 6.8 shows that in this case there are significant differences between the measured dissociation points and those predicted, based upon the predicted methanol content of the remaining aqueous phase. The measurements suggest that more methanol is lost to the vapour phase than that predicted. Further measurements are required, including measurement of the methanol content of the vapour phase to validate the data.

Table 6.2. Experimental and predicted data from tests with methane and 15 weight% methanol using large volume QCM rig.

	Hydrate dissociation conditions		Vapour water content ppmV at hydrate dissociation T/P		Methanol concentration in aqueous at hydrate dissociation conditions
Aqueous mole%	T / °C ± 0.1	P / bara ± 0.4	Experimental	Predicted	Predicted Wgt%
0.5927	-0.3	47.7	154	147	12.5
0.4528	3.1	63.7	164	149	11.7
0.3046	7.7	96.3	155	156	10.0

Table 6.3. Experimental and predicted data from tests with methane and 25 weight% methanol using large volume QCM rig.

	Hydrate dissociation conditions		Vapour water content ppmV at hydrate dissociation T/P		Methanol concentration in aqueous at hydrate dissociation conditions
Aqueous mole%	T / °C ± 0.1	P / bara ± 0.4	Experimental	Predicted	Predicted Wgt%
0.4035	-0.1	62.7	114	115	20.3
0.3169	1.2	63.9	117	125	18.9

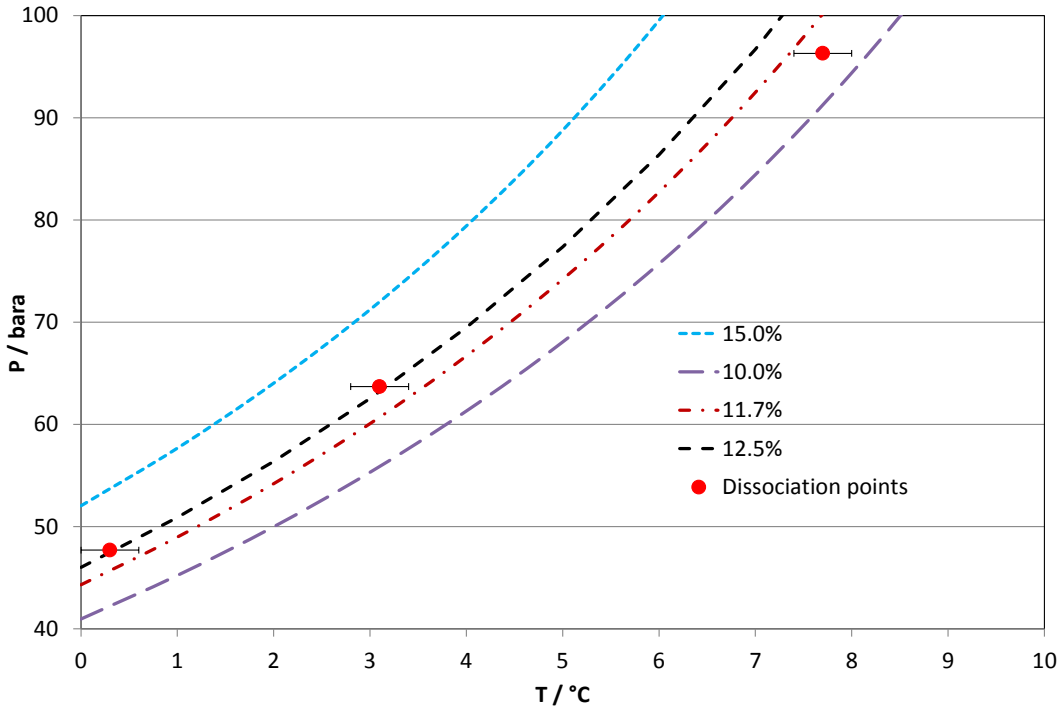

Figure 6.7. Experimental dissociation points for hydrates formed from methane in the presence of low aqueous cut systems with aqueous methanol with a feed composition of 15 weight%.

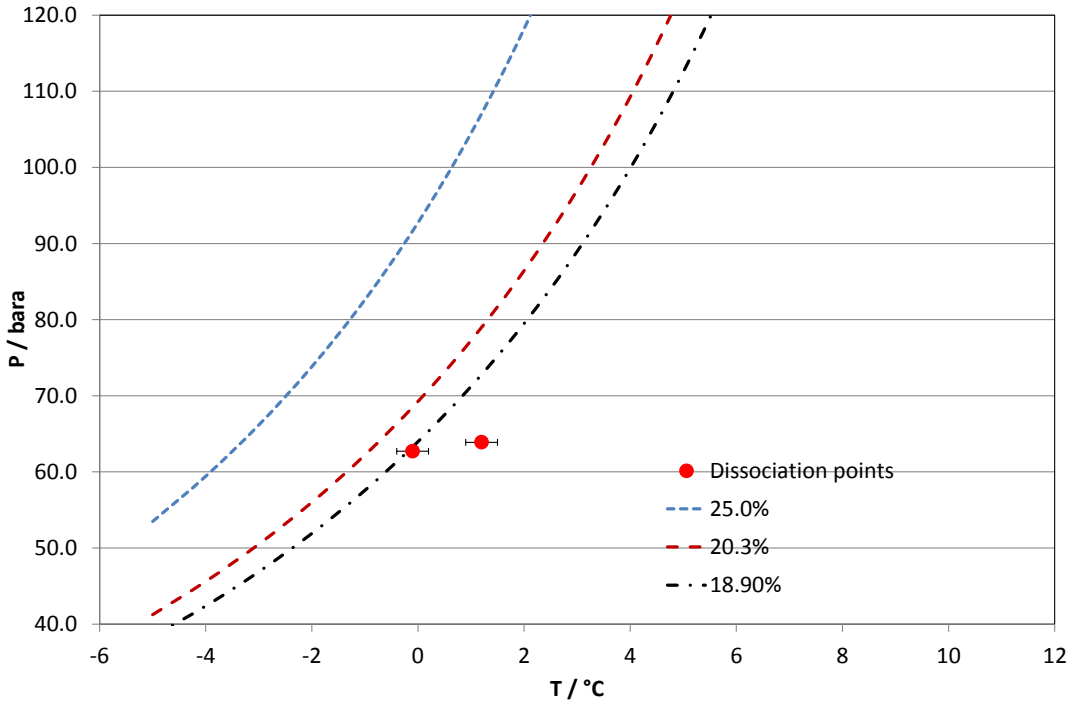

Figure 6.8. Experimental dissociation points for hydrates formed from methane in the presence of low aqueous cut systems with aqueous methanol with a feed composition of 25 weight%.

6.2.5. Conclusions

The use of QCM for hydrate dissociation point measurements was first developed at Heriot-Watt as part of an EPSRC funded research project during 1995 to 1997 [11], following on from that the method was patented in 1999 [12]. Experimental data generated using the developed equipment have been used in different industry funded research projects and published in two papers [13, 14]. The method is included in Sloan and Koh (2008) [1] as a possible method for hydrate equilibrium measurements. Recent publications indicate that the method is being used by other researchers [15, 16].

6.3. Identification of unknown solids forming in a dew pointing and mercaptan removal unit

This work demonstrates the use of QCM in association with other analytical tools for identifying unknown solids forming in a process facility. The solids were seen to be forming in a lean oil sample at temperatures around –30 ºC, causing flow restriction. The aims of the work were identify the solids and in addition investigate different options to avoid problems resulting from solids formation.

The original work programme is given below.

1. Identify the type of solid by step-cooling/step-heating to find its formation and melting conditions, using visual and QCM techniques.
2. Estimate the amount of solids formed at operating conditions (e.g., -30 ºC).
3. GC analysis to find out the composition of the original fluid.
4. GC analysis of the remaining fluid after cooling to -30 ºC.
5. Effect methanol on the solids. Why methanol, as was known, removes them? How much methanol is required if injected on a continuous basis? (testing at least 3 concentrations).
6. Initial tests to identify other potential inhibitors (4 different products or two products at 2 different concentrations, depending on the results in previous steps).

The following is a report detailing the experimental equipment, test fluids, tests and results, discussions and conclusions.

6.3.1. Experimental Equipment

The atmospheric pressure QCM set-up described in Chapter 2, Section 2.4.1 was used for measuring the formation and melting of solids.

A Varian 3400 GC fitted with an Agilent 'HP-1' megabore column with an FID was used for measurement of the composition of the lean oil samples. A Varian CP3800 GC fitted with a Haysep 3 metre column using TCD in series with FID was used for measurements of the water content of the lean oil samples.

6.3.2. Test Fluids

Studies investigating the type of solids formed, the effect of methanol, and the effectiveness of wax inhibitor chemicals were conducted using a sample brought back from the processing plant. Tests to measure the water content of the test fluid were conducted using further samples collected from the dew-pointing & mercaptan removal unit at a later date. The composition of the initial sample and the later sample are shown together in Table 6.4 below. As can be seen from Table 6.4 there were some differences between the two samples. Three 1 litre samples were collected at the later sampling time. Analysis of fluids from each container showed that there was no significant difference in composition between them.

The methanol used was 99+% pure. Three wax inhibitor samples provided by Clariant Oil Services were used. The inhibitors names were DODIFLOW LC 3256, 3257 and 3258.

Table 6.4. Composition in mass% of each component of the two different test samples used in this study.

Carbon number	Earlier sample	Later sample
C_{6s}	0.08	0.66
C_{7s}	32.43	38.78
C_{8s}	40.71	39.16
C_{9s}	16.79	14.04
C_{10s}	6.72	5.15
C_{11s}	2.23	1.40
C_{12s}	0.74	0.49
C_{13s}	0.31	0.20
C_{14s}	0.00	0.10
C_{15s}	0.00	0.01

6.3.3. Tests and Results

6.3.3.1. Solids Identification (Initial tests)

In the first instance tests were conducted using the low pressure QCM based apparatus as described in Chapter 2, section 2.4.1.

The results from a test with the lean oil sample in which the temperature was changed step-wise (30 minutes for each step), starting at 10 ºC reducing to –45 ºC and then returning to 10 ºC, are given in Figure 6.10. As can be seen from Figure 6.10 the solids appearance temperature was ~-25 ºC and the solids disappearance temperature was ~-6 ºC. Comparing Figures 6.9 and 6.10 shows that the pattern of RF change with temperature is similar. Due to this initial result it was considered that the solids may be heavier hydrocarbons crystallizing at low temperatures.

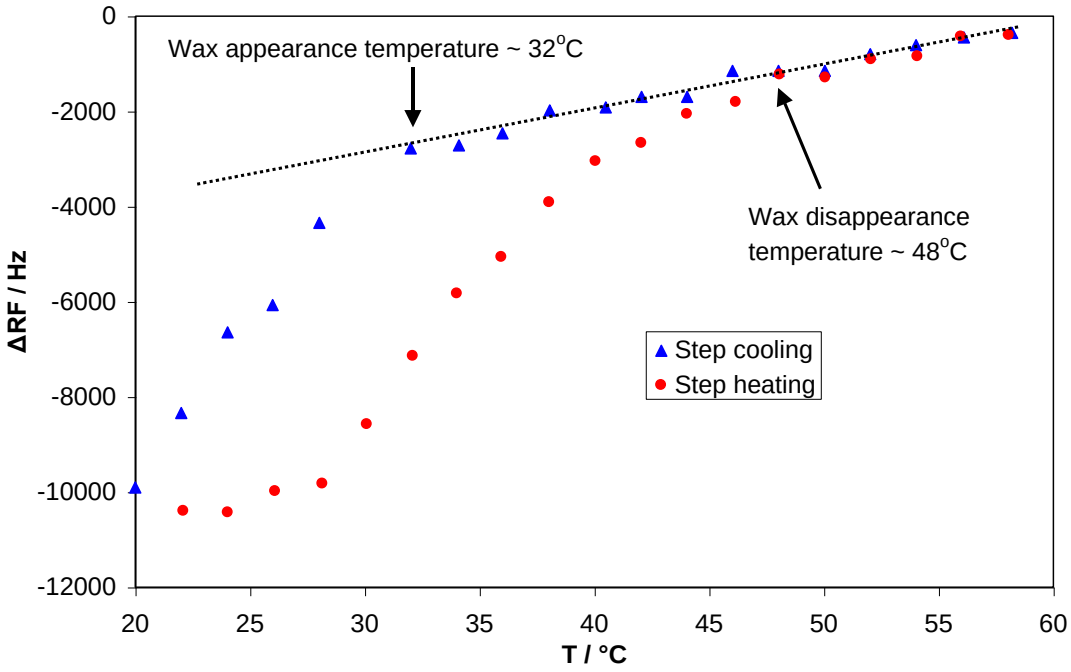

Figure 6.9. Example of WAT and WDT determination for a black oil using a QCM.

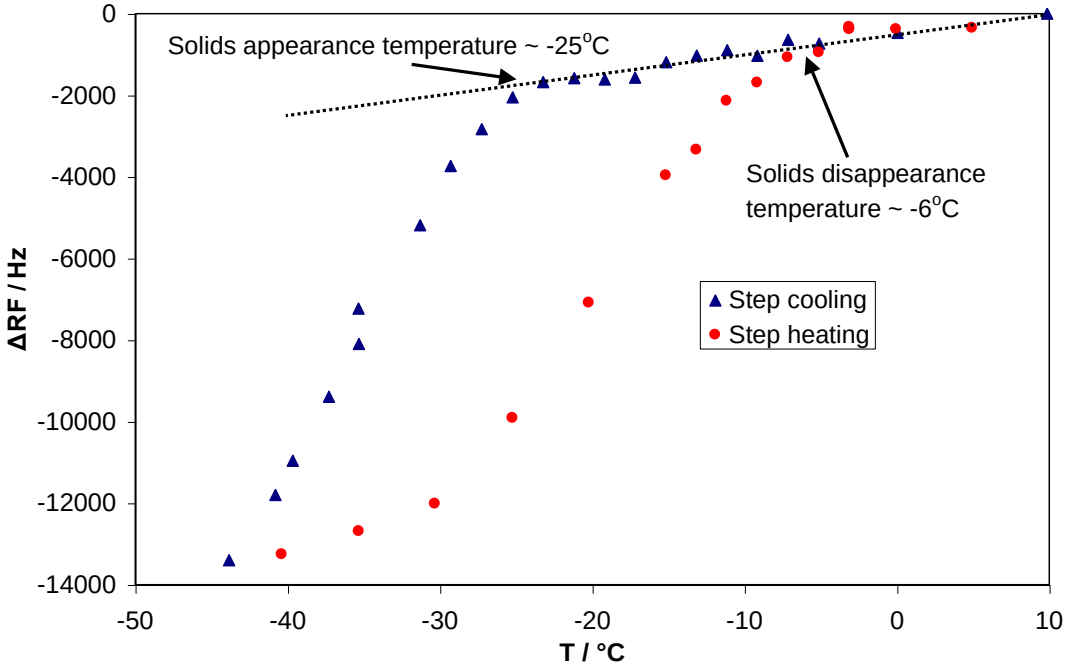

Figure 6.10. Plot of data for QCM test with lean oil sample.

Visual observations were also conducted using small 10 cc vials suspended in a low temperature circulator. On cooling the sample to –60 ºC it was difficult to identify the formation of solids, as the test sample did not become cloudy, whereas in a typical wax test, wax formation could be detected in the bulk of the test sample. Some solids were seen to

adhere to the vial walls above the top meniscus of the sample. These solids were seen to melt, on step-heating at a temperature close to –7 ºC.

6.3.3.2. Compositional Analysis

Two compositional analyses were conducted using GC. One for the original lean oil and one for a sample taken from a vial that had been cooled initially to –60 ºC and then held at –30 ºC for 24 hours. The aim was to take a "solids free" sample from the cooled sample and find if the composition differed from that of the original sample. The preliminary data are given in Table 6.5 below. As can be seen from Table 6.5 there was no significant difference between the compositions of the two samples. The heaviest hydrocarbon number present is C_{14}, and only in trace amounts. The lack of heavier hydrocarbons and the lack of any compositional differences between the original and cooled samples suggest that the solids are not associated with crystallization of hydrocarbons. In addition there was no cloud seen in the cooled sample as is usually observed when hydrocarbon solids crystallize from solution.

Table 6.5. Compositional analysis of the original and cooled lean oil samples.

Carbon number	Original lean oil Mass %	Cooled lean oil Mass%
C_{6s}	0.08	0.06
C_{7s}	32.43	32.31
C_{8s}	40.71	40.56
C_{9s}	16.79	16.84
C_{10s}	6.72	6.82
C_{11s}	2.23	2.24
C_{12s}	0.74	0.80
C_{13s}	0.31	0.35
C_{14s}	0.00	0.03

6.3.3.3. Effect of Methanol

It is known that methanol is currently being successfully used in the facility to remove problems associated with the formation of solids in the Cold Box. Tests were conducted using the QCM to investigate the effect of methanol on the build-up of solids on surfaces. Tests were conducted with different methanol concentrations added to the lean oil. In these tests methanol was added by mass to the lean oil hence the ppm values are given in ppm mass. For each dilution the fluid was continuously cooled from 10 ºC to –40 ºC and maintained at this temperature for 6 hours. The fluid was then heated to –30 ºC and allowed to equilibrate for 1 hour. The difference between the RF measured at -30 ºC on continuous cooling and that after cooling to –40 ºC and reheating to –30 ºC gave an indication of the

relative amount of solids adhering to the QCM for each dilution. Figure 6.11 shows a plot of the change in RF for each dilution. As can be seen for 1000 and 400 ppm mass of methanol there was no difference between the RF on cooling to -30ºC and that measured after reheating. However for methanol concentrations less than 400 ppm mass, the difference increased with decreasing methanol concentration indicating that if the methanol concentration is reduced to less than 400 ppm mass then solid build-up may occur. Clearly, the amount of methanol required is a function of the amount solid forming material in the sample/fluid, which could change in the field/factory as a function of feed and/or process variations.

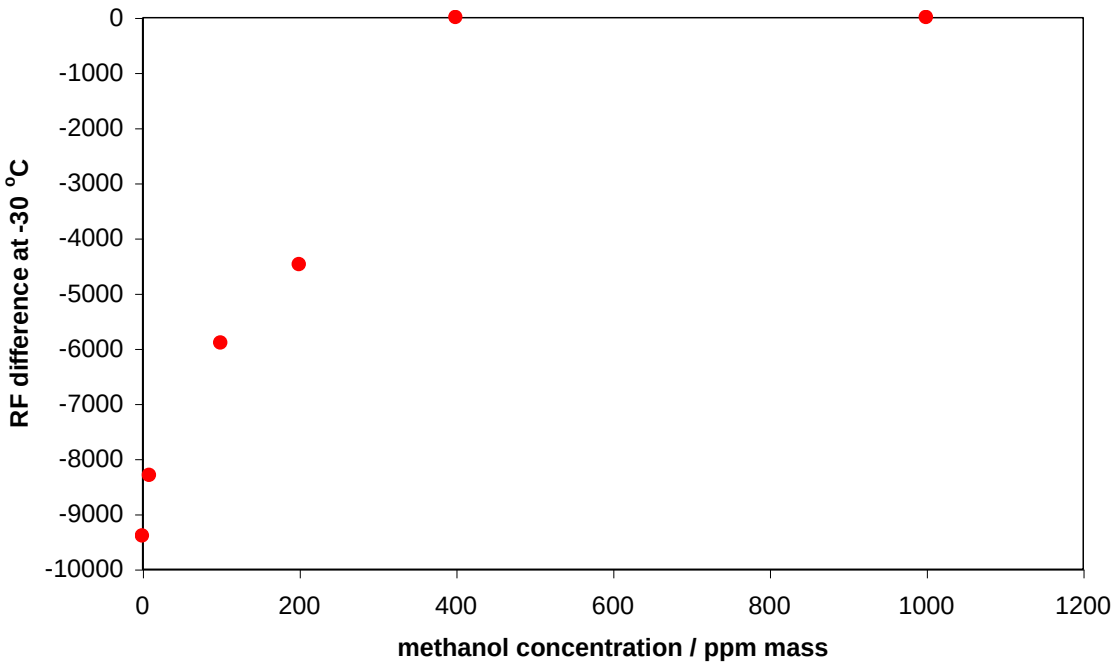

Figure 6.11. Plot showing the difference between the RF measured at -30 ºC on continuous cooling and that after cooling to –40 ºC and reheating to –30 ºC from tests with different methanol concentrations in ppm mass.

6.3.3.4. Investigation of Potential Chemical Additives

Three chemical additives, DODIFLOW LC 3256, 3257 and 3258, aimed at reducing problems caused by hydrocarbon solids in fluids similar to the lean oil being studied in this work, were procured from Clariant Oil Services. QCM tests were conducted with each of the additives at a concentration of 500 ppm mass. In each test the sample temperature was changed step-wise (30 minutes for each step), starting at 10 ºC reducing to –45 ºC and the returning to 10 ºC. In all cases solid build-up was seen by a marked difference in the RF

between the data recorded on cooling and that recorded on heating as shown in Figure 6.10. This indicated that these additives had no significant effect on the solids build-up.

6.3.3.5. Solids Identification (further tests)

From the compositional and chemical additive results it appeared that the solids are not heavier hydrocarbons crystallizing at low temperatures. The fact that methanol removes the problem indicates that the solids may be ice formed from dissolved water coming out of solution at low temperatures. Dissolved water is well known to be a potential problem, when it comes out of solution at low temperatures in jet fuels and hydraulic fluids. One approach to remove dissolved water is to use calcium chloride. Two QCM tests were conducted, one with the original oil, and one with a sample of oil that had been mixed with calcium chloride pellets. In both tests the sample was cooled to –45 ºC and then step-heated. The step-heating data from the test with the original oil is shown in Figure 6.12. The RF value at 5 ºC was taken as zero. As can be seen from Figure 6.12 the plot is similar to that shown in Figure 6.10 with a solids melting point of close to –7 ºC. The step-heating data from the test with the calcium chloride treated sample is shown in Figure 6.13. In this test the RF value at 20 ºC was taken as zero. As can be seen from Figure 6.13 the reduction in RF was much less compared to the original oil test and there was no solids melting point. The data from both tests are plotted together in Figure 6.14. This test indicated that the solids are most probably ice forming from dissolved water coming out of solution at low temperatures, a problem that can be removed using calcium chloride pellets or similar compounds.

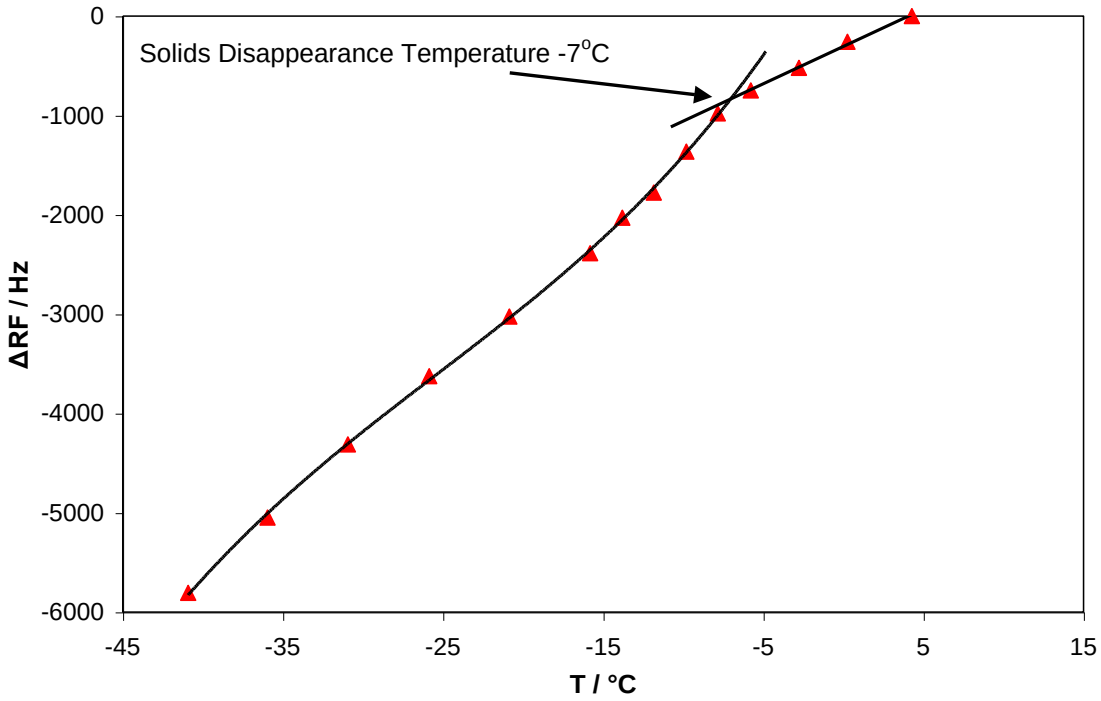

Figure 6.12. Plot of step-heating data for test with original untreated lean oil.

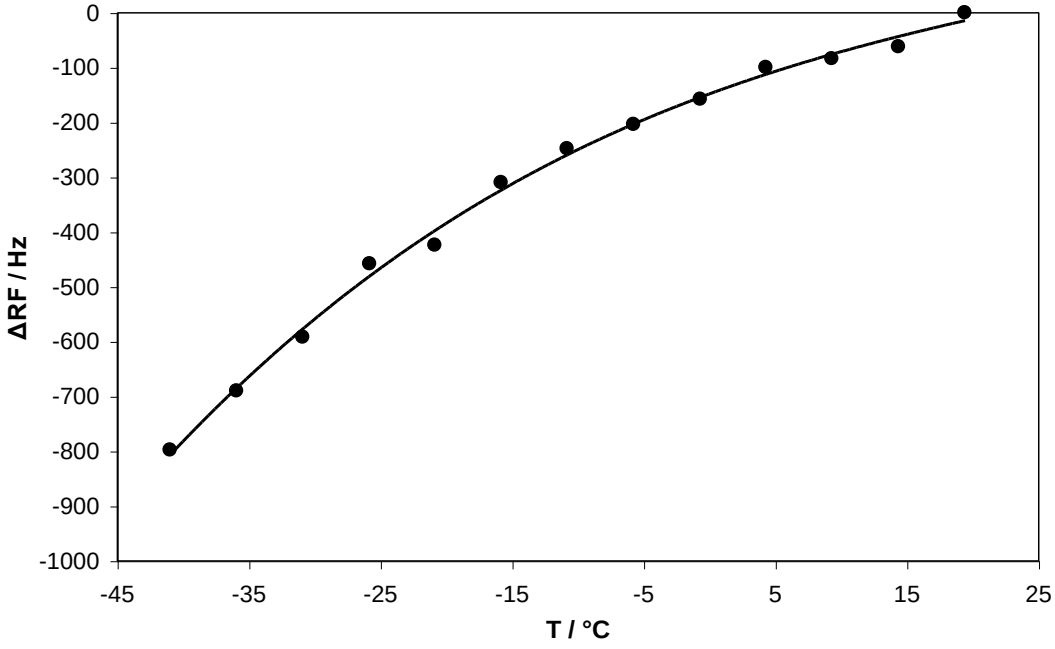

Figure 6.13. Plot of step-heating data for test with lean oil after being contacted with calcium chloride to remove dissolved water.

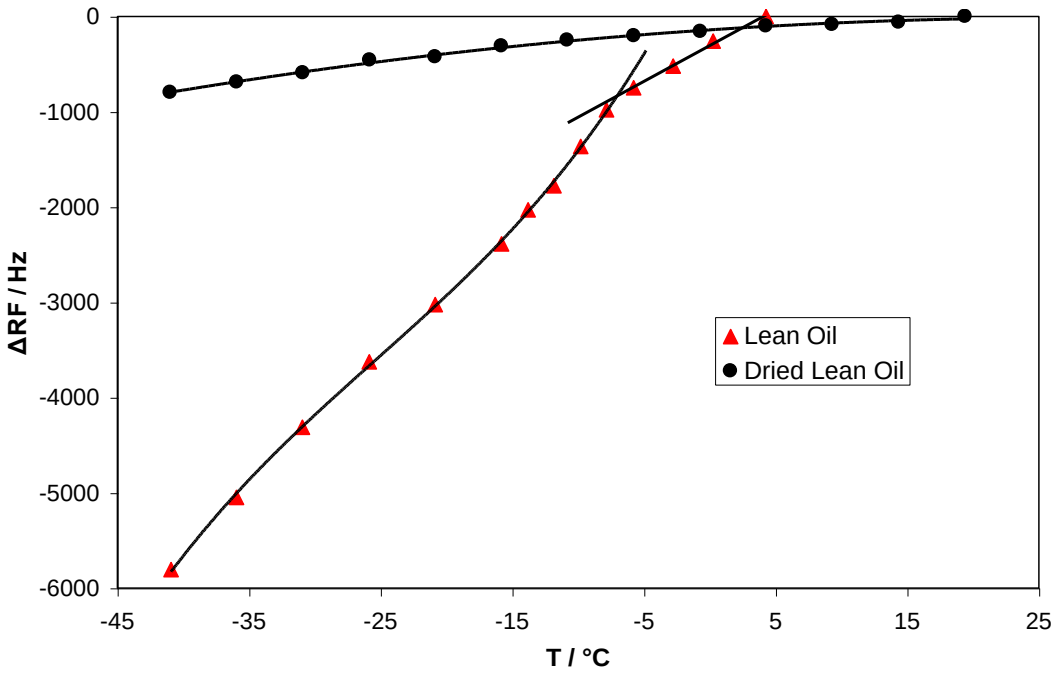

Figure 6.14. Plot of step-heating data for tests with original lean oil sample and lean oil after being contacted with calcium chloride to remove dissolved water.

6.3.3.6. Tests to Confirm Solids ID and Measure Concentrations

The initial testing was conducted using the initial sample. Three litres of condensate taken from the dew pointing and mercaptan removal were received at a later date for further tests. The results of the work on the first sample strongly indicated that the problems encountered were as a result of ice formation. Further work was conducted using the later samples. The aim of the work was to confirm that water was the source of the problem and to measure the amount of water present. Two methods were available to measure the water content of the samples GC and QCM. The GC method was tried first being the most rapid method. Successive measurements confirmed that water was present in all of the samples, however the results were not repeatable. It was thought that the presence of a micro-emulsion of water droplets in the test samples maybe the reason for the lack of repeatability. Subsequent tests using the QCM approach for water content measurement supported this hypothesis. The tests are described below:

In the QCM tests a portion of one of the later samples was dried using calcium chloride. Water was then added by mass to the sample. For each dilution the sample was cooled and then step-heated to find the temperature at which the RF on heating matched the RF measured on cooling. This was taken as the temperature at which water coming out of

solution on cooling re-dissolved on heating, the RF being reduced by the presence of water on its surface, hence the saturation point. Tests were carried out with dilutions of 50, 100 and 150 ppm by mass water. A thermodynamic model, HWHYD, was used to predict the water content of a simulated fluid at different temperatures, matching the measured saturation temperature for the water content at 100 ppm by mass of water. The experimental and predicted water contents are plotted together in Figure 6.15. The saturation temperature of the test sample was measured, using the QCM, to be 28 ºC and as can be seen from Figure 6.15 this gives an estimated water content of 263 ppm on a mass basis. As the saturation temperature of the test sample was above laboratory temperature (21 ºC) it can be assumed that non dissolved (i.e., free) water will be present in the sample in the form of a micro-emulsion supporting the conclusion regarding the reason for non-repeatable measurements obtained using the GC. Figure 6.15 also shows that on reducing the fluid temperature to –30 ºC the equilibrium water content will be reduced to around 11 ppm. This information can be used to estimate the amount of water that may come out of solution on cooling and forming ice.

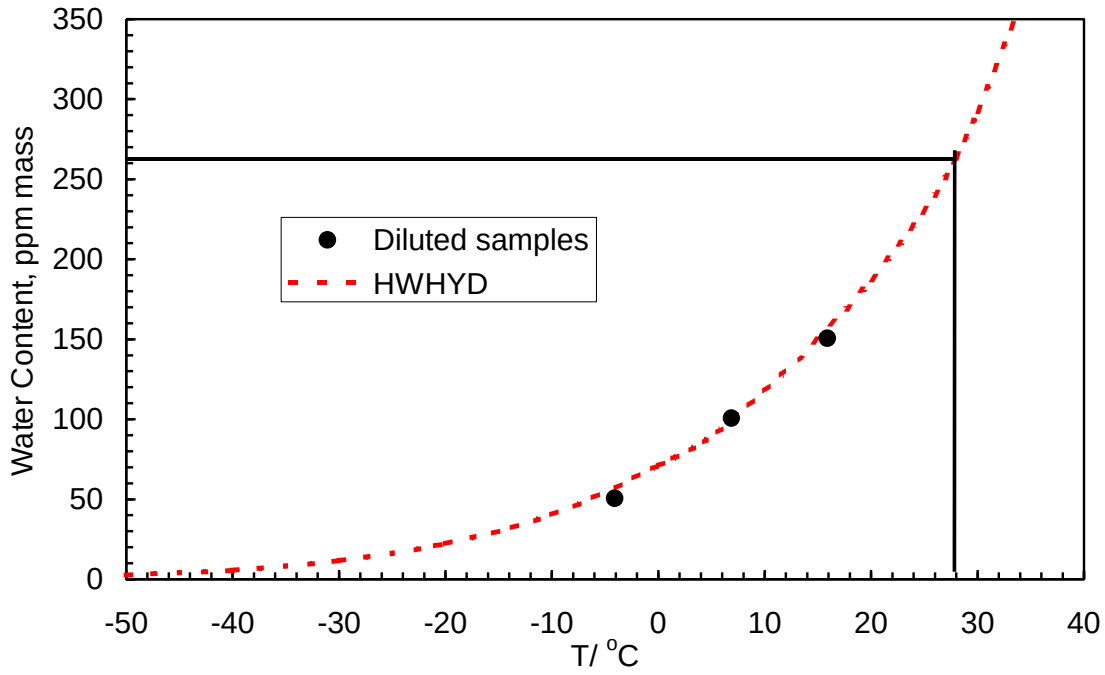

Figure 6.15. Plot showing water saturation temperatures for gravimetrically prepared samples along with predictions using HWHYD for a simulated sample. The test sample with unknown water content had a measured saturation temperature of 28 ºC giving an estimated water content of 263 ppm.

6.3.3.7. Discussions

The initial tests, particularly the QCM data, suggested that hydrocarbon solids formed on cooling may be the source of the solids problem encountered at low temperatures. The GC measurements showed that there was no significant C_{15}+ content and no significant compositional differences between the original sample and that cooled to remove solids. This along with the failure of wax inhibitors to prevent solids suggested that solid hydrocarbons were not to the cause. Subsequent tests, QCM and GC, showed that water was present and that a micro-emulsion was also present. The effect of methanol was clearly demonstrated, in that at concentrations higher than 400 ppm mass no solids were seen to form. It strongly suggests that the reason methanol is preventing solid formation is due to the freezing point depression caused by its presence in the water coming out of solution on cooling.

One other possible cause of the solids was the potential presence of triethylene glycol (TEG). The reason for this being the use of TEG in drying the gas prior to the dew-pointing & mercaptan removal unit and the solids melting temperature recorded using QCM being close to –6 ºC. In the course of this investigation QCM tests were also conducted on pure heptane, octane and nonane. Solid formation was also detected in these samples and the solid melting point was lower, the higher the carbon number. Literature data shows that the solubility of water in these fluids is lower, the higher the carbon number. As TEG will not be present in these pure samples it is not likely that it is the solid being formed. It also indicated that the melting point of the solids, ice, as measured by the QCM is related to the solubility of the water in the sample. Also, the tests results are in good agreement with the model predictions based on pure water solubility. However, it is not possible to rule out the possibility of the presence of small quantities of TEG, though this does not have any significant effect on the recommended remedial measures. Finally, the preceding findings suggest that TEG is unlikely to be the cause of the solids formation at low temperature.

6.3.3.8. Conclusions and Recommendations

From this study it was concluded that-

- The formation of hydrocarbon solids at low temperatures is not the cause of the solids problem.

- Methanol injection at a rate of over 400 ppm by mass can prevent the formation of solids.
- None of the chemical treatments aimed at removing/reducing problems associated with the crystallization of hydrocarbon solids were effective for the solids formed in the fluids tested in this work.
- The later condensate samples collected from the dew-pointing & mercaptan removal unit contain significant amounts, around 263 ppm by mass, of water both dissolved and in the form of a micro-emulsion.
- Calcium Chloride can be used to remove the water, both dissolved and non-dissolved from the sample. Obviously, there are other chemicals that could be used for this purpose.

It was recommended to analyse the water content of the samples using and alternative technique, such as Karl Fischer, to the QCM technique used in the study for confirmation of the water content. There are a number of alternative approaches to water removal available, such as filters and desiccants, and it was recommended to conduct trials with different methods to establish the most effective and efficient for this fluid. Overall this project showed how the QCM could be used in association with other analytical tools for identifying unknown solids and identifying possible remediation strategies.

6.4. Deposition of diesel performance additives

As indicated in the introduction the increasing pressure at which diesel is being injected in engines has potentially been associated with deposition of additives leading to restricted and blocked injectors. Investigating this is challenging due to the high pressures and high temperatures involved. Testing using engines is costly and time consuming. This work was aimed at investigating the possibility of using a QCM mounted in a high pressure cell to indicate the occurrence of solids deposition. Initial work was carried out using a 29,000 psia (2000 bara) rated cell that is normally used for hydrate dissociation point measurements. Following success in initial tests a higher pressure, 40,000 psia (2760 bara) set-up was developed with the capability of simulating instantaneous pressure increase from 3,000 to 40,000 psia. The equipment, methods, test fluids and results from the work are presented in this section.

6.4.1. Experimental equipment

In the initial testing a 35 ml high pressure (maximum 29,000 psia) cell was used. The cell has an integrated metal jacket allowing for circulation of fluids using a temperature controlled circulator. The pressure was measured using a 30,000 psia Quartzdyne transducer with an accuracy of ±10 psi. A QCM was mounted inside the cell, using high pressure electrical feed-throughs, such that it was completely surrounded by the test fluids. The electrical properties of the QCM, Resonant Frequency (RF) and Conductance (G) were measured using an Impedance Analyzer. The pressure and electrical properties of the QCM were continuously recorded. A photograph of the rig is shown in Figure 6.16 below. In the tests reported here the cell was connected directly to a high pressure (maximum 29,000 psia) pump and the sample was not mixed. The pump was used to control the cell pressure.

Following the success of the initial tests a new experimental set-up was designed and built with the following capabilities:

- Test pressures up to 43,500 psia.
- Temperatures up to 200 °C.
- High pressure cell (87,000 psia) and pump, allowing for instantaneous increase of pressure in test cell to 43,500 psia.

In brief, the set-up is comprised of a higher and a lower pressure side. The higher pressure side consists of a 100 ml, 87,000 psia rated cell and pump. The higher pressure side has a pressure transducer and two busting discs. The lower pressure side is comprised of a 35 ml, 43,500 psia rated test cell. The low pressure side is equipped with a pressure relief valve to prevent over-pressurization. A pneumatic, push in type valve, is used to allow instantaneous release of pressure from the high pressure side to the low pressure side. For the tests detailed here the test cell was fitted with high-pressure electric feed-throughs enabling a QCM to be mounted in the test fluids. As in previous work the QCM was oriented horizontally and located at the lower end of the test cell. A 5 MHz QCM was used in all cases. The test cell is located in an oven enabling tests to be conducted at temperatures up to 200 °C. A photograph of the set-up is shown in Figure 6.17.

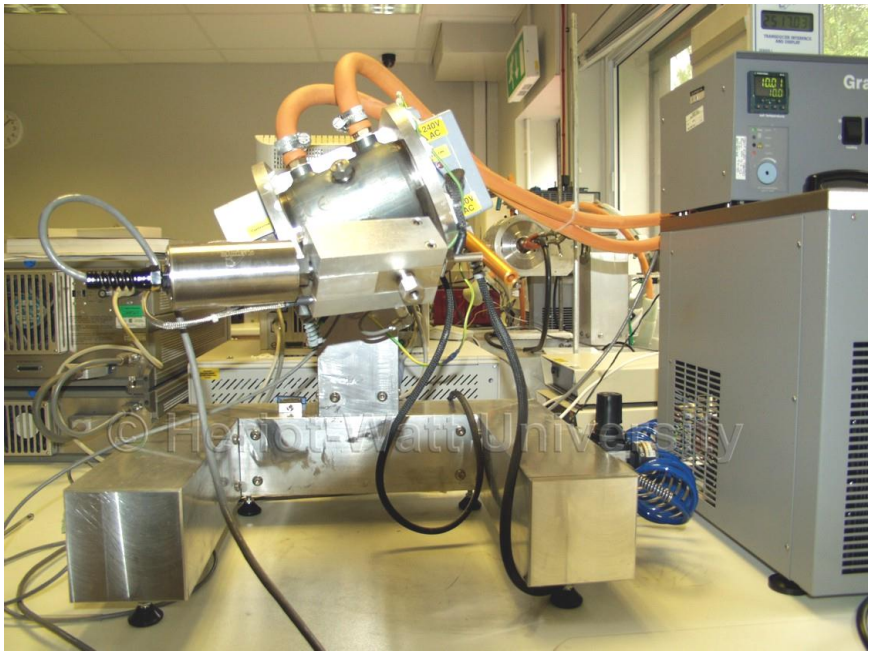

Figure 6.16. Picture of High Pressure Rig

Figure 6.17. Picture of new high pressure diesel test rig. From left, diesel compression rig, oven containing test cell, impedance analyzer and PC for recording data.

6.4.2. Methods

In the initial tests using the 29,000 psia rated rig, the test fluids were loaded into the clean dry high pressure cell and pump. The cell temperature was set at 50 °C throughout the tests. The pressure of the cell was initially set to close to 500 psia and then was increased step-wise, by injecting fluid using the high pressure pump, up to a maximum of 29,000 psia, allowing sufficient time for equilibration at each step. This was adjudged to be when the pressure was stable and there was no significant change in RF or G over a period of no less than 15 minutes.

In the tests with the new rig, the higher pressure side was cleaned and evacuated and the test diesel was injected in under vacuum. Then, the test cell was clean and dried and filled with test diesel prior to connecting to the inlet pipe from the higher pressure side. In the tests the pressure was increased stepwise from ~1,000 to ~3,000 psia and then instantaneously, to a final pressure, close to 40,000 psia. This was achieved by increasing the pressure in the higher pressure side to ~79,000 psia before opening the pneumatic valve. In all of the tests the pressure was held at close to the final pressure for at least 20 hours.

6.4.3. Test fluids

Two test fluids were used in the initial tests using the 29,000 psia rated rig.

- Un-additized base fuel (dried)
- Additized (1000 ppmw additive) base fuel (dried)

Four test fluids were used in the new 40,000 psia rated rig.

- Un-additized base fuel (dried)
- Additized base fuel (dried) known to have been used in engine with blocked injectors
- Base fuel (dried) with Polyisobutylene Succinimide (PIBSI) A
- Base fuel (dried) with PIBSI B

6.4.4. Results

6.4.4.1. Initial tests

An initial test was conducted with the un-additized base fuel. As this test was successful, in that a stable RF and G were recorded at each pressure step between 500 and 29,000 psia, the test was repeated with a new fluid sample. Figure 6.18 shows both changes in RF and G for the first two tests. As can be seen, from Figure 6.18, RF increases with pressure whereas G reduces. It can also be seen that the repeatability is good, especially for RF.

Following the two tests with the base fuel a test was conducted, using the same QCM, with the additized (1000 ppm additive) base fuel. Figure 6.19 shows a plot comparing the data from the test with the un-additized base fuel and the test with the additized (1000 ppm additive) base fuel. As can be seen there is little significant difference in G, however there is

a significant reduction in RF at pressures over 25,000 psia for the test with the additized base fuel when compared to the test with the un-additized base fuel.

A reduction in RF is normally indicative of solids deposition. Following the test the surface of the QCM was examined using FTIR to see if any indication of the material that had deposited, based on the RF results, could be detected. No significant difference between this and a blank QCM could be detected. This might be expected due to the small amount of solids deposited, roughly estimated to be around 1 µg.

At the last pressure step, close to 29,000 psia, it was noted that the RF reduced over time and was still reducing after 120 hours at this pressure. The point shown in Figure 6.19 is the RF value after 120 hours and represents a reduction in RF of close to 2,000 Hz when compared to the value taken from the trendline with the un-additized base fuel. In the initial tests with the un-additized base fuel the sample was not kept at a pressure close to 29,000 psi for an extended period of time, hence one test with the un-additized base fuel was conducted, using a second QCM to find if any reduction in RF would be detected with the un-additized base fuel. Figure 6.20 shows the change in RF at each pressure step for this third test with the base un-additized fuel compared with the first test with the un-additized base fuel. The sample was kept at a pressure close to 29,000 psia for 70 hours and as can be seen there was no significant reduction in RF when compared to the trendline for the first test with un-additized base fuel. In the case of the additized base fluid, after 70 hours, the RF had reduced over 1,200 Hz compared to the trendline for the un-additized base fuel.

A final test was then conducted with the additized base fuel using the second QCM. Figure 6.21 shows the change in RF at each pressure step for this second test with the additized base fuel compared with the first test with un-additized base fuel. As can be seen there was a reduction in RF at the highest pressure, close to 29,000 psia, when compared to the trendline for the un-additized base fuel, however the reduction was not as significant (close to 500 Hz) compared to the first test with additized base fuel. In addition the RF was not seen to continuously decline. In this case the RF was stable within 1 hour of being set at 29,000 psia and remained stable for 70 hours.

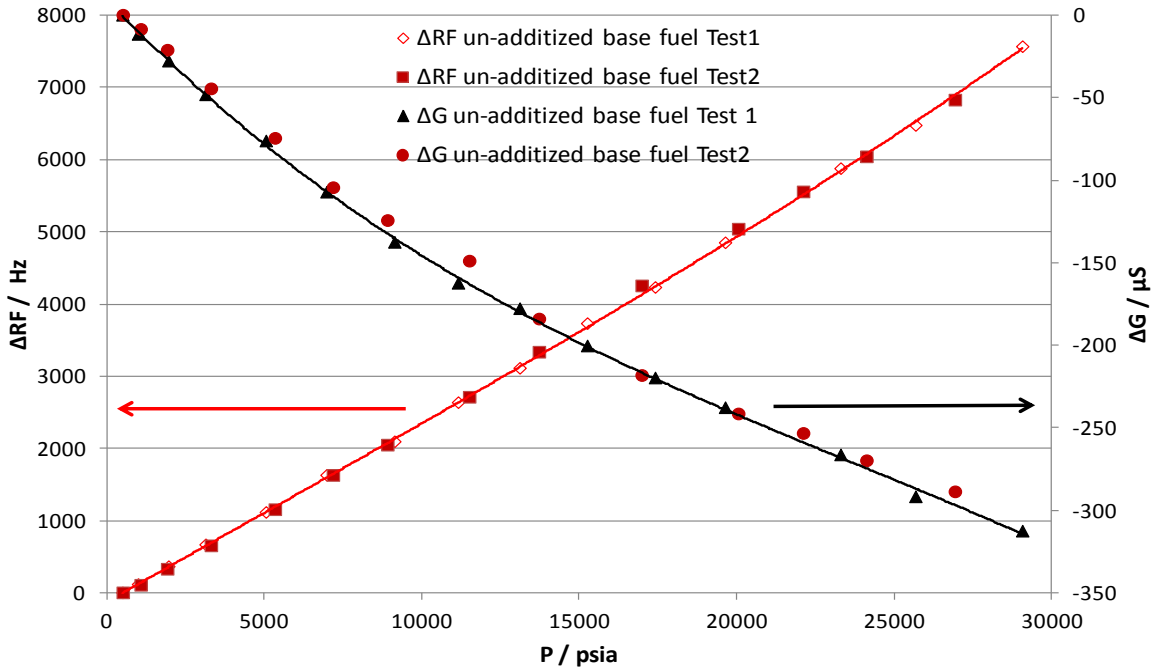

Figure 6.18. Plot showing changes in RF and G with pressure for two tests with the un-additized base fuel (Sample 1), trendlines fitted through un-additized base fuel experimental data.

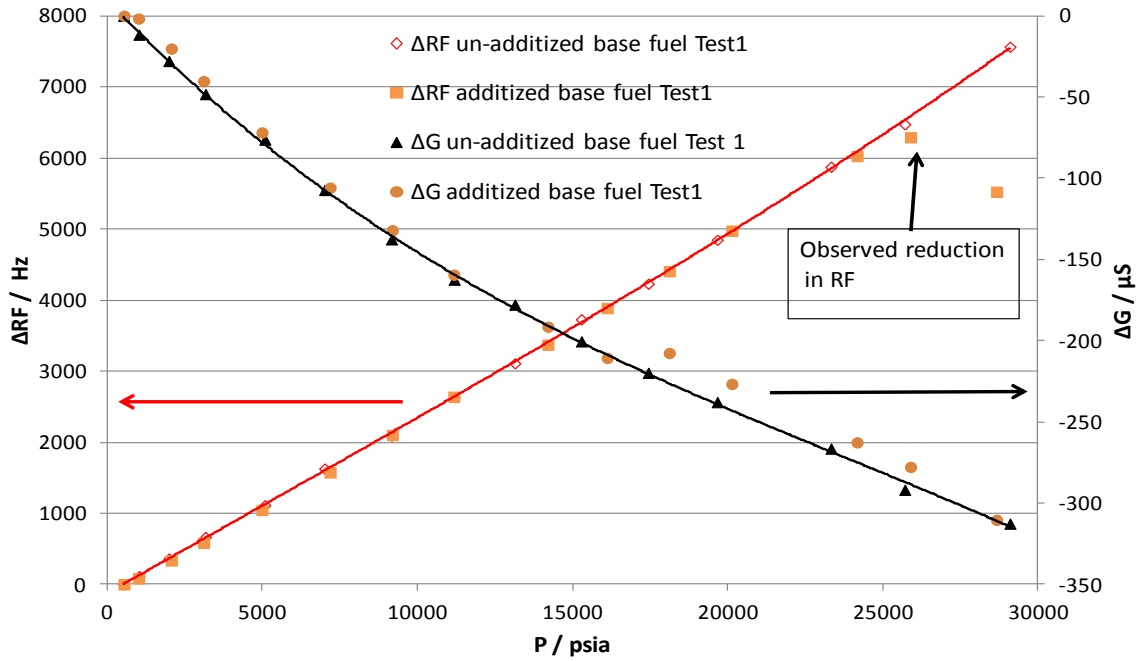

Figure 6.19. Plot showing changes in RF and G with pressure for Test 1 with un-additized base fuel and test with additized (1000 ppm additive) base fuel, trendlines fitted through un-additized base fuel experimental data.

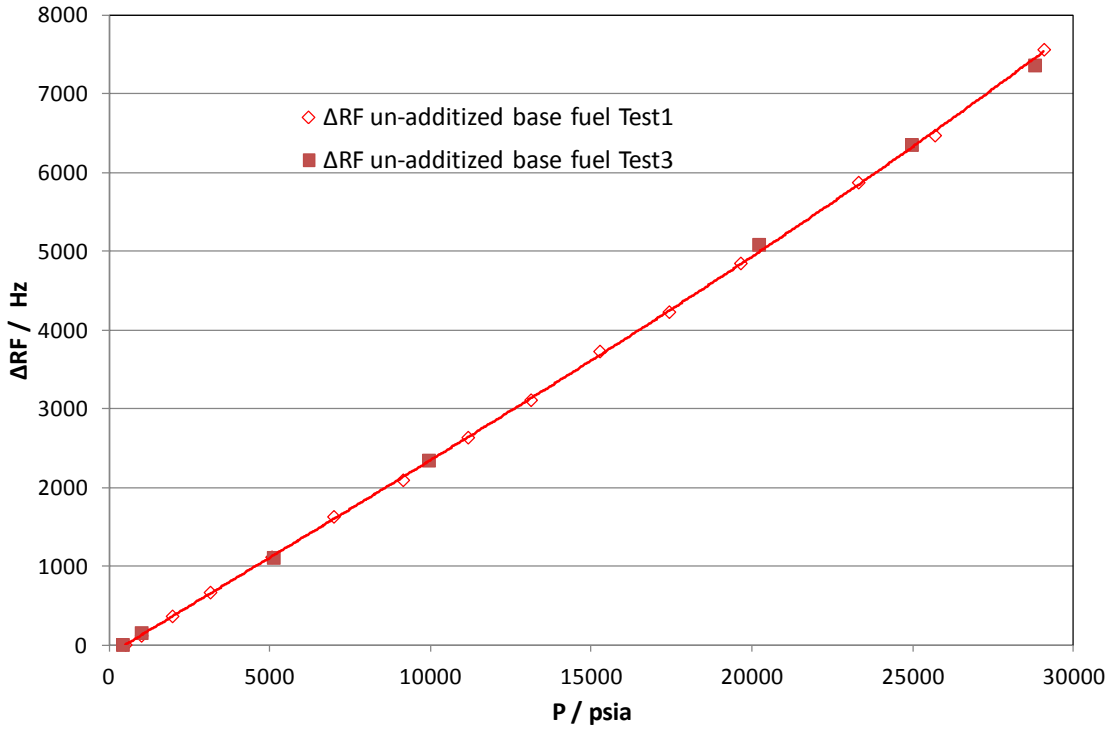

Figure 6.20. Plot showing changes in RF with pressure for Tests 1 and 3 with un-additized base fuel (Sample 1), trendline fitted through un-additized base fuel Test 1 experimental data.

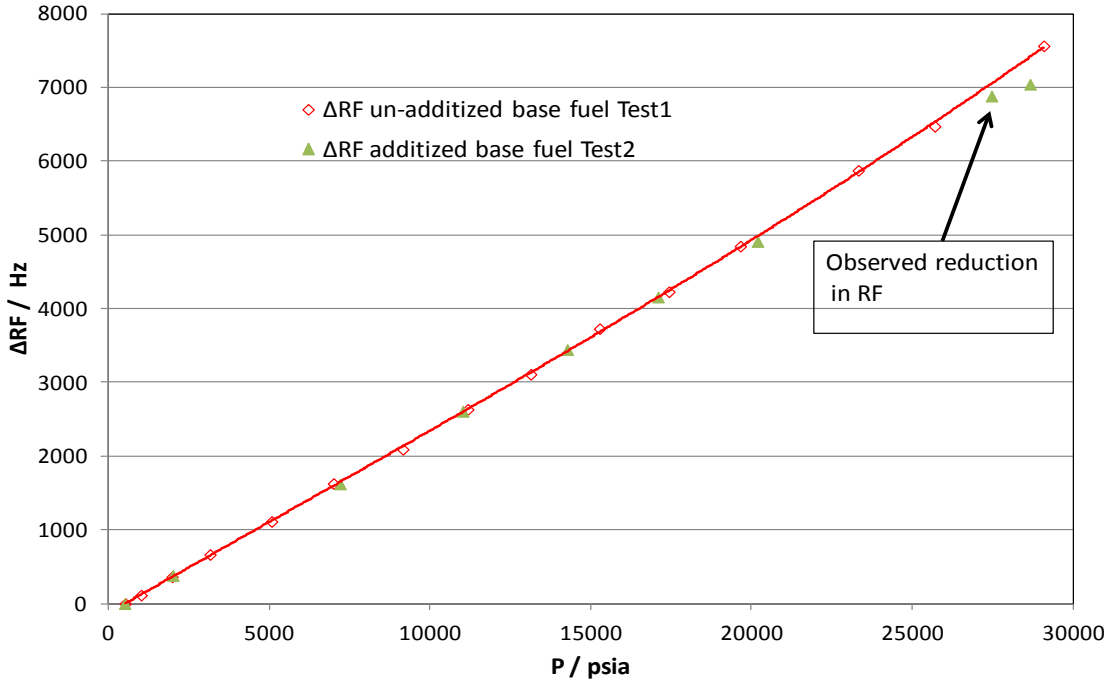

Figure 6.21. Plot showing changes in RF with pressure for Test 1 with the un-additized base fuel (Sample 1) and Test 2 with additized base fuel, trendline fitted through un-additized base fuel Test 1 experimental data.

6.4.4.2. Tests at 40,000 psia

The first two tests with the new 40,000 psia rig were with a sample of un-additized dried base fuel and an additized sample of base fuel which had been used in an engine when the

injectors blocked. The changes RF with time for the two tests, after the instantaneous pressurisation to 40,000 psia, are shown in Figure 6.22. As can be seen in the test with the base fuel the RF was relatively stable, whereas in the test with the additized fuel it was seen to continuously reduce with time, indicating solids deposition.

The changes RF with time for the second two tests, after the instantaneous pressurisation to 40,000 psia, are shown in Figure 6.23 along with the data from the test with the un-additized dried base fuel. As can be seen for both the additized samples the RF reduced continuously with time indicating solids deposition. It can also be seen from Figure 6.23 that the rate of RF decline between the two samples was different indicating that it may be possible to screen PIBSI for their potential to cause deposition in injectors.

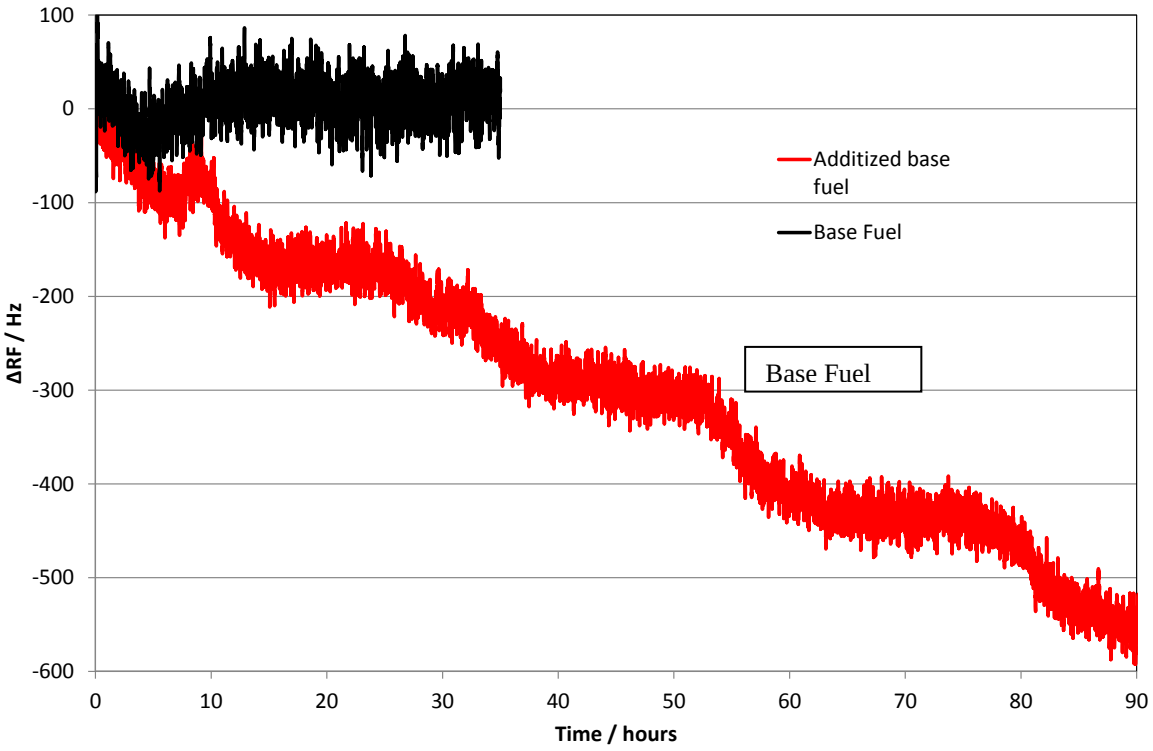

6.22. Change in RF with time in tests with un-additized and additized base fuel. Test pressure 40,000 psia, test temperature 90 °C.

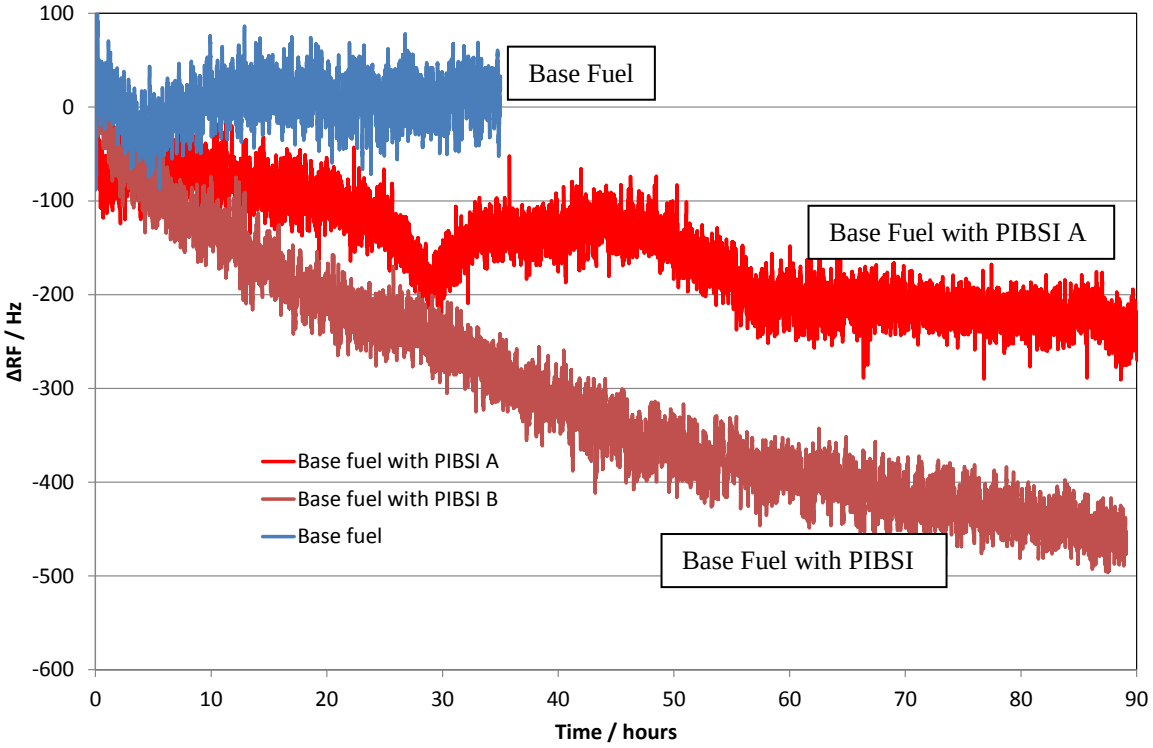

6.23. Change in RF with time in tests with un-additized and additized base fuel with two different PIBSIs. Test pressure 40,000 psia, test temperature 90 °C.

6.4.5. Conclusions

The tests with diesel fuels show that the QCM can be used to measure deposition at high pressures, up to 40,000 psia. This can enable identification of fuels and additive mixtures that may cause restricted or blocked injectors. In addition, screening of commonly used additives, such as PIBSIs can be conducted within a reasonable timeframe and without the requirement for long term testing using engines. As discussed previously QCM based equipment has been used up to high temperatures, over 430 °C, making the QCM a good option for studying solids deposition in a wide variety of challenging environments.

6.5 Evaluation of anti-deposition coatings for scale and wax

6.5.1. Introduction

The main purpose of applying an internal coating to a pipeline is to enhance flow efficiency by reducing surface roughness. In addition, the coating protects the internal surface from corrosion prior to installation and operation of the pipeline. However, flow efficiency can be further compromised by the adherence of solids to the pipeline wall, ultimately resulting in a reduction in pipeline diameter and increasingly turbulent flow. In the oil industry the main four types of substances are scale, wax, hydrates and asphaltene.

Scale formation is often caused by mixing of seawater and formation water giving rise to precipitation of barium and strontium sulphate [17]. Wax formation mainly occurs as a result of a temperature reduction in the reservoir fluid as it is transported from the wellhead. Hydrates also form when fluids cool in subsea pipelines. Asphaltenes tend to flocculate when factors such as pressure and temperature change. The majority of the solids that form remain in suspension and do not contribute to the amount of material adhering to the pipeline wall. There are other undesirable consequences of their formation such as increase fluid viscosity that can be caused by wax formation [18] and total pipeline blockages that can be caused by hydrate formation [19]. Studies have been carried out on factors influencing scale adhesion [20, 21], however for wax, hydrates and asphaltenes there does not appear to be many studies.

An ideal internal coating would not allow the initial adhesion of solids. Factors known to have a bearing upon the initial fouling of a surface by scale, which can be influenced by a surface coating, are surface roughness and surface energy or wettability. In the case of scale it has been shown that surface defects and irregularities will influence surface adhesion [20, 21].

This section details two studies on factors affecting surface deposition and the effectiveness of anti-depositional surface coatings. The first study compared scale adhesion tendencies on uncoated QCMs and QCMs coated with different epoxy resin systems. The second study again used QCMs, coated with an anti-depositional coating, to investigate surface fouling by scale, wax and hydrates.

6.5.2. Investigation of scale adhesion on different epoxy resins applied to QCMs

A brief study of scale adhesion on QCMs coated with four different epoxy resins was carried out. The amount of scale adhering to the different QCMs was compared with that adhering to blank uncoated QCMs. The resin adhering to the QCM, by increasing its mass, reduced the RF as would be expected. The additional RF reduction associated with the adhesion of scale was the main parameter of interest in this study.

6.5.2.1. Experimental equipment

QCMs with a resonant frequency of 5 MHz and a diameter of 1.4 cm were used. The RF was measured using an Impedance/Gain-Phase Analyzer. The different epoxy resins were applied to the QCMs by E. Wood Ltd. For the purposes of identification the four epoxy resins have been named A, B, C and D.

6.5.2.2. Test fluids

For the tests, reported in this communication, where sea and formation water were mixed, synthetic fluids were made up. Typical compositions of seawater and Forties formation water were used to make up the fluids from salts and sulphates in the laboratory. The concentration of ions in each fluid is given in Table 6.6. The mixing of these fluids gives rise to the formation of barium, calcium and strontium sulphate scales.

Table 6.6. Concentration of ions in the synthetic sea and formation water.

Ion	Forties formation water ppm	Seawater ppm
$Na_{(+1)}$	29370	10890
$Ca_{(+2)}$	2809	428
$Mg_{(+2)}$	504	1368
$K_{(+1)}$	372	460
$Sr_{(+2)}$	574	0
$Ba_{(+2)}$	252	0
$SO_{4(-2)}$	0	2960
$Cl_{(-1)}$	52360	19760

6.5.2.3. Experimental methods and results

In this test the RF of the coated QCM plus two blanks were measured. The QCMs were then submersed in a mixed electrolyte solution representing a typical Forties formation water. A synthetic seawater was then added to give a 10 % by volume mix of seawater at which significant scale formation occured. The mixture was then left for 30 minutes after which time the QCMs were removed, washed in clean water and then dried. The RF was then remeasured and the change recorded. The principle of the test was that the RF would fall significantly if scale adhered to the surface of the QCM. The changes in RF were converted to mass changes based upon 1Hz change being equivalent to 1 nanogram. The relationship between change in RF and change in mass is based upon the Sauerbrey equation as given in Chapter 2 Equation 2.1, Page 14.

The test was repeated three times to monitor the build-up of scale. The results of the three tests are shown together in Figure 6.24. In this bar chart the three columns for each QCM represent the cumulative build-up of scale on the QCM surface. It is clear that the QCM coated with resin C shows significantly less scale build-up compared to the other coated QCMs and the blank QCMs. From Figure 6.24, it appears that the QCMs coated with resin A, B and D have more scale on than the blank QCMs, however this variation is within the expected variation for the test.

As there is naturally some scatter in the results, due to the relatively random nature of the scale deposition, four further coated QCMs were used for this test and the same trend was seen as is shown in the results shown in Figure 6.25. In Figure 6.25 the cumulative mass of scale adhering to the QCM over two submersions are presented for each QCM. As with the previous test it is clear that coating C showed significantly less scale adhesion than the other coatings. After the tests had been completed the surfaces of the QCMs were studied using a scanning electron microscope (SEM). The SEM pictures backed up the conclusion that less scale had adhered to the QCMs coated with epoxy resin C.

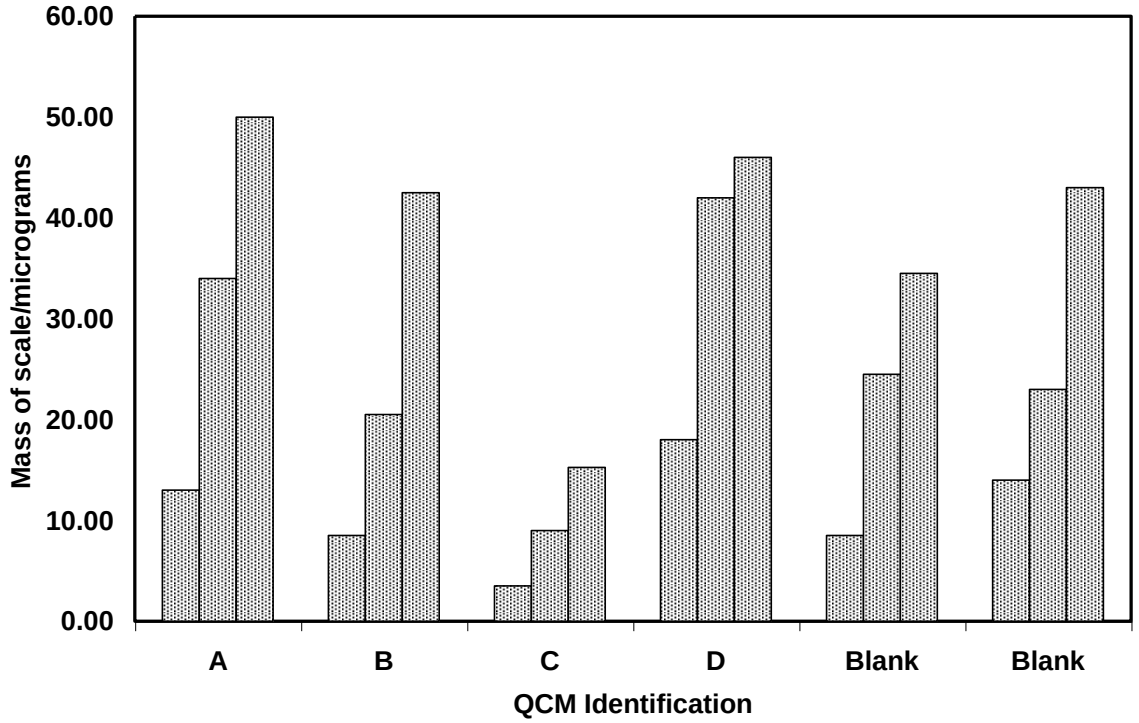

Figure 6.24. Mass of scale adhering to QCMs coated with different epoxy resins over 3 submersions.

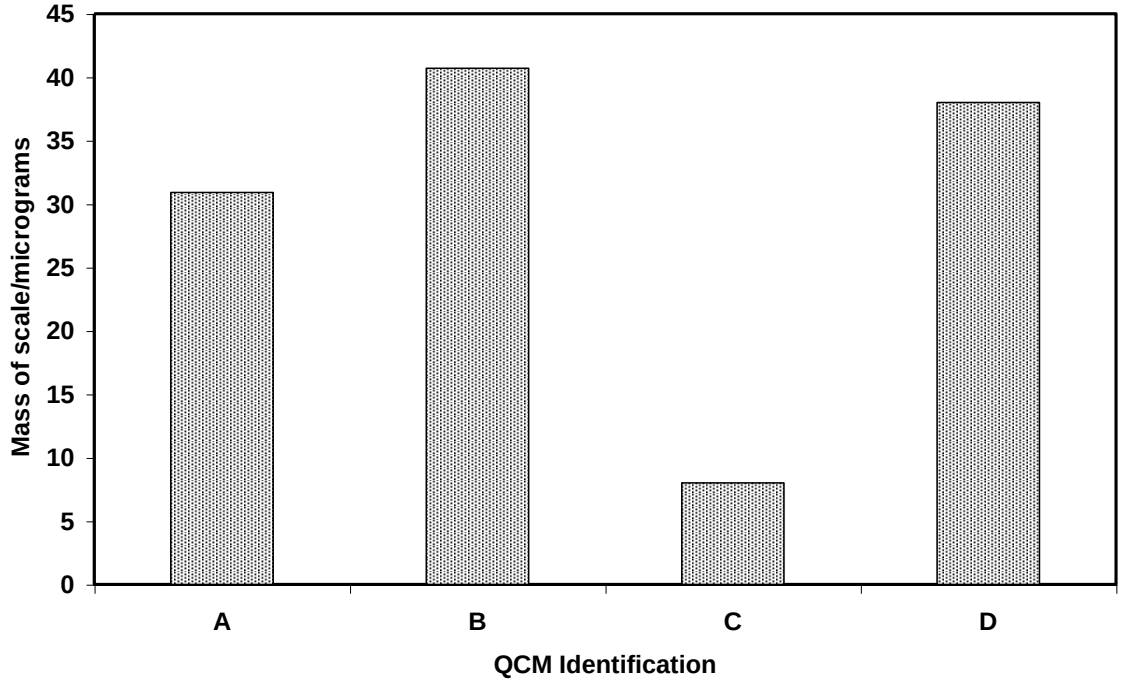

Figure 6.25. Cummulative mass of scale adhering to QCMs coated with different epoxy resins over 2 submersions**.**

6.5.3. Evaluation of anti-depositional coating (copon ep2306hf) for wax, scale and hydrate fouling using QCM technology

A series of tests were conducted to investigate the potential benefits of an anti-depositional coating, COPON EP2306HF, which is used extensively for internal coating of pipelines. The tests were made using coated and uncoated QCMs and studied surface fouling by wax, scale and hydrates. This section details the equipment, methods and results.

6.5.3.1. Experimental equipment

QCMs with a resonant frequency of 5 MHz and a diameter of 2.5 cm were used. The QCMs used were either blank as supplied, blank polished, coated on one side with anti-depositional coating (COPON EP2306HF) or with a roughened surface on one side. The rough surface was made by scratching the surface of a QCM coated with a cellulose paint. The coated QCMs had different depths of paint applied one was 30 microns and one 45 microns. In all of the tests the QCM under study was held in a Teflon holder as shown in Figure 6.26. The QCM holder was designed so that it could be submersed in the test fluid as shown in Figure 6.27. The test fluids were contained in a stainless steel beaker surrounded

by a water jacket. The water jacket was connected to a heater/chiller so that the temperature of the fluid could be raised and lowered. The resonant frequency of the QCM was measured and logged using an Impedance/Gain-Phase Analyzer in communication with a PC fitted with an HPIB board. The test fluids were continuously mixed using a magnetic stirrer. A platinum resistance temperature probe mounted in the water jacket was used to monitor the temperature.

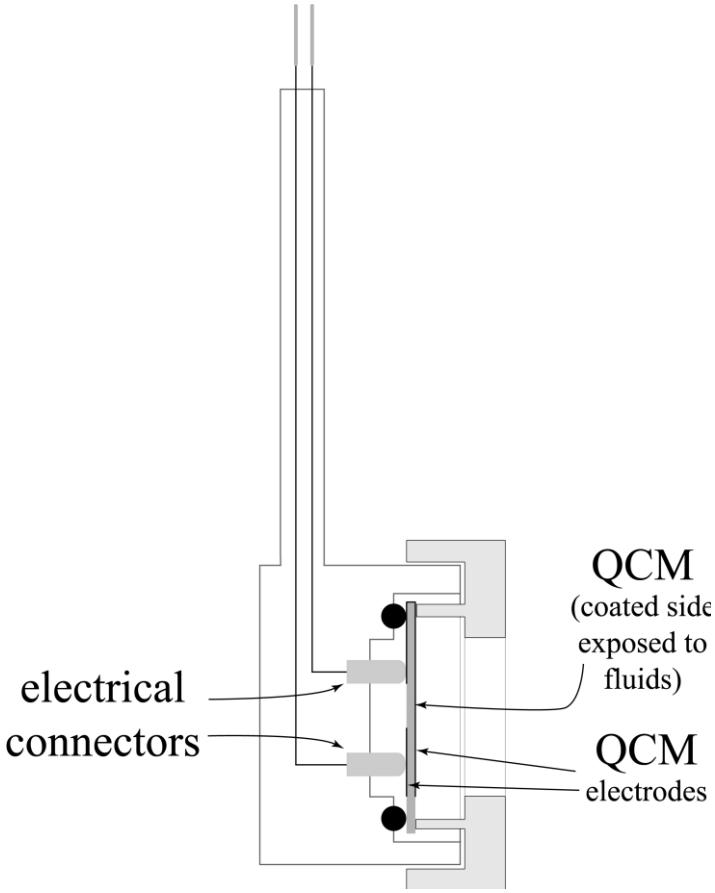

Figure 6.26. Schematic of Teflon QCM holder.

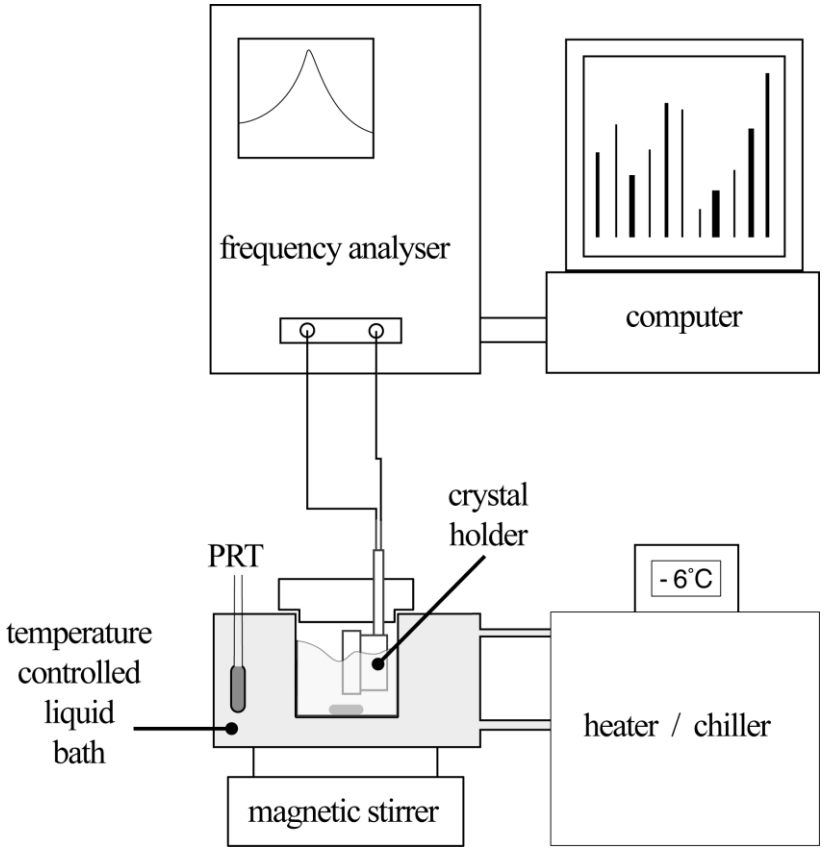

Figure 6.27. Schematic of QCM adhesion rig used for wax scale and hydrate measurements.

6.5.3.2. Experimental methods and results

6.5.3.2.1. Wax adhesion measurements

The wax adhesion measurements were made by cooling a hydrocarbon fluid, surrounding the test QCM, from a temperature where no wax was present to temperatures when wax was present. The temperature at which wax appears in a fluid is commonly known as the wax appearance temperature (WAT). One set of measurements was carried out with a hydrocarbon fluid composed of heptane and microcrystalline wax (0.5 mass% microcrystalline wax). The microcrystalline wax was commercially available wax termed "low melting point". The WAT of the mixture was around 10.8 °C. The amount of wax deposited, estimated from the change in resonant frequency (Equation 2.1, Page 14), was measured at -8.1 °C for QCMs with paint coatings of 30 and 45 microns, a blank QCM and a QCM which had been painted and the surface roughened. The results of these measurements are plotted in Figure 6.28. As can be seen from Figure 6.28 the amount of wax adhering to the QCM with a roughened surface was significantly greater compared to the painted QCMs

and the blank QCM. The accuracy of the measurement technique was estimated to be ±100 micrograms. This means that there is no significant difference between the mass of wax adhering to the painted QCMs and the blank QCM. From this test it is also clear that the difference in thickness of the paint coating had no influence on the mass of wax adhering to the QCM surface.

A second series of wax adhesion measurements was conducted with a separator condensate sample with a WAT around 19.8 °C. In these tests a blank QCM, a highly polished blank QCM and a QCM with a paint coating of 45 microns were tested. The amount of wax adhering to the QCMs was measured at 5.8 °C. The experimental measurements are plotted in Figure 6.29. The results, shown in Figure 6.29, indicate that the three QCMs had similar amounts of wax adhering to their surfaces. The painted QCM had slightly less wax adhesion, however the difference is close to the expected experimental repeatability of the tests. The result also shows that the performance of the highly polished QCM is no better in terms of preventing wax adhesion compared to the blank QCM.

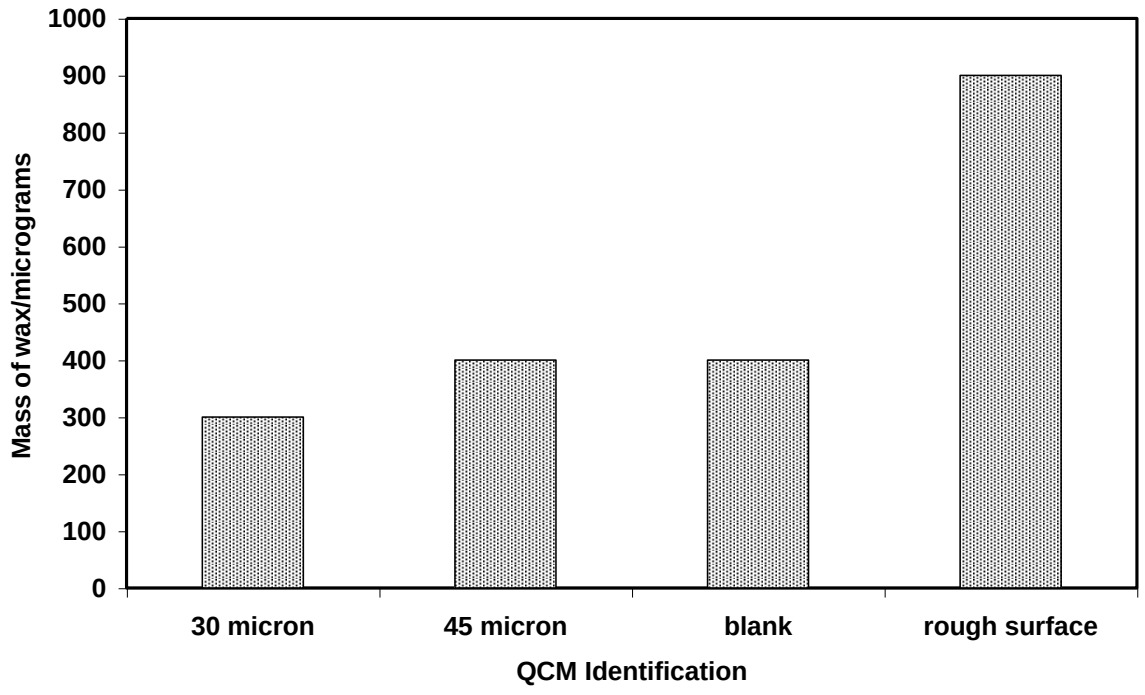

Figure 6.28. The amount of wax adhering to QCMs at 265K in tests with heptane and microcrystalline wax.

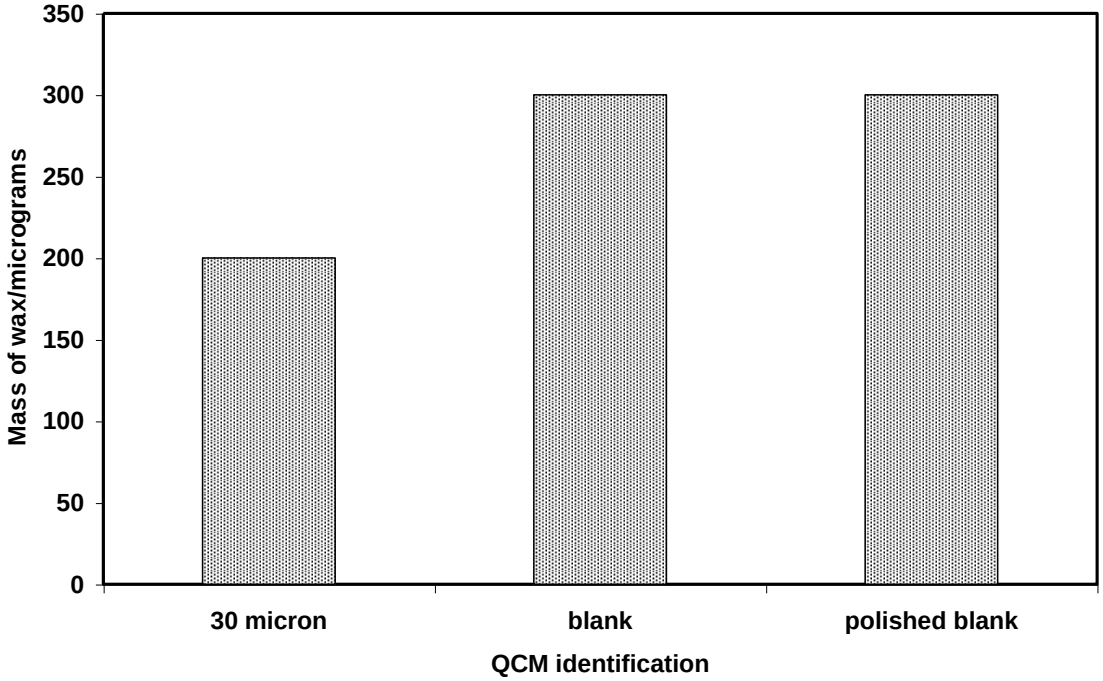

Figure 6.29. The amount of wax adhering to QCMs at 279K in tests with a separator condensate.

6.5.3.2.2. Scale adhesion measurements

The scale tests were made using the same QCM holder and equipment as for the wax measurements (Figures 6.26 and 6.27). The heater chiller was not operated during the scale tests as all tests were conducted at laboratory temperature. The method for the scale tests was that 200 cc of an aqueous solution of sodium carbonate (1 gm per liter) was poured into the stainless steel beaker. Following this 200 cc of an aqueous solution of calcium chloride (1 gm per liter) was added. As soon as these two aqueous solutions mixed calcium carbonate, or limescale, began to precipitate according to the following reaction:

$$CaCl_2 + Na_2CO_3 \Rightarrow CaCO_3 + 2NaCl$$

Some of the limescale adhered to the surface of the QCM causing the resonant frequency to decline. After around 20 minutes the decline in the resonant frequency with time was seen to be negligible and so the test was terminated. The QCM and the apparatus were then

washed with water, without removing the scale adhering to the test QCM. The procedure was then repeated two further times.

The scale adhesion tests as described above were conducted on a QCM with a 45 microns thick paint coating, a blank QCM and the QCM with the roughened surface as used in the wax adhesion measurements. The cumulative mass of scale adhering to the surfaces of the QCM are plotted in Figure 6.30. As can be seen from Figure 6.30 the amount of scale adhering to the surface of the QCM with the rough surface was significantly greater than that adhering to the painted and blank QCMs. The painted and blank QCMs showed a similar result, within the experimental error estimated to be similar to the wax adhesion tests ±100 micrograms.

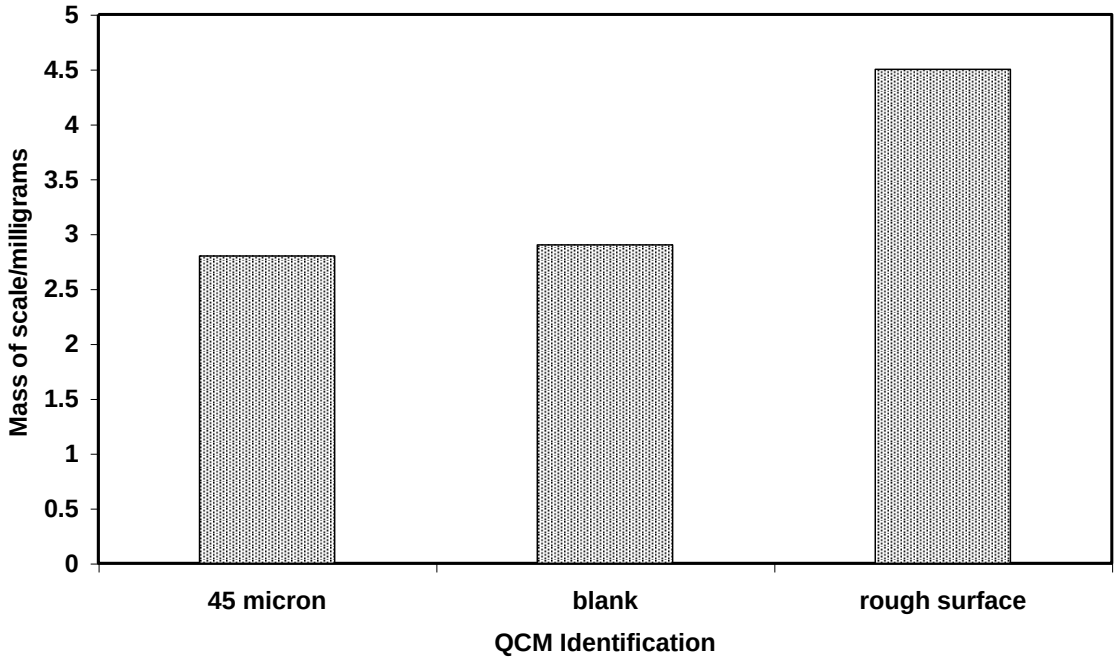

Figure 6.30. Mass of scale adhering to coated QCM and QCMs with different surface finishes.

6.5.3.2.3. Hydrate adhesion measurements

The hydrate tests were made using the same QCM holder and equipment as for the wax and scale measurements (Figures 6.26 and 6.27). Both water and cyclopentane were added to the steel beaker. Cyclopentane was used in this study because it can form hydrates at atmospheric pressure and at temperatures below 6.8 °C. Hydrates were formed at 0.8 °C and the resonant frequency of the test QCM was monitored. Tests were conducted on a QCM coated with paint with a thickness of 45 microns, a blank QCM and a QCM with a roughened

surface. In all cases there was no significant change in resonant frequency on hydrate formation indicating that the hydrates were not adhering to the QCM surface. This was the case even when most of the contents of the beaker were solid. Previous work at HWU forming gas hydrates in water droplets on the surface of a QCM also showed this outcome in that there was no significant change in the resonant frequency of the QCM on hydrate formation. If ice formed then this would strongly adhere to the QCM as seen by a very significant shift in the resonant frequency of the test QCM.

6.5.4. Conclusions

This study shows that:

- QCM technology is an attractive tool for studying/screening anti-depositional coatings for surface fouling solids such as scale, wax, hydrates and asphaltenes.
- Studies using QCMs showed that more wax and scale adhered to rough surfaces than smooth or polished surfaces.
- Tests with QCMs coated with anti-depositional paint, COPON EP2306HF, showed the benefits of the coating compared to a rough surface.
- Tests on the adhesion of hydrates to surfaces showed that hydrates do not appear to bond strongly to surfaces by comparison with ice. This may be due to the low surface energy of the hydrate crystals.
- The conclusions regarding the benefits of anti-depositional coatings compared to rough surfaces from QCM tests with scale were backed up using a new dynamic rig.

6.6. Conclusions

The work presented in this chapter shows that:

- QCM based equipment has been proven to be a good rapid alternative for hydrate dissociation point measurements and that it can be used for indicating loss of volatile inhibitors to the vapour phase in low water cut systems. The developed methods have been patented, are an accepted method and are being used by other researchers.
- QCM can be used in association with other analytical tools to help identify solids that are depositing and evaluate remediation strategies.

- The QCM can be used up to very high pressures, 40,000 psia, and this coupled with its ability to be used up to high temperatures makes it a useful tool for studying solids deposition in challenging environments such as in high pressure diesel injectors.
- The QCM can be used to evaluate the ability of anti-depositional coatings applied to internal pipeline surfaces to reduce the deposition of solids such as scale and wax.

6.7. References

[1] Sloan, E.D., and Koh, C.A., *Clathrate Hydrates of Natural Gases*, 3rd Edition, Taylor & Francis, ISBN 978-0-8493-9078-4 (2008).

[2] Østergaard, K.K., Tohidi, B., Burgass, R.W., Danesh, A., and Todd, A.C. *Hydrate Equilibrium Data of Multi-Component Systems in the Presence of Structure-II and Structure-H HeavyHydrate Formers*, Journal of Chemical and Engineering Data 46 (2001).

[3] Anderson, R., Mozaffar, H., and Tohidi, B., *Development of a crystal growth inhibition based method for the evaluation of kinetic hydrate inhibitors*, Proceedings of the 7th International Conference on Gas Hydrates (ICGH 2011), Edinburgh, Scotland, United Kingdom, July 17-21, 2011.

[4] Chua, P. C., and Kelland, M. A., *Study of the Gas Hydrate Anti-agglomerant Performance of a Series of n‑ Alkyl-tri(n‑ butyl)ammonium Bromides*, Energy Fuels 2013, 27, 1285−1292.

[5] Tohidi, B., Burgass, R.W., Danesh, A., Todd, A.C., and Østergaard, K.K. *Improving the Accuracy of Gas Hydrate Dissociation Point Measurements*, Annals of the New York Academy of Sciences, 912, 924-931 (2000).

[6] Deva Kumar, M.L.S., Drakshayani, S., and Vijaya Kumar Reddy, K., *Effect of Fuel Injection Pressure on Performance of Single Cylinder Diesel Engine at Different Manifold Inclinations*, International Journal of Engineering and Innovative Technology, Volume 2, Issue 4, October (2012).

[7] Mc Geehan, J.A., and Ryason, P.R., *Preventing Catastrophic Camshaft Lobe Failures in Low Emission Diesel Engines*, International Falls Fuels and Lubricants Meeting and Exposition, Baltimore, Maryland, October 16-19, (2000).

[8] Barker, J., Richards, P., Snape, C., and Meredith, W., *Diesel Injection Deposits-An Issue That Has Evolved With Engine Technology*, Society of Automotive Engineers, Paper number 2011-01-1923, (2011).

[9] Deaton, W.M., and Frost, E.M. Jr., *Gas Hydrates and Their Relation to the Operation of Natural-Gas Pipe Lines*, U.S. Bureau of Mines Monograph 8, p. 101, (1946).

[10] Avlonitis, D., *Multiphase Equilibria in Oil-Water Hydrate Forming Systems*, M.Sc. Thesis, Heriot-Watt University, Edinburgh, Scotland (1988).

[11] Danesh, A., Todd, A.C., Tohidi, B., and Burgass, R., *Applicability of Oscillating Quartz Crystal in Measuring Fluid Properties in Laboratory or Downhole*, EPSRC research grant final report, ref No: GR/K63641, (1997).

[12] Burgass, R., Todd, A.C., Danesh, A., and Tohidi, B., *Clathrate Hydrate Dissociation Point Detection and Measurement*, U.S. Patent Number 6,298,724 (1999).

[13] Burgass, R., Tohidi, B., Danesh, A. and Todd, A.C., *Application of Quartz Crystal Microbalance to Gas Hydrate Stability Zone Measurements*, 4th International Conference on Gas Hydrates, Yokohama, Japan, 19-23 May (2002).

[14] Mohammadi, A.H., Tohidi, B. and Burgass, R., *Equilibrium Data and Thermodynamic Modeling of Nitrogen, Oxygen and Air Clathrate Hydrates*, Journal of Chemical and Engineering Data, 48, 612-616 (2003).

[15] Lee, B.R., Sa, J.H., Park, D.H., Cho, S., Lee, J., Kim, H.J., Oh, E., Jeon, S., Lee, J.D., and Lee, K.H., *"Continuous" Method for the Fast Screening of Thermodynamic Promoters of Gas Hydrates Using a Quartz Crystal Microbalance*, Energy Fuels, 26, 767-772, (2012).

[16] Park, D.H., Lee, B.R., Sa, J.H., and Lee, K.H., *Gas-Hydrate Phase Equilibrium for Mixtures of Sulfur Hexafluoride and Hydrogen*, J. Chem. Eng. Data, 57, 1433-1436, (2012).

[17] Yuan M., Todd, A.C., and Sorbie K.S., Marine and Petroleum Geology, Vol. 11, No. 1, 1994.

[18] Edwards, R.T., Industrial and Engineering Chemistry, 49(4), 750-757, 1957.

[19] Tohidi, B., Danesh, A., Burgass, R. W., and Todd, A. C., SPE 28478, 1994.

[20] Pulliam,G.R., Journal of American ceramic society, Vol. 42, No10, pp. 477-481.

[21] Griffith, A.A., Philadelphia Trans. Roy. Soc. London, A221, 1920, pp. 163-198.

CHAPTER 7 - CONCLUSIONS & FUTURE WORK

The conclusions that can be made from the work presented in this thesis are summarised below, following which suggestions for future work are given.

7.1. Wax

The conclusions form **Chapters 2 and 3** which presented the work relating to the development and validation of QCM based equipment for wax measurements are as follows.

- Tests with synthetic fluids using the small volume (5 ml test fluid) QCM glass tube assembly showed that accurate measurements of WAT (Wax Appearance Temperature) and WDT (Wax Disappearance Temperature) could be made. The fact that the generated data for the solubility of hexatriacontane agreed with literature data from three sources and predictions made using the Heriot-Watt Wax model (HWWAX) confirms the accuracy of the measurements.
- The QCM method for measuring WAT and WDT values can be used for stabilised and live reservoir fluids at a wide range of P / T conditions.
- A temperature controlled QCM rig has been developed that can be used for making measurements of wax adhesion tendency at pipeline conditions, mimicking temperature gradients between oil and pipeline wall.
- The use of a multi-cell ambient pressure set-up to screen inhibitors at different dose rates has been demonstrated. The QCM method can give more information regarding inhibitor performance than pour point testing alone.
- The use of the temperature controlled QCM rig to screen inhibitors at different dose rates has been demonstrated. The results agreed with standard cold finger test results for the same fluid and inhibitors. The temperature controlled QCM set-up has distinct advantages in terms of the amount of fluid required, the information obtained and the capability to run tests at field conditions.
- It may be possible to use QCM test data to investigate the possibility of blending inhibitors to improve performance in cases where one inhibitor is not able to reduce wax adhesion across the whole range of conditions encountered at pipeline conditions.
- The three separate case studies presented in **Chapter 3** show how the QCM based equipment has been used to provide information on WAT and WDT values for a live oil and a condensate. In addition to enable selection of inhibitors based upon

performance at both atmospheric and pressurized conditions. It is suggested that further studies will be conducted enabling the equipment and methods to become accepted as a reliable option improving or complimenting existing technologies.

7.2. Asphaltene

The results from the work presented in **Chapters 4 and 5**, aimed at developing and validating QCM based equipment for asphaltene measurements are as follows:

- The heptane titration tests showed that the QCM can be used to measure the onset of asphaltene precipitation and adhesion for stabilised crude oils. This makes the method applicable for use in ASTM D6703 – 07 and ASIST determination for stabilised crude samples.
- The difference between the asphaltene onset, in terms of the amount of heptane injected per "g" oil, between tests with step-wise and continuous injection suggests that more research is required to optimise procedures. In addition it suggests that the true point of asphaltene may not be being correctly measured in tests with continuous solvent injection.
- The tests at pressure show that QCM based equipment can be used to measure the asphaltene onset conditions in live fluids at high pressure/high temperature conditions. The high sensitivity of the QCM to very small amounts of deposition may make it more sensitive than some other experimental methods for detecting asphaltene onset conditions.
- The tests comparing live oil without and with inhibitor indicate that the effectiveness of the inhibitor at reducing deposition can be evaluated. As reducing the deposition of asphaltenes on surfaces is arguably the most important aim of inhibitor injection QCM could be considered as the best option for inhibitor screening and optimisation. Although not investigated in this work it is expected that inhibitor evaluation can also be conducted for stabilised oil with solvent injection.
- The first case study presented in **Chapter 5** shows that using the QCM in heptane titration testing allows for comparison of asphaltene stability in fluids composed of different blends of reservoir fluids.
- The second case study shows that the QCM based equipment can be used to detect deposition of asphaltenes in live reservoir fluids. As discussed in **Chapter 2** a QCM itself has been used at pressures up to 3,000 bara and 430 °C hence with suitably constructed vessels it is possible to make measurements at any realistic reservoir

conditions. The second case study also showed how the set-up can be used to evaluate inhibitor performance in terms of reducing asphaltene deposition and also to optimise inhibitor dose rate at field conditions.

7.3. Hydrate

The use of QCM for hydrate dissociation point measurements is described in this thesis. The method was patented in 2001, it was included as a listed method for making hydrate phase equilibrium measurements by Sloan and Koh 2008. The method was published in 2002 and has been adopted for use by other researchers. In this thesis the potential use of dissociation points measured with the aim of indirectly measuring inhibitor distribution is investigated. The experimental data, if found to be reliable and repeatable, could be used for validating predictions and comparing with experimental data, measured by different approaches.

7.4. Ice, diesel additives and anti-depositional coatings

The use of QCM, combined with other analytical tools to identify solids that had deposited in a processing facility, was described in **Chapter 6**. Other studies have been conducted including one that was used to optimise the type of chemical that was best for removal of gunk in a pipeline. In addition laboratory tests were designed and conducted to give information regarding the optimum slug size and residence time for complete removal of the gunk.

The validation of QCM capability to measure solids deposition in high pressure diesel injectors, as presented in **Chapter 6**, opens up a new avenue of research and the potential development of an industry standard testing procedure.

The use of QCM to investigate the effectiveness of anti-deposition coatings for scale and wax is detailed in **Chapter 6**. This work as with the work on ice and diesel additives demonstrates the potential uses of QCM based laboratory equipment to carry out laboratory based research that can enable initial screening and optimisation work aimed at developing and validating new products.

7.5. Future work

As there is significant scatter for the WAT and WDT values obtained using different methods it is suggested to assemble a set of test fluids, including synthetic mixtures condensates and black oils, and sending samples to different laboratories employing different techniques by way of conducting a comparison of measured values for one set of fluids.

A recent publication by Parlak et al. (2013) [1] describes the potential for decoupling mass adsorption from fluid viscosity and density in QCM measurements using normalized conductance modelling. This means that it is possible to separate out the mass deposition only and may improve the precision of wax measurements and potentially other measurements.

The difference in the asphaltene onset in terms of volume of heptane added per "g" oil, between tests with step-wise and continuous heptane injection suggest that equilibrium was not being achieved with continuous injection. It is suggested to conduct further tests to validate this observation as it may raise questions regarding the reliability of asphaltene onset measurements made using continuous solvent injection. This may also be the case for measurements of asphaltene onset using continuous pressure reduction.

In general there are fewer avenues to validate the accuracy of QCM based measurements for asphaltenes when compared to those for wax measurements. In the case of wax measurements there is literature data available for synthetic mixtures and in the case of wax inhibitors it was possible to run a parallel study with another laboratory. For asphaltenes it is suggested to run further tests to validate the developed equipment and methods, preferably by conducting parallel studies on identical sample with other laboratories.

One interesting observation from the second asphaltene case study presented in **Chapter 4** was that, as shown in Figure 4.3, there were two trends depending upon P/T conditions, either reducing RF indicating asphaltene deposition or increasing RF indicating asphaltene dissolution. The reversibility of asphaltene precipitation/flocculation/deposition has been the subject of a significant number of publications and is considered to be an important issue. It is suggested to conduct further tests to validate the results and explore the phenomenon in further details.

This thesis shows the potential uses for QCM based equipment for use with wax, asphaltene scale and hydrate. It has also been shown in previous work to be capable of being used for a variety of other measurements such a saturation pressure measurements and scale tests. The development of a multi-tasking rig that can be used for a variety of measurements should be considered. The attributes of the rig could be as follows:

- Wide P/T range
- High speed magnetic mixer, preferably with shear/torque measurements
- Variable volume
- Option for locally cooled QCM
- Option for QCM to be in contact with low volume of liquid condensate or aqueous phase
- Salt and acid gas resistant materials

Some of the capabilities of the rig may be as follows:

- WAT and WDT for reservoir fluids
- Asphaltene deposition envelope measurements
- Hydrate phase boundary measurements with normal, low or high aqueous fractions
- Wax adhesion tendency measurements with different shear rates and temperature gradients
- Asphaltene deposition tendency measurements with different shear rates
- Wax inhibitor evaluation with reservoir fluids including effect of shear rates and temperature gradients
- Asphaltene inhibitor evaluation including effect of shear rate
- Saturation pressure measurements including bubble point using volume change and QCM, and potentially dew point using locally cooled QCM
- Evaluation of anti-deposition coatings

In addition to measuring QCM RF and conductance it is also possible to measure the decay in resonance, or dissipation factor, once the AC voltage is turned off. This was described by Hirao et al. (1993) [2] and Rodahl et al. (1996) [3]. The term QCM-D associated with this approach is a trademark owned by Q-sense AB, Gothenburg, Sweden. The dissipation factor can be used to give more information about the film in contact with the

QCM surface in comparison to using only changes in RF and conductance. For example it can be used to sense changes in the softness and any structural changes that may occur. In the case of viscoelastic materials such as wax adhering to the QCM, using only the change in RF tends to underestimate the amount of solids adhering, whereas using the dissipation factor a more accurate value may be obtained. The potential advantages of using QCM-D technology for measurements with wax, asphaltene and hydrate would be worth investigating in future studies.

7.6. References

[1] Parlak, Z., Biet, C., and Zauscher, S., *Decoupling mass adsorption from fluid viscosity and density in quartz crystal microbalance measurements using normalized conductance modeling*, Measurement Science and Technology, 24 (2013), 085301 (9pp).

[2] Hirao, M., Ogi, H., and Fukuoka, H., *Resonance Emat system for acoustoelastic stress measurement in sheet metals*, Review of Scientific Instruments 64 (11): 3198–3205 (1993).

[3] Rodahl, M., and Kasemo, B., *A simple setup to simultaneously measure the resonant frequency and the absolute dissipation factor of a quartz crystal microbalance*, Review of Scientific Instruments 67 (9): 3238–3241 (1996).